

Dissertation der Fakultät für Biologie der
Ludwig-Maximilians-Universität München

Necroptosis and apoptosis
in the primate ovary

München, 2019

Konstantin Bagnjuk



Diese Dissertation wurde
unter der Leitung von

Prof. Dr. Artur Mayerhofer und PD Dr. Lars Kunz

im Bereich Zellbiologie – Anatomie III
des Biomedizinischen Centrums

der Ludwig-Maximilians-Universität München angefertigt

Erstgutachter: PD Dr. Lars Kunz
Zweitgutachterin: Prof. Dr. Gisela Grupe
Tag der Abgabe: 06.11.2019
Tag der Prüfung: 08.01.2020

Eidesstattliche Erklärung

Ich versichere hiermit an Eides statt, dass ich, Konstantin Bagnjuk diese Dissertation selbständig und ohne unerlaubte Hilfsmittel angefertigt habe. Die vorliegende Dissertation wurde weder ganz, noch teilweise einer anderen Prüfungskommission vorgelegt. Zu keinem früheren Zeitpunkt habe ich versucht eine Dissertation einzureichen oder an einer Doktorprüfung teilzunehmen.

München, den 06.11.19

Konstantin Bagnjuk

Für meine Familie

„Ausdauer und Entschlossenheit sind zwei Eigenschaften, die bei jedem Unternehmen den Erfolg sichern.“

Lew Nikolajewitsch Tolstoi

Directory

List of abbreviations	V
List of figures	VII
Publications and contributions	VIII
Summary	XI
Zusammenfassung	XIII
1 Introduction	1
1.1 Life and death in the healthy primate ovary	1
1.1.1 Follicle selection	2
1.1.2 Luteal phase	5
1.2 Granulosa cell tumors – malignancies of the ovary	6
1.3 Understanding cell death	7
1.3.1 Once upon a time there was apoptosis	8
1.3.1.1 SMAC as a role model	11
1.3.2 Necroptosis is programmed necrosis	12
1.3.2.1 Sphingolipids regulate cell fate	15
1.4 Humans are not mice	18
1.4.1 Experimental organisms for the human ovary	19
1.4.2 Cellular models for the human ovary	21
1.4.2.1 Granulosa cell tumor cell lines	22
2 Aims and expectations	23
3 Results	24
3.1 Publication 1 (Bagnjuk et al. 2019)	24
3.2 Publication 2 (Du, Bagnjuk et al. 2018)	46
3.3 Publication 3 (Bagnjuk, Kast et al. 2019)	56
4 Discussion	68
4.1 LGCs – a model for human LLCs	69
4.2 Let’s rethink luteal regression in the human ovary	70
4.3 The aim to give back the ability to decide	74
4.3.1 Necroptosis is to consider in <i>in vitro</i> follicle maturation	75
4.3.2 GCTs may be sensitive to SMAC mimetics	78
4.4 Future scenarios	79
5 References	82
6 Acknowledgements	i
7 List of publications	iv

List of abbreviations

Abbreviation	Full name	Abbreviation	Full name
AA	Amino acid	FADD	Fas associated via death domain
ACD	Accidental cell death	FAS/CD95	Fas cell surface receptor
AChE	Acetylcholinesterase	FASLG	Fas Ligand
ADP	Adenosine diphosphate	FF	Follicular fluid
aGCT(s)	Adult granulosa cell tumor(s)	Fig	Figure
AKT	Protein Kinase B	FOXL2	Forkhead Box L2
AMH	Anti-Muellerian hormone	FSH	Follicle stimulating hormone
APAF	Apoptotic peptidase activating factor	FSHR	FSH-receptor
ASAH1	Acid ceramidase	GC(s)	Granulosa cell(s)
BAK	BCL2 antagonist/killer 1	GCT(s)	Granulosa cell tumor(s)
BAX	BCL2 associated X protein	GnRH	Gonadotropin releasing hormone
BCL2	B-Cell CLL/Lymphoma 2 or BCL2 apoptosis regulator	h	Hour
BIR	Baculoviral IAP repeat domain	hCG	Human chorionic gonadotropin
BIRC	Baculoviral IAP repeat containing protein	HeLa	Henrietta Lacks
BOK	BCL2 family ovarian killer protein	HSP90AA1	Heat shock protein 90a family class A member 1
BV6	Bivalent SMAC mimetic V6	IAP(s)	Inhibitor of apoptosis protein(s)
<i>C. jacchus</i>	<i>Callithrix jacchus</i>	IDO	Indoleamine 2,3-dioxygenase
C134W	Cysteine to tryptophan mutation at amino acid number 134	IFM	In vitro follicle maturation
CARD	Caspase recruitment domain	IOM	In vitro oocyte maturation
CASP	Caspase	IVF	In vitro fertilization
CER	Ceramide, N-acyl-sphingosine	jGCT(s)	Juvenile granulosa cell tumor(s)
CerS	Ceramide synthase	LDL-R	Low Density Lipoprotein Receptor
cFLIP	Cellular FLICE-like inhibitory protein	LGC(s)	Luteinized granulosa cell(s)
CG	Chorionic gonadotropin	LH	Luteinizing hormone
cIAP	Cellular inhibitor of apoptosis protein	LLC(s)	Large lutein cell(s)
CL	Corpus luteum	<i>M. mulatta</i>	<i>Macaca mulatta</i>
cm	Centimeter	MAPK	Mitogen-activated protein kinase
COS	Controlled ovarian stimulation	MLKL	Mixed lineage kinase domain-like pseudokinase
CYP11A1	Cytochrome P450 family 11 subfamily A member 1	mm	Millimeter
DAMP(s)	Damage-associated molecular pattern(s)	MOMP	Mitochondrial outer membrane permeabilization
DIABLO	Direct IAP-binding protein with low pI	mRNA	Messenger ribonucleic acid
DNA	Deoxyribonucleic acid	NCCD	Nomenclature Committee on Cell Death
DOI	Digital object identifier	Nec1	Necrostatin-1
e.g.	Exempli gratia	Nec1s	Necrostatin-1 stable isoform
E2	Estradiol	NF-κB	Nuclear factor kappa-B
ER	Endoplasmic reticulum	nm	Nanometer
et al.	Et aliae / et alii	No.	Number

Abbreviation	Full name	Abbreviation	Full name
NSA	Necrosulfonamide	SMPD1	Acid sphingomyelinase
OHSS	Ovarian hyperstimulation syndrome	Sph	Sphingosine
P4	Progesterone	StAR	Steroidogenic acute regulatory protein
PARP1	Poly (ADP-ribose) polymerase 1	TLR	Toll like receptor
PCD	Programmed cell death	TMA	Tissue micro array
PCR	Polymerase chain reaction	TNF α	Tumor necrosis factor alpha
PGF2 α	Prostaglandin F _{2a}	TNFRSF	Tumor necrosis factor receptor superfamily
PI3K	Phosphoinositide-3-Kinase	TRADD	TNFRSF1A-associated death domain protein
Q-VD-OPH	5-(2,6-difluorophenoxy)-3-[[3-methyl-2-(quinoline-2-carbonylamino)butanoyl]amino]-4-oxopentanoic acid	TRAF	TNF receptor associated factor
qRT-PCR	Quantitative RT-PCR	UB	Ubiquitin
RCD	Regulated cell death	UBA	Ubiquitin-associated domain
RHIM	RIP homotypic interaction motif	US	United States of America
RIG	Retinoic acid inducible gene	Vol.	Volume
RING	Really interesting new gene domain	vs.	Versus
RIP	Receptor interacting protein kinase	XIAP	X-linked inhibitor of apoptosis protein
ROS	Reactive oxygen species	Z-VAD-FMK	Methyl 5-fluoro-3-[2-[[3-methyl-2-(phenylmethoxycarbonylamino)-butanoyl]amino]propanoylamino]-4-oxopentanoate
RT	Reverse transcription	ZBP	Z-DNA Binding Protein
S1P	Sphingosine-1-phosphate	μ m	Micrometer
S357/T358	Amino acid number 357 is a serine and 358 is a threonine	2D	Two-dimensional
SEER	Surveillance, Epidemiology and End Results program	3 β -HSD	3 β -Hydroxysteroid dehydrogenase/ Δ^{5-4} isomerase
SK	Sphingosine kinase	3D	Three-dimensional
SM	Sphingomyelin	402C -> G	Cytosine to Guanine mutation at base number 402
SMAC	Second mitochondria-derived activator of caspases		

List of figures

Figure 1 Schematic illustration of the life history of one selected primordial follicle	3
Figure 2 Apoptosis mechanisms	11
Figure 3 Necroptosis and the sphingolipid metabolism	15
Figure 4 Sphingolipid building blocks	16
Figure 5 Graphical summary of publication 1 (Bagnjuk et al. 2019).....	24
Figure 6 Graphical summary of publication 2 (Du, Bagnjuk et al. 2018)	46
Figure 7 Graphical summary of publication 3 (Bagnjuk, Kast et al. 2019).....	56

Publications and contributions

Publication 1 (Bagnjuk et al., 2019)

Necroptosis in primate luteolysis: a role for ceramide

Konstantin Bagnjuk, Jan Bernd Stöckl, Thomas Fröhlich, Georg Josef Arnold, Rüdiger Behr, Ulrike Berg, Dieter Berg, Lars Kunz, Cecily Bishop, Jing Xu & Artur Mayerhofer
Cell Death Discovery, Vol. 5, No. 67, 2019, DOI: 10.1038/s41420-019-0149-7

A. Mayerhofer and L. Kunz conceived of this study. R. Behr provided sections of marmoset ovary. D. and U. Berg provided IVF-derived follicular fluid for cell extraction. K. Bagnjuk isolated cells from follicular fluid, conducted all cell culture experiments including immunocytochemistry, Western Blot and live cell imaging. JB Stöckl performed mass spectrometry measurements and analyzed the data. C. Bishop provided contributions to RT-PCR and transcriptomic analysis of microarray data and together with K. Bagnjuk she conducted the immunohistochemistry experiments. JB. Stöckl, K. Bagnjuk, A. Mayerhofer T. Fröhlich and GJ. Arnold collectively designed and interpreted the mass spectrometry experiments. GJ. Arnold and T. Fröhlich supervised the mass spectrometry approach. A. Mayerhofer, L. Kunz, J. Xu and K. Bagnjuk designed the experiments and interpreted the results. K. Bagnjuk wrote the manuscript under the supervision of A. Mayerhofer. L. Kunz and J. Xu corrected the manuscript. All co-authors helped to revise the manuscript and approved the final version to be submitted for publication.

Hereby we confirm the stated contributions to the mentioned publication (Publication 1).

Konstantin Bagnjuk

Prof. Dr. Artur Mayerhofer

PD Dr. Lars Kunz

Publication 2 (Du, Bagnjuk et al., 2018)

Acetylcholine and necroptosis are players in follicular development in primates

Yongrui Du*, Konstantin Bagnjuk*, Maralee S. Lawson, Jing Xu & Artur Mayerhofer

Scientific Reports, Vol. 8, No. 6166, 2018, DOI: 10.1038/s41598-018-24661-z

*co-first author

A. Mayerhofer conceived of this study and together with J. Xu they designed the experiments. Y. Du, K. Bagnjuk, J. Xu and A. Mayerhofer jointly supervised this work. Together with J. Xu and MS. Lawson, Y. Du conducted the follicle culture experiments and he analyzed and interpreted the gathered results. Y. Du drafted the manuscript. K. Bagnjuk performed the RT-PCR and immunohistochemistry experiments. Together with A. Mayerhofer he analyzed and interpreted the results. MS. Lawson provided contributions to immunohistochemistry. A. Mayerhofer, J. Xu and K. Bagnjuk revised the manuscript.

Hereby we confirm the stated contributions to the mentioned publication (Publication 2).

Konstantin Bagnjuk

Dr. Yongrui Du¹

Prof. Dr. Artur Mayerhofer

PD. Dr. Lars Kunz

Publication 3 (Bagnjuk, Kast et al., 2019)

Inhibitor of apoptosis proteins are potential targets for treatment of granulosa cell tumors – Implications from studies in KGN

Konstantin Bagnjuk*, Verena Jasmin Kast*, Astrid Tiefenbacher, Melanie Kaseder, Toshihiko Yanase, Alexander Burges, Lars Kunz, Doris Mayr, Artur Mayerhofer

Journal of Ovarian Research, Vol. 12, No. 76, 2019, DOI: 10.1186/s13048-019-0549-6

*co-first author

A. Mayerhofer, L. Kunz and D. Mayr conceived of the study and directed the work. T. Yanase provided KGN. A. Burges was the surgeon and he obtained the consent of the patients. D. Mayr provided the TMA. K. Bagnjuk designed the experiments and together with VJ. Kast he performed the cellular studies and evaluated the results. M. Kaseder performed qRT-PCR. K. Bagnjuk, VJ. Kast and A. Mayerhofer drafted the manuscript. A. Tiefenbacher performed immunohistochemical studies. All authors contributed to and agreed on the final manuscript.

Hereby we confirm the stated contributions to the mentioned publication (Publication 3).

Konstantin Bagnjuk

Verena Jasmin Kast

Prof. Dr. Artur Mayerhofer

PD. Dr. Lars Kunz

Summary

The ovary is one of the most dynamic organs in the human body, bearing resting, developing and dying follicles as well as the corpus luteum (CL). This is a temporary endocrine gland, which develops after ovulation, produces hormones (e.g. progesterone), but eventually regresses. Accordingly, controlled cell death events in ovarian follicles and the CL are inevitably for reproduction and, consequently, make life feasible. However, the underlying mechanisms of cell death in the human ovary mostly remain elusive.

One reason for this lack of knowledge is the poor accessibility of translational models. Human luteinized granulosa cells (LGCs) from patients undergoing *in vitro* fertilization (IVF) are assumed to offer a good model for the primate CL. LGCs produce progesterone during the first days of culture. Eventually, they lose this ability and die like their counterparts *in vivo*. While apoptosis represents one way for the CL to die, necroptosis – a form of programmed cell death (PCD) – was recently discovered in LGC culture as another possibility. The present work manifests necroptosis in the CL of humans, common marmosets (*Callithrix jacchus*) and rhesus macaques (*Macaca mulatta*) *in situ*. In the latter it was only evident in the late stages, suggesting necroptosis during luteal regression. Resemblance of transcriptomic and proteomic data of *in vivo* derived monkey CL and *in vitro* cultured human LGCs, confirmed these cells as a suitable model. Interestingly, both datasets demonstrated coherent upregulation of the ceramide (CER, *N*-acyl-sphingosine) salvage pathway over culture and in the late CL. Recently, CER was shown to induce necroptosis in other cellular systems. Consistently, the addition of a synthetic analog of this lipid to the LGC culture led to elevated signs of necroptosis in the present study. Furthermore, the pharmacological reduction of the cellular CER content indicated the opposite effect by improving LGC viability.

In contrast to follicular granulosa cells (GCs) *in vivo*, isolated LGCs do not proliferate in culture. Subsequently, these cells are inappropriate to study necroptosis during follicle development. 3D-cultured monkey follicles are well suited to discover mechanisms in dividing follicular GCs. With the present work, necroptosis was verified in this system and blocking the aforementioned type of PCD was shown to improve follicular growth. Further exploring in this setting, the trophic action of acetylcholine was confirmed, which represents a substantial local signaling factor within the ovary.

During follicular development, many follicles grow but only one becomes mature. The other follicles eventually become atretic and perish. In some rare settings, the cell death events involved are evaded by degenerated GCs. A consequence can be the development of granulosa cell tumors (GCT), for which surgery has so far been the only effective treatment method. The idea to “trick” the endogenous inhibitor of apoptosis proteins (IAPs) by analogs of the second mitochondria-derived activator of caspases (SMAC) yields new treatment options. In the present work, heterogenous expression of the IAP machinery in GCTs and a model cell line (KGN) was confirmed and apoptosis was successfully induced by the SMAC mimetic BV6 in this cell line.

Collectively, the data suggest necroptosis as a physiological event during follicular development, as well as in luteal regression, and link the latter to the CER salvage pathway. Further, a proof of concept that SMAC mimetics are capable to induce apoptosis in a GCT cell line is provided. In the future, these findings might help patients suffering from GCTs, improve IVF outcome by opposing luteal dysfunction or render targets for fertility control by affecting CL lifetime.

Zusammenfassung

Das Ovar ist eines der dynamischsten Organe im menschlichen Körper. Es enthält neben den ruhenden, wachsenden und sterbenden Follikeln auch das corpus luteum (CL). Dieses ist eine temporäre endokrine Drüse, die nach dem Eisprung entsteht, um Hormone (z.B. Progesteron) zu produzieren. Im Laufe des Zyklus bildet sich das CL jedoch wieder zurück. Demnach sind die kontrollierten Zelltodvorgänge, die die ovariellen Follikel und das CL regulieren, unausweichlich für die Fortpflanzung, die wiederum das Leben überhaupt erst möglich macht. Nichtsdestotrotz sind die Mechanismen, die im menschlichen Ovar für diese Vorgänge verantwortlich sind, weitestgehend unbekannt.

Ein Grund für diese Wissenslücke ist der Mangel an Modellen, die auf den Menschen übertragbar sind. Es wird angenommen, dass humane luteinisierte Granulosazellen (LGCs) von Patientinnen, die sich einer künstlichen Befruchtung (IVF) unterziehen, ein gutes Modell für das CL von Primaten darstellen. Während der ersten Tage in Kultur produzieren LGCs Progesteron, schließlich verlieren sie diese Fähigkeit jedoch und sterben, genau wie ihr Gegenstück *in vivo*. Während die Apoptose ein bereits bekannter Zelltodmechanismus im CL ist, kam vor kurzem mit der Entdeckung der Nekroptose – einer Form des programmierten Zelltods (PCD) – in der LGC Kultur eine weitere Möglichkeit auf. In der vorliegenden Arbeit konnte gezeigt werden, dass auch in den CL von Menschen, Weißbüschelaffen (*Callithrix jacchus*) und Rhesusaffen (*Macaca mulatta*) Nekroptose vorkommt. Bei der zuletzt genannten Spezies war diese Zelltodform nur im späten CL ersichtlich, was bedeuten könnte, dass Nekroptose eine Rolle während der Luteolyse spielt. Die Ähnlichkeit zwischen den Transkriptomdaten von *in vivo* gereiften Affen CL und den Proteomdaten von *in vitro* kultivierten LGCs bestätigte dabei die gute Übertragbarkeit des verwendeten Modellsystems. Interessanterweise war in beiden Datensätzen der Ceramid (CER, *N*-Acyl-Sphingosin) Recycling Signalweg sowohl über die Kulturzeit als auch im späten CL hochreguliert. Vor kurzem wurde in anderen zellulären Systemen gezeigt, dass CER Nekroptose auslöst. Damit übereinstimmend führte die Zugabe eines synthetischen Analogons dieses Lipids zur LGC Kultur in der vorliegenden Arbeit zu mehr Nekroptose. Im Gegensatz dazu verbesserte die pharmakologische Senkung des zellulären CER Spiegels die Vitalität der LGCs.

Anders als die folliculären Granulosazellen (GCs) *in vivo*, teilen sich isolierte LGCs nicht in Kultur. Aus diesem Grund ist dieses Modell ungeeignet, um die Nekroptose während der

Follikelentwicklung zu studieren. Im Gegensatz dazu stellen 3D kultivierte Affenfollikel ein passendes Modell dar, um die Mechanismen in sich teilenden, follikulären GCs zu verstehen. In der vorliegenden Arbeit konnte in diesem Modellsystem Nekroptose nachgewiesen werden und gleichzeitig gezeigt werden, dass das Blockieren dieses PCD zu verbessertem Follikelwachstum führt. Zusätzlich konnte die trophische Aktivität von Acetylcholin, einem wichtigen Signalfaktor im Ovar, bestätigt werden.

Während der Follikelentwicklung wachsen viele Follikel, jedoch reift nur ein einzelner zum Graafschen Follikel heran. Die anderen werden atretisch und sterben schließlich. In seltenen Fällen umgehen entartete GCs jedoch den damit verbundenen Zelltod, was dazu führen kann, dass sich ein Granulosazelltumor (GCT) entwickelt. Derzeit gilt die operative Entfernung des GCTs als die einzige kurative Behandlungsmaßnahme. Die Idee künstliche sekundäre mitochondriale Caspase-Aktivatoren (SMAC) einzusetzen, um endogene Apoptose-Inhibitor-Proteine (IAPs) „auszutricksen“, liefert neue Behandlungsmöglichkeiten. In der aktuellen Arbeit konnte gezeigt werden, dass die IAP-Maschinerie sowohl heterogen in GCTs als auch in einer Modellzelllinie (KGN) exprimiert wird und dass Apoptose in KGN durch das SMAC-Mimetikum BV6 ausgelöst werden kann.

Die vorliegende Arbeit legt den Schluss nahe, dass Nekroptose ein physiologisches Ereignis während der Follikelentwicklung und der Luteolyse ist und dass der zuletzt genannte Prozess in Verbindung mit dem CER-Signalweg steht. Zusätzlich wird der Machbarkeitsnachweis dafür geliefert, dass SMAC-Mimetika in der Lage sind, Apoptose in einer GCT-Zelllinie auszulösen. Zukünftig könnten diese Ergebnisse genutzt werden, um GCT-Patientinnen zu helfen, die IVF-Erfolgschancen durch die Bekämpfung der lutealen Dysfunktion zu erhöhen oder um neue Zielmoleküle für die Schwangerschaftsverhütung zu liefern, die die Lutealphase verkürzen.

1 Introduction

Right now, there are roughly 7,700,000,000 humans on our planet. The population will reach approximately 11 billion people in 2100, as projected by the United Nations in 2019 ¹. Even if all of us would drastically reduce our ecological footprint, earth capacity is assumed to reach its limit at a maximum of 10 billion people ². Consequently, overpopulation represents a threat, which this and emerging generations will have to face.

On the contrary, *in vitro* fertilization (IVF) has been developed to help people with an unfulfilled desire to have children. Although the first IVF baby was already born in 1978 ³, this technique still bears drawbacks, as success rates are low and the implicit hormonal treatment detrimentally affects women ^{4,5}. To contribute to a solution to the opposing problems of infertility and overpopulation, it is important to understand the biology of human reproduction.

Living organisms on our planet developed different ways of reproduction to maintain their species. Primates, including humans, reproduce biparentally. This form of propagation has evolved over time ⁶ and in contrast to asexual reproduction, it depends on two genetically different parents. For that purpose, nature developed two complex systems to produce, protect and mature the gametes, which make life feasible. In females, the ovaries facilitate this crucial task. Therefore, it is important to understand the mechanisms that govern this certain organ to conquer some of the threats of our time.

1.1 Life and death in the healthy primate ovary

To paraphrase reproduction, people would use words like creation, fecundity, pregnancy and life but not inflammation, self-destruction and cell death. Paradoxically it is exactly those latter words that provide the most accurate description of the prevailing mechanisms in the ovary. This complex biological system is the primary reproductive organ in women and comprises various structures that are dynamically altered to protect, develop and select the seed of life – the oocyte. Most of these processes are dominated by cell death events, which determine the fate of every single oocyte and decide whether pregnancy occurs or not. In the female embryo, a non-proliferating pool of gametes is formed and before birth, a significant proportion already

vanishes by self-destructive cell death. This “sorting-out” proceeds over the whole prepubertal as well as the reproductive life. Whereas in every menstrual cycle, ovulation and corpus luteum regression (luteolysis) come in addition, which represent events governed by inflammation and cell death (Fig. 1). Therefore in a healthy ovary, cell death events parallel normal development and function.

1.1.1 Follicle selection

Follicles are cellular conglomerates to preserve the largest and probably most precious cell in the human body – the oocyte (104 - 121 μm in the preovulatory follicle^{7,8}). The earliest form is the primordial follicle, which represents the resting pool of gametes in the ovary and consists of one oocyte and a layer of flat granulosa cells (GCs). Collectively they have an average diameter of 44 μm ^{9,10}. These follicles already start emerging 4 months after conception *in-utero*¹¹ and at this point, female embryos harbor around 7 million oocytes. Until birth, the majority (6 million) of this pool will vanish and by puberty, less than 400,000 follicles will survive^{12,13}. Within the reproductive life of a woman (around 36 years after menarche), only 0.007 % (around 500) of all produced oocytes will ever mature to a final stage and ovulate. The overwhelming majority (> 99.99 %) will degenerate and become atretic¹⁴. If atresia does not work properly, this can lead to some reproductive disorders including the polycystic ovarian syndrome and premature menopause, both of which go in front of infertility^{15,16}. Furthermore, compromised cell death mechanisms might lead to more severe diseases like cancer¹⁷. Together these facts indicate the importance of cell death during follicle selection in healthy women.

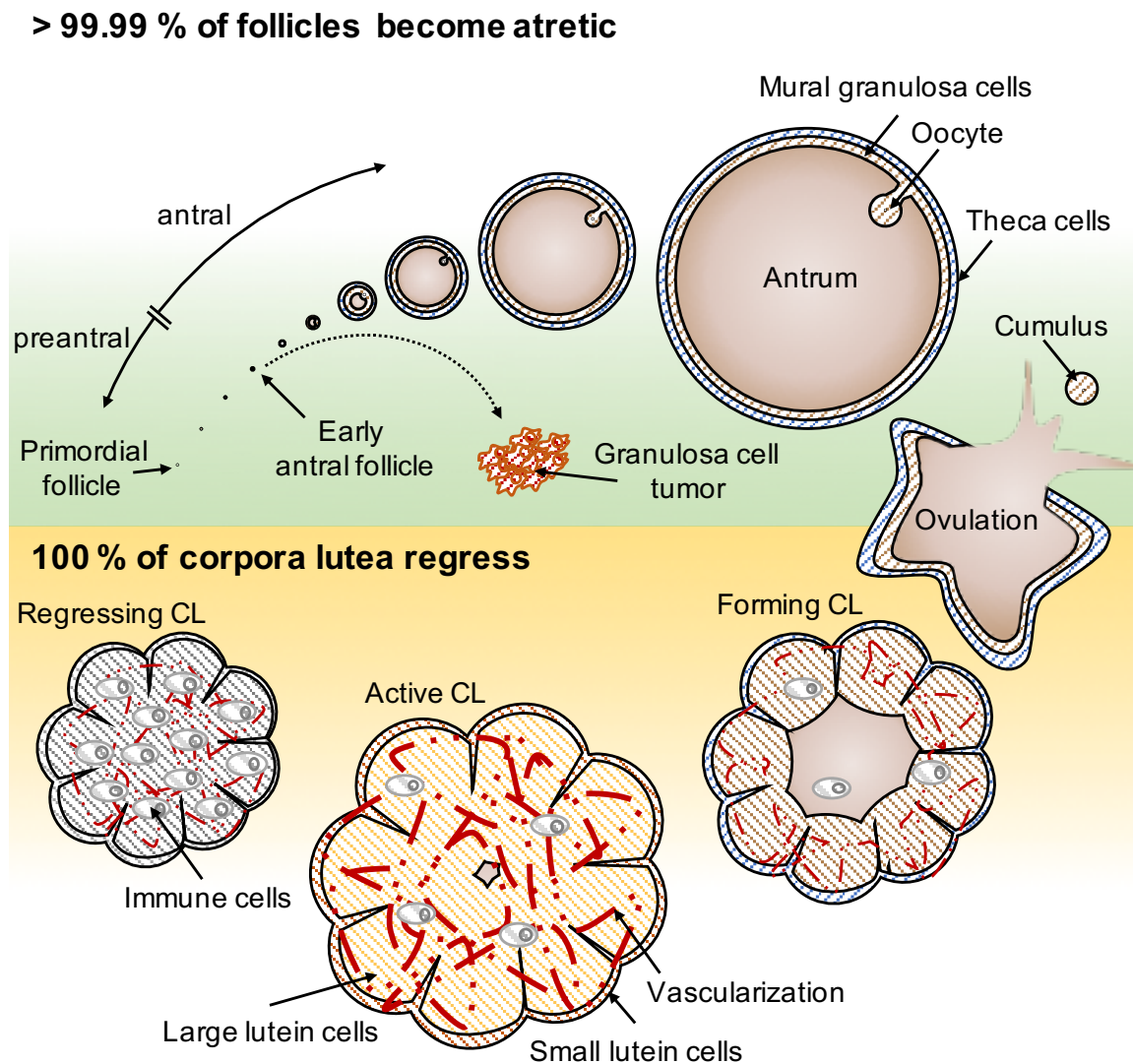


Figure 1 Schematic illustration of the life history of one selected primordial follicle

The green part describes the lifetime of one primordial follicle from left to right. The primordial follicle develops through preantral (gonadotropin-independent) and antral (gonadotropin-dependent) stages. Preantral stages include primordial, primary and secondary stages. In the early antral follicle, a cavity (antrum) is formed. Antral volume is strongly increased over follicular development. More than 99 % of all primordial follicles will never attain the preovulatory stage but become atretic and die. Granulosa cell tumors might develop during the follicular phase from proliferating granulosa cells (GCs). The cumulus consists of an oocyte that is surrounded by GCs. Mural GCs are encased by theca cells. Theca cells are not present in primordial and primary follicles and GCs change their shape from flat to cubical between these two stages. The preovulatory follicle is schematically depicted in 2x magnification (diameter = 4 cm; *in vivo* it is 2 cm). Ovulation and subsequently release of the cumulus into the fallopian tube separate the follicular from the luteal phase, whereas the latter is depicted in the orange part from right to left. Post-ovulation, in the forming corpus luteum (CL) the residual granulosa and theca cells differentiate into large and small lutein cells, respectively. Strong vascularization is a hallmark of a functioning, active CL. Immune cells can be observed in the CL in every stage, however, the amount strongly increases in the regressing CL. In this latter luteal stage the CL is endocrinologically inactive and its regression is governed by cell death events.

Follicular development occurs during the whole life of a woman and describes the morphological and cellular changes of the oocyte bearing structures (Fig. 1). It starts with the activation of a bulk of resting primordial follicles. The exact number of recruited follicles, however, depends on the remaining pool and subsequently alters over life. It has been proposed that a maximum of 900 follicles per month will change their state from resting to growing in a 14-year-old girl. On the contrary, in a 40-year-old woman, only 100 of these structures are recruited from the primordial pool¹⁸. With activation, GCs become cubical in the primary follicle stage and recruit a theca cell layer in the secondary stage. In the early antral stage, a follicular fluid (FF)-filled cavity (antrum) is formed^{19,20}. Beyond this point, growth becomes gonadotropin-dependent. The size drastically increases to reach a maximum of around 2 cm in the preovulatory follicle (Fig. 1 depicts a 2x magnification of the preovulatory follicle). This enlargement by over 40,000 % (vs. the primordial follicle (44 μm)) is primarily due to the increased FF volume and GC number⁹.

As stated above, only a marginal fraction of all follicles will ever reach this size. In the primordial stage, atresia leads to exclusion of low quality and DNA-damaged oocytes by apoptosis²¹. Although altered GC number has been hypothesized as a selection marker, it is very likely that the oocyte quality and grade of DNA damage are the driving forces in primordial follicle atresia²²⁻²⁵.

For the proliferative follicular stages, evidence is growing that GCs play the key role in defining follicular fate²⁶. Further it is thought that apoptosis is the predominant form of cell death²⁷. The preantral stages are regulated by factors GCs produce, e.g. inhibin²⁸, steroids²⁹ and anti-Muellerian hormone (AMH)³⁰. As indicated by genetic manipulation experiments in mice, these stages have been proposed to be gonadotropin (e.g. follicle stimulating hormone (FSH)) independent³¹. However, *in vitro* and *in vivo* studies in humans³²⁻³⁴ and primates^{35,36} led to the conclusion that FSH, in a concentration-dependent manner, is beneficial but not crucial for preantral follicle development. Besides apoptosis^{37,38}, autophagy³⁹ has been proposed as a form of cell death governing follicles at these stages. However, this still needs to be proven in primates including humans.

Nevertheless, it is unanimously accepted that antral follicle growth is FSH-dependent and predominantly occurs during the reproductive life, which is governed by the complex hormone profile of the menstrual cycle²⁶ that can be measured in the bloodstream⁴⁰. These endocrine

changes are a result of the crosstalk between the hypothalamus, the pituitary gland and the ovary⁴¹. In the latter organ, FSH fulfils a critical role. Upon binding to the corresponding FSH-receptor (FSHR)⁴², expression of which is a determinant for follicle survival or death⁴³, FSH leads to estradiol (E2) production⁴⁴ and selection of the dominant follicle⁴⁵ through activation of protein kinase A and the subsequent pathways⁴⁶. Additionally, produced E2 is able to directly block apoptosis^{47,48}. Although other regulators of atresia are known⁴⁹⁻⁵¹, the actions of FSH, FSHR, E2 and apoptosis are thought to explain follicle development and atresia in the antral stages.

1.1.2 Luteal phase

The follicular phase is followed by ovulation and the luteal phase. During ovulation, the oocyte and the directly surrounding GCs (cumulus cells) leave the follicle and move into the fallopian tube. The residual cells (mural GCs and theca cells) form a structure that is crucial for fertility - the corpus luteum (CL) (Fig. 1). The factor that enables the differentiation from granulosa to large lutein cells (LLCs) and from theca to small lutein cells is a hormone that peaks just prior to ovulation and is named after its mode of action, luteinizing hormone (LH)⁵². During this metamorphosis-like process, GCs change their shape and enzymatic machinery⁵³, which allows them to produce progesterone (P4)⁵⁴. The key function of this steroid is to prepare the endometrium for implantation of a fertilized oocyte⁵⁵, but it also affects ovarian FSH levels and subsequently the next follicular wave. In a normal menstrual cycle, the CL stops producing P4 (functional luteolysis) and regresses structurally within 14 days post ovulation. If distorted, this process may also account for luteal phase defects. For fertility, it is crucial that the setup and depletion of the CL occur in a time-dependent (around 14 days) manner. If luteal phase is shortened or prolonged, embryo implantation and the subsequent follicular phase may be disturbed. Importance of the CL in pregnancy and *in vitro* fertilization became obvious⁵ when luteal dysfunction led to implantation failures and miscarriages, which could be rescued by P4 supplementation⁴. It is now known, that up to 40 % of all women amid their reproductive life (20 - 40 years) show luteal phase defects with irregular length⁵⁶. Luteal phase defects can lead to early pregnancy wastage post conception and result from premature luteolysis or disturbed CL formation. Each of these two malfunctions can be a consequence of compromised vascularization and gonadotropin defects⁵⁷. However, the underlying mechanisms from induction to execution of luteal regression in humans remain poorly understood.

1.2 Granulosa cell tumors – malignancies of the ovary

The latest evaluation of the Robert Koch Institute (<https://www.krebsdaten.de>) revealed, that 1 of 71 women in Germany will probably develop ovarian cancer during her lifetime, and in the US the Surveillance, Epidemiology and End Results (SEER) program of the National Cancer Institute (<http://seer.cancer.gov>) has estimated that around 22,530 women will be diagnosed with ovarian cancer in 2019.

It is often projected that approximately 5-8 % of these incidents can be traced back to ovarian sex cord and stromal tumors, among which granulosa cell tumors (GCTs) are the most common (90 %) types^{58,59}. Unfortunately, this estimation is based on a publication from 1992⁶⁰. A personal, yet unpublished statement of the Munich Cancer Registry (<https://www.tumorregister-muenchen.de/>) revealed that between 2008 and 2018, 2.36 % (5799) of all female inhabitants (2.46 million) of the Munich area have been diagnosed with ovarian cancer. However, only 2.41 % (140) of these patients have evidentially been diagnosed with a GCT.

The recurrent and advanced stage GCTs are associated with high mortality rates (up to 80 %). In clinics, unfortunately, the tendency is visible that treatment options for all ovarian cancers are tailored to the most common type (ovarian epithelial cancer, 90 %), which surely will not improve viability rates of GCT patients⁵⁹.

GCTs are classified into two groups, the adult (aGCT, 95 %) and the juvenile (jGCT, 5 %)⁶¹. This separation was initially established due to the frequency these forms appear in “young” and “old” patients. Normally, jGCTs emerge during the first 30 years of life (90 %), however in rare cases they have been found in elder patients⁶². On the other hand, aGCTs are most frequently found in 50 to 55-year-old patients, as only few cases being reported in young individuals⁶³. Nowadays, the grouping is also based on evaluation of a mutation in the *FOXL2* gene (402C→G; C134W) that exclusively is found in 97 % of all aGCTs^{64,65}. The size of aGCTs usually ranges between 5-15 cm and their solid (soft to firm) and yellowish colored tissue typically contains blood-filled cysts. Nevertheless, the tumor morphology can strongly vary between different GCT patients⁶¹.

GCTs derive from follicular GCs of unknown stage, however there is at least some evidence that they stem from early antral follicles ⁶⁶ (Fig. 1). Based on their origin and steroidogenic nature, these tumors express FSHR and produce various hormones, including E2 and inhibin ⁶⁷. They are often recognized by elevated pre-pubertal and post-menopausal E2 levels. AMH, which is strongly expressed by GCTs, can additionally be used as a diagnostic marker ⁵⁸.

Every day spontaneous mutations with the potential to lead to tumors occur in healthy organisms. However, a cellular quality control mechanism (apoptosis) will kill these malfunctioning cells. In some rare cases, cells evade this suicide mode to survive. If these error-prone cells manage it to pass the immune system unnoticed, a tumor is formed ⁶⁸. GCTs have been shown to follow this paradigm of cell death evasion ⁶⁹. To fight this rare cancer, it is important to understand the general mechanisms behind cell death, where GCTs accomplish to sustain natural suicide signals.

1.3 Understanding cell death

The term necrosis stems from the Greek language and means “mortification” or “killing”. In the past, all cell death forms were described by this single term and were perceived as coincidental events (accidental cell death, ACD). In 1842 Carl Vogt made a meaningful observation, which altered this view. He observed a reproducible event of “disappearing” cells, which accomplished tadpole development ⁷⁰. Although Vogt did not use this wording, his work described regulated cell death (RCD) for the first time.

In 1972 another biological hallmark was created by the definition of apoptosis ⁷¹. This cell death form exhibits typical morphological signs like cell shrinkage and membrane blebbing. The same key parameters were described by Schweichel and Merker, but the corresponding cell death form was named necrosis type 1 ⁷². Among necrosis type 1 (apoptosis), specific characteristics of necrosis type 2 and 3 were postulated by these authors. Based on the typical morphology and the current knowledge, type 2 necrosis can be referred to autophagy. However, type 3 necrosis retained its coincidental character over many years. And still, the scientific language epitomizes “necrosis” with unregulated, accidentally occurring cell death with typical morphological signs like ballooning and membrane leakage, as described by type 3 necrosis ⁷³.

Yet, in 2005 a regulated cell death form with morphological signs of necrosis (type 3) was discovered and termed necroptosis⁷⁴. With this determination, science again proved its ability to solve coincidence, as the so thought accidental occurring (type 3) necrosis was found to harbor an underlying mechanism. 2018 the Nomenclature Committee on Cell Death (NCCD) published their definitions of 12 forms of RCD next to ACD, which are distinguishable by their morphological, biochemical and functional characteristics⁷⁵. Apoptosis is already known to be a crucial mechanism within the ovary, especially during follicular development⁷⁶. However, whether the newly discovered forms of cell death exist in the primate ovary, remains to be evaluated.

1.3.1 Once upon a time there was apoptosis

Apoptosis is a RCD, known to play crucial roles in many physiological processes including ovarian function⁷⁶⁻⁷⁸. In general, apoptotic events are classified by the mode of activation, e.g. intrinsic (mitochondrial) or extrinsic (receptor-dependent) (Fig. 2). Both pathway variants will lead to exhibition of key characteristics, such as nuclear fragmentation (karyorrhexis), chromatin condensation (pyknosis) and formation of apoptotic bodies (blebbing) which allow for the differentiation of apoptosis from other forms of cell death^{72,75}.

The fundamental step of intrinsic apoptosis execution is the permeabilization of the outer mitochondrial membrane (MOM), which is tightly controlled⁷⁵ and enabled by members of the apoptosis regulator protein family (BCL2), namely BCL2 associated X protein (BAX), BCL2 antagonist/killer 1 (BAK) and BCL2 family ovarian killer protein (BOK)^{79,80}. Induced by various stimuli, including DNA damage⁸¹, reactive oxygen species (ROS)⁸², endoplasmic reticulum (ER) stress⁸³ and withdrawal of growth factors^{84,85}, MOM-pore formation is irreversibly executed. As a result, mitochondrial factors, such as cytochrome c⁸⁶ and second mitochondria-derived activator of caspases (SMAC)⁸⁷ are released into the cytosol (Fig. 2).

Apoptotic peptidase activating factor 1 (APAF1) binds cytochrome c and caspase 9 (CASP9) to form the apoptosome, which activates CASP9^{88,89}. Further downstream, this complex activates the effector caspases 3 and 7 (CASP3, CASP7) by cleavage⁹⁰. Subsequently these proteases cleave a variety of cellular proteins to induce cell death. Just as activation of CASP3

and CASP7 represent intermediate steps of apoptosis, cleavage of poly(ADP-ribose) polymerase 1 (PARP1) is recognized as a terminal step of apoptosis and therefore serves as a valid marker ⁹¹.

SMAC deprives inhibitor of apoptosis proteins (IAPs), like cellular inhibitor of apoptosis 1 and 2 (cIAP1, cIAP2, also known as BIRC2 and BIRC3, respectively) or X-linked inhibitor of apoptosis (XIAP, sometimes referred to as BIRC4), of their anti-apoptotic ability ⁹². Although well conserved within the family, IAPs execute different functions to block apoptosis. XIAP, for example, directly binds caspases to inhibit apoptosis ⁹³. cIAP1 and cIAP2 on the contrary do not directly inhibit caspases. However, they harbor E3 ubiquitin ligase domains, which enable them to ubiquitinate the receptor interacting protein kinase 1 (RIP1) and subsequently activate the canonical, pro-survival NF- κ B pathway ⁹⁴ (Fig. 2). Upon binding by SMAC, IAPs forfeit their abilities and eventually the non-canonical NF- κ B pathway and apoptosis are induced.

As the name adumbrates, extrinsic apoptosis principally relies on extracellular signals, which interact with specific receptors. These so-called death receptors include tumor necrosis factor receptor superfamily members (TNFRSF) and the Fas cell surface receptor (FAS, also known as CD95) ⁹⁵. After interaction of a ligand (e.g. TNF α , FASLG) with the respective death receptor, a signaling complex is formed to regulate the activity of initiator caspase 8 (CASP8) ⁹⁶. In TNF α -induced apoptosis, the adaptor protein TNFRSF1A-associated death domain protein (TRADD) acts as an anchor for TNF receptor associated factor 2 and 5 (TRAF2, TRAF5), cIAP1, cIAP2 and RIP1 ^{97,98} (Fig. 2). Within this complex (complex I), posttranslational modification status of RIP1 is of special interest, since polyubiquitinated RIP1 (facilitated by cIAP1 and cIAP2) enables cell survival and inflammatory pathways like mitogen-activated protein kinase (MAPK) and canonical NF- κ B pathways ⁹⁹⁻¹⁰¹. However, in the presence of endogenous SMAC or other IAP antagonists ¹⁰², cIAP1/2 are inhibited and RIP1 subsequently is de-ubiquitinated. Thus, the pro-survival pathways are terminated and initiator CASP8 is activated, which in turn will lead to the execution of CASP3 dependent apoptosis ⁷⁵. After CASP3/7 activation, intrinsic and extrinsic apoptosis are indistinguishable.

Extrinsic apoptosis **Intrinsic apoptosis** **Survival (NF-κB)**

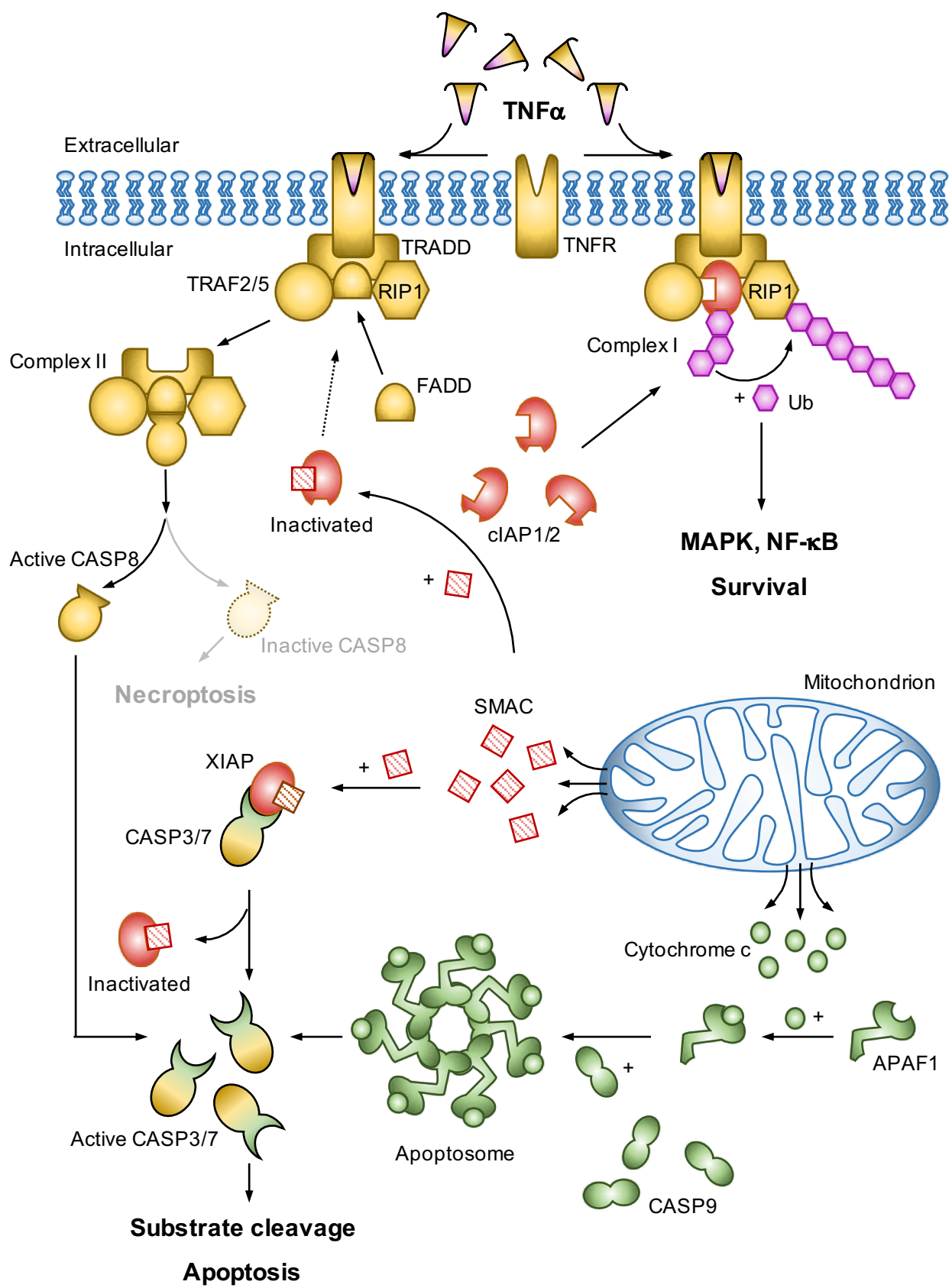


Figure 2 Apoptosis mechanisms

Schematic illustration of intrinsic and extrinsic apoptosis. Extrinsic apoptosis is exemplarily illustrated for the actions of TNF α . The color code distinguishes between the three alternate pathways, extrinsic apoptosis (yellow), intrinsic apoptosis (green) and survival (purple). Molecules that are shared by more than one pathway, e.g. CASP3/7, are multicolored appropriately. SMAC and IAPs are highlighted in red as they play key roles in regulating all three pathways. cIAP1/2 act as molecular switches between death and survival. Upon TNF α ligation and in the presence of these molecules, RIP1 is polyubiquitinated and the pro-survival pathways (NF- κ B and MAPK) are activated. In the absence of cIAP1/2 activity, complex II is formed. It consists of TNFR, TRADD, FADD, RIP1 and TRAF2/5. CASP8 can be recruited via FADD, which in turn will enable activation of this peptidase. Active CASP8 is able to cleave and subsequently activate CASP3 and CASP7. These two so-called executioner caspases cleave cellular substrates and induce cell death. CASP3/7 can be inactivated by XIAP, which in turn can be inactivated by SMAC that is released from mitochondria during intrinsic apoptosis. Cellular stress and other factors induce permeabilization of the mitochondrial membrane that leads to the release of cytochrome c and SMAC into the cytosol. SMAC acts on IAPs, whereas cytochrome c interacts with APAF1 and CASP9 to form the apoptosome. This complex enables CASP9 peptidase activity, which subsequently activates CASP3 and CASP7. From this point onwards, extrinsic and intrinsic apoptosis are indistinguishable. Abbreviations: TNF α = tumor necrosis factor α ; TNFR = TNF receptor (TNFRSF1A); TRADD = TNFRSF1A associated via death domain; TRAF = TNF receptor associated factor; RIP1 = receptor interacting protein kinase 1; FADD = Fas associated via death domain; CASP = caspase; cIAP = cellular inhibitor of apoptosis protein; XIAP = X-linked inhibitor of apoptosis protein; Ub = Ubiquitin; MAPK = mitogen-activated protein kinase pathway; NF- κ B = nuclear factor κ B pathway; APAF1 = apoptotic peptidase activating factor 1.

1.3.1.1 SMAC as a role model

One goal all organisms aim for is to stay alive. Tumor cells brought this to perfection by actively evading apoptosis¹⁰³. Among other features they facilitate this by upregulation of IAPs¹⁰⁴⁻¹⁰⁷, which are present in all cells to regulate the equilibrium between apoptosis and survival. In humans, 8 members belong to this family (genes: *BIRC1-8*). The structural characteristic that is shared by all of these proteins is a zinc-binding domain, namely baculoviral IAP repeat domain (BIR)¹⁰⁸, which facilitates protein-protein interactions. Prominent members of this family are the human *BIRC2*, *BIRC3* and *BIRC4*. The translated products are often referred to as cIAP1, cIAP2 and XIAP, respectively. Each of these proteins contains three BIR domains¹⁰⁹, one ubiquitin-associated domain (UBA)¹¹⁰ and one really interesting new gene domain (RING)¹¹¹. Additionally, cIAP1 and 2 harbor a caspase recruitment domain (CARD)¹¹². By their ability to bind and ubiquitinate key substrates within various cellular properties, including cell migration¹¹³⁻¹¹⁵, extracellular matrix modelling¹¹⁶ or tumor progression¹¹⁷ IAPs are able to influence these.

However, their main function is to regulate the fate of cells. For this cIAP1, cIAP2 and XIAP all bind caspases¹¹⁸, but XIAP is the only IAP that directly inhibits these peptidases^{93,119,120}. cIAP1 and cIAP2 control caspases by ubiquitination^{120,121}, an ability that also affects several other pathways, e.g. NF- κ B¹²²⁻¹²⁵ (Fig. 2), mitogen activated protein kinase (MAPK)¹²⁶ and PI3K/AKT pathway¹²⁷.

This impact on cell death or survival and the fact that cIAP1/2 and XIAP are upregulated in many tumors makes them promising targets in cancer therapy^{67,128-130}. To develop appropriate therapeutics, the trick is to imitate nature as evolution already created a tool to inactivate IAPs, namely SMAC or its rodent homolog direct IAP-binding protein with low pI (DIABLO). Mechanistically, SMAC is released from mitochondria upon membrane permeabilization (Fig. 2). Subsequently it inactivates IAPs by binding the BIR domains with its N-terminus. Four amino acids (AA) (Alanin-Valin-Prolin-Isoleucin) are crucial for this purpose^{109,131}. Based on this knowledge, small molecules, so-called SMAC mimetics have been developed to mimic these four AA. There are various of these compounds in preclinical and clinical (phase 1 and 2) trials, showing promising results, as summarized by Owens et al.¹³². In GCTs however, the expression of IAPs and effects of SMAC mimetics are poorly understood⁶⁷.

1.3.2 Necroptosis is programmed necrosis

In scientific parlance the term necrosis describes an accidentally occurring cell death (ACD). Paradoxically, the 2005 discovered necroptosis is named after this randomly occurring cell death but is tightly regulated through specific pathways^{74,75}. It is now well accepted that various stimulants are able to induce necroptosis through death receptors (TNFRSF1A, CD95)¹³³, toll like receptors (TLR3, TLR4)¹³⁴, nucleic acid sensors (Z-DNA binding protein, ZBP1)¹³⁵, retinoic acid responders (retinoic acid inducible gene 1, RIG1)¹³⁶ and adhesion receptors (e.g. CD44)¹³⁷. However, in most settings necroptosis was only inducible, if apoptosis-related proteins such as CASP8 are blocked or totally retrieved from the system¹³⁸ (Fig. 3). Within the signaling pathways that govern necroptosis or apoptosis, there are molecular switch proteins, like CASP8, which regulate the outcome of a receptor-ligand association, as the same interaction (e.g. TNFRSF1A with TNF α) sometimes exhibits a range of effects, from survival over inflammation to cell death.

TNF α -induced necroptosis is a well described pathway that is evidentially interlinked with apoptosis and cell survival (Fig. 3). Herein several molecules, including RIP1 and CASP8, act as molecular switch proteins to change the pathway outcome from survival to cell death¹³⁹. Post-translational modifications, including ubiquitination and phosphorylation, play a crucial role in this context, as stated above and summarized by Tang et al.⁷³. Upon TNF α ligation one of three processes can follow. First, in the presence of IAPs, the pro-survival NF- κ B pathway will be executed. If these proteins are not available or inhibited, the CASP8-dependent death pathway branch can be activated (Fig. 2), which leads to extrinsic apoptosis induction. In the third scenario, CASP8 is inactivated through specific proteins like cellular FLICE-like inhibitory protein (cFLIP)¹⁴⁰ or caspase inhibitors like Z-VAD-FMK and Q-VD-OPH¹⁴¹, which in turn might lead to necroptosis.

This third branch in TNF α -signaling relies on RIP1 and receptor interacting protein kinase 3 (RIP3) kinase activities^{142,143}. As RIP1 and RIP3, both harbor a RIP homotypic interaction motif (RHIM)¹⁴⁴, they can interact with each other. Upon phosphorylation of RIP1 and RIP3, the formation of the necrosome is enabled^{145,146}, which facilitates recruitment of mixed lineage kinase domain-like pseudokinase (MLKL)^{147,148} (Fig. 3). Although RIP1 seems to be crucial in TNF α -signaling, there is also evidence for necroptotic pathways where RIP1 is dispensable (e.g. TLR-dependent necroptosis in macrophages¹³⁴ and virus-dependent necroptosis in mice^{135,149}). Within the necrosome, RIP3 phosphorylates MLKL at S357/T358, which subsequently is able to oligomerize to tetra- and octamers¹⁵⁰. This process has been shown to depend on the chaperone heat shock protein 90 α family class A member 1 (HSP90AA1)¹⁵¹ and phosphatidylinositol^{152,153}. Oligomerized MLKL induces membrane permeabilization by forming channels or pores with a diameter of 4 nm^{150,154,155}. Interestingly, rodent and primate MLKL are utterly different from each other. Mouse MLKL does not oligomerize to tetramers¹⁵⁰, is phosphorylated at a different residue and it is not sensitive to necrosulfonamide (NSA), a potent necroptosis blocker in human cells¹⁴⁷.

Taken together, this cell death form exhibits morphological signs of type 3 necrosis⁷² and strongly depends on MLKL and RIP kinases. Although it has been discovered in 2005, there are only few evidences for this cell death form to occur in the primate ovary, as species differences between humans and rodents are present. However, recent findings in cellular and histological studies might hint to a physiological necessity of necroptosis in GCs^{156,157}.

Necroptosis

Ceramide pathway

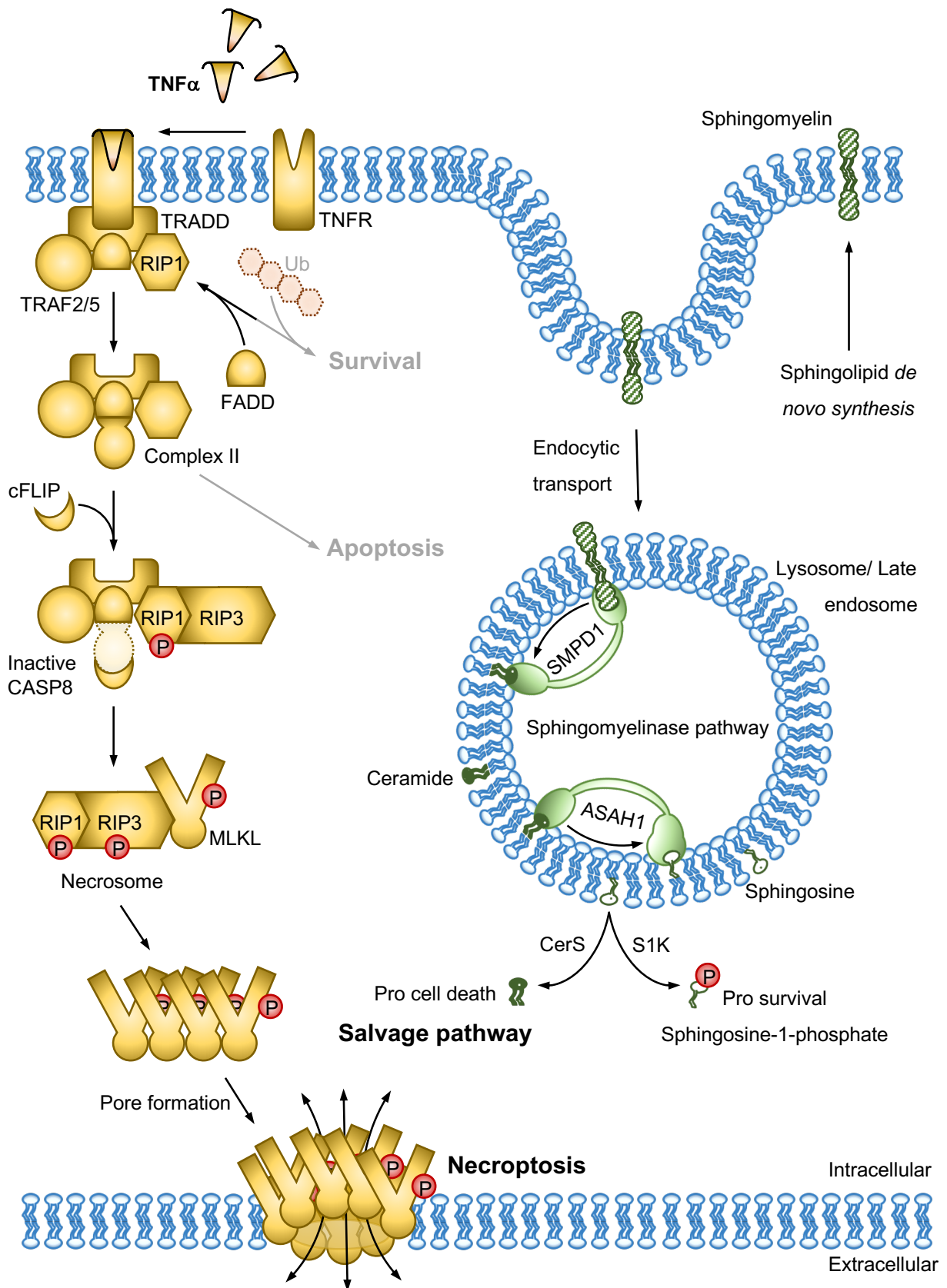


Figure 3 Necroptosis and the sphingolipid metabolism

Necroptosis (yellow) and the sphingolipid metabolism (green) represent two pathways that might be interlinked. Yet, there is not much evidence for such a hypothesis. The cell death pathway is schematically depicted as a consequence of TNF α ligation. Upon interaction between ligand and receptor and in the absence of polyubiquitinated RIP1 the “death” complex II is formed, which activates CASP8-dependent apoptosis. However, if CASP8 is inhibited (e.g. by cFLIP) RIP1 is phosphorylated, which induces recruitment of RIP3. Together with MLKL these three proteins form the necrosome. Within the necrosome RIP3 and MLKL are phosphorylated, which facilitates MLKL oligomerization (tetramers and octamers in humans), membrane permeabilization and subsequently necroptosis. The sphingolipid metabolism can be described by three independent pathways. A simplified sphingolipid metabolism is depicted by green key molecules. *De novo* sphingolipid synthesis utilizes sphingosine and palmitate and the subsequent metabolites to generate the storage form sphingomyelin. Sphingomyelin can be transported via membranes and through endocytic transport. Within an acidic compartment like a late endosome or lysosome the storage form can be metabolized to ceramide (sphingomyelinase pathway). This step is facilitated by the acid sphingomyelinase (SMPD1). The acid ceramidase (ASAH1) degrades ceramide to sphingosine, which is a more soluble form that can exit membranes and enter the cytosol. Sphingosine can be phosphorylated to sphingosine-1-phosphate by the sphingosine-1 kinase (S1K) or utilized in the salvage pathway to generate ceramide via a ceramide synthase (CerS). These two metabolites possess opposite functions. Ceramide is known to induce cell death and sphingosine-1-phosphate preferably supports survival.

1.3.2.1 Sphingolipids regulate cell fate

Sphingolipids are bioactive lipids, found in all eukaryotic organisms and consist of a sphingosine (Sph) backbone, which can be linked to any fatty acid through an amid bond¹⁵⁸. The headgroup, linked to the primary hydroxyl group of the Sph backbone further increases complexity in sphingolipids¹⁵⁹ (Fig. 4). Based on the marked difference that results from these three building blocks, it is apparent that sphingolipids offer infinite possibilities for functions. Indeed, it has been shown that members of this class affect the cytoskeleton, endocytosis, cell cycle, senescence, cell migration, inflammation, survival and cell death¹⁶⁰⁻¹⁶³.

The central molecule of the sphingolipid metabolism is ceramide (CER; *N*-acyl-sphingosine, Fig. 4)¹⁶⁴, which can be generated by *de novo* synthesis, breakdown of sphingomyelin or the salvage pathway (Fig. 3).

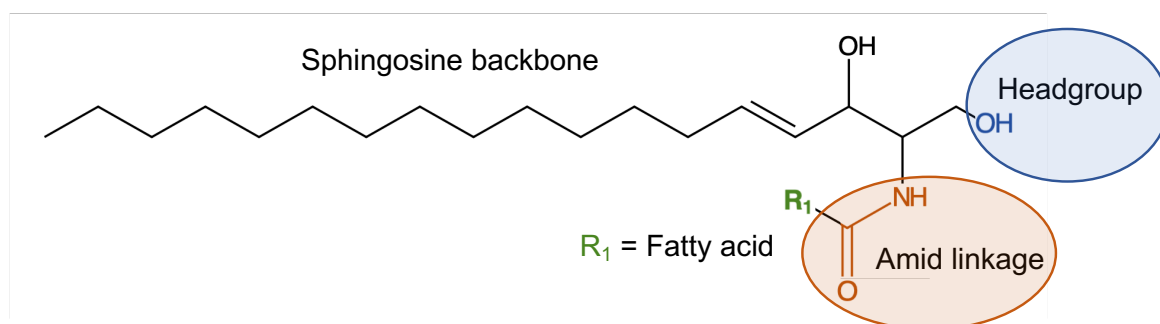


Figure 4 Sphingolipid building blocks

Sphingosine is a molecule with 18 C atoms and a polar hydroxyl headgroup (blue). It can be linked to a fatty acid of varying acyl chain length (R_1 , *N*-acyl, green) by an amid linkage (orange) to form a ceramide (*N*-acyl-sphingosine). The hydroxyl group can be substituted by a variety of molecules to form complex sphingolipids (e.g. phosphocholine in sphingomyelin, one or more sugar residues in a glycosphingolipid).

In short, *de novo* synthesis starts with fusion of serine and palmitate to 3-keto-dihydrosphingosine by the serine palmitoyl transferase¹⁶⁵. After reduction and subsequent acylation by a ceramide synthase (CerS) and further processing by a desaturase, ceramide is formed^{166,167}. This central molecule can act as a signaling molecule or be further processed by phosphorylation (ceramide kinase)¹⁶⁸ or glycosylation (glycosyl-/galactosyl ceramide synthases)¹⁶⁹. Furthermore, CER can be degraded to Sph by acid or neutral ceramidases or processed to sphingomyelin (SM) by sphingomyelin synthases¹⁷⁰. SM acts as a storage form of CER and can be broken down to this bioactive lipid by sphingomyelinases (acid (SMPD1), neutral and alkaline) upon induction^{171,172}. Sph is based on its amphipathic nature, is soluble in aqueous solutions (30 % in cytosol) and organic solvents (70 % in membranes) and is, therefore, recognized as a transportation form of insoluble sphingolipids¹⁷³. This molecule can be phosphorylated to sphingosine-1-phosphate (S1P) by sphingosine kinases¹⁷⁴, or be further degraded by the sphingosine-1-phosphate lyase to ethanolamine-phosphate and hexadecenal to subsequently exit the sphingolipid metabolism¹⁷⁵. Another possibility for Sph conversion is the salvage pathway, which basically represents a recycling process to re-generate CER¹⁷⁶ (Fig. 3). This pathway starts with the degradation of SM or other complex sphingolipids within acidic compartments, namely late endosomes and lysosomes, to generate Sph that is transported to a CerS containing compartment. The CER, which results from the Sph conversion, can act as a signaling molecule or be used for the regeneration of more complex sphingolipids. Interestingly, the salvage pathway was estimated to account for 50 – 90 % of the sphingolipid biosynthesis, as it offers a more efficient energy balance compared to *de novo* synthesis¹⁷⁶⁻¹⁷⁸.

Most sphingolipids are ubiquitously present in lipid membranes. However, there is clear evidence that *de novo* production of CER is restricted to the endoplasmic reticulum, from where it gets transported to the Golgi apparatus to be processed to SM, which in turn is transported through vesicles to any other membrane. SM degradation predominantly occurs in lysosomes or the plasma membrane¹⁷⁹. Interestingly, in most organisms the cellular contents of the storage form (SM), CER, S1P and the transportation form (Sph) strikingly differ. For example, 10 times more SM is present in cells compared to CER, which in turn is an order of magnitude more concentrated than Sph¹⁸⁰ and S1P is rarely found. Therefore, slightly manipulated activity and expression of enzymes, such as sphingomyelinases (e.g. acid; SMPD1), ceramidases (e.g. acid; ASAH1) or sphingosine kinases (SK1 or SK2) tremendously affect the levels of their products and subsequently their effects.

A special interest lies in CER and S1P as these molecules have multiple times been shown to influence cell fate based on their ratio¹⁸¹. It has consistently been shown that S1P- and CER-effects oppose each other¹⁸². Lysosomal CER, for example, has been shown to activate cathepsin D and therefore was linked to TNF α - and mitochondria-dependent apoptosis¹⁸³. Furthermore, CER was shown to activate protein kinase C ζ and apoptosis in stem cells¹⁸⁴. Another group has implicated the involvement of SMPD1 activity and subsequently CER production in tumor cell stress response and apoptosis upon radiation therapy¹⁸⁵. General importance of this protein and its metabolites was supported by experiments in mouse oocytes, showing that disruption of the gene encoding SMPD1 (*smpd1*), or exogenous addition of S1P rescues these cells¹⁸⁶. A mechanistic link of CER to mitochondria was proposed by the effects of sphingolipids in intrinsic apoptosis (HeLa and mouse cells)¹⁸⁷. Indeed, it was demonstrated that CER forms channels in the outer mitochondrial membranes^{158,188}. The feature of CER to induce cell death in various cell types and species is currently tried to be utilized by scientists in ovarian cancer¹⁸⁹ and other tumors^{182,190}.

Over time, more evidence has accumulated that CER plays a role in both, apoptosis and necroptosis. For example, CER was shown to induce necroptosis in trophoblasts during preeclampsia¹⁹¹ and in monocytic like cells¹⁹². Mechanistically, CER accumulation was shown to occur downstream of RIP1 activation during necroptosis¹⁹³. RIP1 dependency was further confirmed by CER associated pore formation in lung cancer cells¹⁹⁴.

In the ovary, CER was shown to induce cell death in cultured GCs and CL of mice ^{195,196}, GCs of hen ^{197,198}, antral follicles and CL of cattle ^{199,200}, GCs and lutein cells of rat ²⁰¹⁻²⁰⁴ and in human GCs ^{205,206}. Nevertheless, most of the studies were conducted before alternate cell death forms like necroptosis were discovered. Thus, some of the above-cited work insufficiently distinguished between cell death forms and may falsely have concluded to apoptosis.

Taken together, CER has been shown to induce cell death, including apoptosis and necroptosis, in various systems. However, it still needs to be elucidated, how the impact of CER on human ovarian physiology has to be interpreted.

1.4 Humans are not mice

Research on human physiology remains a challenging task, as most experiments cannot be executed on human individuals. Scientists, therefore, developed an inventory of models and used experimental organisms to overcome this limitation, though some drawbacks have to be considered. Leonelli and Ankeny distinguished between model and experimental organisms ²⁰⁷, whereas the latter ones were defined as species that are studied but do not necessarily represent other species. However, they render deep insights into specific interesting phenomena or characteristics of the studied species. Contrary to this, model organisms are studied for translational insights into more complex organisms. Accordingly to these two scientists model organisms are: “... *non-human species that are extensively studied in order to understand a range of biological phenomena, with the hope that data, models and theories generated will be applicable to other organisms, particularly those that are in some way more complex than the original.*” ²⁰⁷.

Next to non-mammalian models (e.g. *Saccharomyces cerevisiae*, *Drosophila melanogaster*, *Caenorhabditis elegans*) there are two mammalian species recognized by the National Institutes of Health Center for Scientific Review (<https://public.csr.nih.gov>) as traditional model organisms - the laboratory mouse (*Mus musculus*) and rat (*Rattus norvegicus domestica*). Some of the fundamental advantages of model organisms are the low costs for animal husbandry, the short generation times, the numerous tools that have been developed over time to genetically manipulate these animals and of course the physical animal size, which makes work easier.

Nevertheless, the benefits come at an expense of significant drawbacks. Scientists argue that studying a handful of well characterized organisms, whilst neglecting other species might drive the academic ecology into a wrong direction ²⁰⁸ by supporting the idea that every conclusion from a model experiment must generally be true for all the other species ²⁰⁹. Unfortunately, the underlying differences between human biology and rodent biology are not respected in a way they should and therefore, inappropriate conclusions are done too often. Mark M. Davis, a highly renowned professor from Stanford University summarized that the mouse is an unsuccessful and poorly translational model for clinical questions regarding human immunity ²¹⁰. This opinion is shared by other researches in a variety of diseases ²¹¹⁻²¹³. Nevertheless, without the experiments in mice, rats and all the other model organisms, scientists never would have accumulated so much knowledge about the fundamental mechanisms in biology. Based on the pros and cons of model organisms, it can be concluded that it wise to utilize these systems to resolve general questions. However, it is doubtful to draw conclusions towards human physiology or pathology, as any gathered hypotheses from mouse experiments need to be proven right in humans or more related systems, like non-human primates. In some research areas like development ²⁰⁹, neurodegeneration ^{211,212} or environmental impact ²¹⁴, it has been shown that the used model organisms do not mirror the situation in humans. In such cases it is advisable to investigate the suitability of an experimental organism.

1.4.1 Experimental organisms for the human ovary

For research purposes on the physiology of the human ovary and probably all other human organs ²¹⁵, non-human primates represent the best suited experimental organisms as evolutionary proximity is much closer compared to rodents ^{216,217}. The latest shared ancestor of humans and mice was on earth around 90 million years ago ²¹⁸. For primates like the New World monkey *C. jacchus* the differential evolution begins around 45 million years ago and for the Old World monkey *M. mulatta* the proximity is even closer with around 30 million years ²¹⁷.

In the ovary obvious differences between rodents and primates concern cycle length (1 month in humans vs. 1 week in rodents) ²¹⁹, offspring number (1 in humans vs. 8 in rodents) ^{220,221}, menses (present in humans but absent in rodents) ²²², gestation length (40 weeks in humans vs. 20 days in rodents) ²²³ and menopause, which is naturally absent in rodents due to the short

life time ^{224,225}. However, there are further discrepancies between these two taxa. E2 has a beneficial effect on primordial follicle development in primates *in-utero* ²²⁶, but exerts opposite effects in mice, where primordial follicle formation occurs *post-natal* ²²⁷. These hormonal differences are also indicated during the peaks of E2 and FSH, where rats, contrary to macaques show high FSH and low E2 levels ²²⁸. Next to the differences during follicular development (e.g. varying impact of E2) and ovulation ²²⁹, the luteal phases significantly differ between taxa ^{230,231}. In contrast to the ultra-short CL lifespan of rats and mice (24 h), primates exhibit a longer luteal phase (14 days). One reason for this discrepancy is the continual expression of inhibin in humans ²³², which downregulates FSH during the luteal phase. In rodents the preovulatory LH surge represses inhibin to facilitate the next follicular wave ²³³. Another big question mark remains on luteal regression in primates. This process is well understood in rats ²³¹ but remains elusive in primates to a large extent ²²⁸. In most species including rodents the uterus secretes prostaglandin F_{2α} (PGF2α) to induce luteolysis. In humans and primates, however, the uterus is dispensable for luteolysis ²³⁴. Another facet that encapsulates primates from the rest of the animal kingdom is the secretion and function of chorionic gonadotropin (CG) to rescue the CL in pregnancy ^{235,236}. Next to primates solely equines do secrete CG, however the function and time of secretion do differ from primate CG ²³⁷.

In respect of these profound differences, model organisms are good opportunities to understand general biological mechanisms. However, the human relevance of any mouse or rat experiment has to be proven in humans or at least in the most related experimental organisms - non-human primates. As studies in living animals are expensive, challenging and frequently meet ethical concerns ²³⁸, cellular or organoid systems from hosts that resemble humans are developed to gain insights. One appropriate experimental system that is readily used in ovarian research is the three-dimensional (3D) culture of follicles, extracted from *in vivo*-developed *M. mulatta* ovaries ^{36,239}. This system offers the possibility to study follicular development *in vitro*, while rendering a deep insight into human physiology. To facilitate this, ovaries are surgically removed and follicles are extracted manually. Afterwards, the follicles can be embedded into an alginate hydrogel to mimic the firmness of the surrounding tissue *in vivo* ²⁴⁰. With this technique it is possible to study age or hormone dependent follicular development that is closely related to the physiological situation in humans ³⁵. Next to the basic research approach, this system might also help cancer patients in future. Nowadays young female cancer patients are offered to have their ovarian tissue be removed and stored before chemotherapy and re-implanted afterwards. This is done with the hope to fully mature a follicle *in vitro* in future to finally

facilitate IVF-dependent pregnancy in these patients ²⁴¹. Although we are quite far from this point yet, the non-human primate system renders the best possibility to understand human follicular development and to reach this aim.

1.4.2 Cellular models for the human ovary

As non-human primates are poorly accessible experimental organisms, it is advisable to employ a primary cellular system, originated from human tissue that resembles the organ of interest for first insights. For the ovary, a possibility was discovered with the invention of IVF ³: human IVF-derived luteinized granulosa cells (LGCs).

Within most IVF procedures the female patients undergo a controlled ovarian stimulation (COS), which aims for the development and maturation of multiple oocytes in one menstrual cycle ²⁴². Although numerous different COS protocols exist to establish this aim, they all include a dose of the so-called “pregnancy hormone” (human chorionic gonadotropin, hCG) to facilitate final follicle and oocyte maturation. ^{243,244} hCG is used in IVF for its chemical similarity to LH. Both of these proteins bind the same receptor (LH receptor) and lead to similar consequences, but to a varying extent ^{245,246}. After COS is realized, oocytes are retrieved by follicle punctuation. To assure that the oocyte is aspirated, all follicular fluid (Fig. 1) is retrieved. During this process, some of the mural GCs are taken along. These cells can be isolated from the follicular fluid and cultivated. Due to the stimulation protocol and especially the final hCG dose, GCs luteinize in culture and subsequently become LGCs, which resemble LLCs of the human CL ²⁴⁷. This can be verified by the presence of progesterone in the LGC culture medium, which follicular GCs are incapable of producing ²⁴⁷. Isolation of LGCs can be established by distinctive cellular characteristics (size of cell aggregates, cell density, adherence speed or epitope presentation (immune cells)) that discern these cells from the remaining contents (e.g. blood and immune cells) of the follicular fluid. Based on this, various methods have been invented to improve LGC isolation. The cell-strainer technique, built on the differences between LGC aggregate size and other cells (red and white blood cells, fibroblasts) yields the most reasonable compromise between purity, speed, simplicity and yield ^{248,249}.

Taken together, due to the lack of appropriate and conveniently accessible animal models, LGCs represent a well-suited cellular model to understand mechanisms of the human and

primate luteal phase. *In vivo*, the luteal phase is induced by a specific hormonal pattern (e.g. LH-surge), which IVF-derived LGCs also were exposed to. In culture, these cells express typical markers of LLCs (e.g. progesterone production), which makes them an adequate cellular model for this cell type. However, as it is a cellular model and cell culture effects might affect the outcomes, it is essential to verify the findings in primate studies.

1.4.2.1 Granulosa cell tumor cell lines

Granulosa cell tumors (GCTs) of the ovary are, as stated above, rare diseases. Thus, primary tissue from cancer patients is not readily accessible. Nevertheless, research on these tumors is necessary to help suffering patients and as a consequence, it is important to utilize any available system to better understand the genetic changes and molecular events of tumorigenesis and tumor proliferation²⁵⁰. Only a few scientists managed to cultivate primary GCT cells, however, a range of GCT-like cell lines have been developed over time. For most cases follicular GCs, isolated from mice, cattle, pigs, monkeys and humans were differentiated by oncogenic transformation, immortalization and radiation into GCT-like cell lines²⁵¹. Unfortunately, most of the available cell lines are from model species (mice) or lack the key characteristics of steroidogenesis and gonadotropin dependence. Next to these *in vitro* differentiated cell lines, there are three publicly available cell lines gathered from patient-derived GCTs (COV434 and KGN)²⁵²⁻²⁵⁴ or granulosa-theca cell tumors (HTOG)²⁵⁵. As the HTOG cell line does not produce steroids and does not respond to gonadotropins, the other two cell lines are more interesting to use for the research on GCTs of the ovary. KGN evolved as the predominant cell line in GCT research, although COV434 was established before²⁵¹. Next to the work that can be done in KGN or COV434, it is essential to use primary patient-derived tumor tissue to compare the outcomes from cellular studies with *in situ* material.

2 Aims and expectations

The present work was based on the findings from previous studies^{156,256,257} with a special interest in necroptosis, which was identified in the culture of human luteinized granulosa cells (LGCs) derived from *in vitro* fertilization (IVF). However, the mechanisms behind this cell death form in the human ovary and its physiological importance remained elusive. Furthermore, LGCs are a widely used model for the investigation of the human ovary. Yet, a broad characterization of these cells on the proteomic level has never been done until now. Another model for the human ovary are KGN cells, which are a granulosa cell tumor (GCT)-derived cell line that could provide insights into cell death mechanisms, which are poorly understood in this type of tumor.

- ⇒ To better understand cultured LGCs and their relevance to *in vivo* situations, a proteomic approach was designed. The key question was whether these cells resemble follicular granulosa cells (GCs) or large lutein cells (LLCs). Based on the hormonal stimulation protocols in IVF and the behavior of LGCs in culture, these cells were expected to be more related to LLCs.
- ⇒ To find a link between basally occurring necroptosis in LGC culture and physiological processes in the human ovary the proteomic data were analyzed and compared to *in vivo* data. This approach identified the ceramide (CER) salvage pathway as a candidate. In the ovary, the link between CER and necroptosis is not well established. Therefore, cellular studies were designed to evaluate the mechanistic coherence of these two pathways *in vitro*.
- ⇒ Contrary to LGCs, *in vitro* cultured primate follicles are a system for the research of follicular development, at least *in vitro*. As the impact of necroptosis on follicular development in primates was not elaborated yet, the present study was designed to address the question, if necroptosis is involved in *in vitro* follicle maturation. Further in this setting, the impact of acetylcholine on primate follicle development was tested to validate its trophic actions found before²⁵⁷.
- ⇒ Next to physiological processes, cell death mechanisms play a significant role in tumors. At the moment there are no treatment options for granulosa cell tumors (GCTs) besides surgery. Therefore, it was questioned on the cellular level, whether SMAC mimetics could offer a treatment possibility in the future and what the underlying mechanism would be.

3 Results

3.1 Publication 1 (Bagnjuk et al. 2019)

Necroptosis in primate luteolysis: a role for ceramide

Konstantin Bagnjuk, Jan Bernd Stöckl, Thomas Fröhlich, Georg Josef Arnold, Rüdiger Behr, Ulrike Berg, Dieter Berg, Lars Kunz, Cecily Bishop, Jing Xu & Artur Mayerhofer

Cell Death Discovery, Vol. 5, No. 67, 2019. DOI: 10.1038/s41420-019-0149-7

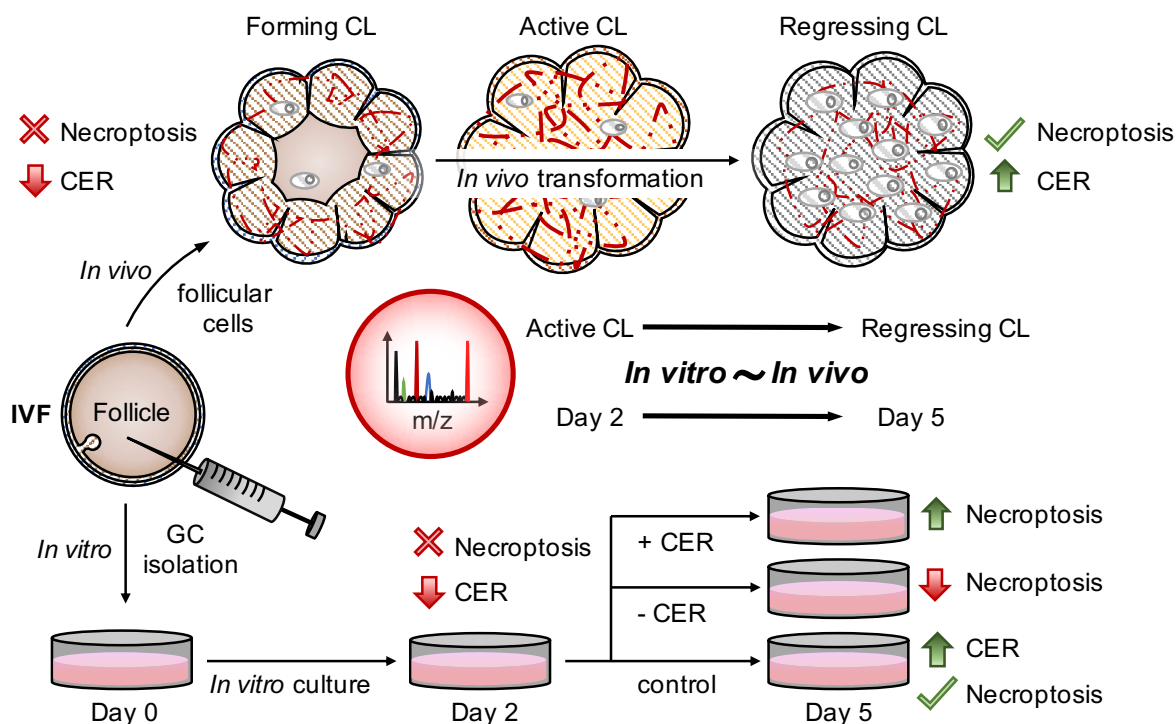


Figure 5 Graphical summary of publication 1 (Bagnjuk et al. 2019)

A proteomic analysis, symbolized by a mass spectrum in the red circle, of cultured LGCs (day 2 to day 5) revealed high similarity between the cell culture model and the regressing rhesus monkey CL *in vivo*. In the latter, signs for necroptosis became evident that were absent in earlier luteal stages. Additionally, the CER salvage pathway was upregulated at the mRNA level. *In vitro* culture of LGCs mimicked this situation, as results indicated necroptosis execution on day 5 of culture, which was absent at day 2 of culture. The CER salvage pathway was likewise upregulated at the protein level. Manipulation of cellular CER concentrations by blocking the CER synthase or by exogenous addition of CER led to reduced or elevated LGC cell death, respectively. (CER = ceramide; LGCs = luteinized granulosa cells)

ARTICLE

Open Access

Necroptosis in primate luteolysis: a role for ceramide

Konstantin Bagnjuk¹, Jan Bernd Stöckl², Thomas Fröhlich², Georg Josef Arnold², Rüdiger Behr³, Ulrike Berg⁴, Dieter Berg⁴, Lars Kunz⁵, Cecily Bishop⁶, Jing Xu⁶ and Artur Mayerhofer¹

Abstract

The corpus luteum (CL) is a transient endocrine organ, yet molecular mechanisms resulting in its demise are not well known. The presence of phosphorylated mixed lineage kinase domain-like pseudokinase pMLKL(T357/S358) in human and nonhuman primate CL samples (*Macaca mulatta* and *Callithrix jacchus*) implied that necroptosis of luteal cells may be involved. In *M. mulatta* CL, pMLKL positive staining became detectable only from the mid-late luteal phase onwards, pointing to necroptosis during regression of the CL. Cell death, including necroptosis, was previously observed in cultures of human luteal granulosa cells (GCs), an apt model for the study of the human CL. To explore mechanisms of necroptotic cell death in GCs during culture, we performed a proteomic analysis. The levels of 50 proteins were significantly altered after 5 days of culture. Interconnectivity analysis and immunocytochemistry implicated specifically the ceramide salvage pathway to be enhanced. *M. mulatta* CL transcriptome analysis indicated in vivo relevance. Perturbing endogenous ceramide generation by fumonisin B1 (FB1) and addition of soluble ceramide (C2-CER) yielded opposite actions on viability of GCs and therefore supported the significance of the ceramide pathway. Morphological changes indicated necrotic cell death in the C2-CER treated group. Studies with the pan caspase blocker zVAD-fmk or the necroptosis blocker necrosulfonamid (NSA) further supported that C2-CER induced necroptosis. Our data pinpoint necroptosis in a physiological process, namely CL regression. This raises the possibility that the primate CL could be rescued by pharmacological inhibition of necroptosis or by interaction with ceramide metabolism.

Introduction

The corpus luteum (CL) forms after ovulation. Upon the ovulatoryluteinizing hormone (LH) surge granulosa and theca cells differentiate into large and small luteal cells, stop dividing and produce progesterone^{1,2}. If conception occurs, chorionic gonadotropin (CG) stimulates survival of the CL and progesterone production. Otherwise the CL shuts down functionally and degenerates structurally.

Knowledge about the molecular events leading to functional and structural regression of the primate CL is limited. Low accessibility and significant differences in luteolytic events between primates and non-primate species may explain this lack of knowledge³. A fraction of the luteal cells undergo apoptosis in humans^{4,5}, and involvement of autophagocytosis was suggested^{6–8}. Both are immunologically silent events, yet other forms of cell death attract immune cells. Immune cells, for example, macrophages, appear to play an indispensable role in ovarian functions⁹ and CD11b positive macrophages invade the nonhuman primate CL during its regression and produce various cytokines and chemokines¹⁰.

Immune cell accumulation in the CL may be a consequence of necroptosis, a process recently suggested to occur in the regressing CL of cows¹¹. Necroptosis is a

Correspondence: Artur Mayerhofer (Mayerhofer@lrz.uni-muenchen.de)

¹Biomedical Center Munich (BMC), Cell Biology, Anatomy III, Ludwig-Maximilians-University (LMU), Grosshaderner Strasse 9, Planegg 82152, Germany

²Laboratory for Functional Genome Analysis LAFUGA, Gene Center, LMU, Feodor-Lynen Strasse 25, Munich 81375, Germany

Full list of author information is available at the end of the article.

Edited by N. Barlev

© The Author(s) 2019



Open Access This article is licensed under a Creative Commons Attribution 4.0 International License, which permits use, sharing, adaptation, distribution and reproduction in any medium or format, as long as you give appropriate credit to the original author(s) and the source, provide a link to the Creative Commons license, and indicate if changes were made. The images or other third party material in this article are included in the article's Creative Commons license, unless indicated otherwise in a credit line to the material. If material is not included in the article's Creative Commons license and your intended use is not permitted by statutory regulation or exceeds the permitted use, you will need to obtain permission directly from the copyright holder. To view a copy of this license, visit <http://creativecommons.org/licenses/by/4.0/>.

combination of events, which include phosphorylation of receptor interacting protein kinase 1 (RIP1) and 3 (RIP3), formation of the necrosome, as well as phosphorylation of mixed lineage kinase domain-like pseudokinase (MLKL, at T357/S358) and its oligomerization to multimers including octamers^{12,13}. Execution of necroptosis is associated with the typical morphological signs of necrosis¹⁴.

Fluidity of the cell membrane and lipid composition change during CL regression, and changes in sphingomyelin levels in combination with cholesterol levels are implicated in the loss of CL function¹⁵. It was shown that activation of the sphingomyelin pathway by Fas cell surface death receptor ligand (FASLG) and consequently production of ceramide led to cell death in bovine luteal cells¹⁶.

Sphingolipid metabolism is complex. Three distinct pathways of ceramide synthesis are known. First, the sphingomyelin degradation pathway leads to generation of ceramide by acid and neutral sphingomyelinases. This pathway is induced by FASLG, TNF α and oxidative stress^{17,18}. Additionally, sphingolipids, especially ceramides, can be produced via *de novo* synthesis starting from serine and palmitoyl-CoA involving a cascaded reaction of 3-ketodihydrospingosine reductase, dihydroceramide synthase and dihydroceramide desaturase in the endoplasmic reticulum¹⁹. Possible inducers of this pathway are heat stress, cannabinoids, chemotherapeutic agents and oxidized low density lipoprotein²⁰. The third pathway is the ceramide salvage pathway. In late endosomes and lysosomes, sphingomyelin and complex sphingolipids are broken down to ceramide and sphingosine^{21,22}. Sphingosine can then be reused to generate ceramide, which gives this pathway its name. Key enzymes of this pathway are acid sphingomyelinase (SMPD1), acid ceramidase (ASAH1) and acid β -glucosidase (GBA1). This pathway has a strong impact on intracellular signalling and has been linked to apoptosis in other cellular systems²³. Recently, ceramide generation or its administration has also been linked to necroptosis^{24,25}.

Human GCs are a unique model for the human CL. GCs stem from patients undergoing IVF and luteinize in culture. Investigations using this model led to the discovery of necroptosis in human GCs, in addition to apoptosis²⁶. Inhibitors of MLKL (necrosulfonamid, NSA) and RIP1 (necrostatin-1, Nec-1) blocked necroptotic cell death. Evidence for *in vivo* relevance of this observation was obtained in ovarian sections of the rhesus macaque (*Macaca mulatta*) and the human, containing both follicles and the CL^{26,27}. Strongest staining for pMLKL(T357/S358) was, however, found in CL samples.

Based on these observations we hypothesized that necroptosis is involved in primate luteolysis. To examine molecular mechanisms, we studied timed primate ovarian tissue, employed human IVF-derived GCs as a cellular model, and performed mass spectrometry and

transcriptomic analysis. The results support that necroptosis occurs during luteolysis in primates, and pinpoint ceramide and the ceramide salvage pathway.

Results

Necroptosis occurs in the human and nonhuman primate CL

Immunohistochemical staining using anti-pMLKL(T357/S358) antibody provided evidence for necroptotic pathway activation in luteal cells of human and nonhuman primates (marmoset and macaque; Fig. 1). The immunoreactive cells were large luteal cells (Fig. 2). Preabsorption controls (Fig. 1e–g) were negative. CL samples from different stages were studied in macaques. While 3- and 7-day-old CL samples were negative for pMLKL(T357/S358) (Fig. 1a, b), cells positive for pMLKL(T357/S358) were evident in the 14 day-old CL (Fig. 1c).

IVF-derived human GCs - a model for the human CL

IVF-derived human GCs luteinize and are considered a model for luteinized GCs of the CL (Fig. 2)²⁶. We attempted to validate this model by using a proteome analysis of GCs cultured for 2 to 5 days. LC-MS/MS data from cultured GCs and literature data of human CL and *in vivo*-developed primate luteal cells stemming from the mid to late luteal phase were compared. The results indicated a high level of similarity. For example, the cholesterol side-chain cleavage enzyme (CYP11A1), a known luteal-cell marker, was highly expressed (24th most abundant of 3642 detected proteins) in cultured GCs³. Progesterone (P4) synthesis in the CL mainly requires three proteins next to CYP11A1, low density lipoprotein receptor (LDL-R), β -hydroxysteroid dehydrogenase (β -HSD) and steroidogenic acute regulatory protein (StAR)⁴⁴. All of these proteins were expressed in GC samples.

Human granulosa cells undergo necroptosis during culture

To examine necrotic events, we analysed LDH levels in medium. After medium change at day 2, we found a relative cytotoxicity of around 20 % ($n = 8$, Fig. 3a) in cells cultured until day 3 (i.e. 1 day of LDH accumulation), if compared to maximally possible LDH. LDH levels were rising over culture time (Fig. 3a). After 3 consecutive days of LDH accumulation, we found a significant difference compared to the samples analysed on day 3 ($*p < 0.05$).

We next studied proteins known to become phosphorylated during necroptosis (RIP1, RIP3, MLKL). Unphosphorylated forms of those were found at all timepoint during culture (Fig. 3b–d). In the beginning of necroptosis RIP1 is phosphorylated. Using anti-pRIP1(S166), we found the specific band, which was stronger on day 1 and 3 of culture if compared to day 5 (Fig. 3b). After RIP1 phosphorylation, RIP3 is recruited and phosphorylated at S227.

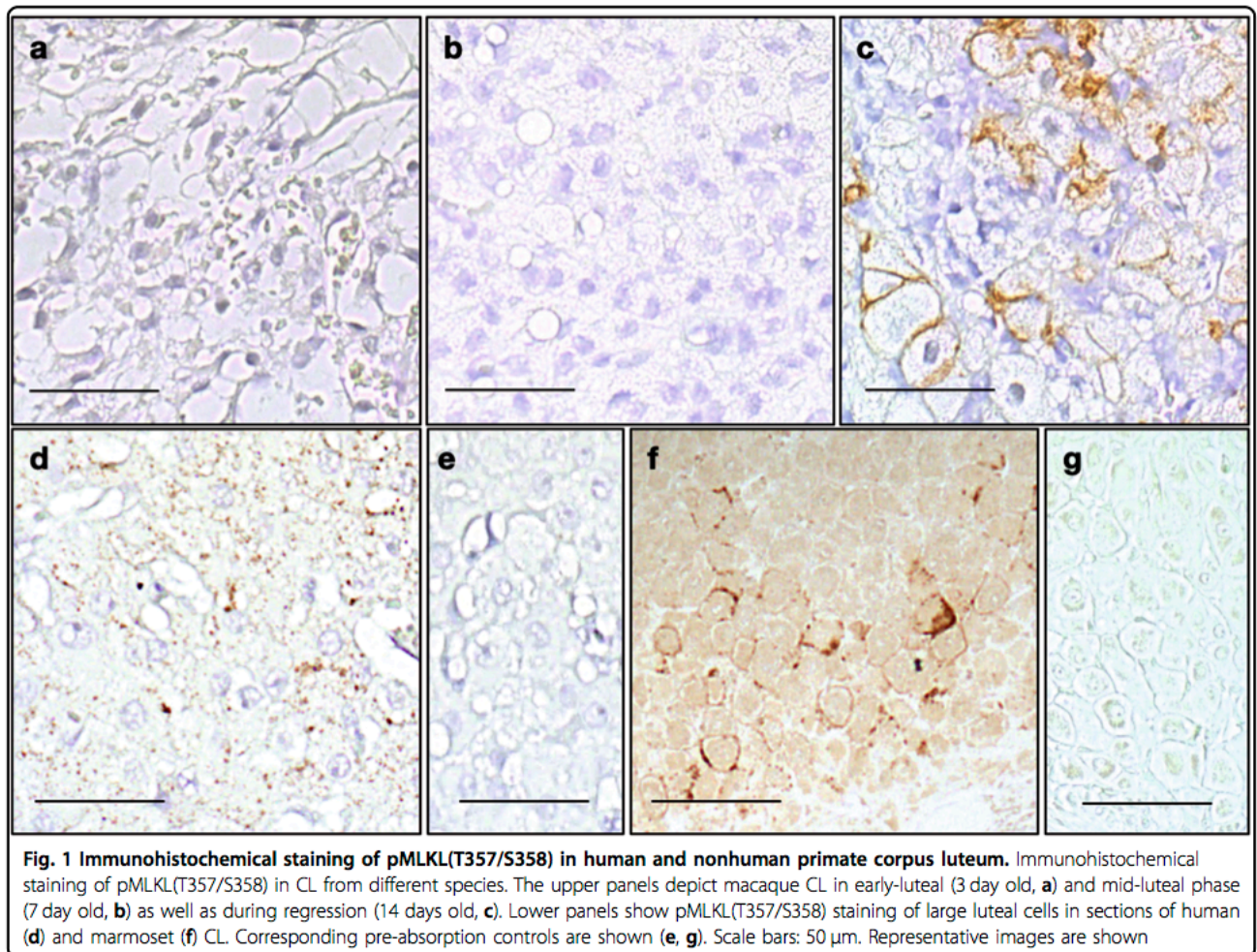


Fig. 1 Immunohistochemical staining of pMLKL(T357/S358) in human and nonhuman primate corpus luteum. Immunohistochemical staining of pMLKL(T357/S358) in CL from different species. The upper panels depict macaque CL in early-luteal (3 day old, **a**) and mid-luteal phase (7 day old, **b**) as well as during regression (14 days old, **c**). Lower panels show pMLKL(T357/S358) staining of large luteal cells in sections of human (**d**) and marmoset (**f**) CL. Corresponding pre-absorption controls are shown (**e**, **g**). Scale bars: 50 μ m. Representative images are shown

An antibody against this phosphorylated peptide revealed a faint band at 62 kDa (Fig. 3c). Evaluation of band intensity showed a slight trend to more RIP3 being phosphorylated at late culture timepoints if compared to day 1. Finally, MLKL is recruited to form the necrosome and oligomerized pMLKL is the executor of necroptosis. Western blots with anti-pMLKL(T357/S358) showed stronger bands at day 3 of cultivation if compared to day 1 (Fig. 3d). Additionally, the oligomerized form was only detectable at day 3 onwards, indicating execution of necroptosis at these timepoints. The specificity of the anti-pMLKL(T357/S358) antibody was tested²⁷. Taken together, the data indicate a trend of enhanced execution of necroptosis during culture time.

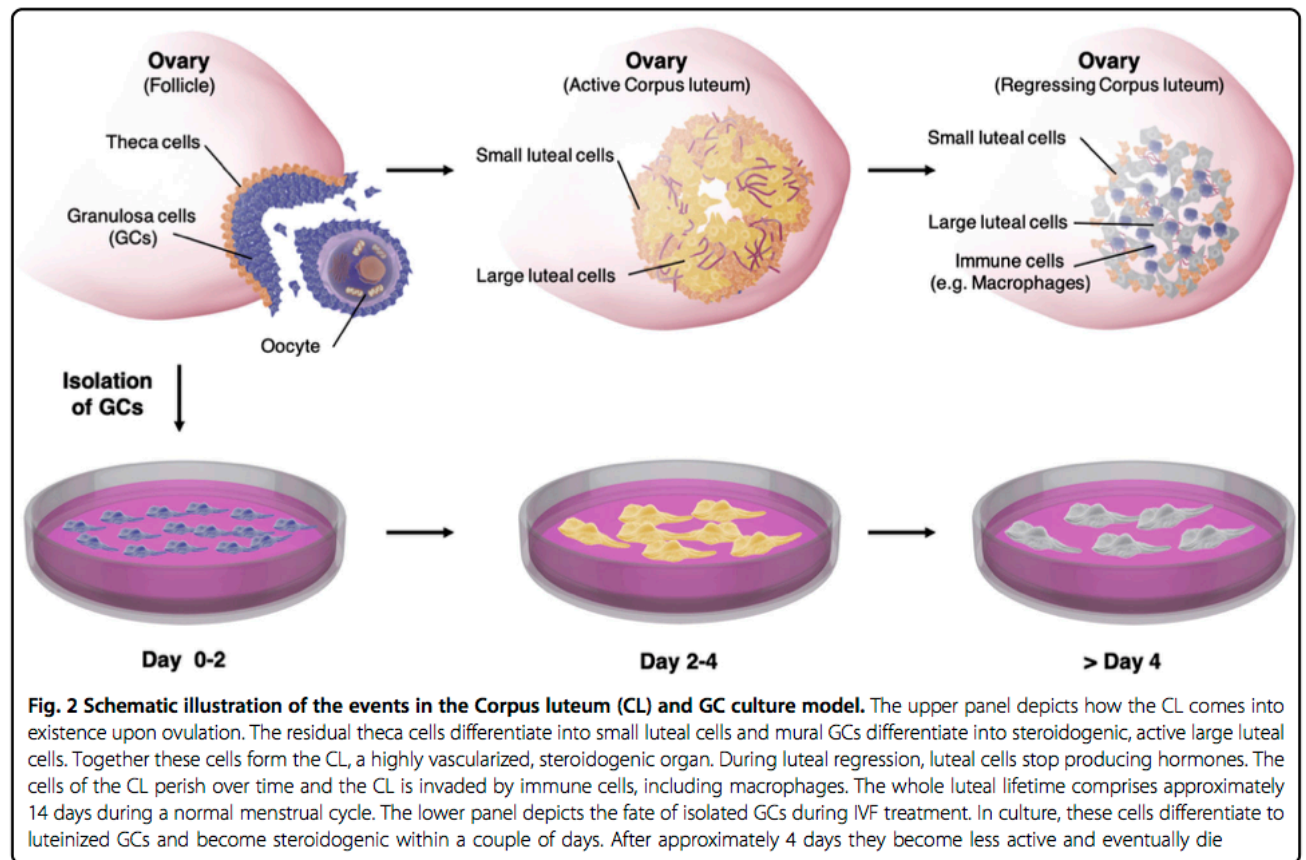
Proteins associated with the ceramide salvage pathway were highly upregulated in GCs over culture period, as well as during in vivo-development of the CL

For GC samples from culture day 2 to 5, LC-MS/MS based proteomic analyses ($n = 5$ per day) were performed and a total of 3642 proteins were identified.

Quantified proteins were prefiltered, based on p value and \log_2 fold change, and underwent a DAVID analysis to

identify functional annotation clusters, which were enriched in day 5 compared to day 2. Three clusters were found (Table 1). The first cluster contained 7 proteins involved in cholesterol biosynthesis, which all showed lower abundance at day 5. The second cluster included mainly translation initiation factors and translation associated proteins, which showed mostly small changes in abundance. The third cluster contained 17 proteins, which were lysosome associated proteins. Most of these proteins are directly involved in the lysosomal ceramide salvage pathway and showed different degrees of raised abundance at day 5 ranging from \log_2 fold change 0.91 (HEXB) to 2.75 (GAA). An overview of the core pathway proteins and corresponding reactions is provided (Fig. 4a). For a detailed pathway see Supplementary Figure 1.

Transcriptomic data of in vivo-developed macaque CL showed that 8 of 14 genes associated with the ceramide salvage pathway were significantly upregulated in the late stage CL relative to the early stage CL in macaques with \log_2 fold change ranging from 0.34 for arylsulfatase A (ARSA) to 1.51 for GM2 ganglioside activator (GM2A). ASAH1, GM2A, HEXA, HEXB, PSAP and SCARB2 were



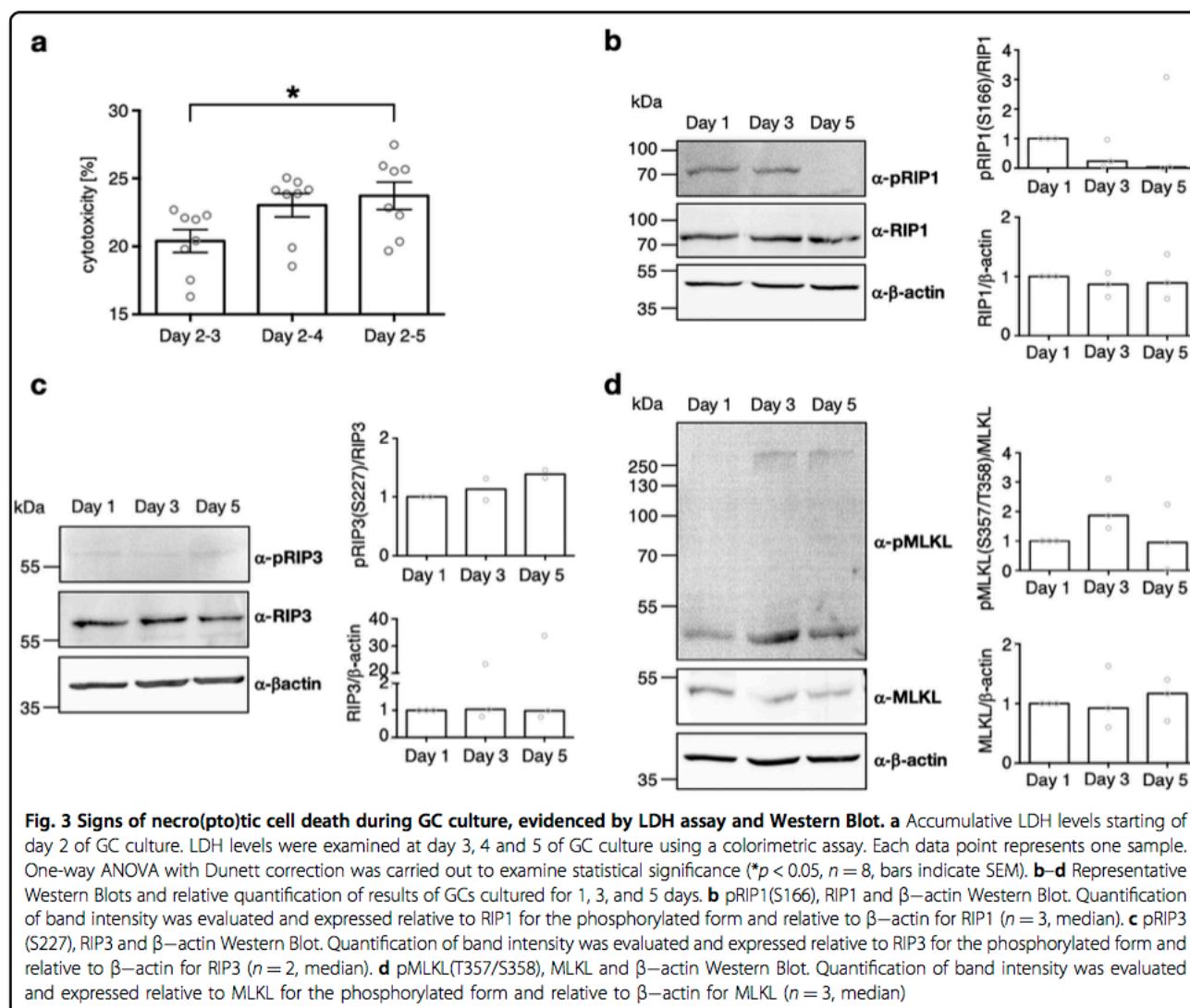
elevated in both the proteomics and the transcriptomics analysis (Supplementary Fig. 2, Supplementary Table 1). Validations employing real-time PCR revealed that the mRNA levels of *ASAHI*, *SMPD1*, *GBA* and *CERS2* were likewise changed compared to the microarray data (data not shown).

The proteomics data were also filtered for q-values < 0.05 to identify highly significant differential abundance of proteins. The resulting 50 proteins were highlighted in a volcano plot (Fig. 4b). Several proteins were already found to be differentially abundant based on the DAVID enrichment analysis above, especially the lysosomal proteins. Granulins (GRN) were reported to have lysosomal activity and cytokine-like functions and were shown to be trafficked by prosaposin (PSAP) to the lysosome⁴⁵. Both, GRN and PSAP were found to be highly abundant in cultured GCs on day 5. The high \log_2 fold change (-4.20) of the cytosolic hydroxymethylglutaryl-CoA synthase (HMGCS1) and the reduction of another protein associated with cholesterol synthesis, namely vigilin (also known as high density lipoprotein-binding protein, HDLBP, \log_2 fold change (-1.08)), became evident. The RNA binding protein vigilin is reported to protect cells from overaccumulation of cholesterol⁴⁶. Collectively, these data point to the ceramide salvage pathway, and

accumulation of its metabolic products ceramide and sphingosine, involved in cell death of in vitro cultured GCs and in vivo-developed CL.

Cell studies using FB1 support a role of the ceramide pathway in GCs viability

The LC-MS/MS data in combination with the transcriptomic data in a nonhuman primate indicated an accumulation of ceramide or sphingosine in cultured GCs and in the regressing CL (Supplementary Fig. 2 and Supplementary Table 1). To further examine this possibility in vitro, immunocytochemical staining of ceramide species and the Golgi apparatus were carried out³⁵. GCs at day 2 and day 5 of culture, as well as after 72 h of treatment with the known ceramide synthase blocker fumonis B1 (FB1, 0.5 μ M) were studied. At day 2, the ceramide staining was mainly localized to the Golgi apparatus, as shown by co-staining with anti-golgin97 (Fig. 4c). After 5 days of culture, cells had grown in size, which was indicated by the larger nuclei and Golgi apparatus. Ceramide staining intensity also increased. In addition to the Golgi apparatus, it was associated presumably with cell membranes of other cell compartments. As expected, FB1 treatment reduced ceramide staining intensity (Fig. 4c). These findings support the LC-MS/MS



and transcriptomic data and show the significance of ceramide synthases in ceramide generation.

Next, we treated GCs with FB1 (0.5 μM) at day 1 of culture and determined cell confluency over a time period of 72 h (Fig. 4d). FB1-treatment increased confluency by $17.6 \pm 11.1\%$ ($n = 6$, Fig. 4d, right diagram) compared to the solvent control. Furthermore, FB1 treatment significantly increased cell number ($7.76 \times 10^4 \pm 0.65 \times 10^4$ cells, $n = 11$) compared to controls ($6.41 \times 10^4 \pm 0.57 \times 10^4$ cells, $n = 11$, Fig. 4d, bar diagram). The data indicate that blocking ceramide synthases and therefore lowering ceramide levels has a positive effect on GC viability.

A soluble ceramide analogue induced a form of necrotic cell death in human GCs

Cell studies with FB1 showed that endogenously produced ceramide has a negative effect on GC viability. To further examine the significance of ceramide in GC

culture, we added the soluble ceramide analogue C2-ceramide (C2-CER, 50 μM) at day 1 or 2 of culture and evaluated confluency, cell number (Fig. 5a), as well as medium LDH levels (Fig. 5b). In the C2-CER-treated group we found significantly reduced confluency after 72 h by $17.5 \pm 2.9\%$ ($n = 9$, Fig. 5a, x/y diagram) compared to the solvent control group. This was accompanied by an augmentation of typical morphological signs of necro(pto)tic cell death, e.g., ballooning (Fig. 5a, images). Additionally, 72 h stimulation with C2-CER significantly reduced cell number to $4.64 \times 10^4 \pm 0.65 \times 10^4$ ($n = 11$), compared to controls ($6.86 \times 10^4 \pm 0.64 \times 10^4$, $n = 11$, Fig. 5a, bar diagram).

We measured accumulation of medium LDH after 24, 48 and 72 h, starting of day 2 of culture. LDH levels and subsequently relative cytotoxicity between day 2–3 were not significantly altered due to C2-CER (50 μM) stimulation (Fig. 5b, $n = 8$, upper diagram). After 48 h (Fig. 5b,

Table 1 DAVID clusters of proteome analysis

Protein name	Gene name	Uniprot accession	log ₂ fold change	p value
Cluster 1: cholesterol biosynthesis				
3-hydroxy-3-methylglutaryl-CoA synthase 1	HMGCS1	Q01581	-4.20	1.8E-04
7-dehydrocholesterol reductase	DHCR7	Q9UBM7	-0.81	2.6E-02
SWI/SNF related, matrix associated, actin dependent regulator of chromatin, subfamily d, member 3	SMARCD3	Q6STE5	-0.97	2.0E-02
Acetyl-CoA carboxylase alpha	ACACA	Q13085	-2.09	1.4E-02
Cytochrome P450 family 51 subfamily A member 1	CYP51A1	Q16850	-2.77	9.1E-03
Farnesyl diphosphate synthase	FDPS	P14324	-0.93	9.4E-04
Isopentenyl-diphosphate delta isomerase 1	IDI1	Q13907	-2.02	3.9E-02
Cluster 2: translation initiation/ translation associated proteins				
Eukaryotic translation initiation factor 3 subunit I	EIF3I	Q13347	-0.70	9.3E-03
Eukaryotic translation initiation factor 3 subunit J	EIF3J	O75822	-0.70	1.8E-02
Eukaryotic translation initiation factor 3 subunit K	EIF3K	Q9UBQ5	-1.63	1.6E-02
Eukaryotic translation initiation factor 3 subunit L	EIF3L	Q9Y262	-0.63	1.4E-02
Eukaryotic translation initiation factor 4A1	EIF4A1	P60842	-0.64	5.5E-03
Heat shock protein family B (small) member 1	HSPB1	P04792	-1.19	2.7E-02
Ribosomal protein L22-like 1	RPL22L1	Q6P5R6	-1.82	3.9E-03
Ribosomal protein L24	RPL24	P83731	-0.67	2.8E-02
Ribosomal protein S14	RPS14	P62263	-0.65	6.8E-03
Cluster 3: lysosomal proteins				
GM2 ganglioside activator	GM2A	P17900	1.39	1.7E-02
N-acetyl-alpha-glucosaminidase	NAGLU	P54802	1.80	9.4E-03
N-acylsphingosine amidohydrolase 1	ASAH1	Q13510	2.57	6.4E-03
Arylsulfatase B	ARSB	P15848	2.43	3.4E-04
Cathepsin A	CTSA	P10619	1.85	3.7E-06
Cathepsin D	CTSD	P07339	1.03	9.8E-04
Fucosidase, alpha-L- 1, tissue	FUCA1	P04066	1.58	3.4E-03
Galactosylceramidase	GALC	P54803	1.81	4.3E-02
Glucosamine (N-acetyl)-6-sulfatase	GNS	P15586	0.94	7.8E-04
Glucosidase alpha, acid	GAA	P10253	2.75	3.6E-02
Hexosaminidase subunit alpha	HEXA	P06865	1.37	4.8E-04
Hexosaminidase subunit beta	HEXB	P07686	0.91	2.9E-04
Neuraminidase 1	NEU1	Q99519	2.12	3.2E-02
Phospholipase B domain containing 2	PLBD2	Q8NHP8	1.04	2.9E-03
Prosaposin	PSAP	P07602	1.06	2.2E-03
Scavenger receptor class B member 2	SCARB2	Q14108	1.51	1.7E-02
Sphingomyelin phosphodiesterase 1	SMPD1	P17405	1.17	6.4E-03

Results of the DAVID annotation clustering. Three clusters were found to be enriched. Every cluster is shown with the corresponding proteins and the changes in abundancies

Table 2 50 significantly differentially abundant proteins between day 2 and day 5 of GC culture

Protein name	Gene name	log ₂ fc	p value
Hydroxymethylglutaryl-CoA synthase, cytoplasmic	HMGCS1	-4.20	1.82E-04
Fibrinogen beta chain	FGB	-4.09	5.47E-03
Fibrinogen alpha chain	FGA	-3.78	7.55E-03
Signal recognition particle subunit SRP72	SRP72	-3.67	1.13E-02
Lanosterol 14-alpha demethylase	CYP51A1	-2.77	9.09E-03
Fatty acid desaturase 2	FADS2	-2.56	6.55E-06
Nucleolar RNA helicase 2	DDX21	-2.32	1.95E-03
Protein transport protein Sec23B	SEC23B	-2.26	1.75E-03
RNA polymerase II-associated protein 3	RPAP3	-2.26	7.72E-03
LIM and cysteine-rich domains protein 1	LMCD1	-2.12	2.76E-03
60 S ribosomal protein L22-like 1	RPL22L1	-1.82	3.90E-03
DnaJ homolog subfamily A member 1	DNAJA1	-1.78	9.18E-03
Arf-GAP domain and FG repeat-containing protein 1	AGFG1	-1.78	9.24E-03
Zinc transporter ZIP14	SLC39A14	-1.73	2.05E-03
EH domain-containing protein 1	EHD1	-1.63	2.14E-03
A-kinase anchor protein 2	AKAP2	-1.61	8.69E-03
Proteasome-associated protein ECM29 homolog	ECM29	-1.56	1.45E-03
Serotransferrin	TF	-1.48	6.79E-03
E3 ubiquitin-protein ligase UBR4	UBR4	-1.32	3.35E-03
Coiled-coil domain-containing protein 47	CCDC47	-1.28	6.43E-03
Plasminogen activator inhibitor 2	SERPINB2	-1.27	2.07E-03
Golgi membrane protein 1	GOLM1	-1.21	3.63E-03
Neuroblast differentiation-associated protein AHNAK	AHNAK	-1.19	3.39E-04
ATP-dependent Clp protease ATP-binding subunit clpX-like, mitochondrial	CLPX	-1.18	2.52E-03
Vigilin	HDLBP	-1.08	2.81E-03
Histone deacetylase 6	HDAC6	-1.00	1.22E-04
Farnesyl pyrophosphate synthase	FDPS	-0.93	9.37E-04
Beta-hexosaminidase subunit beta	HEXB	0.91	2.88E-04
N-acetylglucosamine-6-sulfatase	GNS	0.94	7.76E-04
Cathepsin D	CTSD	1.03	9.81E-04
Putative phospholipase B-like 2	PLBD2	1.04	2.91E-03
Prosaposin	PSAP	1.06	2.20E-03
Integrin alpha-1	ITGA1	1.10	1.94E-03

Table 2 continued

Protein name	Gene name	log ₂ fc	p value
Sphingomyelin phosphodiesterase	SMPD1	1.17	6.37E-03
Adenylate kinase isoenzyme 1	AK1	1.17	5.85E-03
ATP synthase mitochondrial F1 complex assembly factor 1	ATPAF1	1.26	5.86E-03
Granulins	GRN	1.34	5.82E-04
Beta-hexosaminidase subunit alpha	HEXA	1.37	4.81E-04
Protein FAM162A	FAM162A	1.38	6.68E-04
Tissue alpha-L-fucosidase	FUCA1	1.58	3.36E-03
Dipeptidyl peptidase 2	DPP7	1.62	1.66E-03
Four and a half LIM domains protein 2	FHL2	1.64	3.14E-03
Fatty acid-binding protein, heart	FABP3	1.70	2.36E-03
Alpha-N-acetylglucosaminidase	NAGLU	1.80	9.35E-03
Vacuolar protein sorting-associated protein VTA1 homolog	VTA1	1.83	7.35E-03
Lysosomal protective protein	CTSA	1.85	3.72E-06
Unconventional myosin-VI	MYO6	1.97	1.89E-03
Arylsulfatase B	ARSB	2.43	3.38E-04
Acid ceramidase	ASAH1	2.57	6.39E-03
Mammalian ependymin-related protein 1	EPDR1	3.50	1.09E-03

Log₂ fold change and p values of the proteins highlighted in the volcano plot shown in Fig. 2

$n = 8$, middle diagram), but not after 72 h (Fig. 5b, lower diagram), the effect of C2-CER on viability reached statistical significance. These results are in line with the confluency measurements (Fig. 5a), but the basal release of LDH is possibly superimposing the effect of C2-CER. Our studies on GCs using exogenously applied soluble C2-CER support the previous findings that ceramide induces a form of necrotic cell death in GCs.

Necrosulfonamid but not the apoptosis inhibitor zVAD-fmk counteracted the effect of C2-CER

To analyse the types of cell death occurring in culture, we stimulated GCs with C2-CER (50 μ M) alone or in combination with NSA (20 μ M) or zVAD-fmk (20 μ M) for 72 h, starting on day 1 or 2 of culture. The addition of NSA had a positive effect on confluency (121.3 ± 8.2 %, $n = 6$, Fig. 5c, upper diagram). Co-treatment with zVAD-fmk had no effect on confluency of C2-CER-treated GCs (102.4 ± 1.9 %, $n = 5$, Fig. 5c, middle diagram). Evaluation of cell numbers after a 72 h stimulation likewise showed a significant positive effect of NSA ($8.50 \times 10^4 \pm 0.53 \times 10^4$ cells, $n = 12$) and no effect of zVAD-fmk ($5.75 \times 10^4 \pm 0.80 \times 10^4$ cells, $n = 8$)

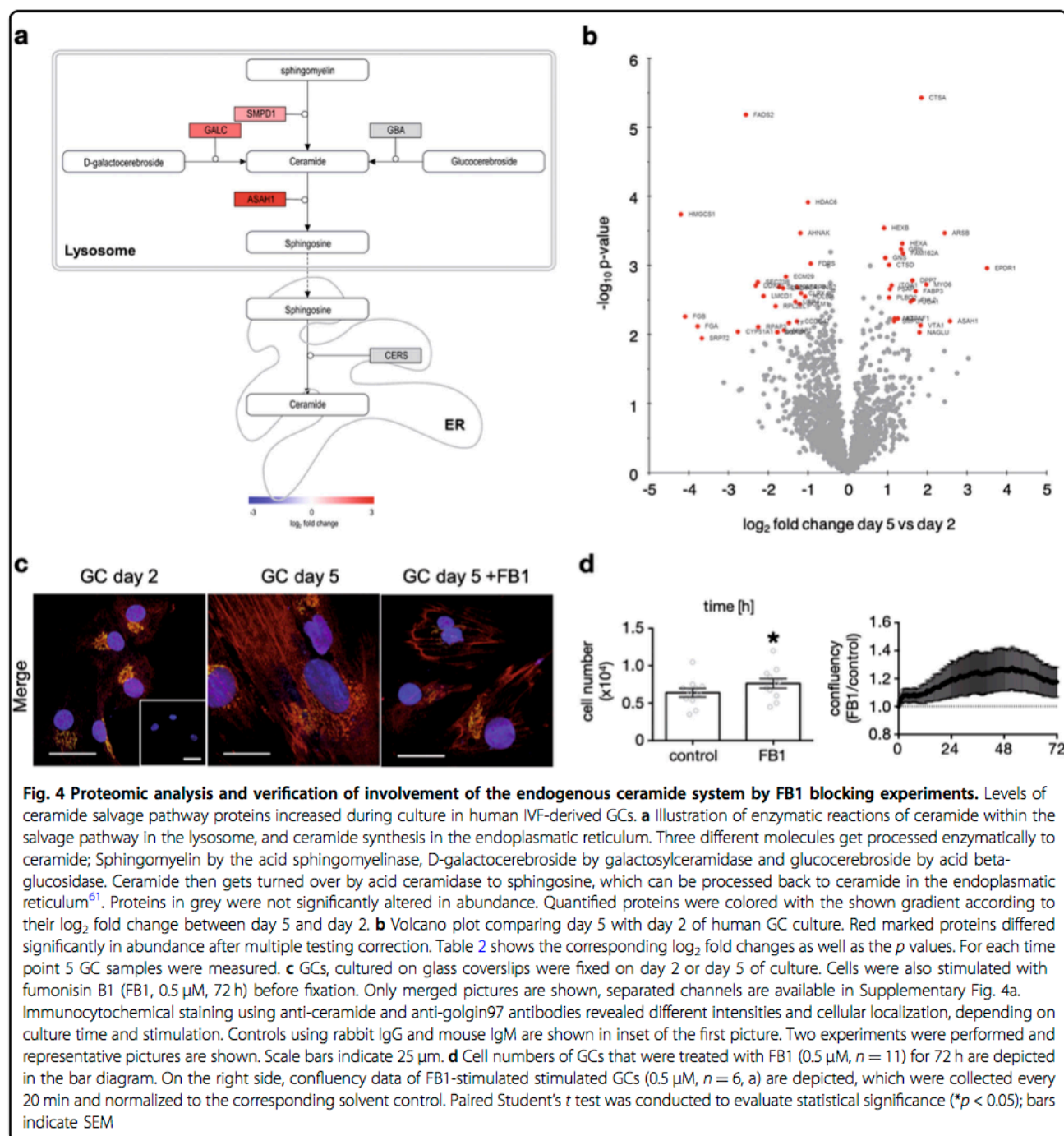


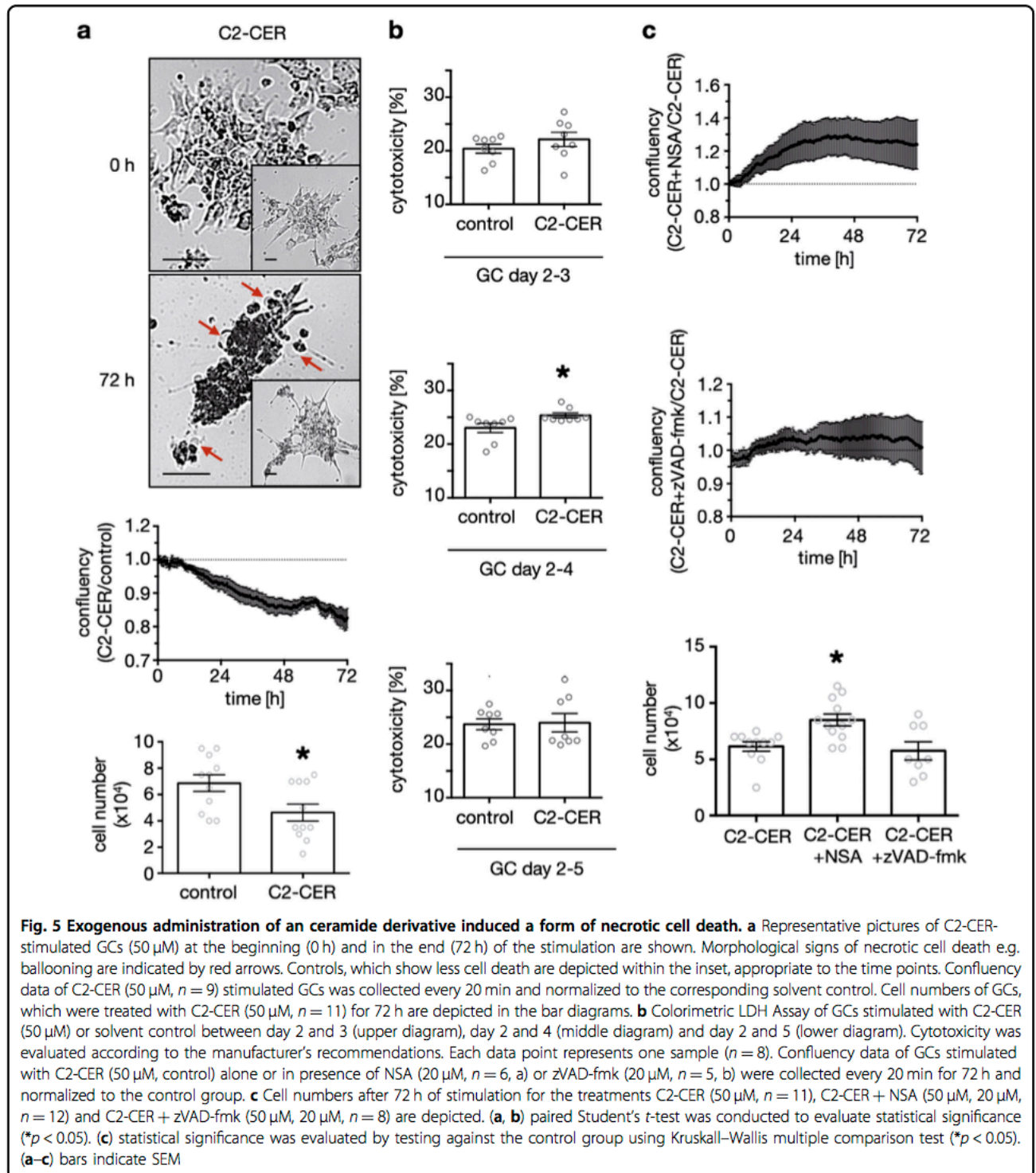
Fig. 4 Proteomic analysis and verification of involvement of the endogenous ceramide system by FB1 blocking experiments. Levels of ceramide salvage pathway proteins increased during culture in human IVF-derived GCs. **a** Illustration of enzymatic reactions of ceramide within the salvage pathway in the lysosome, and ceramide synthesis in the endoplasmic reticulum. Three different molecules get processed enzymatically to ceramide; Sphingomyelin by the acid sphingomyelinase, D-galactocerebroside by galactosylceramidase and glucocerebroside by acid beta-glucosidase. Ceramide then gets turned over by acid ceramidase to sphingosine, which can be processed back to ceramide in the endoplasmic reticulum⁶¹. Proteins in grey were not significantly altered in abundance. Quantified proteins were colored with the shown gradient according to their \log_2 fold change between day 5 and day 2. **b** Volcano plot comparing day 5 with day 2 of human GC culture. Red marked proteins differed significantly in abundance after multiple testing correction. Table 2 shows the corresponding \log_2 fold changes as well as the p values. For each time point 5 GC samples were measured. **c** GCs, cultured on glass coverslips were fixed on day 2 or day 5 of culture. Cells were also stimulated with fumonisins B1 (FB1, 0.5 μ M, 72 h) before fixation. Only merged pictures are shown, separated channels are available in Supplementary Fig. 4a. Immunocytochemical staining using anti-ceramide and anti-golgin97 antibodies revealed different intensities and cellular localization, depending on culture time and stimulation. Controls using rabbit IgG and mouse IgM are shown in inset of the first picture. Two experiments were performed and representative pictures are shown. Scale bars indicate 25 μ m. **d** Cell numbers of GCs that were treated with FB1 (0.5 μ M, $n = 11$) for 72 h are depicted in the bar diagram. On the right side, confluency data of FB1-stimulated stimulated GCs (0.5 μ M, $n = 6$, a) are depicted, which were collected every 20 min and normalized to the corresponding solvent control. Paired Student's t test was conducted to evaluate statistical significance (* $p < 0.05$); bars indicate SEM

in comparison to C2-CER-only treatment ($6.14 \times 10^4 \pm 0.42 \times 10^4$ cells, $n = 11$, Fig. 5c, bar diagram).

As MLKL phosphorylation and oligomerization are the known terminal steps of necroptosis, we examined by western blot analyses whether the addition of C2-CER (50 μ M, 72 h starting of day 1 or 2) is able to increase pMLKL (T357/S358). We detected bands corresponding to the monomeric and the oligomeric form of pMLKL in the C2-CER treated and the solvent group, yet without a

significant difference ($n = 5$, Supplementary Fig. 3b). A high degree of variability became evident. Co-treatment of C2-CER (50 μ M) and NSA (20 μ M) yielded a significant reduction of pMLKL(T357/S358) levels, when compared to the group solely treated with C2-CER ($n = 5$, Supplementary Fig. 3c).

We also cultured GCs in the presence of NSA (20 μ M, Supplementary Fig. 3a) for 72 h between day 2 and 5 and performed immunocytochemistry. As expected, we found



increased ceramide staining over culture time, which unexpectedly was reduced upon addition of NSA (Supplementary Fig. 3a). To explore possible off-target effects, we conducted the same experiment using a blocker, which is known to have less off-target effects and acts as an

upstream inhibitor of necroptosis by targeting RIP1, namely necrostatin 1s (Nec-1s, 20 μ M, Supplementary Fig. 4b)⁴⁷. This experiment yielded comparable results supporting the hypothesis that ceramide generation and necroptosis are interlinked pathways.

Discussion

Necrosis and necroptosis are generally linked to harmful or pathological processes⁴⁸. Our cellular studies combined with the analysis of luteal samples indicate that necroptosis occurs in the CL of nonhuman primates and humans, as a physiological process linked to luteolysis, which is possibly fuelled by ceramide actions.

To date, very little is known about a physiological role of necro(pto)sis⁴⁹. For example, during development of *C. elegans*, the linker cell helps to shape gonads in male worms and dies afterwards, lacking apoptosis marker but exhibiting morphological signs of necrosis⁵⁰. In nonhuman primates, a functional study using ovarian follicle culture indicated involvement of necroptosis in follicular death²⁷. A cell culture study in human GCs revealed spontaneously occurring necroptosis, which was further stimulated upon addition of a peptide (ARP) corresponding to a splice variant of acetylcholinesterase²⁶. We now document phosphorylation of MLKL at T357/S358 in large luteal cells of regressing CL in macaques. Necroptotic cells were likewise identified in other primate species, including marmosets and humans, though the exact stages of the CL were not known. Furthermore, we assessed necroptotic cell death of GCs in a time course experiment, using pRIP1(S166), pRIP3(S277), pMLKL (T357/S358) and their unphosphorylated counterparts. We found necroptosis to occur over culture time. Due to pMLKL oligomerization at day 3 and 5 of culture we concluded that execution of necroptosis takes place on and after day 3 of culture. These results were supported by increasing LDH concentrations in culture medium over time.

As GCs differentiate in culture and also die over time, we reasoned that the culture of IVF-derived GCs is an apt model to explore possible mechanisms of necroptotic cell death related to the events in the CL. Results of a proteomic analysis of GCs allowed us to identify the ceramide salvage pathway. Many contributing enzymes were consistently upregulated, leading to the hypothesis that localization and/or quantity of sphingolipid species could change^{20,51}. Comparison between the proteomic and the transcriptomic data indicated a high degree of similarity in protein and gene expression patterns between the two datasets, especially components involved in the ceramide salvage pathway, which indicated its physiological relevance. As both, GC necroptosis and elevated expression of ceramide salvage proteins take place during GC culture, we explored whether these pathways may be interlinked.

The salvage pathway may result in accumulation of two principle metabolites, ceramide and sphingosine²⁰. Ceramide accumulation during necroptosis was shown before and was linked to *de novo* lipogenesis⁵². However, proteins associated with the synthesis of fatty acids were not changed in cultured GCs (ATP citrate lyase, ACLY; fatty

acid synthase, FASN; fatty acid elongase1 and 5, ELOVL1 and 5) or were even strongly downregulated (acetyl-CoA carboxylase α , ACACA, $\log_2FC = -1.74$). Hence, we concluded that ceramide stems from the salvage pathway. An immunocytochemical approach endorsed the LC-MS/MS data, and ceramide levels increased with culture time. Addition of the ceramide synthase blocker FB1^{31,32,53} reduced ceramide staining. FB1 also improved cell viability. Taken together, these results lead us to conclude that ceramide accumulation has a negative effect on GC viability by inducing cell death.

We also challenged GCs with a soluble, cell permeable ceramide analogue, C2-CER. It decreased cell viability. The change in confluency became evident during the first 48 h of imaging and was only marginally altered afterwards. Likewise, we found slightly but statistically significantly higher LDH levels due to C2-CER treatment albeit only after 48 h, a result which points at a necrotic form of cell death. Typical morphological signs of necro(pto)sis, including ballooning and cell burst, were evident in the C2-CER treated groups⁵⁴.

The results obtained in GCs are in line with previous data^{11,55,56}, which indicated that ceramide is associated with apoptosis or necroptosis in non-primate GCs. To further examine the forms of cell death in GCs, we tested the actions of NSA and zVAD-fmk. NSA is a known inhibitor of MLKL that covalently modifies Cys88, and subsequently blocks MLKL oligomerization and execution of cell death⁵⁷. This blocker had a positive effect on confluency and cell number, which was lowered by C2-CER, whereas zVAD-fmk lacked such actions. While all these results point to the ability of C2-CER to induce necroptosis in GCs, Western Blot studies indicated that the known necroptosis executioner protein, i.e., phosphorylated MLKL, was not further elevated upon treatment. However, the addition of NSA reduced MLKL phosphorylation and lowered oligomerization of MLKL compared to C2-CER treated groups¹². Human GCs are patient-derived primary cells and exhibit a large degree of variability²⁶. It is possible that this fact contributes to the inability to decide from this type of experiment whether or to what degree the ongoing necroptotic events in GCs may be further enhanced by exogenous C2-CER.

Previous research showed that ceramide accumulation occurred downstream of RIP1 activation in TNF α -induced necroptosis⁵⁸. However, there is also a link between ceramide production, general perturbation in cell metabolism and cell death⁵⁹. We found that the addition of inhibitors targeting two steps in necroptosis, NSA and Nec-1s, both reduced ceramide staining. Clearly, while off-target actions of the drugs can not be ruled out, this may also indicate that ceramide production is complexly regulated in GCs and linked to necroptotic cell death.

In summary, results obtained in a cellular model and in vivo-developed CL from humans and nonhuman primates, indicate that necroptotic cell death contributes to the demise of the CL. This implicates necroptosis as a physiologically occurring event in the ovary. We suggest that the ceramide salvage pathway has a role in CL regression. Increased endogenous ceramide production is proposed as an inducer of this form of necrotic cell death in GCs. The cellular results also raise the possibility that the primate CL could be rescued by pharmacological inhibition of necroptosis or by modulation of ceramide metabolism. The applicability of such an approach in luteal-phase dysfunctions remains to be tested⁶⁰.

Materials and methods

Culture and treatment of human IVF-derived GCs

The use of human IVF-derived GCs was approved by the ethics committee of the Ludwig-Maximilians University in Munich and each patient approved the use of cells. GCs were isolated from follicular fluid (FF), as previously described^{28–30}. In brief, pooled FF from at least two patients was filtered (40 μ m EASYstrainer, Grainer Bio-One, Kremsmünster, A), and the residuum was washed and backwashed with medium (1:1 DMEM/F12, Thermo Fisher Scientific, Waltham, MA, USA). Afterwards, cells were singularized through a 0.9 \times 40 mm syringe (B.Braun Melsungen, Melsungen, GER) and centrifuged at 800 g for 3 min. Next, cell pellet was re-suspended in DMEM/F12 medium, supplemented with fetal calf serum (FCS, 10 %), penicillin (100 U/ml) and streptomycin (100 μ g/ml), and counted using Neubauer chamber method. A total of 10^5 cells were seeded per 35 mm² plate (Sarstedt AG & Co. KG, Nümbrecht, GER) and cultivated at 37 °C and 5 % CO₂. After 24 h of cultivation (day 1), non-adherent cells were removed by washing. For immunocytochemistry, cells were trypsinized at day 1 of culture and seeded onto glass coverslips in a 24 well plate (10^4 cells/well, Sarstedt AG & Co. KG, Nümbrecht, GER). All experiments were carried out using cell culture medium.

For live cell experiments, GCs were stimulated with a synthetic, soluble and cell permeable ceramide analogue alone (C2-ceramide, 50 μ M, Enzo Life Sciences Inc., Farmingdale NY, USA) or in combination with either the MLKL inhibitor necrosulfonamid (NSA, 20 μ M, Cat. No. 5025) or the pan-caspase (apoptosis) inhibitor z-VAD-fmk (20 μ M, Cat. No. 2163). Both inhibitors were ordered from Tocris Bioscience (Bristol, UK). Further, a widely used ceramide synthase inhibitor fumonisins B1 (FB1, 0.5 μ M, Enzo Life Sciences Inc., Farmingdale NY, USA) was administrated to block endogenous ceramide generation^{31,32}. All experiments were carried out for at least six times if not described otherwise.

Confluency measurement and cell counting

Confluency of GCs between day 1 and day 5 of culture was measured for a period of 72 h, as described before²⁶. For cell counting experiments, cells were rinsed with PBS post treatment, trypsinized and counted using the Neubauer chamber method. All experiments were carried out for at least eight times if not described otherwise.

Immunohistochemistry

We immunohistochemically stained pMLKL(T357/S358) using the specific antibody (ab187091, Abcam, Cambridge, UK) to identify necroptosis in tissue sections of macaque, marmoset (*Callithrix jacchus*) and human ovaries. Samples from macaques were consecutive sections of those described previously³³. Additional samples were provided by the Oregon National Primate Research Center, Oregon Health & Science University (Beaverton, OR, USA) collected during days 3–5 (early), days 7–8 (mid) and days 14–16 (late) after the midcycle LH surge in a previous study³⁴. Marmoset samples are from the German Primate Center (Göttingen, GER) and were taken from the histological sample archive of the Platform Degenerative Diseases. The samples were fixed in Bouin's solution and embedded in paraffin. All immunohistochemistry procedures were conducted as previously described²⁷. In brief, sections were deparaffinized, antigens were retrieved using the HIER method, and endogenous peroxidase was blocked with H₂O₂ (3 in 10% methanol). Further, unspecific binding was prevented by incubation with 10 % goat serum in PBS. Positive antibody staining resulted from complexing of antigen bound primary antibody with biotinylated secondary antibody and avidin (ABC kit). Pre-absorption of anti-pMLKL(T357/S358) antibody using the respective peptide (ab206929, Abcam, Cambridge, UK) was done as previously described²⁷. Immunohistochemical staining was carried out on three human CL samples, two marmoset CL samples and three timed series of macaque CL samples.

Immunocytochemistry

To determine expression and localization of ceramide over culture time, we used a monoclonal anti-ceramide antibody (anti-CER, clone MID15B4, Enzo Life Sciences Inc., Farmingdale, NY, USA) in an immunocytochemical approach. This antibody detects different ceramide species including dihydroceramide, C16- and C24-ceramide³⁵. Furthermore, anti-golgin97 antibody (Thermo Fisher Scientific, Waltham, MA, USA) was used to examine ceramide localization. Cells were stimulated at day 2 of culture with 0.5 μ M FB1, 20 μ M Necrostatin-1s (Nec-1s, a potent RIP1-kinase inhibitor) or 20 μ M NSA for 72 h. After 5 days of culture and 72 h of stimulation, GCs were fixed in a 4% formaldehyde solution and permeabilized on ice using 0.2% Triton X-100 in PBS. To block unspecific binding, cells

were incubated with 5 % goat serum in PBS. Specific immuno-decoration was achieved during 1.5 h incubation at room temperature. After three 5 min wash steps with 0.1 % Triton X-100 in PBS, a fluorophore-antibody conjugate was used to visualize specific antibody binding. For detection of anti-CER binding, Rhodamine conjugated F(ab')₂ fragment goat anti-mouse IgM (Jackson ImmunoResearch Inc., West Grove, PA, USA) was used (kindly provided by D. Dormann laboratory (Ludwig-Maximilians University, Department of Cell Biology, Munich, GER). Anti-golgin97 antibody was detected using Alexa488 conjugated donkey anti-mouse IgG (H + L) (Thermo Fisher Scientific, Waltham MA, USA). As controls, mouse serum IgG (Sigma-Aldrich, St. Louis, MI, USA) and IgM (Thermo Fisher Scientific, Waltham MA, USA) were used. Examination by confocal microscopy was conducted at the bioimaging core facility of the Biomedical Center (Ludwig Maximilians University, Munich, GER) using an inverted Leica SP8 microscope, equipped with lasers for 405, 488, 552 and 638 nm excitation. Images were acquired with a HC PL APO 63 × /1.40 oil objective. Fluorescence was recorded with hybrid photo detectors (HyDs), and DAPI with a conventional photomultiplier tube. All experiments were carried out for at least three times.

LDH assay

Pierce LDH Cytotoxicity Assay Kit (PI, Thermo Fisher Scientific, Waltham, USA) was carried out as recommended by the manufacturer and described previously²⁶. In brief, GCs were isolated and pools of at least 2 patients were cultured for 24 h. At day 1 of culture the cells were trypsinized and seeded at 10⁴ cells/well in 96-well plates. At day 2 of culture growth medium was changed and cells were treated with C2-CER (50 μM) or solvent control. After 1, 2 or 3 days of stimulation LDH levels were measured using a microplate reader (FLUOStar Optima, BMG Labtech, Ortenberg, GER). To calculate cytotoxicity a serum control, serum free control and controls treated with lysis buffer before measurement (max LDH) were included.

Protein isolation and western blot

Protein isolation and Western Blot were conducted as previously described^{26,27}. In brief, GCs were lysed after 1 to 5 days of culture using RIPA buffer containing protease and phosphatase inhibitors (PI, Thermo Fisher Scientific, Waltham, USA). A total of 10 μg protein per lane was loaded on a 12 % SDS gel and run under constant current (30 mA/gel). After blotting (100 V, 65 min) and blocking with 5 % non-fat dry milk in Tris-buffered saline with Tween 20 (TBS-T, 50 mM Tris-HCl, 150 mM NaCl, 0.1 % Tween 20, pH 7.4), anti-pRIP1 (S166), anti-pRIP3(S227) both from Cell Signaling Technology (Danvers, MA, USA) and anti-pMLKL

(T357/S358) antibodies were administered to decorate these phosphorylated proteins. To visualize specific binding, HRP-conjugated goat anti-rabbit antibody (Jackson ImmunoResearch Inc., West Grove, PA, USA) was used. As loading controls, anti-RIP1, anti-RIP3 (both from Cell Signaling Technology, Danvers, MA, USA), anti-MLKL (ab184718, Abcam, Cambridge, UK) and anti-β-actin (A5441, Sigma-Aldrich, St. Louis, MI, USA) antibodies were used. Preabsorption of anti-pMLKL was previously published²⁷. All experiments were carried out five times if not described otherwise.

Protein mass spectrometry (LC-MS/MS)

GCs cultured for 2 to 5 days were analyzed using a label-free approach. LC-MS/MS was performed as previously described³⁶. In brief, 2.5 μg total proteins were reduced using DTT, alkylated and digested at 37 °C with LysC for 4 h followed by trypsin overnight. LC-MS/MS was performed with an Ultimate 3000 RSLC chromatography system coupled to a 5600⁺ mass spectrometer.

Raw files were processed using MaxQuant (version: 1.5.8.3) and default settings with the following exceptions: (a) label-free quantification was set to on; (b) "LFQ minimum ratio count" was set to 1; and (c) the "match between runs" feature was turned on. As databases, the human Swiss-Prot subset (Release 06/2017) and the common contaminants from MaxQuant were used³⁷. For protein identification, the data were searched with a target decoy approach resulting in a < 1% False Discovery Rate (FDR). The mass spectrometry data were submitted to the ProteomeXchange Consortium via the PRIDE partner repository (identifier PXD010658). Statistical analysis was done with Perseus (version 1.6.0.7). The samples were first grouped based on their day of cultivation. For pair-wise comparisons, a minimum of 4 values in at least one group were required. The filtered and imputed data were used to calculate log₂ fold changes with a two-sided Welch's *t*-test. Multiple Testing correction was performed using the Permutation-based FDR (5% FDR) which is based on calculation of *q*-values and provided with Perseus. Proteins with a *q*-value < 0.05 and a log₂ fold change > |0.6| were considered significantly different in abundance. For the "DAVID Functional Annotation Clustering", proteins were filtered less stringent with a *p* value < 0.05 and a log₂ fold change > |0.6|^{38,39}. This list was then analyzed with the DAVID online tool to build annotation based clusters according to the GO terms (molecular function, biological process and cellular component) and the reactome pathway database. Only clusters where at least one annotation component had a corrected *p* value (Benjamini) < 0.01 and an enrichment score > 2.5 were seen as significantly enriched.

Pathway illustrations were done with pathvisio^{40,41}. The volcano plot was performed with Microsoft Excel

(Redmond, USA) using the results from the Welch's *t*-test mentioned above.

Microarray and real-time PCR

This was a retrospective study assessing mRNA levels of target genes in rhesus macaque CL samples collected during day 3–5 (early) and day 14–16 (late) after the midcycle LH surge in a previous study⁴². The normalized and log transformed (base 2) microarray data were downloaded from the NCBI Gene Expression Omnibus repository (<https://www.ncbi.nlm.nih.gov/gds>) Dataset Series #GSE10367⁴². The target genes searched were *ARSA*, *ASAH1*, *CTSA*, *GALC*, *GBA*, *GLA*, *GLB1*, *GM2A*, *HEXA*, *HEXB*, *NEU1*, *PSAP*, *SCARB2*, and *SMPD1*. The RNA samples used for microarray analysis were used to synthesize cDNA, as described previously⁴². Real-time PCR was performed using TaqMan Gene Expression Assays (Thermo Fisher Scientific, Waltham, MA, USA) and Applied Biosystems 7900HT Fast Real-time PCR System (Thermo Fisher Scientific, Waltham, MA, USA), as previously described⁴³, for selected genes including *ASAH1* (Assay ID: Hs00602774_m1), *CERS2* (Assay ID: Hs00371958_g1), *GBA* (Assay ID: Hs00986836_g1), and *SMPD1* (Assay ID: Hs003679347_g1). Mitochondrial ribosomal protein S10 (*MRPS10*) served as the internal control.

Statistical analysis

Graphs were constructed in Prism 6 running under Mac OS X, whereby statistical analysis of cell counts, LDH Assays, Western Blot and gene expression were done using the same program and two-sided Student's *t* test. LDH Assay with more than two groups were analysed using One-way ANOVA with Dunnett correction. Cell count experiments with more than two independent groups were analysed using Kruskal–Wallis multiple comparison test. *P* values < 0.05 were considered as significant. The microarray transcriptome analysis was performed using the GeneShifter (VizX Labs, Seattle, WA, USA) software and the Affymetrix Expression Console, as described previously⁴².

Acknowledgements

We thank Kim-Gwendolyn Dietrich and Astrid Tiefenbacher for expert support. Further we thank Idoya Lahortiga and Luk Cox for the allowance to use the graphical content from www.somersault1824.de for Fig. 2. This work was performed in partial fulfilment of the requirements of a Dr. rer. nat. thesis (KB) at LMU. Grant support: Deutsche Forschungsgemeinschaft (DFG) MA1080/19-2, NIH/OD P51OD011092.

Author details

¹Biomedical Center Munich (BMC), Cell Biology, Anatomy III, Ludwig-Maximilians-University (LMU), Grosshaderner Strasse 9, Planegg 82152, Germany. ²Laboratory for Functional Genome Analysis LAFUGA, Gene Center, LMU, Feodor-Lynen Strasse 25, Munich 81375, Germany. ³Platform Degenerative Diseases, German Primate Center, Kellnerweg 4, Göttingen 37077, Germany. ⁴A.R.T. Bogenhausen, Prinzregentenstrasse 69, Munich 81675, Germany. ⁵Department Biology II, Division of Neurobiology, LMU, Grosshaderner Strasse 2, Planegg 82152, Germany. ⁶Division of Reproductive &

Developmental Sciences, Oregon National Primate Research Center, Oregon Health & Science University, 505 NW 185th Avenue, Beaverton, Oregon 97006, USA

Conflict of interest

The authors declare that they have no conflict of interest.

Publisher's note

Springer Nature remains neutral with regard to jurisdictional claims in published maps and institutional affiliations.

The online version of this article (<https://doi.org/10.1038/s41420-019-0149-7>) contains supplementary material, which is available to authorized users.

Received: 15 January 2019 Accepted: 22 January 2019

Published online: 11 February 2019

References

- Richards, J. S., Russell, D. L., Ochsner, S. & Espey, L. L. Ovulation: new dimensions and new regulators of the inflammatory-like response. *Annu. Rev. Physiol.* **64**, 69–92 (2002).
- Green, C., Chatterjee, R., McGarrigle, H. H., Ahmed, F. & Thomas, N. S. p107 is active in the nucleolus in non-dividing human granulosa lutein cells. *J. Mol. Endocrinol.* **25**, 275–286 (2000).
- Devoto, L. et al. The human corpus luteum: life cycle and function in natural cycles. *Fertil. Steril.* **92**, 1067–1079 (2009).
- Shikone, T. et al. Apoptosis of human corpora lutea during cyclic luteal regression and early pregnancy. *J. Clin. Endocrinol. Metab.* **81**, 2376–2380 (1996).
- Morales, C. et al. Different patterns of structural luteolysis in the human corpus luteum of menstruation. *Hum. Reprod.* **15**, 2119–2128 (2000).
- Mizushima, N. et al. A protein conjugation system essential for autophagy. *Nature* **395**, 395 (1998).
- Grzesiak, M., Knapczyk-Stwora, K. & Słomczyńska, M. Induction of autophagy in the porcine corpus luteum of pregnancy following anti-androgen treatment. *Can. J. Physiol. Pharmacol.* **67**, 933–942 (2016).
- Bulling, A. et al. Identification of an ovarian voltage-activated Na⁺-channel type: hints to involvement in luteolysis. *Mol. Endocrinol.* **14**, 1064–1074 (2000).
- Wu, R., Van der Hoek, K. H., Ryan, N. K., Norman, R. J. & Robker, R. L. Macrophage contributions to ovarian function. *Hum. Reprod. Update* **10**, 119–133 (2004).
- Bishop, C. V. et al. Changes in immune cell distribution and their cytokine/chemokine production during regression of the rhesus macaque corpus luteum. *Biol. Reprod.* **96**, 1210–1220 (2017).
- Hojo, T. et al. Programmed necrosis - a new mechanism of steroidogenic luteal cell death and elimination during luteolysis in cows. *Sci. Rep.* **6**, 38211 (2016).
- Huang, D. et al. The MLKL channel in necroptosis is an octamer formed by tetramers in a dyadic process. *Mol. Cell Biol.* **37**, <https://doi.org/10.1128/mcb.00497-16> (2017).
- Galluzzi, L. et al. Molecular mechanisms of cell death: recommendations of the Nomenclature Committee on Cell Death 2018. *Cell Death & Differ.* **25**, 486–541 (2018).
- Linkermann, A. & Green, D. R. Necroptosis. *N. Eng. J. Med.* **370**, 455–465 (2014).
- Carlson, J. C., Buhr, M. M. & Riley, J. C. Plasma membrane changes during corpus luteum regression. *Can. J. Physiol. Pharmacol.* **67**, 957–961 (1989).
- Pru, J. K., Hendry, I. R., Davis, J. S. & Rueda, B. R. Soluble Fas ligand activates the sphingomyelin pathway and induces apoptosis in luteal steroidogenic cells independently of stress-activated p38MAPK. *Endocrinology* **143**, 4350–4357 (2002).
- Kim, M. Y., Linardic, C., Obeid, L. & Hannun, Y. Identification of sphingomyelin turnover as an effector mechanism for the action of tumor necrosis factor alpha and gamma-interferon. Specific role in cell differentiation. *J. Biol. Chem.* **266**, 484–489 (1991).
- Goldkorn, T. et al. H₂O₂ acts on cellular membranes to generate ceramide signaling and initiate apoptosis in tracheobronchial epithelial cells. *J. Cell. Sci.* **111**(Pt 21), 3209–3220 (1998).

19. Menaldino, D. S. et al. Sphingoid bases and de novo ceramide synthesis: enzymes involved, pharmacology and mechanisms of action. *Pharmacol. Res.* **47**, 373–381 (2003).
20. Kitatani, K., Idkowiak-Baldys, J. & Hannun, Y. A. The sphingolipid salvage pathway in ceramide metabolism and signaling. *Cell Signal.* **20**, 1010–1018 (2008).
21. Smith, E. R. & Merrill, A. H. Jr. Differential roles of de novo sphingolipid biosynthesis and turnover in the “burst” of free sphingosine and sphinganine, and their 1-phosphates and N-acyl-derivatives, that occurs upon changing the medium of cells in culture. *J. Biol. Chem.* **270**, 18749–18758 (1995).
22. Ogretmen, B. et al. Biochemical mechanisms of the generation of endogenous long chain ceramide in response to exogenous short chain ceramide in the A549 human lung adenocarcinoma cell line. Role for endogenous ceramide in mediating the action of exogenous ceramide. *J. Biol. Chem.* **277**, 12960–12969 (2002).
23. Takeda, S., Mitsutake, S., Tsuji, K. & Igarashi, Y. Apoptosis occurs via the ceramide recycling pathway in human HaCaT keratinocytes. *J. Biochem.* **139**, 255–262 (2006).
24. Mizumura, K. et al. Sphingolipid regulation of lung epithelial cell mitophagy and necroptosis during cigarette smoke exposure. *FASEB J.: Off. Publ. Fed. Am. Soc. Exp. Biol.* **32**, 1880–1890 (2018).
25. Zhang, X. et al. Ceramide nanoliposomes as a MLKL-dependent, necroptosis-inducing, chemotherapeutic reagent in ovarian cancer. *Mol. Cancer Ther.* **17**, 50–59 (2018).
26. Blohberger, J. et al. Readthrough acetylcholinesterase (AChE-R) and regulated necrosis: pharmacological targets for the regulation of ovarian functions? *Cell Death Dis.* **6**, e1685 (2015).
27. Du, Y., Bagnjuk, K., Lawson, M. S., Xu, J. & Mayerhofer, A. Acetylcholine and necroptosis are players in follicular development in primates. *Sci. Rep.* **8**, 6166 (2018).
28. Mayerhofer, A. et al. Functional dopamine-1 receptors and DARPP-32 are expressed in human ovary and granulosa luteal cells in vitro. *J. Clin. Endocrinol. Metab.* **84**, 257–264 (1999).
29. Mayerhofer, A., Föhr, K. J., Sterzik, K. & Gratzl, M. Carbachol increases intracellular free calcium concentrations in human granulosa-lutein cells. *J. Endocrinol.* **135**, 153–159 (1992).
30. Mayerhofer, A., Sterzik, K., Link, H., Wiemann, M. & Gratzl, M. Effect of oxytocin on free intracellular Ca²⁺ levels and progesterone release by human granulosa-lutein cells. *J. Clin. Endocrinol. & Metab.* **77**, 1209–1214 (1993).
31. Wang, E., Norred, W. P., Bacon, C. W., Riley, R. T. & Merrill, A. H. Inhibition of sphingolipid biosynthesis by fumonisins. Implications for diseases associated with *Fusarium moniliforme*. *J. Biol. Chem.* **266**, 14486–14490 (1991).
32. Kim, S. H., Singh, M. P., Sharma, C. & Kang, S. C. Fumonisin B1 actuates oxidative stress-associated colonic damage via apoptosis and autophagy activation in murine model. *J. Biochem. Mol. Toxicol.* e22161 (2018). <https://doi.org/10.1002/jbt.22161>. Epub ahead of print.
33. Kunz, L. et al. Ca²⁺-activated, large conductance K⁺ channel in the ovary: identification, characterization, and functional involvement in steroidogenesis. *J. Clin. Endocrinol. Metab.* **87**, 5566–5574 (2002).
34. Xu, F. & Stouffer, R. L. Existence of the lymphatic system in the primate corpus luteum. *Lymphat. Res. Biol.* **7**, 159–168 (2009).
35. Cowart, L. A., Szulc, Z., Bielawska, A. & Hannun, Y. A. Structural determinants of sphingolipid recognition by commercially available anti-ceramide antibodies. *J. Lipid Res.* **43**, 2042–2048 (2002).
36. Schmid, N. et al. Characterization of a nonhuman primate model for the study of testicular peritubular cells - comparison with human testicular cells. *Mol. Hum. Reprod.* <https://doi.org/10.1093/molehr/gay025> (2018).
37. Cox, J. & Mann, M. MaxQuant enables high peptide identification rates, individualized p.p.b.-range mass accuracies and proteome-wide protein quantification. *Nat. Biotechnol.* **26**, 1367–1372 (2008).
38. Huang da, W., Sherman, B. T. & Lempicki, R. A. Systematic and integrative analysis of large gene lists using DAVID bioinformatics resources. *Nat. Protoc.* **4**, 44–57 (2009).
39. Huang da, W., Sherman, B. T. & Lempicki, R. A. Bioinformatics enrichment tools: paths toward the comprehensive functional analysis of large gene lists. *Nucleic Acids Res.* **37**, 1–13 (2009).
40. van Iersel, M. P. et al. Presenting and exploring biological pathways with PathVisio. *BMC Bioinforma.* **9**, 399 (2008).
41. Kutmon, M. et al. PathVisio 3: an extendable pathway analysis toolbox. *PLoS Comput. Biol.* **11**, e1004085 (2015).
42. Bogan, R. L., Murphy, M. J., Stouffer, R. L. & Hennebold, J. D. Systematic determination of differential gene expression in the primate corpus luteum during the luteal phase of the menstrual cycle. *Mol. Endocrinol.* **22**, 1260–1273 (2008).
43. Xu, J. et al. Anti-Mullerian hormone is produced heterogeneously in primate preantral follicles and is a potential biomarker for follicle growth and oocyte maturation in vitro. *J. Assist. Reprod. Genet.* **33**, 1665–1675 (2016).
44. Chaffin, C. L., Dissen, G. A. & Stouffer, R. L. Hormonal regulation of steroidogenic enzyme expression in granulosa cells during the peri-ovulatory interval in monkeys. *Mol. Hum. Reprod.* **6**, 11–18 (2000).
45. Zhou, X. et al. Prosaposin facilitates sortilin-independent lysosomal trafficking of progranulin. *J. Cell Biol.* **210**, 991–1002 (2015).
46. Cheng, M. H. & Jansen, R. P. A jack of all trades: the RNA-binding protein vigilin. *Wiley Interdiscip. Rev. RNA* **8**, 1448 (2017).
47. Takahashi, N. et al. Necrostatin-1 analogues: critical issues on the specificity, activity and in vivo use in experimental disease models. *Cell death & Dis.* **3**, e437–e437 (2012).
48. Zhou, W. & Yuan, J. Necroptosis in health and diseases. *Semin. Cell Dev. Biol.* **35**, 14–23 (2014).
49. Grootjans, S., Vanden Berghe, T. & Vandenabeele, P. Initiation and execution mechanisms of necroptosis: an overview. *Cell Death Differ.* **24**, 1184 (2017).
50. Abraham, M. C., Lu, Y. & Shaham, S. A morphologically conserved non-apoptotic program promotes linker cell death in *Caenorhabditis elegans*. *Dev. Cell* **12**, 73–86 (2007).
51. Wang, S. W. et al. Regulation of ceramide generation during macrophage apoptosis by ASMase and de novo synthesis. *Biochim. Et. Biophys. Acta (BBA) - Mol. Cell Biol. Lipids* **1851**, 1482–1489 (2015).
52. Parisi, L. R., Li, N. & Atilla-Gokcumen, G. E. Very long chain fatty acids are functionally involved in necroptosis. *Cell Chem. Biol.* **24**, 1445–1454.e1448 (2017).
53. Domijan, A. M., Zeljezic, D., Milic, M. & Peraica, M. Fumonisin B(1): oxidative status and DNA damage in rats. *Toxicology* **232**, 163–169 (2007).
54. Vandenabeele, P., Riquet, F. & Cappe, B. Necroptosis: (last) message in a bubble. *Immunity* **47**, 1–3 (2017).
55. Santana, P. et al. Ceramide mediates tumor necrosis factor effects on P450-aromatase activity in cultured granulosa cells. *Endocrinology* **136**, 2345–2348 (1995).
56. Witty, J. P., Bridgham, J. T. & Johnson, A. L. Induction of apoptotic cell death in hen granulosa cells by ceramide. *Endocrinology* **137**, 5269–5277 (1996).
57. Liao, D. et al. Necrosulfonamide inhibits necroptosis by selectively targeting the mixed lineage kinase domain-like protein. *MedChemComm* **5**, 333–337 (2014).
58. Sawai, H., Ogiso, H. & Okazaki, T. Differential changes in sphingolipids between TNF-induced necroptosis and apoptosis in U937 cells and necroptosis-resistant sublines. *Leuk. Res.* **39**, 964–970 (2015).
59. Sentelle, R. D. et al. Ceramide targets autophagosomes to mitochondria and induces lethal mitophagy. *Nat. Chem. Biol.* **8**, 831–838 (2012).
60. Devoto, L., Kohen, P., Munoz, A. & Strauss, J. F. 3rd Human corpus luteum physiology and the luteal-phase dysfunction associated with ovarian stimulation. *Reprod. Biomed. Online* **18**(Suppl 2), 19–24 (2009).
61. Fabregat, A. et al. The reactome pathway knowledgebase. *Nucleic Acids Res.* **46**, D649–d655 (2018).

Supplement File

Supplement Fig. 1: Pathway illustration of known reactions of sphingolipid metabolism and the ceramide salvage pathway.

Metabolites are shown in rectangular boxes with rounded corners and proteins in rectangular boxes colored according to the log₂ fold change between day 5 and day 2. Proteins were colored with the shown gradient according to their log₂ fold change. Proteins with no significant change in abundancies are shown in grey.

Supplement Fig. 2: Illustration of ceramide salvage pathway associated genes/proteins generated by transcriptomic/proteomic analysis.

LFQ values and log₂ transformed transcriptome data for specified proteins/genes are shown in column diagrams. In most cases, the tendency was the same for proteomic and transcriptomic data. P-values and fold changes are shown in Supplement Tab. 1 and p < 0.05 is marked with an asterisk (*). Proteomic data, n = 5; transcriptomic data, n = 8. Error bars indicate SEM.

Supplement Fig. 3: Confocal microscopy images of immunostained GCs and Western blot results showing actions of NSA

(a) GCs, cultured on glass coverslips were fixed on day 2 or 5 of culture, or stimulated with NSA (20 μM, 72 h) before fixation. Immunocytochemical staining using anti-ceramide and anti-golgin97 antibodies revealed different intensities and loci due to culture time and stimulation. Controls using mouse IgG and IgM are shown in insets of the first column. Three independent experiments were conducted, and representative pictures are shown. Scale bars indicate 50 μm.

(b, c) Western Blot of GCs stimulated for 72 h either with (b) the solvent control, (b, c) 50 μM C2-CER alone or (c) in combination with 20 μM NSA showed phosphorylation of MLKL at T357/S358, and oligomerization. In all groups, monomeric pMLKL(T357/S358) bands at <55 kDa and octameric pMLKL(T357/S358) at >250 kDa were evident. The Western Blots were evaluated by quantification of 5 independent experiments per group. Intensity of the pMLKL(T357/S358) bands (monomeric + oligomeric) were normalized to the MLKL band. Representative blots are shown. (b, c) paired Student's *t*-test was conducted to evaluate statistical significance (*p < 0.05);

means and SEM are shown.

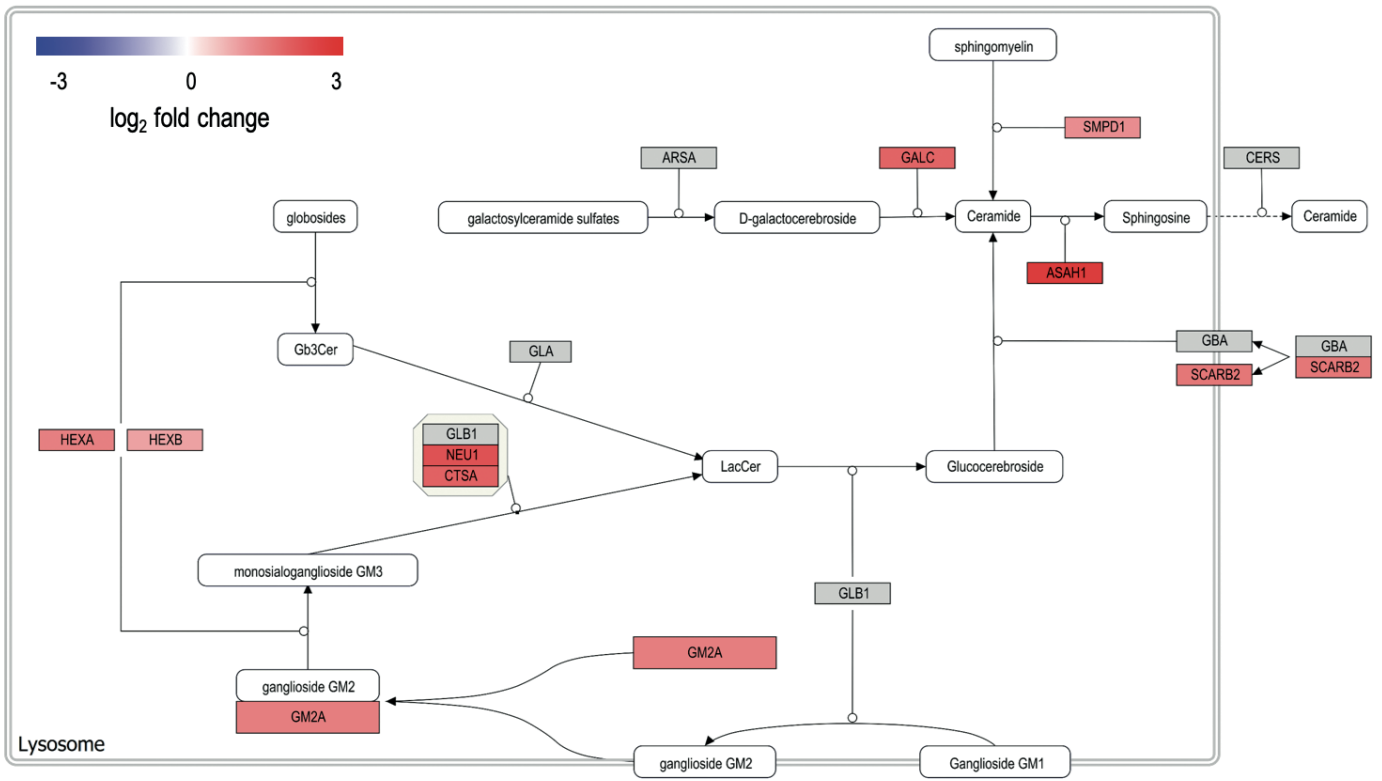
Supplement Fig. 4: Confocal microscopy images of immunostained GCs showing actions of FB1 and Nec1s.

(a) GCs, cultured on glass coverslips were fixed on day 2 (left column) or day 5 (middle column) of culture, with or without stimulation by FB1 (0.5 μ M, 72 h, right column) before fixation. Controls using rabbit IgG and mouse IgM are shown in insets of the first row. (b) In another experiment GCs were cultured the same way but stimulated with Nec-1s (20 μ M, 72 h, right column) instead of FB1. Immunocytochemical staining using anti-ceramide and anti-golgin97 antibodies revealed different intensities and cellular localization, depending on culture time and stimulation. Two independent experiments were performed and representative pictures are shown. Scale bars indicate 25 μ m (a) and 50 μ m (b).

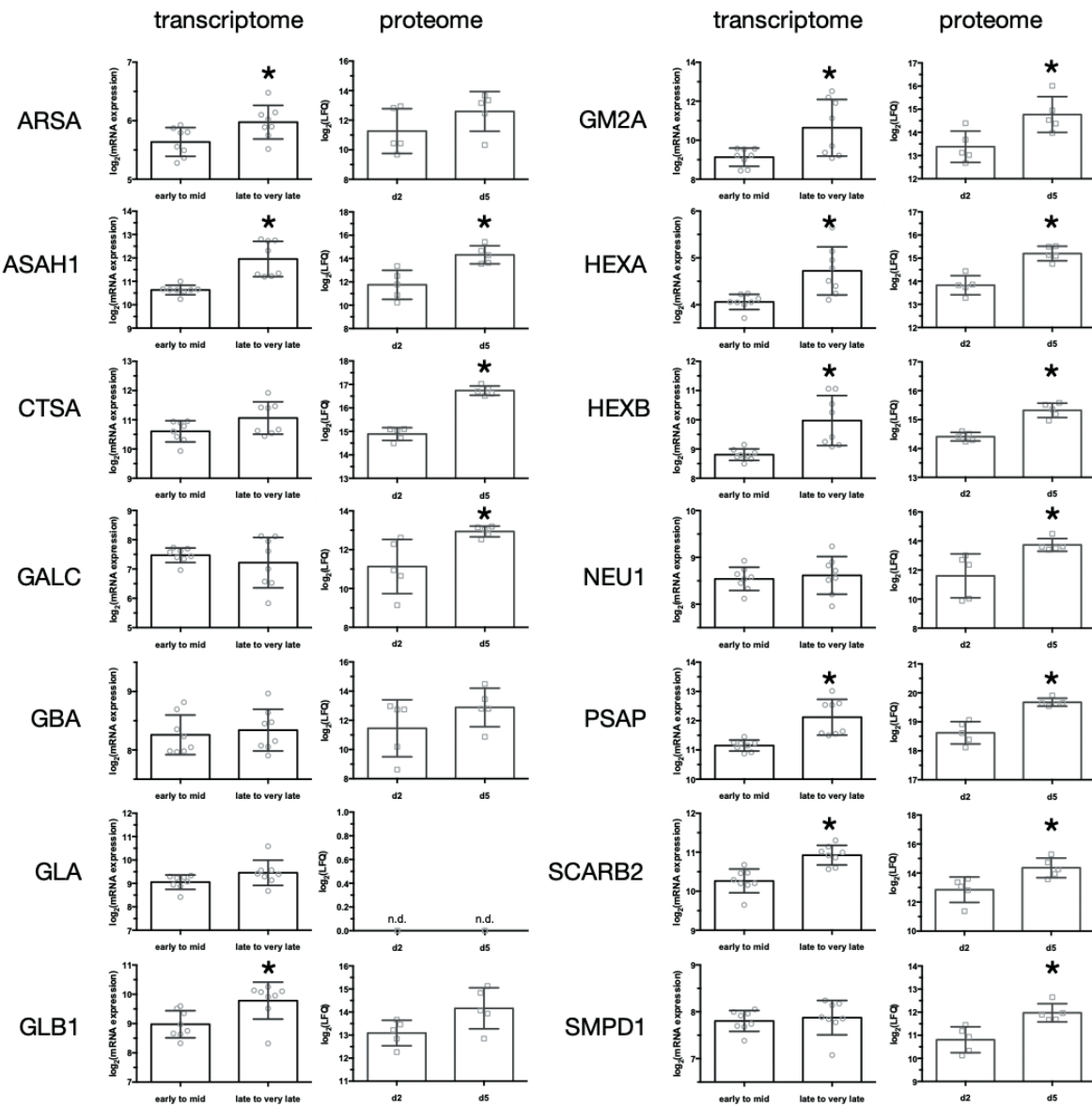
Supplement Tab. 1: The levels of proteins and genes (mRNA) involved in ceramide salvage pathway, which were upregulated after 5 days of culture in human IVF-derived GCs and in the late stage macaque CL, respectively.

The p-values resulted from Student's *t*-test with Welch's correction analysis of log₂ fold change values of protein and mRNA expression data of cultured GCs and timed macaque CL.

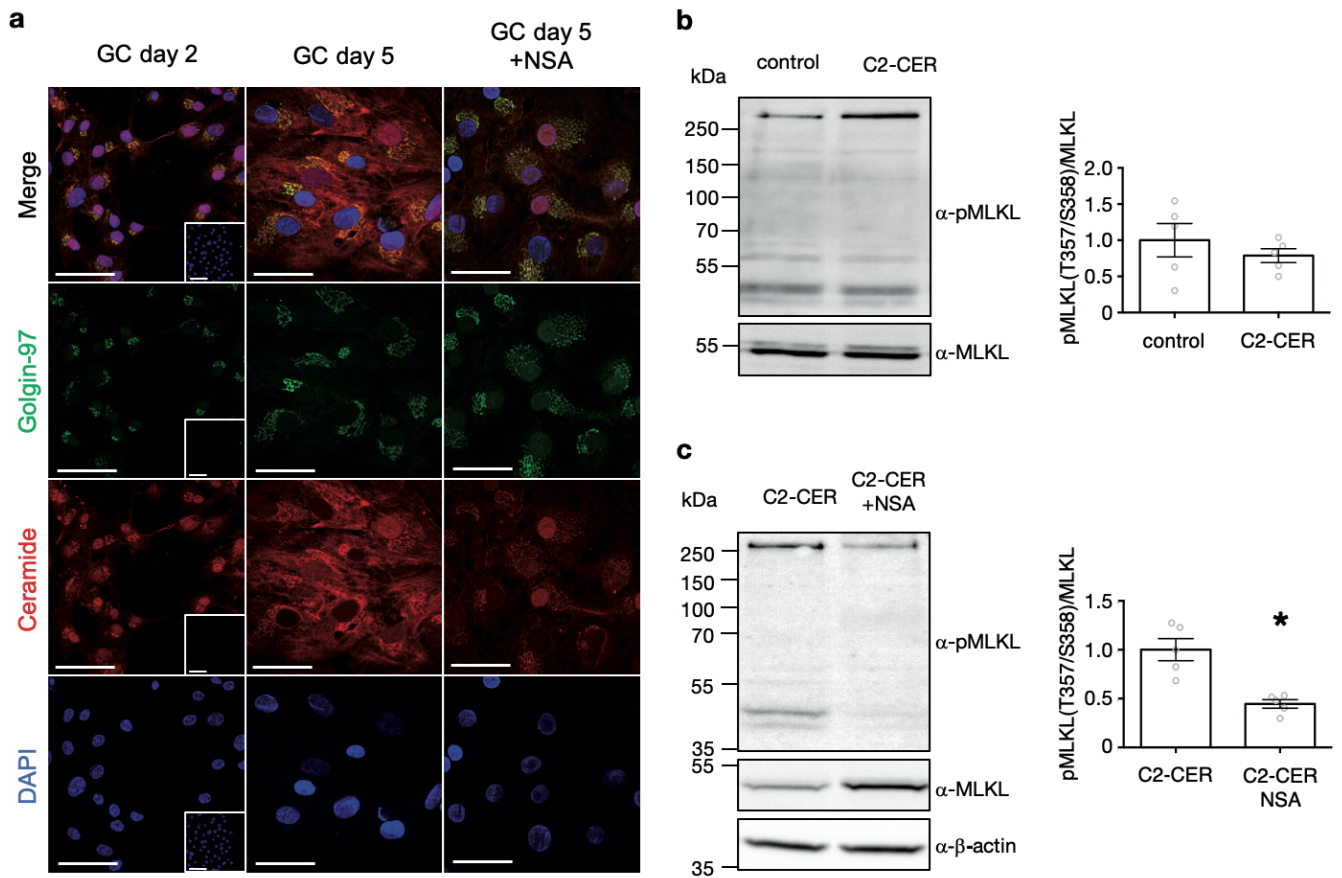
Supplement Figure 1



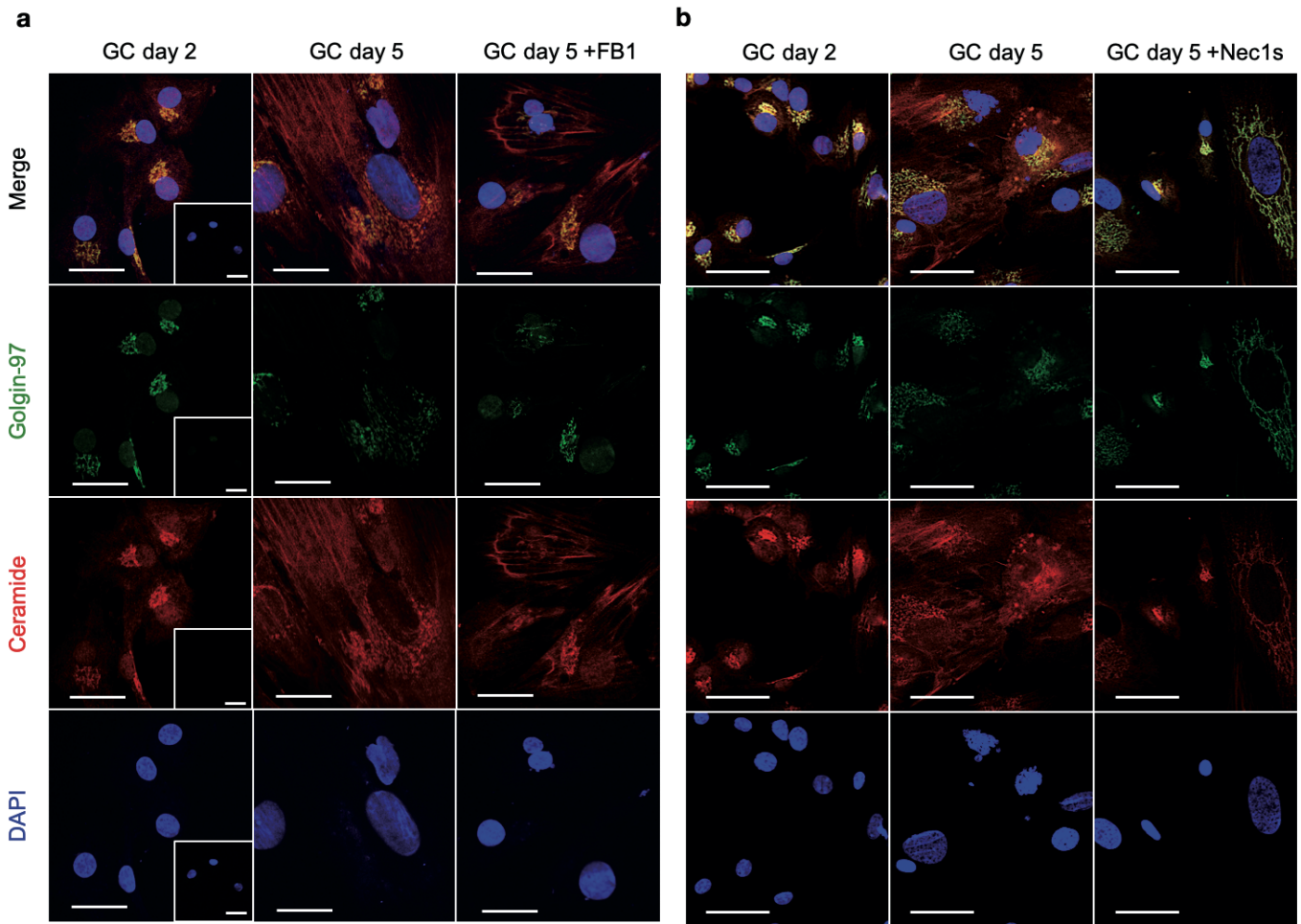
Supplement Figure 2



Supplement Figure 3



Supplement Figure 4



Supplement Table 1

		protein levels (GC d5 vs. d2)		mRNA levels (late vs. early CL)	
gene name	protein name	p value	log2 FC	p value	log2FC
ARSA	arylsulfatase A	0.181	1.329	0.024	0.338
ASAH1	acid ceramidase	0.006	2.568	0.001	1.326
CTSA	cathepsin A	3.72E-06	1.848	0.071	0.456
GALC	galactocerebrosidase	0.043	1.809	0.439	-0.252
GBA	glucosylceramidase	0.217	1.427	0.649	0.081
GLA	a-galactosidase A	n.d.	n.d.	0.091	0.399
GLB1	b-galactosidase	0.058	1.073	0.011	0.807
GM2A	GM2 ganglioside activator	0.017	1.389	0.014	1.510
HEXA	hexosaminidase subunit a	4.81E-04	1.369	0.004	0.662
HEXB	hexosaminidase subunit b	2.81E-04	0.911	0.002	1.168
NEU1	sialidase 1	0.032	2.124	0.661	0.075
PSAP	prosaposin	0.002	1.056	0.001	0.967
SCARB2	lysosomal membrane protein 2	0.017	1.510	0.001	0.661
SMPD1	acid sphingomyelinase	0.006	1.166	0.646	0.071

3.2 Publication 2 (Du, Bagnjuk et al. 2018)

Acetylcholine and necroptosis are players in follicular development in primates

Yongrui Du*, Konstantin Bagnjuk*, Maralee S. Lawson, Jing Xu & Artur Mayerhofer

Scientific Reports, Vol. 8, No. 6166, 2018, DOI: 10.1038/s41598-018-24661-z

*co-first author

***In vitro* 3D-culture of primate follicles**

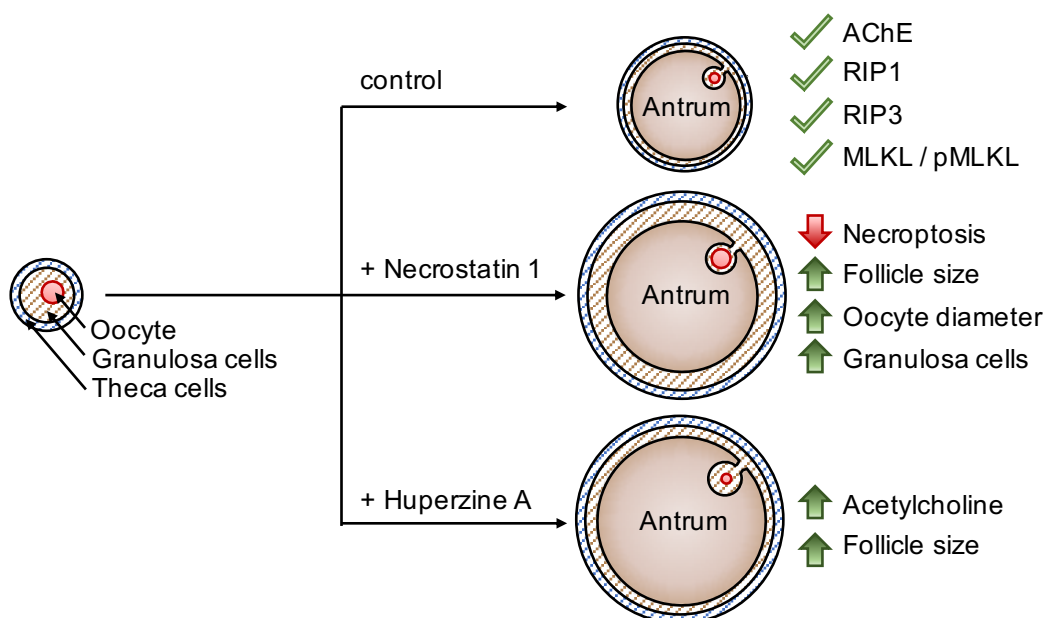


Figure 6 Graphical summary of publication 2 (Du, Bagnjuk et al. 2018)

Secondary rhesus monkey follicles were cultured under the influence of necrostatin 1 or Huperzine A. The expression of the necroptotic machinery and acetylcholinesterase were verified. Addition of necrostatin 1 blocked necroptosis and consequently improved follicle growth by increasing the follicle and oocyte size and the granulosa cell number. Huperzine A blocked endogenous acetylcholinesterase, which elevated acetylcholine levels and increased follicle size.

SCIENTIFIC REPORTS

OPEN

Acetylcholine and necroptosis are players in follicular development in primates

Yongrui Du^{1,2}, Konstantin Bagnjuk³, Maralee S. Lawson¹, Jing Xu^{1,4} & Artur Mayerhofer³

Acetylcholine (ACh) in the ovary and its actions were linked to survival of human granulosa cells *in vitro* and improved fertility of rats *in vivo*. These effects were observed upon experimental blockage of the ACh-degrading enzyme (ACh esterase; AChE), by Huperzine A. We now studied actions of Huperzine A in a three-dimensional culture of macaque follicles. Because a form of programmed necrotic cell death, necroptosis, was previously identified in human granulosa cells *in vitro*, we also studied actions of necrostatin-1 (necroptosis inhibitor). Blocking the breakdown of ACh by inhibiting AChE, or interfering with necroptosis, did not improve the overall follicle survival, but promoted the growth of macaque follicles from the secondary to the small antral stage *in vitro*, which was correlated with oocyte development. The results from this translational model imply that ovarian function and fertility in primates may be improved by pharmacological interference with AChE actions and necroptosis.

Acetylcholine (ACh) is known as an important neurotransmitter of the central and the peripheral nervous systems. Its actions are mediated by nicotinic and muscarinic receptors. In addition, ACh is also produced by non-neuronal cells in various organ systems. Roles of non-neuronal ACh are emerging in the skin, the respiratory system, the cardiovascular system, the immune systems and the reproductive system^{1–4}.

In the ovary, granulosa cells are producers and targets of ACh^{5,6}. Previous studies, mainly using cultured granulosa cells collected from patients undergoing *in vitro* fertilization, implicated ACh in the regulation of cell viability and proliferation. ACh induced muscarinic receptor-mediated elevations of intracellular Ca²⁺ levels and transcription factor expression, activation of ion channels and breakdown of gap junction communication, which resulted in trophic, growth-promoting actions^{4,7–10}. Studies in mice indicated that follicle-stimulating hormone (FSH) stimulated ACh production by granulosa cells¹¹. Thus, ACh could participate in mediating FSH-actions in the avascular compartment of the ovary. Studies in the bovine corpus luteum were also in line and supported the trophic action of ACh in the ovary¹².

In neurons, ACh is cleaved and deactivated by acetylcholinesterase (AChE). AChE was also expressed by granulosa cells collected from patients undergoing *in vitro* fertilization¹³. Blocking AChE activity by a potent and selective inhibitor, Huperzine A, consequently enhanced granulosa cell survival in culture¹³. A subsequent systemic study in rats demonstrated that Huperzine A, when applied locally to the ovarian bursa, increased intra-ovarian ACh levels and promoted specifically the growth of preantral follicles to the early antral stage¹⁴. Furthermore, the treatment significantly enhanced antral follicle maturation, ovulation and fertility outcomes. Since AChE blockers are commonly used in the treatment of Alzheimer's disease¹⁵, they could be explored as agents to facilitate ovarian follicular development via regulating granulosa cell viability and proliferation.

The study mentioned above¹³ also led to the insight that cultured human granulosa cells can die not only by apoptosis, but also by necroptosis, i.e. programmed necrotic cell death, which was not previously described in ovarian cells^{13,16–19}. Necroptosis involves necrosome assembly, i.e., a cascade of interacting kinases cumulating in the execution of necrotic cell death. Interfering with activities of necrosome components, e.g., by necrostatin-1,

¹Division of Reproductive & Developmental Sciences, Oregon National Primate Research Center, Oregon Health & Science University, 505 NW 185th Avenue, Beaverton, Oregon, 97006, USA. ²Department of Reproductive Medicine, Tianjin Central Hospital of Gynecology Obstetrics, No 156 Nankai Sanma Road, Nankai District, Tianjin, 300100, China. ³BMC Munich, Cell Biology, Anatomy III, Ludwig-Maximilians-University, Grosshaderner Str. 9, D-82152, Planegg, Martinsried, Germany. ⁴Department of Obstetrics and Gynecology, School of Medicine, Oregon Health & Science University, 3181 SW Sam Jackson Park Road, Portland, Oregon, 97239, USA. Yongrui Du, Konstantin Bagnjuk, Jing Xu and Artur Mayerhofer jointly supervised this work. Correspondence and requests for materials should be addressed to A.M. (email: Mayerhofer@lrz.uni-muenchen.de)

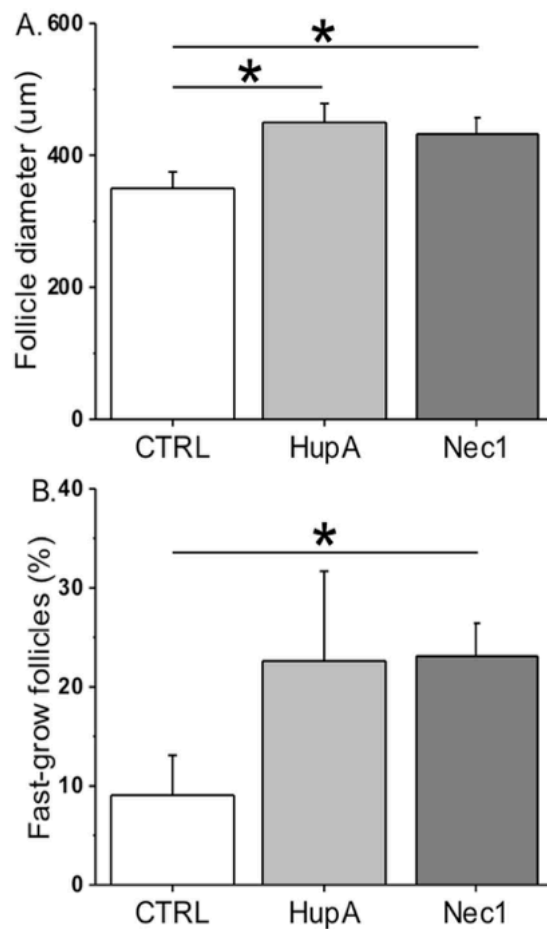


Figure 1. The effects of Huperzine A and necrostatin-1 on rhesus macaque follicle growth after 5 weeks of culture in an alginate matrix. Follicle growth was presented as follicle diameters (A) and as percentages of fast-grow follicles (diameter $\geq 500 \mu\text{m}$) versus total growing follicles (B). CTRL, vehicle control; HupA, Huperzine A addition; Nec1, necrostatin-1 addition. *Significant difference between treatment groups ($P < 0.05$). Data are presented as the mean \pm SEM with 18–31 follicles and 5 animals per experimental group.

inhibited necroptosis in cultured human granulosa cells¹³. While the existence of necroptosis in the rodent ovary remains to be determined, follicular expression of phosphorylated mixed lineage kinase domain-like protein (MLKL), pMLKL(S358) as a necroptosis marker, was detected in the human and nonhuman primate antral follicles by immunohistochemistry¹³. This implies physiological relevance of necroptosis in the primate ovary. It remains to be studied, which factors trigger ovarian necroptosis¹⁹. Although necroptosis occurred in cultured granulosa cells, there are no insights into its regulation, aside from a peptide derived from a splice variant of *ACHE*, namely “read-through variant” (*ACHE-R*)^{20,21}, which enhanced this process¹³.

Based on the results obtained in human granulosa cells and in the systemic rat study, additional experiments were designed, in which the consequences of (1) pharmacological manipulation of ACh breakdown and (2) interference with necroptosis were studied in nonhuman primate growing follicles from the secondary to the small antral stage *in vitro*.

Results

Huperzine A treatment. Under control conditions, *in vitro*-developed macaque antral follicles produced ACh, which was detectable in the culture media. Huperzine A addition during culture increased ($P < 0.05$) media concentrations of ACh compared with the vehicle control group (1.23 ± 0.09 versus $0.93 \pm 0.06 \mu\text{M}$; $n = 26$ and 17 follicles from 5 animals, respectively).

The percentage of rhesus macaque follicles that survived relative to the total number cultured was $56 \pm 9\%$ in the vehicle control group at culture week 5. Huperzine A addition had no effect on follicle survival after 5 weeks of culture ($58 \pm 11\%$) compared with controls.

Rhesus macaque follicles that survive *in vitro* can be divided into distinct cohorts based on their growth by week 5 as previously described²². While non-growing follicles remained at the preantral stage throughout 5 weeks of culture, growing follicles formed an antrum at week 3. The percentages of growing versus total surviving follicles were comparable between the vehicle control and Huperzine A group (50 ± 7 versus $73 \pm 13\%$). However, though starting with equivalent sizes in the beginning of culture, growing follicles attained larger ($P < 0.05$) diameters at week 5 of culture in the Huperzine A group compared with those of the vehicle control group (Fig. 1A). Growing follicles with diameters $\geq 500 \mu\text{m}$ at culture week 5 were termed as fast-grow follicles, as previously

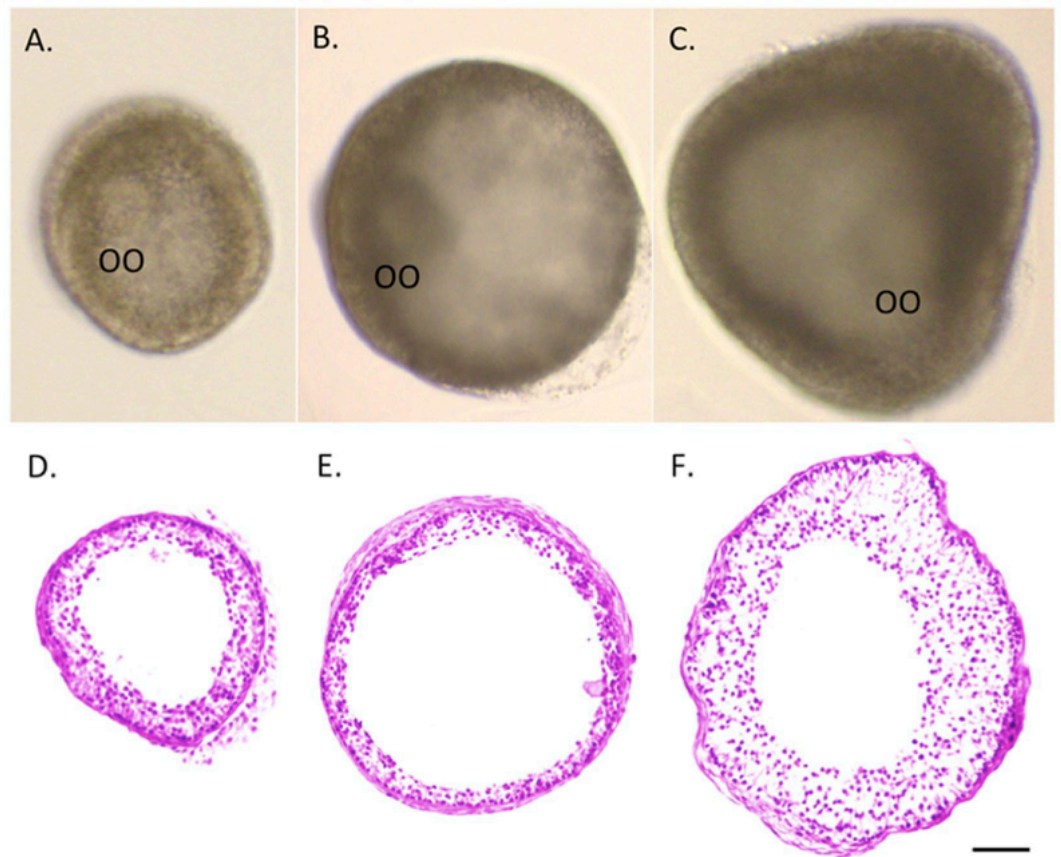


Figure 2. *In vitro*-developed rhesus macaque follicles following 5 weeks of culture in an alginate matrix with exposure of the control vehicle (A), Huperzine A (B) and necrostatin-1 (C) were stained with hematoxylin and eosin, respectively (D,E,F). OO, oocyte. Scale bar = 100 μ m.

described²². There were no significant differences between the vehicle control and Huperzine A group on the percentages of fast-grow versus total growing follicles at culture week 5 (Fig. 1B).

Following 5 weeks of culture, hematoxylin and eosin staining of follicles (the largest sections of follicles to show the relative follicle diameters and the thickness of follicle walls) from the vehicle control (Fig. 2A and D) and Huperzine A (Fig. 2B and E) groups revealed a morphology similar to that observed in *in vivo*-developed small antral follicles in primates²³, in terms of a spherical shape with an oocyte and an antral cavity, multiple layers of granulosa cells and an intact basement membrane.

In vitro-developed macaque antral follicles produce appreciable amounts of ovarian steroid hormones, including progesterone (P4), androstenedione (A4) and estradiol (E2), into the culture media, as reported previously²². Huperzine A addition did not statistically alter media P4, A4 or E2 concentrations produced by growing follicles compared with those of the vehicle controls at culture week 5 (P4: 11 ± 4 versus 8 ± 4 ng/ml; A4: 3 ± 2 versus 5 ± 3 pg/ml; E2: 487 ± 175 versus 289 ± 88 pg/ml).

Healthy, germinal vesicle stage oocytes surrounded by cumulus cells were obtained from *in vitro*-developed macaque antral follicles after 5 weeks of culture in the vehicle control and Huperzine A groups (Fig. 3A). Huperzine A treatment did not alter the oocyte diameters relative to the control group (Fig. 3B).

Necrostatin-1 treatment. Neither the follicle survival rates nor the percentage of growing versus total surviving follicles at culture week 5 were altered by necrostatin-1 treatment relative to the vehicle control group (survival: 64 ± 10 versus $56 \pm 9\%$; growth: 69 ± 15 versus $50 \pm 7\%$). However, diameters of growing follicles at culture week 5 were larger ($P < 0.05$) in the necrostatin-1 group than those of the vehicle control group (Fig. 1A). In addition, percentages of fast-grow follicles were greater ($P < 0.05$) following necrostatin-1 exposure compared with those of the vehicle controls (Fig. 1B). Hematoxylin and eosin staining at culture week 5 showed that follicles cultured with necrostatin-1 had an extensively developed granulosa layer (Fig. 2C and F) relative to follicles in the vehicle control group (Fig. 2A and D).

There were no statistically significant differences between the vehicle control and necrostatin-1 group on the media concentrations of P4 (8 ± 4 versus 5 ± 2 ng/ml), A4 (5 ± 3 versus 2 ± 2 pg/ml) or E2 (289 ± 88 versus 723 ± 265 pg/ml) produced by growing follicles at culture week 5. *In vitro*-developed macaque antral follicles in the necrostatin-1 group produced healthy, germinal vesicle stage oocytes surrounded by cumulus cells. Compared with the vehicle controls, the oocyte diameters at week 5 increased ($P < 0.05$) in follicles following necrostatin-1 exposure (Fig. 3B).

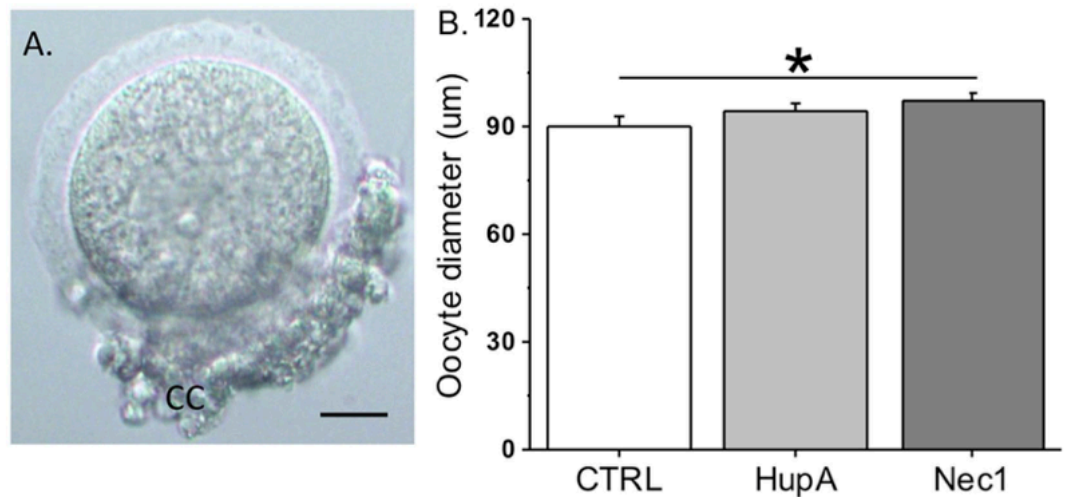


Figure 3. The effects of Huperzine A and necrostatin-1 on oocyte growth in rhesus macaque antral follicles after 5 weeks of culture in an alginate matrix. Oocytes obtained were surrounded by cumulus cells (A; representative from the vehicle control group). Oocyte growth was determined by measuring oocyte diameters. CC, cumulus cells; CTRL, vehicle control; HupA, Huperzine A addition; Nec1, necrostatin-1 addition. *Significant difference between treatment groups ($P < 0.05$). Data are presented as the mean \pm SEM with 18–31 oocytes per experimental group. Scale bar = 25 μm .

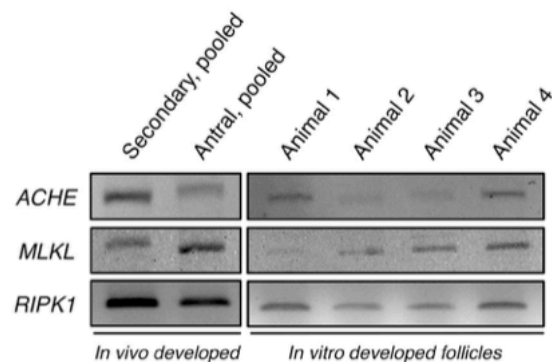


Figure 4. RT-PCR analysis on the expression of acetylcholinesterase (*ACHE*), mixed lineage kinase domain-like protein (*MLKL*), receptor-interacting serine/threonine-protein kinase 1 (*RIPK1*) by *in vivo*-developed secondary and antral follicles pooled from 4 macaques, respectively, as well as by *in vitro*-developed antral follicles (under control culture conditions) from 4 individual macaques. Electrophoresis and Midori Green staining were performed using the same protocol for all gels. Results were cropped and grouped. Original gels are provided in the supplemental dataset.

Expression of *ACHE* and of necrosome components. The mRNA expression of *ACHE* and the necrosome components (*MLKL*, receptor-interacting serine/threonine-protein kinase 1 or *RIPK1*) were detected in *in vivo*-developed macaque secondary and antral follicles (Fig. 4). *In vitro*-developed antral follicles from all 4 macaques expressed *ACHE*, *MLKL*, *RIPK1*, as identified by RT-PCR (Fig. 4). Amplicon identities were confirmed by sequencing.

In addition, *RIPK1* and *RIPK3* proteins were readily detected in the preantral and antral follicles, mainly in granulosa cells, of macaque ovaries by immunohistochemistry (Fig. 5A). Granulosa cells of some *in vivo*-developed macaque follicles were stained for pMLKL(S358) (Fig. 5A). Positive immunostaining of pMLKL(S358) was also detected in the cytoplasm of granulosa cells in *in vitro*-developed antral follicles from all 4 macaques (Fig. 5B). No pMLKL(S358)-positive staining was evident in negative control sections (Fig. 5A and C) or *in vitro*-developed antral follicles cultured with necrostatin-1 (Fig. 5D).

Discussion

The present study utilized a three-dimensional follicle culture system²² to explore roles of ACh and necroptosis during primate follicular development. Pharmacological inhibition of ACh-breakdown was achieved by *ACHE*-blocker Huperzine A. Necroptosis was inhibited by intercepting *RIPK1* actions using necrostatin-1. Both approaches enhanced follicular development from the secondary to the small antral stage *in vitro*. The results

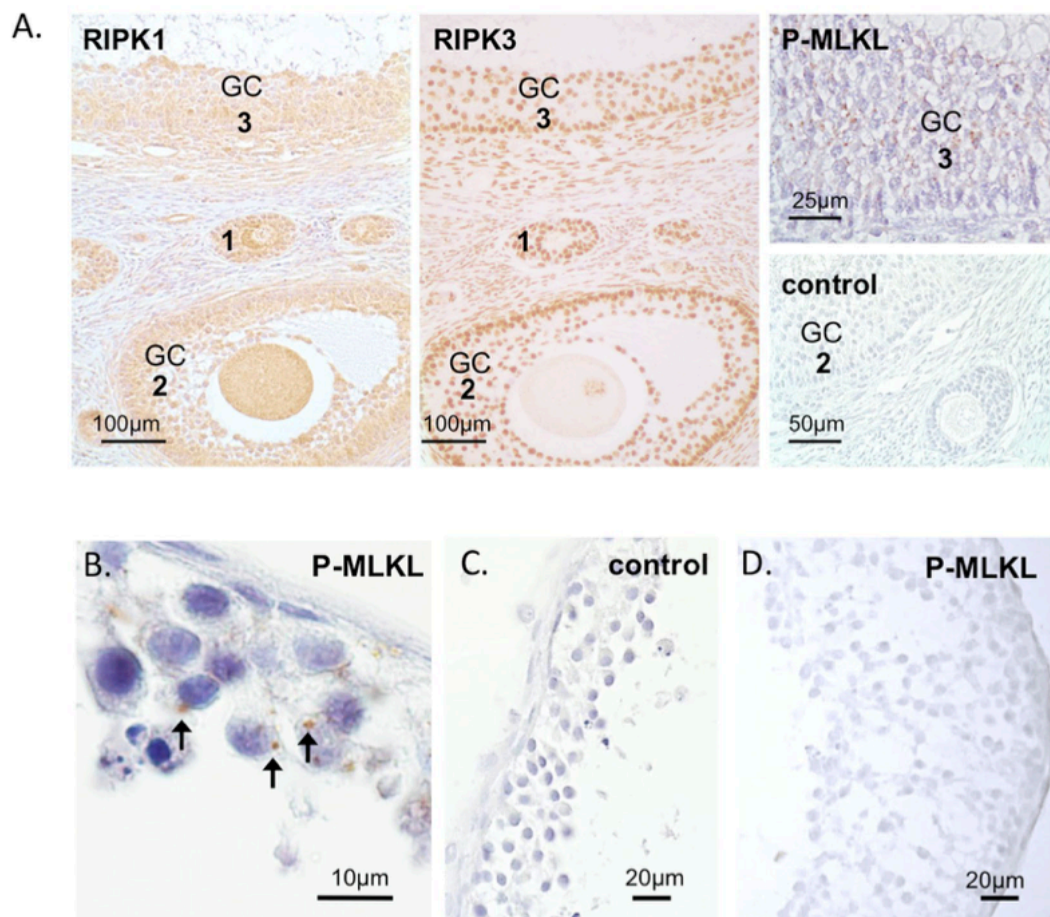


Figure 5. Immunohistochemical detection of necroptosis-related proteins in macaque ovarian follicles. Receptor-interacting serine/threonine-protein kinase 1 (RIPK1) and 3 (RIPK3) were identified in *in vivo*-developed preantral (1), small antral (2) and large antral (3) follicles, mainly in granulosa cells (GC) (A). Granulosa cells of some follicles were stained for phosphorylated mixed lineage kinase domain-like protein, pMLKL(S358) (A). Positive staining of pMLKL(S358) was also detected in the granulosa cells of *in vitro*-developed small antral follicles cultured under control conditions (B; arrows), but not in the negative controls (A,C) or follicles cultured with necrostatin-1 (D). Counterstaining was performed using haematoxylin.

of the present study performed in a translational model reveal previously unknown roles for ACh/ACHE and necroptosis in follicular development, and indicate that pharmacological agents, which target these processes, may be suitable to enhance follicular development.

ACh production and some of its actions were previously identified in granulosa cells of the ovarian follicle. ACh acted via muscarinic receptors, which were detected in macaque and human ovarian follicles⁴. Downstream actions studied in human granulosa cells included among others breakdown of gap junctions and increasing proliferation^{7,8}. Further studies in granulosa cells obtained from patients undergoing *in vitro* fertilization demonstrated the positive impact of ACh on cell viability in culture¹³. The addition of Huperzine A, which blocks ACHE actions²⁴, generated similar outcomes¹³. In a follow-up systemic study in rats, Huperzine A administration to the ovarian bursa elevated ovarian ACh levels, specifically enhanced the growth of preantral follicles, improved ovulation, and increased overall fertility¹⁴. When the same concentration of Huperzine A was used for macaque follicle culture in the present study, it promoted follicle growth from the secondary to the small antral stage, as indicated by larger follicle diameters, implying a trophic action of ACh in granulosa cells. ACh levels produced by *in vitro*-developed follicles increased following Huperzine A treatment, as demonstrated in the current study, and higher bioavailable ACh stimulated granulosa cell proliferation and viability in macaque follicles, which is consistent with previous studies.

The previous study in rats¹⁴ showed that Huperzine A treatment increased the number of small antral follicles *in vivo*. However, in our current study, blocking ACHE actions did not increase the overall survival of macaque follicles developed *in vitro*, which could be due to the fact that follicle survival involves both granulosa cell and oocyte viability. Oocytes may have an important role in regulating follicular development²⁵. In this context, expression of receptors for ACh in rhesus macaque preovulatory follicle-derived oocytes⁷ indicates that the oocyte could be a direct target of ACh. Future studies are warranted to determine whether oocytes from preantral and small antral follicles are affected by ACh and what the outcomes are.

Once ovarian follicles start to grow, they either reach the preovulatory stage or undergo atresia. Apoptosis of oocytes and granulosa cells has been intensively studied and is suggested to be the underlying mechanism of follicular atresia throughout species^{26,27}. Recently, necroptosis was described in cultured human granulosa cells¹³, which could be intercepted by drugs targeting the necrosome¹⁶. In human granulosa cells, the RIPK1 inhibitor necrostatin-1 and the MLKL blocker necrosulfonamide reduced necroptosis significantly¹³. A specific marker pMLKL(S358) was detected in human and macaque granulosa and luteal cells, which provided first evidence of necroptosis in the primate ovary¹³.

Consistently, the present study demonstrated expression of the necrosome components *MLKL* and *RIPK1* in macaque follicles developed *in vivo* and *in vitro*. RIPK1, RIPK3 and pMLKL(S358) proteins were also detected in macaque ovarian follicles. The presence of pMLKL(S358) clearly indicated ongoing necroptosis in macaque follicles. To further explore involvement of necroptosis in follicular development, necrostatin-1 was introduced into the follicle culture system with the same concentration as what was used in human granulosa cell culture¹³. Macaque secondary follicles cultured in the presence of necrostatin-1 grew larger than the control follicles as indicated by increased follicle diameters, greater percentages of fast-grow follicles and well-developed granulosa layers. Therefore, besides apoptosis, necroptosis appears to be an important additional mechanism in regulating follicular cell death, at least in the primate ovary.

Although diameters of *in vitro*-developed antral follicles increased following either Huperzine A or necrostatin-1 exposure, more fast-grow follicles were obtained only from the necrostatin-1 group containing oocytes with larger diameters. It could be due to a suboptimal dose of Huperzine A employed, the greater impact of necroptosis in follicular growth, in general. These points, which are the heart of the question how follicular growth is regulated, require additional studies. Growth of follicles is also reflected by active E2 production by well-developed granulosa cells, specifically in the necrostatin-1-treated follicles, though the differences in media E2 levels did not reach statistical significance. Results from the current study suggest that inhibition of necroptosis has the potential to promote primate follicular development, which may be used to improve outcomes of *in vitro* follicle maturation protocols.

Several ACHE-blockers are used clinically for the treatment of Alzheimer's disease^{15,28,29}. Necroptosis-blockers are being developed and tested for treatment of various medical conditions¹⁵. It appears conceivable that these agents could also be used to manipulate follicular development, either by enhancing granulosa cell proliferation or by interfering with granulosa cell necroptosis. Studies are warranted to explore their effectiveness in treatment of ovarian dysfunction.

It is not clear whether the cholinergic system in the ovary⁶ is affected by circulating ACHE or the related enzyme, butyrylcholine-esterase (BCHE). Both enzymes break down ACh and were active in human follicular fluid¹³. ACHE and BCHE increase in the circulation with age in women³⁰. Hence, it seems that changes in the circulating levels of these enzymes could be superimposing factors affecting the fate of ovarian follicles by lowering available ACh. The age-related decline of the functional ovarian reserve is thought to be a consequence of follicular atresia, which ultimately leads to depletion of the ovarian follicle pool, and hence, menopause^{26,27,31}. Studies are now warranted to explore the involvement of ACh/ACHE and necroptosis in the process of follicular atresia.

In summary, both Huperzine-A and necrostatin-1 promoted overall follicular development during encapsulated three-dimensional culture in rhesus macaques, presumably by fostering granulosa cell proliferation (actions of elevated ACh) and limiting granulosa cell necroptosis (actions of interference with RIPK1). The results reveal, for the first time, the importance of local ACh and necroptosis in the regulation of primate folliculogenesis, which supports the potential of pharmacological interference of ACHE actions and necroptosis as novel approaches to improve ovarian functions in women.

Methods

Animal use and ovary collection. The general care and housing of rhesus macaques (*Macaca mulatta*) were provided by the Division of Comparative Medicine, Oregon National Primate Research Center (ONPRC), Oregon Health & Science University, as previously described²². Animals were pair-caged in a temperature-controlled (22 °C), light-regulated (12 L: 12D) room. The diet consisted of Purina monkey chow (Ralston-Purina, Richmond, IN, USA) and was provided twice a day supplemented with fresh fruit or vegetables once a day. Water was provided *ad libitum*. Animals were treated according to the National Institutes of Health's Guide for the Care and Use of Laboratory Animals. Protocols were approved by the ONPRC Institutional Animal Care and Use Committee²².

Ovaries were collected from 5 animals at necropsy (8–14 year old) by the Pathology Services Unit, via the ONPRC Tissue Distribution Program. Euthanasia was not performed for the current study, but was due to health issues unrelated to reproductive health. Ovaries were immediately transferred into HEPES-buffered holding media (Cooper Surgical, Inc., Trumbull, CT, USA) and kept at 37 °C for follicle isolation³².

Follicle isolation, encapsulation and culture. The process of follicle isolation, encapsulation and culture was previously reported²². Briefly, the ovarian cortex was cut into 1 × 1 × 1 mm cubes. Follicles were mechanically isolated using 31-gauge needles. Secondary follicles (diameter 125–225 μm) met criteria for encapsulation if they exhibited an intact basement membrane, 2–4 layers of granulosa cells and a healthy centrally located oocyte.

Follicles were individually transferred into 5 μl 0.25% (w/v) sterile sodium alginate (FMC BioPolymers, Philadelphia, PA, USA)-PBS (137 mM NaCl, 10 mM phosphate, 2.7 mM KCl, Invitrogen, Carlsbad, CA, USA). The droplets were gelled in 50 mM CaCl₂, 140 mM NaCl, 10 mM HEPES solution (pH 7.2). Each encapsulated follicle was placed in individual wells of 48-well plates containing 300 μl alpha minimum essential medium (Invitrogen) containing 6% (v/v) human serum protein supplement (Cooper Surgical, Inc.), 0.5 mg/ml bovine fetuin, 5 μg/ml insulin, 5 μg/ml transferrin, 5 ng/ml sodium selenite (Sigma-Aldrich, St Louis, MO, USA), and 3 ng/ml recombinant FSH (NV Organon/Merck Sharp & Dohme, Oss, Netherlands)²².

Target gene	Direction	Sequence	<i>Macaca mulatta</i> fitness	Accession number
MLKL	Forward	5'- TAC AGT CAG CAG AGT GCA GG -3'	85%	<i>H. sapiens</i> NM_152649.2 <i>M. Mulatta</i> XM_015126624.1
	Reverse	5'- ACC GTT TGT GGA TGA CCT GG -3'	95%	
RIPK1	Forward	5'- TGG GCG TCA TCA TAG AGG AAG -3'	100%	<i>H. sapiens</i> NM_003804 <i>M. Mulatta</i> XM_015135439.1
	Reverse	5'- CGC CTT TTC CAT GTA AGT AGC A -3'	100%	
ACHE	Forward	5'- TTC CTC AGT GAC ACC CCA GA -3'	100%	<i>H. sapiens</i> NM_000665.4
	Reverse	5'- GGG GAG AAG AGA GGG GTT AC -3'	100%	<i>M. Mulatta</i> NM_001128088.2

Table 1. Information about oligonucleotide primers used for RT-PCR. Note that primers were designed using *Homo sapiens* RNA sequences. Except *MLKL* forward (85%) and *MLKL* reverse (95%), all primers are 100% identical to *Macaca mulatta* sequences. Sequences of PCR products obtained matched *Macaca mulatta* sequences as confirmed upon sequencing.

Follicles from each of the five animals were randomly assigned to 3 experimental groups (12 follicles/monkey/group): (a) vehicle control (0.025% ethanol), (b) 10 μ M Huperzine A (42643; Sigma-Aldrich), and (c) 20 μ M necrostatin-1 (sc-200142; Santa Cruz Biotechnology, Inc., Santa Cruz, CA, USA). Follicles were cultured at 37 °C in a 5% O₂ environment (in 6% CO₂/89% N₂) for 5 weeks. Media (150 μ l) was collected and replaced every other day, and stored at -20 °C²².

Follicle survival and growth. Follicle survival, growth and antrum formation were assessed weekly using an Olympus CK-40 inverted microscope and an Olympus DP11 digital camera (Olympus Imaging America Inc., Center Valley, PA, USA), as described previously²². Follicle growth was determined by measuring the distance from the outer layer of cells at the widest diameter and then the diameter perpendicular to the first measurement by the same individual. The mean of the two values determined the follicle's overall diameter. The measurements were performed using ImageJ 1.6.0 software (National Institutes of Health, Bethesda, MD, USA). Follicles were considered atretic if the oocyte was dark or not surrounded by a layer of granulosa cells, the granulosa cells appeared dark or fragmented, or the follicle diameter decreased.

Follicle histology. Randomly selected *in vitro*-developed antral follicles from all three groups were harvested at culture week 5 and fixed in in 4% paraformaldehyde-PBS solution for 3 hours at room temperature. Follicles were embedded in HistoGel (Thermo Scientific, Kalamazoo, MI, USA) before being dehydrated in ascending concentrations of ethanol (70–100%) and embedded in paraffin. Five micrometer sections were cut by the Histopathology-Morphology Research Core at ONPRC, and stained with hematoxylin and eosin as previously described²².

Culture media assays. To determine the efficiency of Huperzine A in blocking ACHE actions in cultured follicles, media samples from the control and the Huperzine A group were analyzed for ACh concentrations using the Amplex Red Acetylcholine/Acetylcholinesterase Assay Kit (A12217; Molecular Probes, Inc., Eugene, OR, USA) according to the manufacturer's instruction, as described previously³³.

In order to assess steroidogenesis in cultured follicles, media samples collected from each culture group were analyzed for P4, A4 and E2 concentrations by the Endocrine Technologies Core at ONPRC. P4 and E2 were assayed to determine granulosa cell steroidogenic function using an Immulite 2000, a chemiluminescence-based automatic platform (Siemens Healthcare Diagnostics, Deerfield, IL, USA)²². A4 was measured by ELISA to determine thecal cell steroidogenic function using an AA E-1000 kit (Rocky Mountain Diagnostics, Inc., Colorado Springs, CO, USA) according to the manufacturer's instruction²².

Oocyte evaluation. Oocyte evaluations were performed on a 37 °C warming plate, as previously described²². Briefly, the cumulus-oocyte complex was dissected out of the follicle in Tyrode's albumin lactate pyruvate (TALP)-HEPES-BSA (0.3% v/v) medium provided by the Assisted Reproductive Technologies Core at ONPRC. Oocytes were then transferred to TALP medium and photographed. Oocyte diameters (excluding the zona pellucida) and conditions were assessed using the same camera and software, as described above.

Expression of ACHE and necrosome components in macaque follicles. This retrospective study included follicles obtained from animals (n = 4) reported in previous research³⁴. Briefly, *in vivo*-developed secondary (30 follicles/monkey) and antral (10 follicles/monkey) follicles were isolated from the cortex and the medulla region of macaque ovaries, respectively, and pooled. *In vitro*-developed antral follicles were collected at the end of culture under control conditions and pooled (10 follicles/monkey). Total RNA was extracted from each follicle pool for reverse transcription, as previously described³⁴. Oligonucleotide primers for PCR (Table 1) were designed using Primer3^{35,36} and synthesized by metabion international AG (Planegg, Germany). PCR was performed to examine expression of *ACHE*, *MLKL* and *RIPK1*, as described previously¹³. PCR products were sequenced by GATC Biotech AG (Konstanz, Germany) and analyzed using BLAST³⁷.

Consecutive sections from paraffin-embedded rhesus macaque ovaries (n = 3) obtained from previous studies^{11,13} were used for immunohistochemistry with antibodies detecting RIPK1 (HPA015257; Sigma-Aldrich), RIPK3 (HPA055087; Sigma-Aldrich) and pMLKL(S358) (ab187091; Abcam, Cambridge, UK), as previously described¹³. Randomly selected paraffin embedded antral follicles (4 follicles from 4 macaques), developed under

control culture conditions³⁴, were obtained for sectioning and immunohistochemistry for pMLKL(S358). To determine the efficiency of necrostatin-1 in blocking necroptosis in cultured follicles, *in vitro*-developed antral follicles harvested from the necrostatin-1 group at week 5 were also stained for pMLKL(S358). Controls were performed with the omission of antibodies or using non-immune serum.

Statistical analysis. Statistical analysis was performed using SigmaPlot 11 software (SPSS, Inc., Chicago, IL, USA). Because follicles from each animal were randomly distributed into the culture groups, the Wilcoxon signed-rank test was used to evaluate differences in follicle survival and percentage of fast-grow follicles, with five individual animals in each experimental group. One-way analysis of variance (ANOVA), followed by the Student-Newman-Keuls post hoc test, was used to analyze diameters of follicles and oocytes, as well as media hormone concentrations, with total follicle numbers indicated in the figure legends which represent follicles obtained from five individual animals. Media ACh concentrations were analyzed using a Student's *t*-test. Differences were considered significant at $P < 0.05$ and values are presented as mean \pm SEM.

Data availability. Data generated during this study are included in this published article and supplementary files. The original raw datasets generated during the current study are available from the corresponding author on reasonable request.

References

1. Beckmann, J. & Lips, K. S. The non-neuronal cholinergic system in health and disease. *Pharmacology* **92**, 286–302 (2013).
2. Fujii, T. *et al.* Physiological functions of the cholinergic system in immune cells. *J. Pharmacol. Sci.* **134**, 1–21 (2017).
3. Wessler, I. K. & Kirkpatrick, C. J. Non-neuronal acetylcholine involved in reproduction in mammals and honeybees. *J. Neurochem.* **142**(Suppl 2), 144–150 (2017).
4. Fritz, S. *et al.* Functional and molecular characterization of a muscarinic receptor type and evidence for expression of choline-acetyltransferase and vesicular acetylcholine transporter in human granulosa-luteal cells. *J. Clin. Endocrinol. Metab.* **84**, 1744–1750 (1999).
5. Mayerhofer, A. & Fritz, S. Ovarian acetylcholine and muscarinic receptors: hints of a novel intrinsic ovarian regulatory system. *Microsc. Res. Tech.* **59**, 503–508 (2002).
6. Mayerhofer, A. & Kunz, L. A non-neuronal cholinergic system of the ovarian follicle. *Ann. Anat.* **187**, 521–528 (2005).
7. Fritz, S. *et al.* Expression of muscarinic receptor types in the primate ovary and evidence for nonneuronal acetylcholine synthesis. *J. Clin. Endocrinol. Metab.* **86**, 349–354 (2001).
8. Fritz, S. *et al.* Muscarinic receptors in human luteinized granulosa cells: activation blocks gap junctions and induces the transcription factor early growth response factor-1. *J. Clin. Endocrinol. Metab.* **87**, 1362–1367 (2002).
9. Kunz, L. *et al.* Ca²⁺-activated, large conductance K⁺ channel in the ovary: identification, characterization, and functional involvement in steroidogenesis. *J. Clin. Endocrinol. Metab.* **87**, 5566–5574 (2002).
10. Kunz, L., Roggors, C. & Mayerhofer, A. Ovarian acetylcholine and ovarian KCNQ channels: insights into cellular regulatory systems of steroidogenic granulosa cells. *Life Sci.* **80**, 2195–2198 (2007).
11. Mayerhofer, A. *et al.* FSH regulates acetylcholine production by ovarian granulosa cells. *Reprod. Biol. Endocrinol.* **4**, 37 (2006).
12. Al-Zi'abi, M. O., Bowolaksono, A. & Okuda, K. Survival role of locally produced acetylcholine in the bovine corpus luteum. *Biol. Reprod.* **80**, 823–832 (2009).
13. Blohberger, J. *et al.* Readthrough acetylcholinesterase (AChE-R) and regulated necrosis: pharmacological targets for the regulation of ovarian functions? *Cell Death Dis.* **6**, e1685 (2015).
14. Urra, J., Blohberger, J., Tiszavari, M., Mayerhofer, A. & Lara, H. E. *In vivo* blockade of acetylcholinesterase increases intraovarian acetylcholine and enhances follicular development and fertility in the rat. *Sci. Rep.* **6**, 30129 (2016).
15. Birks, J. Cholinesterase inhibitors for Alzheimer's disease. *Cochrane Database Syst. Rev.* **25**, CD005593 (2006).
16. Linkermann, A. & Green, D. R. Necroptosis. *N. Engl. J. Med.* **370**, 455–465 (2014).
17. Holler, N. *et al.* Fas triggers an alternative, caspase-8-independent cell death pathway using the kinase RIP as effector molecule. *Nat. Immunol.* **1**, 489–495 (2000).
18. Vanlangenakker, N., Vanden Berghe, T. & Vandenabeele, P. Many stimuli pull the necrotic trigger, an overview. *Cell Death Differ.* **19**, 75–86 (2012).
19. Grootjans, S., Vanden Berghe, T. & Vandenabeele, P. Initiation and execution mechanisms of necroptosis: an overview. *Cell Death Differ.* **24**, 1184–1195 (2017).
20. Soreq, H. & Seidman, S. Acetylcholinesterase—new roles for an old actor. *Nat. Rev. Neurosci.* **2**, 294–302 (2001).
21. Zimmermann, M. Neuronal AChE splice variants and their non-hydrolytic functions: redefining a target of AChE inhibitors? *Br. J. Pharmacol.* **170**, 953–967 (2013).
22. Xu, J. *et al.* Fibrin promotes development and function of macaque primary follicles during encapsulated three-dimensional culture. *Hum. Reprod.* **28**, 2187–2200 (2013).
23. Gougeon, A. Dynamics of human follicular growth: morphologic, dynamic, and functional aspects. In: Leung, P. C. K. & Adashi, E. Y. editors. *The Ovary*. San Diego, CA, USA: Elsevier Academic Press, pp. 25–43 (2004).
24. Wang, R. & Tang, X. C. Neuroprotective effects of huperzine A. A natural cholinesterase inhibitor for the treatment of Alzheimer's disease. *Neurosignals* **14**, 71–82 (2005).
25. Kidder, G. M. & Vanderhyden, B. C. Bidirectional communication between oocytes and follicle cells: ensuring oocyte developmental competence. *Can. J. Physiol. Pharmacol.* **88**, 399–413 (2010).
26. Richardson, S. J., Senikas, V. & Nelson, J. F. Follicular depletion during the menopausal transition: evidence for accelerated loss and ultimate exhaustion. *J. Clin. Endocrinol. Metab.* **65**, 1231–1237 (1987).
27. Matsuda, F., Inoue, N., Manabe, N. & Ohkura, S. Follicular growth and atresia in mammalian ovaries: regulation by survival and death of granulosa cells. *J. Reprod. Dev.* **58**, 44–50 (2012).
28. Howes, M. R., Fang, R. & Houghton, P. J. Effect of Chinese Herbal Medicine on Alzheimer's Disease. *Int. Rev. Neurobiol.* **135**, 29–56 (2017).
29. Damar, U., Gersner, R., Johnstone, J. T., Schachter, S. & Rotenberg, A. Huperzine A as a neuroprotective and antiepileptic drug: a review of preclinical research. *Expert Rev. Neurother.* **16**, 671–80 (2016).
30. Sklan, E. H. *et al.* Acetylcholinesterase/paraoxonase genotype and expression predict anxiety scores in health, risk factors, exercise training, and genetics study. *Proc. Natl. Acad. Sci. USA* **101**, 5512–5517 (2004).
31. Wallace, W. H. & Kelsey, T. W. Human ovarian reserve from conception to the menopause. *PLoS One* **5**, e8772 (2010).
32. Xu, J., Bishop, C. V., Lawson, M. S., Park, B. S. & Xu, F. Anti-Müllerian hormone promotes preantral follicle growth, but inhibits antral follicle maturation and dominant follicle selection in primates. *Hum. Reprod.* **31**, 1522–1530 (2016).
33. Steffl, M. *et al.* Non-neuronal acetylcholine and choline acetyltransferase in oviductal epithelial cells of cyclic and pregnant pigs. *Anat. Embryol. (Berl.)* **211**, 685–690 (2006).

34. Xu, J. *et al.* Anti-Müllerian hormone is produced heterogeneously in primate preantral follicles and is a potential biomarker for follicle growth and oocyte maturation *in vitro*. *J. Assist. Reprod. Genet.* **33**, 1665–1675 (2016).
35. Untergasser, A. *et al.* Primer3 - new capabilities and interfaces. *Nucleic Acids Research* **40**, e115 (2012).
36. Koressaar, T. & Remm, M. Enhancements and modifications of primer design program Primer3. *Bioinformatics* **23**, 1289–1291 (2007).
37. Altschul, S. F., Gish, W., Miller, W., Myers, E. W. & Lipman, D. J. Basic local alignment search tool. *J. Mol. Biol.* **215**, 403–410 (1990).

Acknowledgements

We are grateful for the assistance provided by members of the Division of Comparative Medicine, the Pathology Services Unit, the Assisted Reproductive Technologies Core, the Endocrine Technologies Core and the Histopathology-Morphology Research Core at ONPRC, OHSU. We gratefully acknowledge Astrid Tiefenbacher and Karin Metzrath at LMU for technical assistance and editorial help, respectively. The study was supported by German Research Foundation (DFG) MA1080/19-2, NIH OD P51OD011092 (ONPRC), TCHGO Hospital Fund. There are no conflicts of interest. This work was done in partial fulfilment of the requirements of a Dr. rer. nat. degree (K.B.) at the LMU Munich.

Author Contributions

Y. Du provided contributions to 1) follicle culture, 2) data analysis, 3) manuscript drafting, and 4) final approval of the version to be submitted for publication. K. Bagnjuk provided contributions to 1) RT-PCR, 2) immunohistochemistry and immunoblotting, 3) manuscript revising, and 4) final approval of the version to be submitted for publication. MS. Lawson provided contributions to 1) follicle culture, 2) immunohistochemistry, and 3) final approval of the version to be submitted for publication. J. Xu provided contributions to 1) experimental design, 2) follicle culture, 3) data analysis and interpretation, 4) manuscript revising, and 5) final approval of the version to be submitted for publication. A. Mayerhofer conceived of the study and provided contributions to 1) experimental design, 2) data interpretation, 3) manuscript drafting and revising, and 4) final approval of the version to be submitted for publication. All authors participated in the writing of the manuscript and approved of the final version.

Additional Information

Competing Interests: The authors declare no competing interests.

Publisher's note: Springer Nature remains neutral with regard to jurisdictional claims in published maps and institutional affiliations.



Open Access This article is licensed under a Creative Commons Attribution 4.0 International License, which permits use, sharing, adaptation, distribution and reproduction in any medium or format, as long as you give appropriate credit to the original author(s) and the source, provide a link to the Creative Commons license, and indicate if changes were made. The images or other third party material in this article are included in the article's Creative Commons license, unless indicated otherwise in a credit line to the material. If material is not included in the article's Creative Commons license and your intended use is not permitted by statutory regulation or exceeds the permitted use, you will need to obtain permission directly from the copyright holder. To view a copy of this license, visit <http://creativecommons.org/licenses/by/4.0/>.

© The Author(s) 2018

3.3 Publication 3 (Bagnjuk, Kast et al. 2019)

Inhibitor of apoptosis proteins are potential targets for treatment of granulosa cell tumors – Implications from studies in KGN

Konstantin Bagnjuk*, Verena Jasmin Kast*, Astrid Tiefenbacher, Melanie Kaseder, Toshihiko Yanase, Alexander Burges, Lars Kunz, Doris Mayr, Artur Mayerhofer

Journal of Ovarian Research, Vol. 12, No. 76, 2019, DOI: 10.1186/s13048-019-0549-6

*co-first author

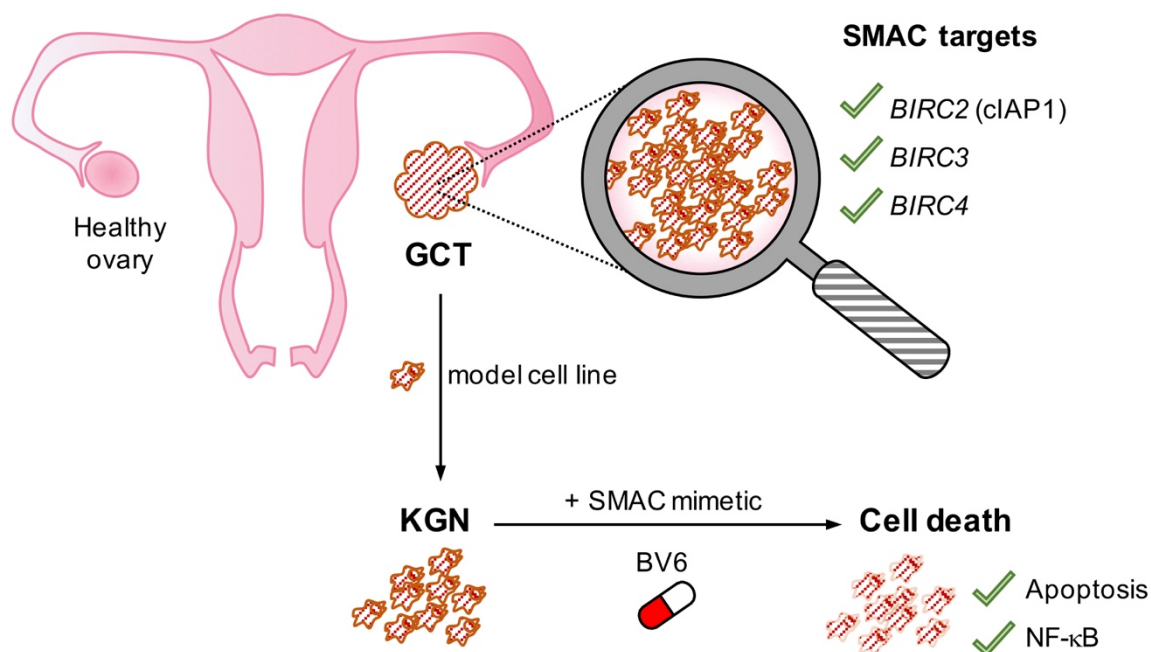


Figure 7 Graphical summary of publication 3 (Bagnjuk, Kast et al. 2019)

The expression of potential SMAC targets in granulosa cell tumors (GCTs) was verified by immunohistochemistry for clAP1 and by PCR for *BIRC2*, *BIRC3* and *BIRC4*. The effects of the SMAC mimetic BV6 on KGN, a GCT cell line, were elaborated *in vitro*. BV6 was able to induce apoptosis in the cell line and affected NF-κB-dependent gene expression. (*BIRC* = gene encoding the baculoviral IAP repeat containing protein; clAP = cellular inhibitor of apoptosis protein; SMAC = second mitochondria-derived activator of caspases)

RESEARCH

Open Access



Inhibitor of apoptosis proteins are potential targets for treatment of granulosa cell tumors – implications from studies in KGN

Konstantin Bagnjuk^{1†}, Verena Jasmin Kast^{1†}, Astrid Tiefenbacher¹, Melanie Kaseder¹, Toshihiko Yanase², Alexander Burges³, Lars Kunz⁴, Doris Mayr⁵ and Artur Mayerhofer^{1*} 

Abstract

Background: Granulosa cell tumors (GCTs) are derived from proliferating granulosa cells of the ovarian follicle. They are known for their late recurrence and most patients with an aggressive form die from their disease. There are no treatment options for this slowly proliferating tumor besides surgery and chemotherapy. In a number of tumors, analogs of the second mitochondria-derived activator of caspases (SMAC), alone or in combination with other molecules, such as TNF α , are evolving as new treatment options. SMAC mimetics block inhibitor of apoptosis proteins (IAPs), which bind caspases (e.g. XIAP), or activate the pro-survival NF- κ B pathway (e.g. cIAP1/2). Expression of IAPs by GCTs is yet not fully elucidated but recently XIAP and its inhibition by SMAC mimetics in a combination therapy was described to induce apoptosis in a GCT cell line, KGN. We evaluated the expression of cIAP1 in GCTs and elucidated the effects of the SMAC mimetic BV-6 using KGN as a model.

Results: Employing immunohistochemistry, we observed cIAP1 expression in a tissue microarray (TMA) of 42 GCT samples. RT-PCR confirmed expression of cIAP1/2, as well as XIAP, in primary, patient-derived GCTs and in KGN. We therefore tested the ability of the bivalent SMAC mimetic BV-6, which is known to inhibit cIAP1/2 and XIAP, to induce cell death in KGN. A dose response study indicated an EC₅₀ \approx 8 μ M for both, early (< 8) and advanced (> 80) passages, which differ in growth rate and presumably aggressiveness. Quantitative RT-PCR showed upregulation of NF- κ B regulated genes in BV-6 stimulated cells. Blocking experiments with the pan-caspase inhibitor Z-VAD-FMK indicated caspase-dependence. A concentration of 20 μ M Z-VAD-FMK was sufficient to significantly reduce apoptosis. This cell death was further substantiated by results of Western Blot studies. Cleaved caspase 3 and cleaved PARP became evident in the BV-6 treated group.

Conclusions: Taken together, the results show that BV-6 is able to induce apoptosis in KGN cells. This approach may therefore offer a promising therapeutic avenue to treat GCTs.

Keywords: Cell death, Ovarian granulosa cell tumor, Apoptosis

Background

Apoptosis can be activated via two different pathways, the extrinsic death receptor pathway and the intrinsic mitochondria associated pathway [1, 2]. Both will execute apoptosis by cleaving and therefore activating caspases, which in turn degrade other proteins, based on their peptidase activity [3]. The intrinsic pathway is induced by the release of

pro-apoptotic molecules from mitochondria, for example cytochrome c, endonuclease G, apoptosis inducing factor (AIF), high temperature requirement protein A2 (HtrA2 also known as OMI) or the second mitochondria-derived activator of caspases (SMAC; or its murine homolog, known as direct inhibitor of apoptosis protein binding protein with low PI (DIABLO)) [2, 4].

SMAC blocks inhibitor of apoptosis proteins (IAPs, e.g. baculoviral IAP repeat containing protein 1–8, BIRC1–8), which are highly expressed in various tumors [5]. Therefore, IAPs are potential targets in oncology. Different SMAC mimetics have been developed to target IAPs [6–8].

* Correspondence: mayerhofer@lrz.uni-muenchen.de

Konstantin Bagnjuk and Verena Jasmin Kast share first authorship.

¹Biomedical Center Munich (BMC), Cell Biology, Anatomy III, Ludwig-Maximilians-University (LMU), Grosshaderner Strasse 9, 82152 Planegg, Germany

Full list of author information is available at the end of the article



Some of these compounds are monovalent and others are bivalent. The latter target two BIR domains simultaneously and have been shown to be more potent [6, 9].

BIRC2 (cIAP1), *BIRC3* (cIAP2), and *BIRC4* (XIAP) are expressed in granulosa cells of ovarian follicles [10]. Tumors, which arise from these cells (granulosa cell tumors (GCTs)), are often steroidogenic and produce estrogen in prepubertal (juvenile GCTs) and postmenopausal woman (adult GCTs) [11]. Adult GCTs usually bear the FOXL2(C134W) mutation. Although these tumors are steroidogenic, it remains unknown whether they grow in a gonadotropin-dependent manner, as shown for other tumors [12, 13].

The majority of patients who suffer from aggressive or recurrent GCTs, where the aggressiveness and probability of relapse is not reflected histologically, die from their disease [11]. Due to the low proliferation speed, chemotherapy is often ineffective and therefore surgery is the only promising way to treat GCTs. In other ovarian malignancies, such as epithelial cancers, chemotherapy is more effective. In these tumors it was shown that reoccurrence might be due to reduced immune-surveillance or drug-resistant cells [14, 15]. In GCTs this option was never discussed but might be of interest in the rare case of effective first line chemotherapy.

To improve the situation for GCT-patients, it is important to develop alternative methods. A widely used model to study this type of tumor is the KGN cell line [16]. These cells are steroidogenic and bear the FOXL2 mutation. It was recently shown that *BIRC2* (cIAP1) and *BIRC4* (XIAP) are expressed in GCTs and in KGN [17]. The examined samples were, however, only very weakly stained for *BIRC2* (cIAP1) and reportedly negative for *BIRC3* (cIAP2). Immunostaining results, as those mentioned, may depend on fixation, antibody specificity and antibody concentration. Negative results do not necessarily rule out expression. Furthermore, in granulosa cells of healthy woman *BIRC2*, *BIRC3* and *BIRC4* expression levels vary during follicular development [18]. Of note, GCTs are thought to stem from proliferating GCs of unknown follicular stage. In the present study we therefore examined expression of *BIRC2* (cIAP1) in 42 GCTs. We next evaluated the actions of the bivalent SMAC mimetic BV-6, which targets XIAP and cIAP1/2 simultaneously, in studies employing KGN.

Results

cIAP1 protein expression in GCTs

We examined cIAP1 expression in 42 ovarian GCTs using a specific anti-cIAP1 antibody. In general, three distinct staining patterns were observed: strong, weak and heterogeneous (Fig. 1a-d). Classification of the tumor-staining by 6 individuals revealed 18.2 \pm 1.6 (43.3%) samples with homogeneously strong cIAP1 expression (Fig. 1a,d), whereas weak expression was observed in only 5.8 \pm 1.3 tumors (13.9%)

(Fig. 1b,d). Heterogeneous staining was found in 18.0 \pm 0.9 samples (42.9%) (Fig. 1c,d). In these samples, some cells showed strong nuclear cIAP1 staining (indicated by arrows), some remained unstained, and others showed weak staining in the cytoplasm. A significant difference ($****p < 0.0001$) was found between the number of strongly versus weakly stained tumors and between the number of heterogeneously versus weakly stained tumors. Negative controls (non-immune rabbit serum instead of antiserum) showed only marginal and non-specific staining (Fig. 1a, Inset).

BIRC2, *BIRC3* and *BIRC4* mRNA is expressed in GCTs and KGN

To elucidate gene expression of IAPs in primary GCT-samples, we conducted a RT-PCR analysis using the listed primers (Table 1). *BIRC2*, *BIRC3*, and *BIRC4* gene expression levels were analyzed in three human GCTs, as well as in KGN. All targets were found in the tested samples (Fig. 1e). The band intensities varied across different tumors, indicating patient-specific expression levels.

BV-6 induces time-dependent cell death in KGN

IAPs are potential targets for tumor treatment. Therefore, we tested the ability of BV-6, a bivalent SMAC mimetic, to induce cell death in KGN [6]. This cell line is known to divide faster in high passages, implicating elevated aggressiveness [19]. Therefore, we examined BV-6 actions in KGN from high (> 80, Fig. 2) and low passages (< 8). (A flowchart of the experiments can be found in the Additional file 1: Figure S1a). Using live cell imaging, we tested 4 concentrations of BV-6, ranging from 0.1 to 50 μ M (Fig. 2a), in comparison to the respective solvent controls (Fig. 2a insets). At low concentrations of BV-6 (0.1 μ M, 1 μ M) cells were not affected within the timeframe of 24 h. At 10 μ M, BV-6 induced cell death, as seen by detached and floating cells. This effect was intensified when 50 μ M of BV-6 was used. The concentration-dependent effects were independent of the passage number (data not shown).

To determine the half maximal effective concentration (EC_{50}) after 24 h, KGN (passages > 80) were treated with increasing concentrations of BV-6 for 24 h and then counted (Fig. 2b). As expected, at low concentrations (0.1–5.0 μ M) cells remained unaffected. However, concentrations above 5 μ M reduced cell numbers. Nonlinear regression analysis described a sigmoidal curve and interpolation revealed an EC_{50} for BV-6 ranging from 7.4 μ M to 8.2 μ M (Fig. 2b, left graph). For the low passages, we found an EC_{50} ranging between 8.1 and 8.6 μ M (Fig. 2c). As the effective concentrations did not substantially vary between high and low passages, all further experiments were implemented on KGN at high passages (> 80).

To further test the defined EC_{50} , cell viability was analyzed using an ATP assay (Fig. 2b, right graph). For this purpose, cells were treated with different concentrations

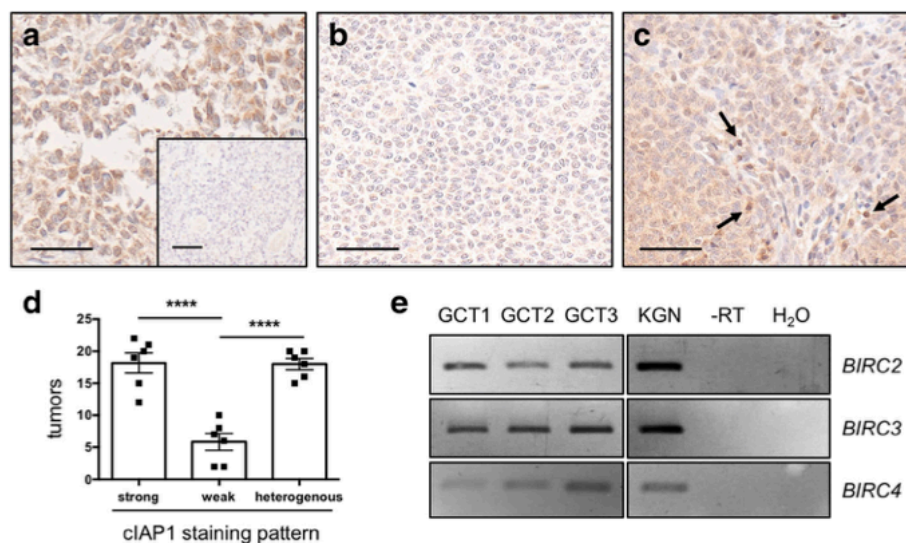
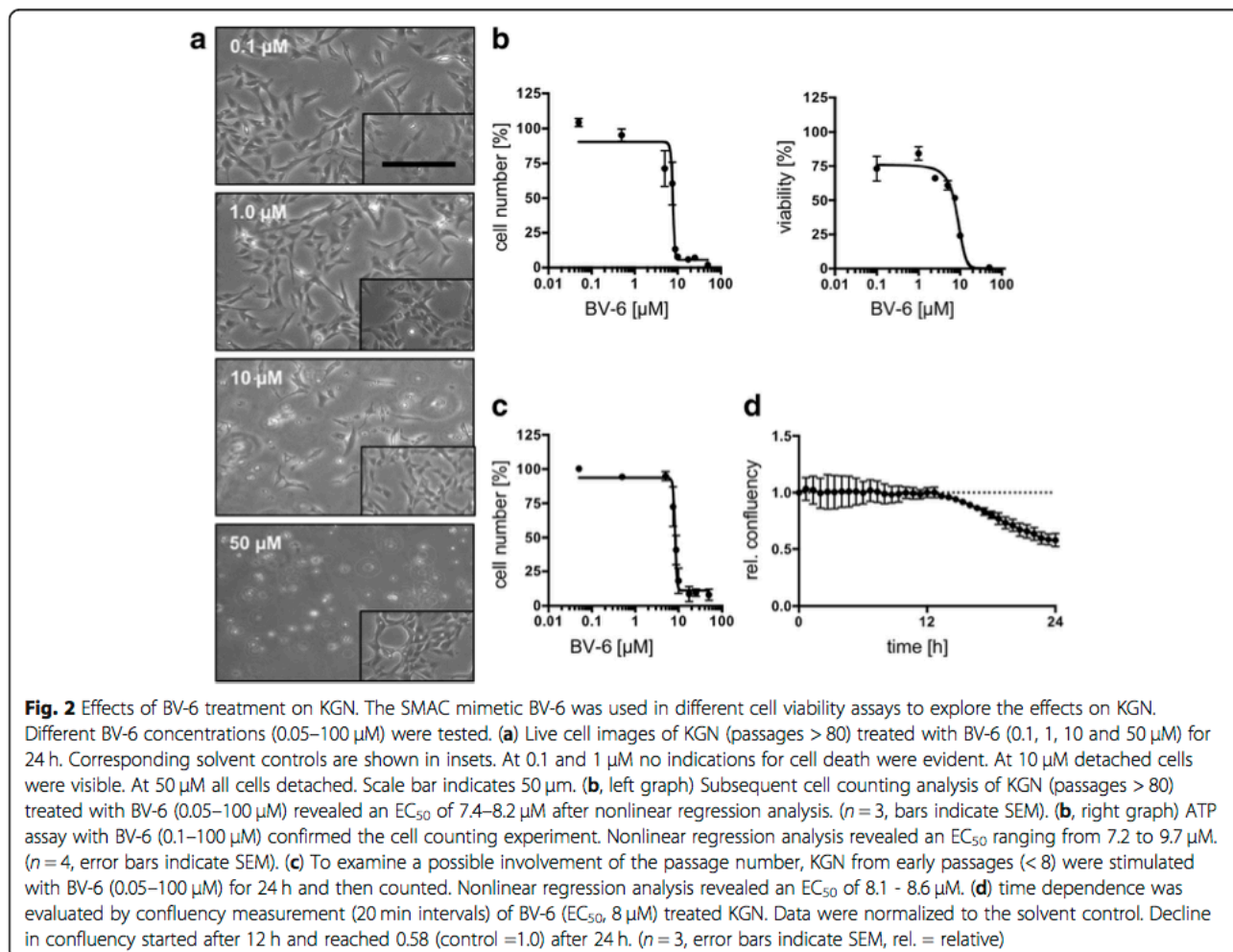


Fig. 1 *BIRC2* (cIAP1), *BIRC3* and *BIRC4* expression in GCTs and KGN. Identification of *BIRC2*, *BIRC3* and *BIRC4* expression at mRNA level in KGN and GCTs and evaluation of cIAP1 protein expression in GCTs. **(a-d)** Expression of cIAP1 in 42 different samples of GCTs were analyzed by immunohistochemistry. **(a,d)** Results of the evaluation, performed by 6 researchers, indicated strong and homogenous cIAP1 staining in 18.2 tumors (mean). **(b,d)** 5.8 tumors (mean) showed weak cIAP1 staining. **(c,d)** Heterogeneous cIAP1 staining was visible in 18.0 tumors (mean). Arrows indicate strongly stained nuclei. **(a-c)** Negative control (rabbit serum) showed no staining (**a**, inset). Scale bars correspond to 50 μ m. **(d)** Shown are the mean values and SEM. **(e)** RT-PCR of three independent GCTs and KGN (primers are described in Table 1). Controls consisted of a no reverse transcription (-RT) sample and a no template (H₂O) sample

Table 1 List of oligonucleotide primers used for RT-PCR studies

Target	Sequence (5' - 3')	Reference	Product size (bp)	
<i>BIRC2</i>	Forward	GAC ATC ATC ATT GCG ACC CAC	NM_001166.4	192
	Reverse	TGG TTT CCA AGG TGT GAG TAC T		
<i>BIRC3</i>	Forward	AGA ACA CCT GAG ACA TTT TCC CA	NM_001165.4	202
	Reverse	GAC ATC ATC ATC GTT ACC CAC A		
<i>BIRC4</i>	Forward	TGT GGA GGA GGG CTA ACT GA	NM_001167.3	83
	Reverse	AGA TAT TTG CAC CCT GGA TAC CA		
<i>TNFα</i>	Forward	ATG AGC ACT GAA AGC ATG ATC C	NM_000594.4	217
	Reverse	GAG GGC TGA TTA GAG AGA GGT C		
<i>MCP-1</i>	Forward	AGG TGA CTG GGG CAT TGA T	NM_002982.3	109
	Reverse	GCC TCC AGC ATG AAA GTC TC		
<i>IL8</i>	Forward	TCT TGG CAG CCT TCC TGA	NM_000584.4	271
	Reverse	GAA TTC TCA GCC CTC TTC		
<i>L19</i>	Forward	AGG CAC ATG GGC ATA GGT AA	NM_000981.3	199
	Reverse	CCA TGA GAA TCC GCT TGT TT		
<i>HPRT</i>	Forward	CCT GGC GTC GTG ATT AGT GA	NM_000194.2	163
	Reverse	GGC CTC CCA TCT CCT TCA TC		
<i>PPIA</i>	Forward	AGA CAA GGT CCC AAA GAC	NM_021130.5	118
	Reverse	ACC ACC CTG ACA CAT AAA		
<i>TBP</i>	Forward	TGC ACA GGA GCC AAG AGT GAA	NM_003194.5	132
	Reverse	CAC ATC ACA GCT CCC CAC CA		



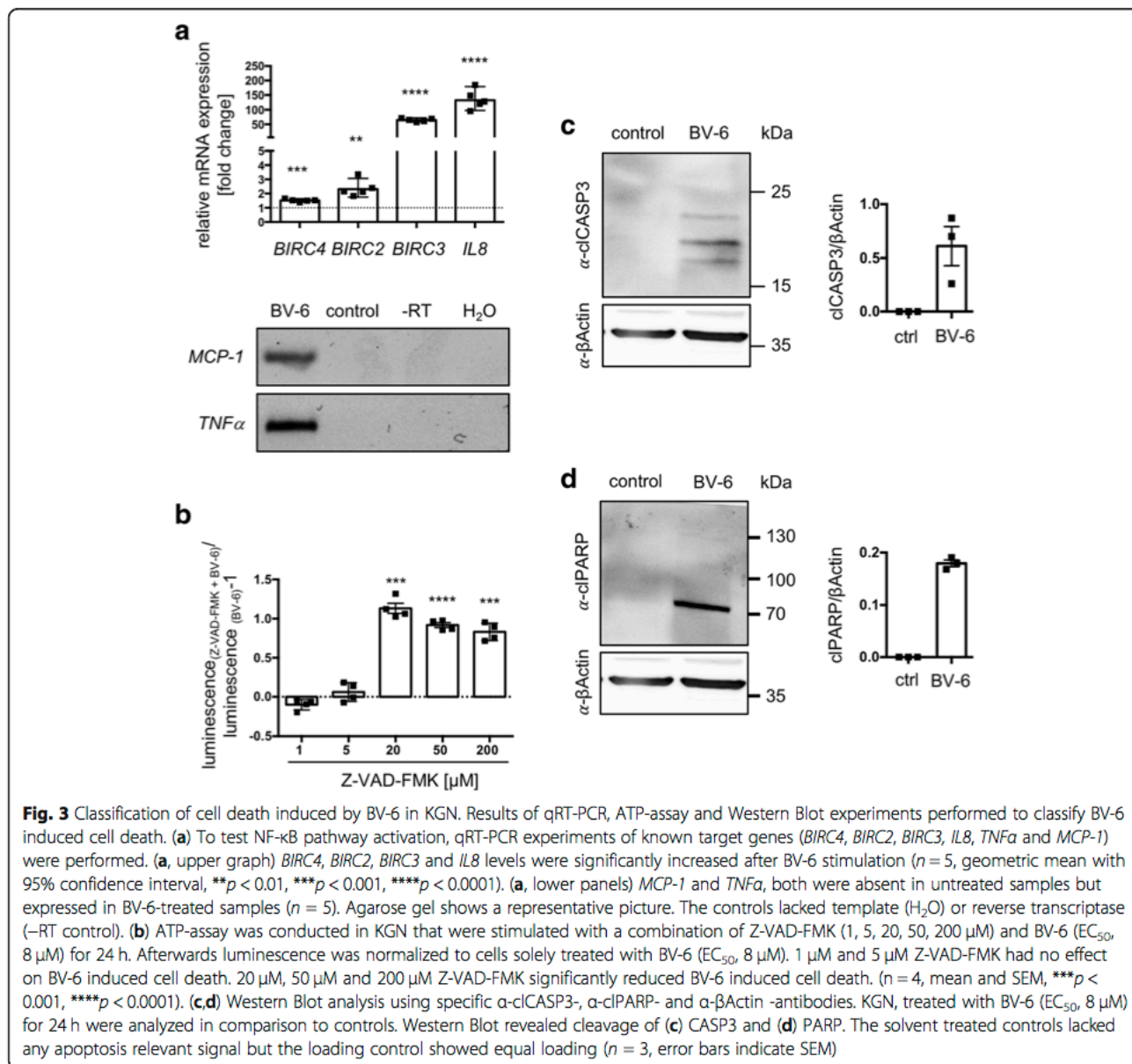
of BV-6 (0.1 to 50 μM) and evaluated after 24 h. In accordance with the results in Fig. 2b, nonlinear regression analysis revealed a half-maximal reduction of viability by 7.2 to 9.7 μM BV-6. Live cell imaging and subsequent measurement of confluency were assessed in BV-6 (EC_{50} , 8 μM) treated KGN. The space occupied by cells (confluency) relative to the maximally available space, was measured in 20 min intervals. Confluency began to decline after 12 h and reached 0.58 after 24 h, as compared to the control (1.0). This result is in line with the other experiments. Taken together, we found an EC_{50} (24 h) of approximately 8 μM for BV-6 in KGN, which is passage-independent but time-dependent.

BV-6 leads to NF- κB activation and apoptosis in KGN

BV-6 is known to block XIAP, cIAP1 and cIAP2 and therefore is able to activate apoptosis through different pathways, including NF- κB activation and direct caspase activation [6]. To examine these possibilities in KGN, we exposed KGN to BV-6 (EC_{50}) for 24 h and examined involvement of NF- κB pathway and caspase activation.

IL8, *MCP-1*, *TNF α* , *BIRC2*, *BIRC3* and *BIRC4* are known NF- κB target genes [20–23]. Therefore, upregulation points to pathway activation. Indeed, all of the tested genes were expressed in BV-6 stimulated KGN (Fig. 3a). *BIRC4*, *BIRC2*, *BIRC3* and *IL8* were upregulated with a fold-change rate of 1.52 \pm 0.04, 2.4 \pm 0.26, 64.9 \pm 2.57 and 133.5 \pm 14.9, respectively (** p < 0.01 for *BIRC2*, *** p < 0.001 for *BIRC4* and **** p < 0.0001 for *BIRC3* and *IL8*). *TNF α* and *MCP-1* were not found in untreated KGN but were present in BV-6 treated samples, as shown in the representative agarose gel (Fig. 3a).

To test involvement of caspases, different concentrations of Z-VAD-FMK in combination with BV-6 (EC_{50} , Fig. 3b) were added to KGN cultures. Z-VAD-FMK is a pan-caspase inhibitor and therefore functions as a blocker of apoptosis [24]. Cell viability was assessed using ATP assays. At low concentrations (1 μM and 5 μM) Z-VAD-FMK had no effect on BV-6 induced cell death. Interestingly, viability was significantly improved at higher doses (20 μM *** p < 0.001, 50 μM **** p < 0.0001 and 200 μM *** p < 0.001).



Next we screened BV-6-treated KGN for apoptotic markers by Western Blot. We used a specific anti-cleaved caspase 3 (α -clCASP3) antibody to detect the intermediate step of apoptosis and anti-cleaved poly (ADP-ribose)-polymerase (α -clPARP) antibody to detect the terminal step of apoptosis [1, 25]. Both, clCASP3 (Fig. 3c) and clPARP (Fig. 3d) were present in three independent samples of BV-6 (8 μM)-treated KGN but completely absent from the corresponding controls. Using an anti- β Actin antibody, equal loading was confirmed.

Discussion

A hallmark of cancer is resistance to cell death [26], which may be related to altered IAP expression profiles. cIAP1 and cIAP2, for example, have been shown to be

overexpressed in various tumors, including cervical cancer, esophageal squamous cell carcinoma, hepatocarcinoma, medulloblastoma, several forms of lung cancer, pancreatic cancer and many more, as summarized by Dubrez et al. [27]. SMAC mimetics, which target intracellular IAPs, are for this reason a hot topic in cancer biology. Some of these compounds are currently being tested in phase I and phase II clinical trials and show promising results [28]. To our knowledge (<https://www.clinicaltrials.gov>), there are several ongoing clinical studies with SMAC mimetics in different solid tumors and lymphomas, however not in GCTs.

Which IAPs are expressed by GCTs is not fully known. Yet a recent work described strong and homogenous expression of XIAP but a weak cIAP1 expression in GCTs

[17]. Immunostaining results may depend on fixation, antibody specificity, as well as many other factors. Therefore, we tested a validated and specific anti-cIAP1 antibody in 42 tumor samples and employed primary GCT samples and KGN for RT-PCR studies. While expression of cIAP1 was strong in most tested GCT samples, the second largest group showed heterogeneous staining. Only a small fraction (13.9%) was weakly stained.

Furthermore, we detected *BIRC3* (cIAP2) mRNA, which in the previous study was not described [17], but was shown to be upregulated in many other tumors [27]. However, in line with the previous study by Leung et al., *BIRC4* (XIAP) was detected. Thus, GCTs are endowed with several IAPs, which render them targets for SMAC mimetics.

Given that *BIRC2*, *3* and *4* are present, we hypothesized that BV-6 may be of special interest [6]. BV-6 targets cIAP1/2 and XIAP, which block apoptosis by directly inhibiting caspases (e.g. XIAP = *BIRC4*), and by activating the pro-survival canonical NF- κ B pathway (e.g. cIAP1/2 = *BIRC2/3*) [6]. We tested BV-6 actions in KGN, a cell line that is widely used for the study of GCTs [16]. NF- κ B was shown to play a role in BV-6 mediated apoptosis [6]. BV-6 stimulation increased the levels of several target genes of this pathway, namely *IL8*, *MCP-1*, *TNF α* , *BIRC2*, *BIRC3* and *BIRC4* in KGN [20–23]. Interestingly, the increase in expression of the 3 tested IAPs varied, with *BIRC3* (cIAP2) showing the strongest effect (fold change = 133.5). It may be possible that upregulation of *BIRC2* and *BIRC3* are cellular attempts to counter apoptosis [21]. TNF α plays an important role in BV-6 induced cell death in many tumor cell lines and is expressed upon BV-6 stimulation in KGN. Therefore, TNF receptor mediated activation of NF- κ B and apoptosis are likely to be involved in BV-6 actions in KGN [6]. As we did not elucidate the whole pathway, e.g. RIP1 ubiquitination and cIAP1/2 degradation, we can not conclude to the full mode of action of BV-6. However, it is likely that cIAP1/2, which ubiquitinate RIP1, are degraded. In turn this may lead to deubiquitylation of RIP1 and subsequently activation of apoptosis or necroptosis through a TNF α autocrine loop [6, 29, 30].

Passaging KGN induces a change in proliferation speed, which might be related to tumor aggressiveness [19]. We tested low and advanced passages for their sensitivity to BV-6 but found no substantial differences. BV-6 -induced cell death in KGN was concentration- ($EC_{50} \approx 8 \mu\text{M}$) and time-dependent. Low concentrations of BV-6 (e.g. $1 \mu\text{M}$) induced cell death in KGN, but longer incubation times (72 h) were needed (Additional file 1: Figure S1b).

In a recent study, a SMAC mimetic alone was reported incapable to induce cell death in KGN [17], but co-applied with a PPAR γ agonist it became effective. The PPAR γ pathway was shown to be relevant in cancer earlier [31, 32]. In the previous study the bivalent SMAC mimetic “compound A”, originally developed by the pioneering group

around Vince [7] was employed. This compound was designed to bind the same IAP domains (BIR2-BIR3) as BV-6, but is chemically different, which could explain the disparate potency [6, 7]. Our results obtained with BV-6 are in line with published work, verifying that some SMAC mimetics induce cell death as single agents in various cancers [6, 33–37].

The Western Blot experiments of our study showed cleaved caspase 3, indicating an intermediate step of apoptosis and cleaved PARP, i.e. a terminal step of apoptosis in BV-6-treated KGN. Furthermore, blocking experiments with the pan-caspase blocker Z-VAD-FMK improved KGN viability [24]. Hence, we conclude that BV-6-induced cell death is mainly apoptosis. Necroptosis (regulated necrosis) has also been described in literature to occur upon SMAC mimetic stimulation in some settings [38]. It is postulated that different cell death pathways are interlinked and might be triggered simultaneously [39]. We attempted to determine a possible involvement of necroptosis and examined phosphorylated MLKL (T357/S358) in BV-6-treated samples by Western Blot, using a validated phosphospecific antibody [40]. Using this marker, we were not able to find signs for necroptotic cell death in KGN. MLKL was evident in every sample but phosphorylation and subsequently oligomerization were not observed (Additional file 1: Figure S1c).

The results obtained in cellular studies are in line with reports showing that apoptosis is induced by BV-6 in many cell types [6], but the effects of different SMAC mimetics in distinct experiment settings and cells may vary. For example, it was found that a SMAC mimetic monotherapy is effective only in a small number of tumor cell lines (< 15%), whereas in combination with exogenously added TNF α or TRAIL, around 50% of the tumor cell lines died [41]. Further, the dependence on cytokines was proposed. In mouse models, for example, it was shown that next to the innate immune system the adaptive immune system plays an important role in SMAC mimetic-mediated cell death [42]. The fact that these compounds not only affect the tumor cell itself but also trigger effector cells like natural killer cells, was shown recently [43]. Lecis and group further supported this hypothesis, as SMAC mimetics affected the tumor niche by exerting immunomodulatory effects on macrophages [44]. Thus, next to their effect on tumor cells, SMAC mimetics have a broad impact on the tumor microenvironment and the immune system. These points can however not be examined in cellular experiments with KGN cells.

In the present work we focused on the SMAC mimetic BV-6 as a potential inducer of apoptosis in KGN. As described, apoptosis is either induced extrinsically (death receptor pathway) or intrinsically (mitochondrial pathway). The extrinsic pathway is executed upon binding of a death ligand (e.g. TNF α) to the corresponding receptor

(e.g. TNFR1). Then initiator caspase (caspase 8) is activated, which leads to further cascaded reactions including caspase 3 activation and cleavage of crucial proteins, including PARP [25, 45]. These steps were readily observed in BV-6-treated KGN and indicate that BV-6 does induce apoptosis.

Taken together, our results may imply that GCTs, which as we found are often positive for cIAP1, albeit in a patient-dependent manner, can possibly be treated by BV-6. The results further suggest that prior to treatment, testing for expression of IAPs may be useful and should be performed.

Conclusions

The SMAC mimetic BV-6 is able to induce apoptosis in KGN, which express XIAP and cIAP1/2. The results imply that these IAPs, if present in primary tumors, may serve as targets for therapeutic approaches.

Methods

Human GCT samples

The ethical committee of the LMU has approved the study (project 390–15) and patients had agreed to the use of the tissue. Samples (approximately 0.5 cm³) from three patients (age 41, 53 and 66 years) undergoing surgery were obtained. Tumor cells were enriched by collagenase digestion in the presence of antibiotics (1% penicillin/streptomycin (Biochrom GmbH, Berlin, Germany)) and subsequent plating on culture wells (HAM's-F12 supplemented with 10% fetal calf serum (FCS)), as described for primary human granulosa cell cultures [26]. RNA was extracted and subjected to RT-PCR.

All patients were diagnosed at the Institute for Pathology (LMU, Munich). The diagnoses were confirmed by an experienced gynecologic pathologist (D.M.).

In addition, two tissue microarrays (TMA) were assembled and used. Archival material of 42 patients with GCT was available. All patients were treated surgically at the same institution (Department of Gynecology, University of Munich). Tissue biopsies ($n = 42$) were taken from representative regions of paraffin-embedded tumor samples (donor) and arrayed into a new recipient paraffin block by using MTA-1 (Micro Tissue Arrayer) from Beecher Instruments, USA.

Culture and treatment of KGN

The human ovarian granulosa-like tumor cell line KGN was obtained from the Riken BioResource Research Centre (Ibaraki, Japan) [16] and the use of this patented cell line was approved by T. Yanase. KGN were cultured in Dulbecco's Modified Eagle Medium/Nutrient Mixture F-12 (DMEM/F-12, Thermo Fisher Scientific, Waltham, MA, USA) supplemented with 10% FCS (Capricorn Scientific GmbH, Ebsdorfergrund, Germany) and 1%

penicillin/streptomycin (Biochrom GmbH, Berlin, Germany) in T75 flasks (Thermo Fisher Scientific, Waltham, MA, USA) under constant temperature (37 °C) and CO₂ concentration (5%). As KGN change in aggressiveness over culture time [19] we used low passages (< 8) and high passages (> 80) for preliminary experiments. As a passage dependence was absent in terms of sensitivity to BV-6 we proceeded with high passages (> 80).

To rule out serum effects, experiments were executed in serum-free DMEM/F-12 media. Therefore, KGN were stimulated for 24 h either with the second mitochondria-derived activator of caspases (SMAC) mimetic BV-6 (0.05–100 μM; Selleck Chemicals LLC, Houston, TX, USA) alone or in combination with the pan-caspase inhibitor Z-VAD-FMK (1–200 μM; Selleck Chemicals LLC, Houston, TX, USA). BV-6 and Z-VAD-FMK were dissolved in water and DMSO (Merck, Darmstadt, Germany), respectively. Solvent controls were included in every experiment. To block caspases before cell death induction, Z-VAD-FMK was applied 2 h prior to BV-6 administration. All experiments were carried out at least 3 times, if not described otherwise.

RT-PCR and qRT-PCR

RT-PCR was conducted as previously described [46, 47]. In brief, total RNA was extracted using RNeasy Plus Micro Kit (Qiagen, Hilden, Germany) and employed for reverse transcription. RT-PCR and qRT-PCR primers (Table 1) were designed using Primer3 and synthesized by metabion international AG (Planegg, Germany) [48]. The qRT-PCR analyses were performed utilizing the QuantiFast SYBR Green PCR Kit (Qiagen, Hilden, Germany). Samples (final cDNA concentration 10 ng/reaction) were measured in duplicates in a LightCycler[®] 96 System (Roche Diagnostics, Penzberg, Germany; melting at 95 °C for 5 min, followed by 40 cycles of denaturation at 95 °C for 10 s and extension at 60 °C for 30 s, and a final melting step with continuous heating (0.5 °C/s from 65 °C to 97 °C) and a cool-down step at 37 °C for 30 s). Results were calculated using the $2^{-\Delta\Delta C_q}$ method and expression was normalized to ribosomal protein L19 (*L19*), hypoxanthine Phosphoribosyltransferase 1 (*HPRT*), peptidylprolyl isomerase A (*PPIA*) and TATA-box binding protein (*TBP*) as endogenous references. After PCR, products were separated and visualized on a 2% agarose gel. Expected bands were cut out, sequenced (GATC Biotech AG, Konstanz, Germany) and analyzed using BLAST tool [49].

Immunohistochemistry of ex vivo GCT using anti-cIAP1 antibody

Immunohistochemical staining of cIAP1 proteins to examine expression patterns in GCTs was done as described in previous work [46, 47]. Two slides of the TMAs, containing a total of 42 tumors in duplicates, were used for this study.

After deparaffinizing, the heat-induced epitope retrieval (HIER) method was applied to retrieve antigens. Afterwards endogenous peroxidase was blocked with a methanol (10%)/H₂O₂ (3%) solution. Unspecific binding was reduced by 10% goat serum in PBS. To detect cIAP1 protein, a polyclonal antibody was used (HPA005513, Sigma Aldrich, St. Louis, MO, USA). As a negative control rabbit serum replaced the primary antiserum. As a secondary antibody a biotinylated goat anti-rabbit antibody (111-065-144, Jackson Immuno Research, Cambridge, UK) was used. After complexing avidin with biotin (ABC reaction) and staining by means of 3,3' diaminobenzidine tetrahydrochloride (DAB), the slides were counterstained with hematoxylin. Images were captured using a Zeiss Axiovert microscope with an Insight Camera (18.2 Color Mosaik). The TMA's were evaluated by 6 different researchers, who classified each tumor into one of the three groups (homogeneously strong staining, weak staining/no staining or heterogeneous staining).

Confluency measurement and live cell imaging

Confluency was measured as described before [40, 47]. In brief, 3×10^5 KGN plated on a 60 mm² culture dish (Sarstedt AG & Co. KG, Nümbrecht, Germany) were stimulated with BV-6 (EC₅₀, 8 μM) or the solvent control and monitored for 24 h using the JuLi™ Br Live Cell Analyzer (NanoEnTek Inc., Seoul, Korea). Pictures were captured every 20 min and confluency was evaluated using the in-built algorithm. The experiments were repeated 3 times.

Images of KGN, stimulated with 0.1, 1, 10, 50 μM BV-6, were also captured using a cell culture microscope with an 10X objective (Leica Biosystems, Wetzlar, Germany).

Viability measurements using cell counting and ATP-assay

EC₅₀ was identified using 2 different methods. First a cell counting experiment was carried out with low passages (< 8) and high passages of KGN (> 80). Therefore 1.5×10^5 cells were seeded on 6 well plates (Sarstedt AG & Co. KG, Nümbrecht, Germany) and incubated over night at 37 °C and 5% CO₂. On the next day the cells were stimulated with BV-6 concentrations ranging from 0.05 to 100 μM or the corresponding solvent control for 24 h. Afterwards cells were trypsinized and counted using the CASY® counting system (OMNI Life Science GmbH & Co KG, Bremen, Germany). Cell counts were normalized to solvent controls. Experiments were repeated at least 3 times.

The CellTiter-Glo® ATP assay Kit (Promega, Mannheim, Germany) was performed following the manufacturer's instructions. In brief 1×10^4 cells/well (KGN passages > 80) were seeded in 96-well plates (Sarstedt AG & Co. KG, Nümbrecht, Germany) and incubated at 37 °C and 5% CO₂. The next day culture media was replaced by

colorless media without supplements. After 2 h, BV-6 (0.1–50 μM) was added and cells were incubated for a time period of 24 h. Further, BV-6 (8 μM) treatment was accompanied by different Z-VAD-FMK concentrations ranging from 0 to 200 μM. Z-VAD-FMK was applied 2 h before BV-6 stimulation to block caspases. Luminescence was measured using a plate reader (FLUOstar Optima, BMG Labtech, Ortenberg, Germany).

Verification of apoptosis hallmarks by Western blot

Apoptosis is a form of cell death that is executed by caspases. Cleavage and therefore activation of caspase 3 is known to be an intermediate step, which leads to cleavage of proteins including PARP that is known to be a terminal step of apoptosis. Therefore, we treated KGN (10^6 cells/60 mm² dish (Sarstedt AG & Co. KG, Nümbrecht, Germany)) with BV-6 (EC₅₀, 8 μM) for 24 h. Afterwards we generated crude protein extracts using RIPA buffer. Western Blot was carried out as described before [40, 46]. 20 μg/lane protein were loaded on 12% SDS-PAGE gels. To detect cleaved caspase 3 a specific α-cIcASP3 antibody (#9664, Cell Signaling Technology, Denver, MA, USA) was used. To detect a cleavage product of PARP the specific α-cIcPARP antibody (#56255, Cell Signaling Technology, Denver, MA, USA) was applied. As a loading control an α-βActin antibody (A5441, Sigma Aldrich, St. Louis, MO, USA) was used. For decoration of bound primary antibody horseradish peroxidase (HRP) conjugated goat α-rabbit or goat α-mouse antibody (Jackson Immuno Research, Cambridge, UK) were used.

Statistics and graphs

Cell culture and live cell imaging pictures were evaluated using FIJI [50]. Construction and statistical evaluation of graphs, including nonlinear regression analyses, were done in Prism 6 (GraphPad, San Diego, CA, USA). The statistical significance between different staining patterns of tumors was evaluated by one-way ANOVA (Tukey; Geisser-Greenhouse correction). Effectiveness of Z-VAD-FMK on BV-6-induced cell death and mRNA expression of NF-κB regulated genes were evaluated statistically by one sample *t*-tests. Final figures were constructed using PowerPoint for Mac 2013 (Microsoft, Redmond, WA, USA).

Additional file

Additional file 1: Figure S1. Workflow of experiments and effects of BV-6 on KGN. (a) Schematic workflow of experiments: First EC₅₀ after 24 h was determined by cell counting and ATP assay in KGN (passage > 80) and by cell counting in a low passage of KGN (< 8). All further experiments were carried out with the determined EC₅₀ and with KGN of higher passages (> 80). Afterwards a Z-VAD-FMK dilution experiment was carried out, using KGN that were treated with BV-6 (EC₅₀). (b) Live cell imaging experiment of stimulated KGN (BV-6, 1 μM) versus the corresponding control for 72 h. The low concentration caused a time-

dependent effect by reducing number of attached cells. Scale bar = 100 μm (c) Western Blot of BV-6 (EC_{50} , 8 μM)-stimulated KGN and the corresponding control. An antibody against phosphorylated (p) MLKL(T357/S358) (ab187091, Abcam, Cambridge, UK) and one against MLKL (ab184718, Abcam, Cambridge, UK) were examined to explore possible induction of necroptosis. MLKL bands were visible, whereas the necroptosis marker (pMLKL) was absent. (TIFF 8189 kb)

Abbreviations

AIF: Apoptosis inducing factor; ATP: Adenosine triphosphate; BIR: Baculoviral IAP repeats; BIRC: Baculoviral IAP repeat containing protein; CASP8: Caspase 8; cIAP: Cellular inhibitor of apoptosis protein; DAB: 3,3'-diaminobenzidine tetrahydrochloride; DIABLO: Direct inhibitor of apoptosis protein binding protein with low PI; EC_{50} : Half maximal effective concentration; FCS: Fetal calf serum; FOXL2: Forkhead Box L2; GCTS: Granulosa cell tumors; HIER: Heat-induced epitope retrieval; HPRT: Hypoxanthine phosphoribosyltransferase 1; HRP: Horseradish peroxidase; HRP: Horseradish peroxidase; HtrA2: High temperature requirement protein A2; IAPs: Inhibitor of apoptosis proteins; IL8: Interleukin 8; KGN: Human ovarian granulosa-like tumor cell line; L19: ribosomal protein L19; MCP-1: Monocyte chemoattractant protein-1; MLKL: Mixed lineage kinase domain-like protein; mRNA: Messenger ribonucleic acid; PPIA: Peptidylprolyl isomerase A; TBP: TATA-box binding protein; α -cCASP3: anti-cleaved caspase 3; α -cPARP: anti-cleaved poly (ADP-ribose)-polymerase

Acknowledgements

We gratefully acknowledge the expert technical help of Kim Dietrich and Carola Herrmann.

Ethics approval and consent to participation

The ethical committee of the LMU has approved the study (project 390–15) and patients had agreed to the use of the tissue for scientific purposes.

Authors' contributions

Konstantin Bagnjuk and Verena Jasmin Kast performed the cellular studies and evaluated the results and together with Artur Mayerhofer drafted the manuscript. Astrid Tiefenbacher performed immunohistochemical studies. Melanie Kaseder performed qRT-PCR experiments. Toshihiko Yanase provided KGN. Dr. Burges was the surgeon and obtained the consent of the patients. Doris Mayr provided TMA. Lars Kunz, Doris Mayr and Artur Mayerhofer conceived of the study and directed the work. All authors contributed to and agreed on the final manuscript.

Funding

Deutsche Forschungsgemeinschaft (DFG), MA1080/19–2 (to AM) and MA4790/4–2 (to DM).

Availability of data and materials

Upon request.

Competing interests

None.

Author details

¹Biomedical Center Munich (BMC), Cell Biology, Anatomy III, Ludwig-Maximilians-University (LMU), Grosshaderner Strasse 9, 82152 Planegg, Germany. ²Department of Endocrinology and Diabetes Mellitus, Faculty of Medicine, Fukuoka University, 7-45-1 Nanakuma, Jonan-ku, Fukuoka City, Japan. ³Frauenklinik Campus Großhadern, Ludwig-Maximilians-University (LMU), Marchioninistraße 15, 81377 Munich, Germany. ⁴Division of Neurobiology, Department Biology II, Ludwig-Maximilians-University (LMU), Grosshaderner Strasse 9, 82152 Planegg, Germany. ⁵Institute for Pathology, Ludwig-Maximilians-University (LMU), 80337 Munich, Germany.

Received: 26 April 2019 Accepted: 31 July 2019

Published online: 14 August 2019

References

1. Hengartner MO. The biochemistry of apoptosis. *Nature*. 2000;407:770.

- Fulda S, Debatin KM. Extrinsic versus intrinsic apoptosis pathways in anticancer chemotherapy. *Oncogene*. 2006;25:4798.
- Degterev A, Boyce M, Yuan J. A decade of caspases. *Oncogene*. 2003;22:8543.
- Saelens X, Festjens N, Vande Walle L, van Gurp M, van Loo G, Vandenabeele P. Toxic proteins released from mitochondria in cell death. *Oncogene*. 2004; 23(16):2861–74.
- Fulda S. Promises and challenges of Smac mimetics as Cancer therapeutics. *Clin Cancer Res*. 2015;21(22):5030.
- Varfolomeev E, Blankenship JW, Wayson SM, Fedorova AV, Kayagaki N, Garg P, et al. IAP antagonists induce autoubiquitination of c-IAPs, NF- κ B activation, and TNF α -dependent apoptosis. *Cell*. 2007;131(4):669–81.
- Vince JE, Wong WW-L, Khan N, Feltham R, Chau D, Ahmed AU, et al. IAP antagonists target cIAP1 to induce TNF α -dependent apoptosis. *Cell*. 2007; 131(4):682–93.
- Petersen SL, Wang L, Yalcin-Chin A, Li L, Peyton M, Minna J, et al. Autocrine TNF α signaling renders human Cancer cells susceptible to Smac-mimetic-induced apoptosis. *Cancer Cell*. 2007;12(5):445–56.
- Lu J, Bai L, Sun H, Nikolovska-Coleska Z, McEachern D, Qiu S, et al. SM-164: a novel, bivalent Smac mimetic that induces apoptosis and tumor regression by concurrent removal of the blockade of cIAP-1/2 and XIAP. *Cancer Res*. 2008;68(22):9384–93.
- Vischioni B, van der Valk P, Span SW, Kruyt FAE, Rodriguez JA, Giaccone G. Expression and localization of inhibitor of apoptosis proteins in normal human tissues. *Hum Pathol*. 2006;37(1):78–86.
- Jamieson S, Fuller PJ. Molecular pathogenesis of granulosa cell tumors of the ovary. *Endocr Rev*. 2012;33(1):109–44.
- Zhou J, Chen Y, Huang Y, Long J, Wan F, Zhang S. Serum follicle-stimulating hormone level is associated with human epidermal growth factor receptor type 2 and Ki67 expression in post-menopausal females with breast cancer. *Oncol Lett*. 2013;6(4):1128–32.
- Gründker C, Emons G. The Role of Gonadotropin-Releasing Hormone in Cancer Cell Proliferation and Metastasis. *Frontiers in Endocrinology*. 2017;8(187).
- Lagana AS, Colonese F, Colonese E, Sofo V, Salmeri FM, Granese R, et al. Cytogenetic analysis of epithelial ovarian cancer's stem cells: an overview on new diagnostic and therapeutic perspectives. *Eur J Gynaecol Oncol*. 2015;36(5):495–505.
- Lagana AS, Sofo V, Vitale SG, Triolo O. Epithelial ovarian cancer inherent resistance: may the pleiotropic interaction between reduced immunosurveillance and drug-resistant cells play a key role? *Gynecologic oncology reports*. 2016;18:57–8.
- Nishi Y, Yanase T, Mu Y, Oba K, Ichino I, Saito M, et al. Establishment and characterization of a steroidogenic human granulosa-like tumor cell line, KGN, that expresses functional follicle-stimulating hormone receptor. *Endocrinology*. 2001;142(1):437–45.
- Leung DTH, Nguyen T, Oliver EM, Matti J, Alexiadis M, Silke J, et al. Combined PPAR γ activation and XIAP inhibition as a potential therapeutic strategy for ovarian granulosa cell tumors. *Mol Cancer Ther*. 2019;18(2):364–75.
- Zhang Y, Yan Z, Qin Q, Nisenblat V, Chang HM, Yu Y, et al. Transcriptome Landscape of Human Folliculogenesis Reveals Oocyte and Granulosa Cell Interactions. *Molecular cell*. 2018;72(6):1021–34.e4.
- Imai M, Muraki M, Takamatsu K, Saito H, Seiki M, Takahashi Y. Spontaneous transformation of human granulosa cell tumours into an aggressive phenotype: a metastasis model cell line. *BMC Cancer*. 2008;8(1):319.
- Stehlik C, De Martin R, Kumabashiri I, Schmid JA, Binder BR, Lipp J. Nuclear factor (NF)- κ B-regulated X-chromosome-linked iap gene expression protects endothelial cells from tumor necrosis factor α -induced apoptosis. *J Exp Med*. 1998;188(1):211–6.
- Wang C-Y, Mayo MW, Korneluk RG, Goeddel DV, Baldwin AS. NF- κ B antiapoptosis: induction of TRAF1 and TRAF2 and c-IAP1 and c-IAP2 to suppress caspase-8 activation. *Science*. 1998;281(5383):1680–3.
- Kang HB, Kim YE, Kwon HJ, Sok DE, Lee Y. Enhancement of NF- κ B expression and activity upon differentiation of human embryonic stem cell line SNUHES3. *Stem Cells Dev*. 2007;16(4):615–23.
- Xing L, Remick DG. Promoter elements responsible for antioxidant regulation of MCP-1 gene expression. *Antioxid Redox Signal*. 2007;9(11): 1979–89.
- Van Noorden CJF. The history of Z-VAD-FMK, a tool for understanding the significance of caspase inhibition. *Acta Histochem*. 2001;103(3):241–51.
- Chaitanya GV, Steven AJ, Babu PP. PARP-1 cleavage fragments: signatures of cell-death proteases in neurodegeneration. *Cell communication and signaling : CCS*. 2010;8:31.

26. Hanahan D, Weinberg RA. Hallmarks of cancer: the next generation. *Cell*. 2011;144(5):646–74.
27. Dubrez L, Berthelet J, Glorian V. IAP proteins as targets for drug development in oncology. *OncoTargets and therapy*. 2013;9:1285–304.
28. Infante JR, Dees EC, Olszanski AJ, Dhuria SV, Sen S, Cameron S, et al. Phase I dose-escalation study of LCL161, an oral inhibitor of apoptosis proteins inhibitor, in patients with advanced solid tumors. *Journal of clinical oncology : official journal of the American Society of Clinical Oncology*. 2014;32(28):3103–10.
29. Bertrand Mathieu JM, Vandenabeele P. The Ripoptosome: death decision in the cytosol. *Mol Cell*. 2011;43(3):323–5.
30. Wertz IE, Dixit VM. Signaling to NF- κ B: regulation by ubiquitination. *Cold Spring Harb Perspect Biol*. 2010;2(3):a003350.
31. Lagana AS, Vitale SG, Nigro A, Sofo V, Salmeri FM, Rossetti P, et al. Pleiotropic Actions of Peroxisome Proliferator-Activated Receptors (PPARs) in Dysregulated Metabolic Homeostasis, Inflammation and Cancer: Current Evidence and Future Perspectives. *Int J Mol Sci*. 2016;17(7).
32. Vitale SG, Lagana AS, Nigro A, La Rosa VL, Rossetti P, Rapisarda AM, et al. Peroxisome proliferator-activated receptor modulation during metabolic diseases and cancers: master and minions. *PPAR Res*. 2016;2016:6517313.
33. Brumatti G, Ma C, Lalaoui N, Nguyen NY, Navarro M, Tanzer MC, et al. The caspase-8 inhibitor emricasan combines with the SMAC mimetic birinapant to induce necroptosis and treat acute myeloid leukemia. *Sci Transl Med*. 2016;8(339):339ra69.
34. McComb S, Aguade-Gorgorio J, Harder L, Marovca B, Cario G, Eckert C, et al. Activation of concurrent apoptosis and necroptosis by SMAC mimetics for the treatment of refractory and relapsed ALL. *Sci Transl Med*. 2016;8(339):339ra70.
35. Opel D, Schnaiter A, Dodier D, Jovanovic M, Gerhardinger A, Idler I, et al. Targeting inhibitor of apoptosis proteins by Smac mimetic elicits cell death in poor prognostic subgroups of chronic lymphocytic leukemia. *Int J Cancer*. 2015;137(12):2959–70.
36. Schirmer M, Trentin L, Queudeville M, Seyfried F, Demir S, Tausch E, et al. Intrinsic and chemo-sensitizing activity of SMAC-mimetics on high-risk childhood acute lymphoblastic leukemia. *Cell Death Dis*. 2016;7:e2052.
37. Steinhart L, Belz K, Fulda S. Smac mimetic and demethylating agents synergistically trigger cell death in acute myeloid leukemia cells and overcome apoptosis resistance by inducing necroptosis. *Cell Death Dis*. 2013;4:e802.
38. Safferthal C, Rohde K, Fulda S. Therapeutic targeting of necroptosis by Smac mimetic bypasses apoptosis resistance in acute myeloid leukemia cells. *Oncogene*. 2017;36(11):1487–502.
39. Chen Q, Kang J, Fu C. The independence of and associations among apoptosis, autophagy, and necrosis. *Signal Transduction and Targeted Therapy*. 2018;3(1):18.
40. Bagnjuk K, Stöckl JB, Fröhlich T, Arnold GJ, Behr R, Berg U, et al. Necroptosis in primate luteolysis: a role for ceramide. *Cell Death Discovery*. 2019;5(1):67.
41. Beug ST, Conrad DP, Alain T, Korneluk RG, Lacasse EC. Combinatorial cancer immunotherapy strategies with proapoptotic small-molecule IAP antagonists. *The International journal of developmental biology*. 2015;59(1–3):141–7.
42. Beug ST, Beauregard CE, Healy C, Sanda T, St-Jean M, Chabot J, et al. Smac mimetics synergize with immune checkpoint inhibitors to promote tumour immunity against glioblastoma. *Nat Commun*. 2017;8.
43. Fischer K, Tognarelli S, Roesler S, Boedicker C, Schubert R, Steinle A, et al. The Smac Mimetic BV6 Improves NK Cell-Mediated Killing of Rhabdomyosarcoma Cells by Simultaneously Targeting Tumor and Effector Cells. *Front Immunol*. 2017;8(202).
44. Lecis D, De Cesare M, Perego P, Conti A, Corna E, Drago C, et al. Smac mimetics induce inflammation and necrotic tumour cell death by modulating macrophage activity. *Cell death & disease*. 2013;4(11):e920-e.
45. Fulda S. Smac mimetics to therapeutically target IAP proteins in Cancer. *Int Rev Cell Mol Biol*. 2017;330:157–69.
46. Du Y, Bagnjuk K, Lawson MS, Xu J, Mayerhofer A. Acetylcholine and necroptosis are players in follicular development in primates. *Sci Rep*. 2018; 8(1):6166.
47. Blohberger J, Kunz L, Einwang D, Berg U, Berg D, Ojeda SR, et al. Readthrough acetylcholinesterase (AChE-R) and regulated necrosis: pharmacological targets for the regulation of ovarian functions? *Cell death & disease*. 2015;6:e1685.
48. Koressaar T, Remm M. Enhancements and modifications of primer design program Primer3. *Bioinformatics*. 2007;23(10):1289–91.
49. Altschul SF, Gish W, Miller W, Myers EW, Lipman DJ. Basic local alignment search tool. *J Mol Biol*. 1990;215(3):403–10.
50. Rueden CT, Schindelin J, Hiner MC, DeZonia BE, Walter AE, Arena ET, et al. ImageJ2: ImageJ for the next generation of scientific image data. *BMC bioinformatics*. 2017;18(1):529.

Publisher's Note

Springer Nature remains neutral with regard to jurisdictional claims in published maps and institutional affiliations.

Ready to submit your research? Choose BMC and benefit from:

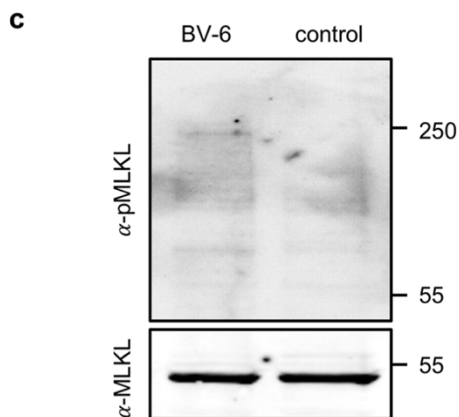
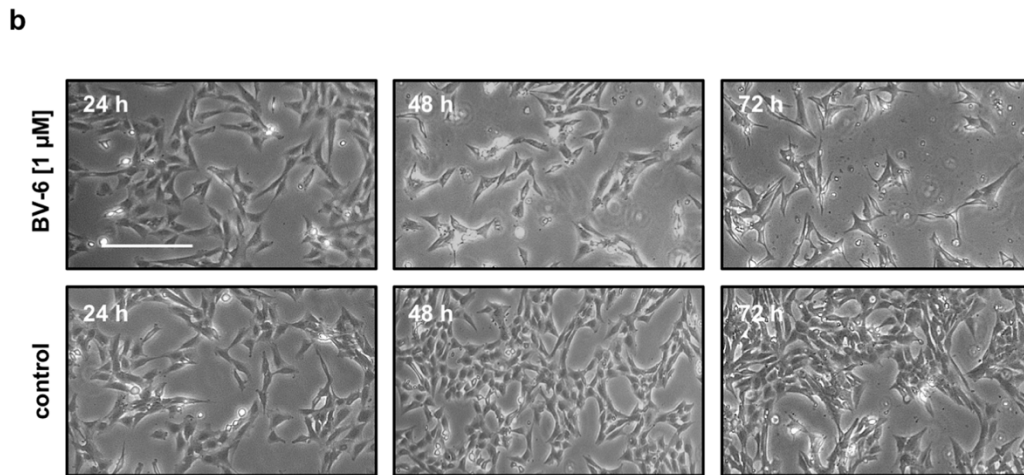
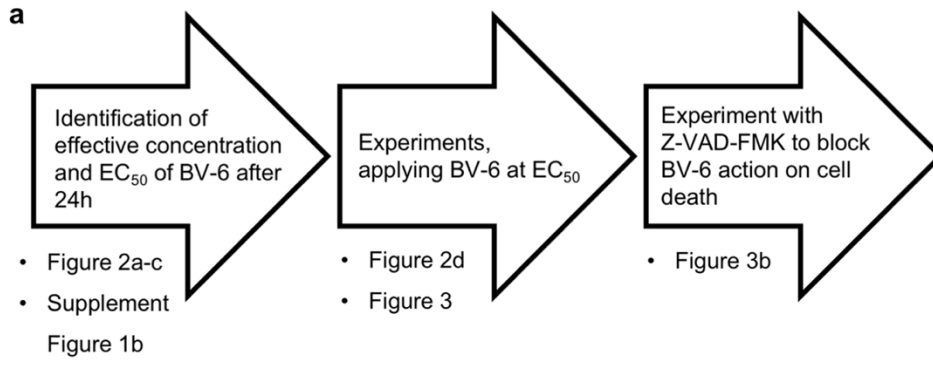
- fast, convenient online submission
- thorough peer review by experienced researchers in your field
- rapid publication on acceptance
- support for research data, including large and complex data types
- gold Open Access which fosters wider collaboration and increased citations
- maximum visibility for your research: over 100M website views per year

At BMC, research is always in progress.

Learn more biomedcentral.com/submissions



Supplementary Figure 1



4 Discussion

Reproduction governs life. In our modern society, however, factors like environmental influence, career goals, financial resources or social pressure affect the reproductive functions and capability. The desire to reproduce is contrasted with the threat of overpopulation, which we will have to face.

On one hand, it is important to help people with an unfulfilled wish for having a family. On the other hand, it is necessary to prevent unwelcomed pregnancy by fertility control techniques rather than induced abortions. To achieve these opposed goals, the biology of human reproduction needs to be understood.

The present work focused on the female part in human reproduction. In particular, the CL was explored, which is a transient organ that produces P4 to regulate fecundity. Low P4 levels have been associated with diminished pregnancy rates ²⁵⁸, which might originate from luteal phase defects or improper large lutein cell (LLC) function ²⁵⁹. Cell death events regulate CL lifetime that in turn manifests in P4 production. Interference with these incidents could hence allow us to maintain or disturb CL function in case of preterm regression or in fertility control, respectively. Subsequently, the interest in this work was concentrated on the ongoing cell death events in the human CL to understand the mechanisms which could be interfered with. The adjusted understanding of CL regression in humans and its implication for fertility control and IVF will be discussed in the following.

Additionally, the discussion will be focused on basic research goals that might yield improvements for fertility preservation in cancer patients. As medicine is evolving, odds for long-term cancer survivors are improving. For pediatric cancer patients this rate fortunately increased up to 70 % ²⁶⁰. However, only half of the counseling oncologists will send their patients to fertility preservation specialists ^{261,262}. This might be due to limited options for fertility preservation in prepubertal patients or the knowledge about current techniques. Hence, the present study touched on two key issues of a prepubertal cancer patient on the way through treatment to contribute to the aim of giving back the patients the ability to decide whether they want to have children or not. A therapy option apart from gonadotoxic chemotherapy and radiation, namely treatment with the small molecule BV6 was evaluated. Furthermore, attempts

were made to improve *in vitro* follicle maturation for fertility preservation, as this technique is ubiquitously suited for female cancer patients.

4.1 LGCs – a model for human LLCs

In reproductive biology there is a lack of translational models to examine the complex ovary, with its vast interspecies difference. A widely used *in vitro* model, namely LGCs, could eliminate this gap of knowledge, if a proper characterization of these cells was performed. All studies that characterized LGCs by big data analysis, used transcriptomic approaches, which depend on mRNA levels²⁶³⁻²⁶⁵. These, however, do not necessarily represent protein levels, a fact that is constituted by publications describing the expression patterns of the steroidogenic acute regulatory protein (StAR) in the ovary. StAR protein expression is restricted to the theca layer and cells of the CL^{266,267}. Although this was verified at the mRNA level before²⁶⁸, a novel transcriptomic analysis indicates strong StAR mRNA expression in GCs of the follicle²⁶⁹. Based on these discrepancies between RNA and protein levels, it is substantial to collect proteomic data of LGCs for a proper characterization of this cellular model. As proteomic data are exclusively available for follicular fluid²⁷⁰, the present study was designed to assess IVF-derived LGCs by mass spectrometry. The particular attention was focused on the changes of LGCs over time *in vitro*, which could actually mimic LLC *in vivo*. However, it has to be considered that IVF-derived LGCs are the product of a clinical intervention on the endocrinological homeostasis. During the course of IVF, COS leads to a defective luteal phase, whereas the explanation for this phenomenon remains indistinct^{271,272}. Next to a variety of hypotheses²⁷³⁻²⁷⁵, supraphysiological hormone levels may be an appropriate answer^{271,275,276}. Nevertheless, IVF-derived LGCs could be the means of choice to tackle the question behind COS-dependent luteal insufficiency.

Upon ovulation the CL is formed, it produces P4 and hence enables pregnancy. Before follicular GCs luteinize, they do not synthesize this steroid, as the key enzyme StAR is missing²⁶⁸. Consequently, the first rise in P4 levels after the LH surge must be due to theca cell actions²⁷⁷. Post luteinization, however, P4 is mainly produced by LLCs^{52,278}. With modern mass spectrometric approaches, it was verified that human IVF-derived LGCs resemble LLCs rather than GCs, as they express StAR and produce P4 *in vitro*²⁴⁷. Although IVF-derived LGCs have been used to make conclusions on follicular GCs^{256,279-281}, the present mass spectrometric data

(e.g. expression patterns of CYP11A1, LDL-R, 3 β -HSD and StAR) and the comparison to literature revealed that cultured LGCs from day 2 onwards more likely resemble the main content of the CL²⁸², the LLCs of the mid-luteal to late (regressing)-luteal phase. This is further supported by yet unpublished results, which showed that P4 levels are highest between day 1 and 2 of culture and decline afterwards.

The mass spectrometric approach supported the assumption that human, IVF-derived LGCs resemble LLCs of the human CL²⁸² of an IVF patient. But yet a cellular model does not fully mimic a whole organ, which is characterized by the interplay between a variety of cells. In the primate CL there are non-steroidogenic and steroidogenic cells²⁸³, whereas the latter ones equate the largest proportion of the CL in volume²⁸⁴. However, endothelial cells play an inevitable role in the vascularization process of this transient organ in the early- and mid-luteal phase. These cells have been shown to interact with steroidogenic cells²⁸⁵ and they are responsible for the connection between the CL and the rest of the human body through the blood stream. Compromised vascularization was linked to premature luteolysis, induced through gonadotropin defects, which led to pregnancy loss⁵⁷. Therefore, steroidogenic activity is strongly dependent on endothelial function, and of course it could be possible that endothelial cells regulate LLCs cell death, or vice versa, by yet unknown factors. Unfortunately, the multicellular behavior cannot readily be examined in the 2D-culture system used in the study. Human LGCs provide insights into the human situation, but come with the drawbacks of cell culture. These drawbacks can, however, be overcome by reproducing the findings in studies with non-human primates *in vivo* or *in situ*.

4.2 Let's rethink luteal regression in the human ovary

The luteal phase can be dissected into three parts, CL formation, maintenance and regression. Especially the mechanisms governing luteal regression in humans remain poorly understood, as most of the research is done in animals like rats²⁸⁶, cattle^{287,288} and sheep²⁸⁹, where CL regression is due to the actions of uterine prostaglandin F_{2 α} (PGF_{2 α}). Although apoptosis is suffice to explain most of the features of a regressing CL in rodents⁴⁹, the situation for the bovine and the primate CL^{290,291} is more complex, as the largest proportion of the occurring cell death remains unexplained. Recent work in the bovine indicated necroptosis during CL regression *in vivo*^{292,293}. Hereby the authors used bovine CL to show that PGF_{2 α} administration

elevates RIP1 and RIP3 mRNA expression. Furthermore, a study by Wang and colleagues²⁹⁴ indicated that PGF2 α administration does induce luteolysis in mice, as seen by lowered P4 levels. The importance for apoptosis in this process, however, was unconvincing, as PARP1 vs. cleaved PARP1 levels remained unchanged and CASP3 levels were only slightly elevated²⁹⁴. This indicates the importance to reflect the process of luteal regression with the gained expertise about cell death forms, even in rodents. In the human CL it was demonstrated that apoptosis is a rare event²⁹⁵. Sugino and Okuda²⁹⁶ summarized that there are tremendous differences between species in terms of luteolysis. This was the motivation to verify the first hints for necroptosis in primate CL regression¹⁵⁶ to improve the understanding of this field in human physiology.

As stated above, most animal models are barely suited for the study of the human CL. The only well-suited animal models are closely related species from the order of primates like *Macaca mulatta* and *Callithrix jacchus*. Contrary to most other animals, uterine PGF2 α was clearly shown to be negligible for luteal function in primates^{297,298}, a fact based on the human and non-human primate anatomy. Nevertheless, in primates PGF2 α can be synthesized locally, which was shown in human LGCs²⁹⁹ and monkey LLCs³⁰⁰. Next to its luteolytic function³⁰¹ and contrary to other prostaglandins³⁰², PGF2 α is able to induce vasoconstriction^{303,304}. Accordingly, this hormone's actions are implicated in myocardial dysfunction^{305,306}, brain injury³⁰⁷ and inflammation³⁰⁸. The vasoconstrictive ability of PGF2 α could strongly affect the highly vascularized CL in the late luteal phase, where this hormone is known to peak³⁰¹. Interestingly, E2 administration is able to induce PGF2 α -dependent functional luteolysis in *M. mulatta*^{309,310}, probably through modifying the cellular PGF2 α receptor localization³¹¹. Accordingly, in *C. jacchus* it was verified that the PGF2 α analogue Cloprostenol is able to induce functional luteolysis³⁰¹. Consistent with other species, PGF2 α plays a role in luteal regression in primates, but the origin and mode of action are different from other model and experimental organisms. Especially the form of cell death that is induced by PGF2 α in primates remains elusive. This, however, was not examined in the present study, as cell death was observed to occur spontaneously in culture²⁸². The possibility that PGF2 α treatment could increase LGC death in culture represents a scenario that therefore remains to be tested. In the present setting, cell death, including necroptosis, could be induced by the withdrawal of the cells from their natural environment and subsequent from the stimulus of luteotrophic factors like hCG or LH³¹². In primates it was demonstrated that withdrawal of pituitary gonadotropin support induces reversible functional luteolysis *in vivo*³¹³. Together with the recent, unpublished findings,

which indicate that hCG is able to reduce necroptosis *in vitro*, the deprivation hypothesis fits the present results. However, the mechanistic mode of action of how deprivation of specific factors eventually induces cell death in the culture system, remains elusive.

Nevertheless, post induction a multifold of cell death events lead to the demise of the CL. This process must include forms of cell death that differ from apoptosis^{290,291}. Data from the present study proposed necroptosis as a mechanism during luteal regression in primates (Fig. 5). A process that can readily be mirrored in a cell culture system (human LGCs), as it was shown that the basally occurring cell culture phenomena are indeed relevant for the *in vivo* situation. The published findings²⁸² are supported by yet unpublished results, which indicate that the “pregnancy hormone” hCG, which rescues the CL *in vivo*^{314,315}, also rescues LGCs in culture by reducing necroptosis.

Although still unknown how necroptosis is initiated in the human CL, there is much evidence for this form of cell death to be important for CL clearance. Necroptosis leads to membrane permeabilization and release of so-called damage-associated molecular patterns (DAMPs), which attract immune cells³¹⁶ (Fig. 3). Just recently there was a proof of concept study in cancer research utilizing this characteristic of necroptosis to actively attract immune cells to a tumor³¹⁷. The hypothesis that CL regression represents an immunological event is old³¹⁸, but it was supported by migrating immune cells³¹⁹. In the bovine, it was demonstrated that this migration occurred upon PGF2 α stimulation³²⁰, supporting the need of an immunogenic cell death. However, this interplay between numerous cells is difficult to evaluate in a cell culture system³²¹. Therefore, to test the possibility that necroptosis is attracting immune cells to the human/primate CL, whole animal studies utilizing primates are needed.

The present study contributed to the understanding of one of the mechanisms that actually execute cell death in the LGC culture and the primate CL. It was pinpointed that CER, a prominent cell death inducer, plays a substantial role in luteal regression in humans and non-human primates, although in an unexpected way. The significant impact of CER on the ovary has been proposed by the capability of sex hormones to regulate the CER metabolism during the menstrual cycle. During the luteal phase, CER was reported to be upregulated in organs of the female reproductive tract, however the ovary was not examined³²². Interestingly, cellular concentrations of CER (Fig. 4) were shown to differ between healthy and malignant tissue of the ovary which makes the ceramide pathway not only interesting in physiology but also in

oncology^{323,324}. In the present study the impact of the CER metabolism on the luteal phase of humans and non-human primates was evaluated. It was demonstrated that enzymes of the CER salvage pathway¹⁷⁶ were upregulated over culture in human LGCs as well as during primate CL regression *in vivo*. Especially SMPD1 and ASAH1 were strikingly upregulated. These enzymes are predominantly located in the endolysosomal compartments^{179,325} and it is known that their activation leads to CER production through the salvage pathway³²⁶ (Fig. 3). By immunocytochemistry it was verified that this upregulation actually led to translocation and increased levels of CER. Translocation of CER between cellular compartments was hypothesized to be important in CL formation³²⁷, however the study was conducted in bovine and shows only few data of the localization of CER. Luteolysis and CER were linked in mice^{195,328} and rats²⁰⁴ before. In mouse studies, luteal endothelial cells were examined. It was indicated that the enzyme, which degrades sphingomyelin to CER is important for TNF α -dependent apoptosis in endothelial cells of the CL but not in lutein cells³²⁸. The impact of ceramide on apoptosis of bovine lutein cells was shown in two independent studies^{200,329}. In human IVF-derived LGCs, CER was also shown to induce apoptosis. Interestingly, in this study clear morphological markers for necrotic cell death were evident²⁰⁶, which support the present findings. Together with the studies in various species cited above, it is irrefutable that CER is able to induce cell death in lutein cells. Although most studies linked CER to apoptosis, some of them lacked clear markers for this type of cell death. Subsequently, these do not contradict the present study. Furthermore, it has to be considered that there are significant interspecies differences for organs of the reproductive tract, which was recently shown by a broad gene transcription analysis between various model and experimental organisms and humans³³⁰. In view of this fact, the results from the present work indicate that ceramide is a cell death inducer and linked to necroptosis, at least in primates during luteal regression.

Western Blot experiments, performed in the frame of the present study, implied that CER accumulation, which actually leads to cell death in the CL, occurs post MLKL phosphorylation in the necroptosis pathway²⁸². Therefore, CER could rather be a necroptosis executioner than a necroptosis inducer. This is in line with recent findings from Parisi et al.¹⁹³, who state that CER accumulation occurs post RIP1 phosphorylation, an upstream event to MLKL phosphorylation. Another study assessing CER nanoliposomes in ovarian cancer models hypothesized a MLKL-dependent but RIP-independent necroptotic cell death¹⁸⁹, further underpinning the recent findings of ceramide executed necroptosis.

With the limitations of work published before, namely incomplete cell death determination, and the present and previous findings, which based on ceramide actions in a variety of systems including human LGCs, the hypothesis of luteal regression in the human and primate CL can be rewritten by adding ceramide-dependent necroptosis as a molecular switch between survival and cell death next to the well-established apoptotic mechanisms in LLCs.

4.3 The aim to give back the ability to decide

According to a recent analysis by Kim et al.²⁶⁰, up to 70 % of all prepubertal cancer patients survive their disease. However, cancer treatment often includes gonadotoxic therapies like chemotherapy or radiation. As techniques regarding fertility preservation parallelly improved over time, there are new practice guidelines for oncologists³³¹, which recently have been updated³³² and should be followed to disclose the possibilities patient have. For female patients, there are currently two well established methods, which are embryo- and oocyte-cryopreservation. Both of these techniques are not suited for a subset of patients including prepubertal girls with immature, gonadotropin irresponsive follicles and patients with E2-sensitive breast cancer or gynecological malignancies³³². The most innovative approach to preserve fertility in female cancer patients is the cryopreservation and transplantation of the ovarian cortex, which already showed promising results^{333,334}. Although still considered as an investigative approach in the US, German reproductive specialists support this technique because of proved success³³⁵. Probably the most significant advantage of this method is that the obligatory surgery can be done immediately without hormonal stimulation and risk for patients. Furthermore, it is suited for patients with immature ovaries, as the transplant is able to restore the normal ovarian function, including endocrinological characteristics. However, it is not known whether this method is suited for leukemia patients or patients with ovarian cancer as risk of reoccurrence could be elevated³³². Right now, prepubertal cancer patients who suffer from the most common pediatric cancer³³⁶, namely leukemia, and ovarian cancer patients have no adequate option to preserve fertility.

To give back these patients the ability to decide, whether they may want to have a family or not, there are three possibilities, whereas adoption is the only established. The other two consist of non-gonadotoxic treatments, which are rare for most cancers, as chemotherapy and radiation are still the place holder in cancer therapy³³⁷, and *in vitro* follicle maturation, which remains in

an investigative state until now. The results of two ^{338,339} of the present studies may, however, contribute to the goal of giving back the patients the ability to decide.

4.3.1 Necroptosis is to consider in *in vitro* follicle maturation

In vitro follicle maturation (IFM) is a clinical approach using preantral follicles to produce preovulatory ones, containing metaphase II oocytes that can readily be fertilized. A derivative of this technique is the *in vitro* oocyte maturation (IOM), which comprises antral follicles (< 13 mm) and is already used in some indications ^{340,341}. With the invention of laparoscopic surgery to acquire preovulatory follicles ³⁴², IVF with its controlled ovarian stimulation (COS) protocol prior to retrieval of mature oocytes became the predominant form of all assisted reproductive technologies. The prosperous birth of Louis Brown ³ through IVF marked the clinical starting point of this technique. However, IOM procedures have been shown to lead to pregnancy ^{340,341}, even without *in vivo* stimulation with gonadotropins,. Therefore, this technique bears advantages for particular cases as reviewed elsewhere ^{239,343,344}. In brief, IOM is of special interest in patients who disproportionately respond to COS (e.g. patients with ovarian hyperstimulation syndrome (OHSS) or polycystic ovary syndrome), or patients with other indications (e.g. fertility preservation due to cancer treatment, premature ovarian failure due to chemotherapy, oophorectomy, autoimmune diseases or infections, genetic abnormalities like Turner 47, XXX syndrome or FSHR mutations). Additionally, IOM is cheaper, as medications for possible OHSS and gonadotropin stimulation are not necessary. Furthermore, the monitoring costs are lowered due to the low impact on the ovarian physiology.

Once IFM becomes a standardized method, it could be utilized for the same indications as IOM, however the main use case would be fertility preservation ²³⁹. Hereby this technique is advantageous as it enables fertility preservation for all women including breast cancer patients, where gonadotropin stimulation should be avoided ³⁴⁵, patients with aggressive cancer, where time is precious and prepubertal girls, who do not harbor developed follicles but have been diagnosed with cancer to be treated by gonadotoxic therapies (e.g. radiation, chemotherapy). In these, sometimes very young patients, ovarian tissue is retrieved for fertility preservation and in most cases transplanted post gonadotoxic treatment to regain fertility ³⁴⁶. This clinical approach has already successfully restored the fertility in patients ³⁴⁷. Although it is very promising in most prepubertal cancer cases, patients who suffer from ovarian malignancies,

leukemia or metastatic cancers are not suited for transplantation of ovarian tissue, as cancer reoccurrence could be promoted by implantation. Therefore, IFM is a technique, worth to be fully developed to render treatment possibilities for these patients. With the present work in primate follicles³³⁸, preclinical insights were gathered that could lead to improvement of IFM one day.

10 years ago it was demonstrated that a secondary primate follicle can be fully matured in 3D-culture *in vitro*^{36,240}, but since then only once a meiotically competent metaphase II oocyte has been developed from human preantral follicles³⁴⁸, indicating a gap of knowledge. Contrary to this, in mice IFM has been established a long time ago³⁴⁹ and it has been shown recently that the whole process from a pool of rodent germ cells to mature oocytes can be established *in vitro*³⁵⁰. These achievements probably can be explained by the frequent use of this model organism in research, but it has also to be considered that the laboratory mouse is much less complex than a human in this perspective. For human follicles it has been shown that a two-phase 3D-culture method is needed to generate a mature follicle³⁴⁸. Hereby the follicles were grown in a firm alginate capsule until the antral stage. Afterwards, the follicle was released from the alginate capsule into a low attachment plate to mimic the *in vivo* environment, as it is thought that follicles move from the firm ovarian cortex to the less rigid perimedullary region during follicular development³⁵¹. In *M. mulatta* a single-phase 3D-culture is sufficient to render metaphase II oocytes³⁶, whereas *C. jacchus* follicles can be fully matured in 2D-culture, indicating the great difference even between closely related species and implicating the complexity of human ovarian physiology. Another explanation for these differences between species in terms of IFM success may be provided by the varying size of preovulatory follicles, where the impact of diffusion of nutrients and oxygen within a follicle is proportional to follicular size. Rodent preovulatory follicles are considerably smaller (around 0.4 mm³⁵²) if compared to *C. jacchus* (2-4 mm^{353,354}), *M. mulatta* (around 7 mm³⁵⁵) or human preovulatory follicles (2 cm⁹). Therefore, the molecular transport through the antrum represents a limiting factor that is important to consider in IFM.

In the study with human follicles, the authors generated an apparently healthy metaphase II oocyte, however they stated that the oocyte and follicle diameter never reached *in vivo* size³⁴⁸. As described above, antral follicle size is primarily determined by the volume of follicular fluid and the number of granulosa cells. Based on the findings in LGCs¹⁵⁶, where these cells have been found to have the ability to die by necroptosis, it can be hypothesized that follicles might

also be governed by necroptosis *in vitro*³³⁸. Therefore, the effects of the RIP1 kinase activity blocker necrostatin-1 (Nec1) on *in vitro* development of secondary follicles of *M. mulatta* in a 3D-culture system³³⁸ have been evaluated. Additionally, the trophic actions of the acetylcholinesterase (AChE) blocker Huperzine A on GC proliferation have been tested. It was found that both supplements improved follicular development as measured by size and cell death markers (Fig. 6). Nec1 is a known necroptosis blocker, but it also blocks the immunomodulatory enzyme indoleamine 2,3-dioxygenase (IDO)³⁵⁶. IDO regulates inflammation and cytokine production via the NF- κ B pathway, mainly in immune cells³⁵⁷. Interestingly, immune cells have been detected in ovarian follicles³⁵⁸⁻³⁶⁰ and Nec1 could block IDO of these cells and therefore change the cytokine pattern, which could affect follicular fate. Although various studies found immune cells in follicular fluid from IVF patients, these cells could also derive from contaminations with surrounding tissue. IVF samples are almost always contaminated with blood and tissue pieces, which can be separated from LGCs during primary cell preparation. Nevertheless, this ambiguous immune cell factor could be overcome in future studies by the use of a more specific Nec1 analogue, namely Nec1s³⁵⁶. In the setting used in the present study, namely *in vitro* cultured monkey follicles, off target effects have not been separated³³⁸, as more specific Nec1 analogues like Nec1s were not readily available at the time of experimental design. Nevertheless, necroptosis was verified by two parameters, which minimize the proportion of possible off-target effects in the interpretations that necroptosis is occurring in primate follicular GCs in culture and might be a factor in follicular atresia^{156,338}. The present study showed that it is possible to improve follicular size and probably GC number by applying a necroptosis blocker or an AChE blocker (Fig. 6). Together with a two-phase 3D-culture system this could improve IFM. However, the addition of more than one supplement needs to be evaluated in future studies, and hereby Nec1s should be used instead of Nec1.

The present results underpin the differences between species in follicular atresia of *in vitro* cultured follicles and during follicular development *in vivo*. Until now³⁶¹ follicular atresia has been equated by apoptosis in most published studies, although never really tested in primate or human follicles. Studies, including the present one^{156,338} shed light on this poorly understood topic of follicular cell death by indicating necroptosis as an important factor, as apoptosis is not the sole cell death mechanism in atresia, at least in IFM.

4.3.2 GCTs may be sensitive to SMAC mimetics

Fertility preservation in patients who underwent gonadotoxic treatment is important, but could be redundant by the development of non-gonadotoxic treatment methods. To accomplish this goal, science is in duty to understand the behavior and characteristics of tumors, to be able to trigger the weak spots without affecting the healthy environment. Therefore, the current study³³⁹ was designed to translate the knowledge about cell death, gathered in GCs³³⁸ and LGCs²⁸², to GCTs with the aim to better understand the ways GCT cells could undergo cell death. For this approach the effects of SMAC mimetics^{123,125,362,363} were assessed in KGN culture and their translational capacity was evaluated by immunohistochemistry³³⁹ (Fig. 7).

Overexpression of IAPs correspond to a poor prognosis in a variety of cancers^{128,364-368}, as these proteins empower tumor cells to evade cell death¹⁰³. In the ovary, expression of IAPs is poorly understood. The Human Protein Atlas³⁶⁹ (<http://www.proteinatlas.org>), which represents an online tool for pathologists, reflects this situation, as it shows, contrary to Leung and colleagues⁶⁷, no staining for cIAP1/2 and XIAP within the stroma of the healthy ovary. For malignancies of the ovary the protein atlas shows significant staining for cIAP1 and XIAP. This is consistent with the present and a recent publication, where XIAP⁶⁷ and cIAP1³³⁹ staining were found in GCTs. In the rat ovary XIAP was expressed in follicles depending on their size, with preovulatory follicles showing the strongest staining³⁷⁰. RNA sequencing data of human follicles of various size²⁶⁹ indicated strongest expression of XIAP in the secondary and antral follicle. For cIAP2 this study showed unchanged but low levels of mRNA during the whole follicular phase, whereas cIAP1 levels were highest in the primary stage. RNA sequencing and the immunohistochemical data from multiple sources, including the present study, propose differential staining patterns for follicles of various stages and between healthy and malignant tissues of the ovary. The gathered results, however, have to be put to the test, as immunohistochemical results always depend on antibody specificity and tissue preparation and RNA data do not necessarily mirror protein expression. Nevertheless, the studies do not refute that the resting pool of primordial follicles show the lowest expression levels for IAPs compared to cancerous tissue, where IAPs are much stronger expressed in. Therefore, SMAC mimetics could indeed be an alternative treatment method for GCTs with a lower gonadotoxic side effect, which could improve the situation for a subset of young cancer patients.

For this study, the bivalent SMAC mimetic BV6 was used to treat the GCT cell line KGN. This compound was chosen for its high potency¹²⁵ and the vast amount of experience from experiments with a variety of cancer cells³⁷¹⁻³⁷⁵. In the present work³³⁹ BV6 was effective in affecting the transcription of NF- κ B-dependent genes and in inducing apoptosis in KGN, as shown by viability assays, Western Blot and qRT-PCR experiments (Fig. 7). Therefore, the aims of this study were reached by supplying a proof of concept that SMAC mimetics alone are able to induce cell death in KGN and based on the expression patterns, these therapeutics might be of interest in future GCT treatments. The question, how BV6 or other SMAC mimetics will act on GCTs *in vivo* remains of interest and cannot be evaluated in the used setting. To further pursue this question xenograft models and primary tumors have to be assessed³⁷⁶. Additionally, other options of interfering with IAPs, such as downregulation of these targets, should be kept in mind for upcoming studies. For this, the antisense oligonucleotide AEG35156 should be considered in future approaches, as this compound showed promising results in preclinical¹¹⁸ and clinical studies³⁷⁷⁻³⁸⁰ with patients having malignancies other than GCTs.

The results of the present study may help to better understand the cell death mechanisms in GCTs and the tools these tumors use to evade cell death (IAP overexpression). With these preliminary findings and its interpretations, it is proposed that SMAC mimetics could be a less gonadotoxic treatment opportunity for GCT patients, although this still needs to be evaluated in xenograft models and clinical studies.

4.4 Future scenarios

The work summarized in this dissertation was performed with the aim to improve the general understanding of the human ovary and to generate basic research knowledge that may be translatable to a clinical application.

The better understanding of the newly discovered cell death form necroptosis during luteal regression in humans renders alternative possibilities for improvement of IVF procedures. Hormonal treatment during IVF represents a significant intrusion into the hormonal homeostasis of the human body and is therefore accompanied by many negative side effects^{381,382}. Next to FSH for follicle development, hCG is used for oocyte maturation and luteal phase support, as the artificially suppressed (through gonadotropin releasing hormone (GnRH)

antagonists³⁸³) LH peak needs to be replaced. The artificial addition of the recombinant “pregnancy hormone” hCG might induce OHSS³⁸⁴, which should be avoided. Interestingly, hormonal stimulation could drastically be reduced by interference with necroptosis, which is now known to be a factor in luteal regression. By reducing the amount of GnRH antagonists during the late follicular phase, a moderate but natural LH surge could occur, which should be sufficient for oocyte maturation. Otherwise stimulation with GnRH agonists³⁸⁵ or recombinant LH could be considered, as this hormone offers a shorter half-life and subsequent lower impact on hormonal homeostasis³⁸⁶. In a next step, during follicle punctuation and oocyte retrieval, Nec1s or other necroptosis inhibitors like NSA could be introduced into the luteinizing follicle to block cell death and therefore support the luteal phase. But, it has to be considered that too many active CL produce supraphysiological levels of hormones that in turn lead to inhibition of LH by a negative feedback loop^{275,276,383,387}. Therefore, necroptosis blockers could selectively be introduced into a specific number of follicles, sufficient enough to sustain the LH shortage and to enable pregnancy. In theory, the un-supplemented CL would undergo regression, whereas the supplemented CL would survive and maintain pregnancy. Supplementation with necroptosis blocker could also be considered in natural cycle IVF to support luteal phase, as hormonal stimulation is avoided in this procedure³⁸⁸. These scenarios have yet not been tested *in vivo*, however, in theory they might improve IVF outcomes and reduce risks of hormonal treatment.

If blocking cell death in the CL is possible, induction would be possible too. Therefore, the knowledge could be translated into contraceptives by induction of necroptosis in the CL. Hereby a body temperature-dependent pump could be introduced into the main artery that supplies the CL with blood. Body temperature is a measurement for the menstrual cycle³⁸⁹, which could render the accurate timing for ovulation, upon which S1P-kinase blockers could be released to the bloodstream through the pump to increase ceramide levels and subsequently induce necroptosis. The CL is the most vascularized structure in the ovary³⁹⁰ and based on the level of vascularization, ovarian compartments would be more or less affected by this treatment. Therefore, the CL could absorb most of the chemical and eventually regress. This hypothesis would lead to evasion of the use of hormones and therefore yield an improvement for the current situation for patients. However, artery devices are not evolved enough for such a use case as they remain a high-risk factor. Such devices have been utilized in cancer therapy³⁹¹, but not for fertility control approaches. Therefore, this idea remains a possible far future scenario.

Next to healthy individuals with fertility issues, GCT patients and prepubertal cancer patients could benefit from the work in this dissertation. For this purpose, IAP antagonists have successfully been used to induce apoptosis in GCT like cells, which improves the understanding of this tumor and opens a wide, recently emerged field of tumor therapeutics³⁹² that are used in clinical trials, namely SMAC mimetics and could also potentially be used for GCTs. Right now, no publications examined gonadotoxicity of SMAC mimetics. This needs to be evaluated before it can be said that SMAC mimetics offer a more gonad friendly alternative to radiation³⁹³ and chemotherapy³⁹⁴. In a next step, a variety of SMAC mimetics that are used in preclinical and clinical trials should be evaluated in KGN and other human GCT cell lines to determine optimal candidates for xenograft studies. Furthermore, the mode of action of these molecules in GCT like cells and other human cells needs further evaluation to be able to estimate possible consequences for the human body.

Next to cancer treatment options, factors that influence IFM have been identified in this study. Although necroptosis has been tagged to represent a substantial factor in GC death, it remains elusive how this affects the outcome of IFM³⁴⁸, as oocyte quality was not assessed in this study. Therefore, necroptosis blockers like Nec1s should be included in studies using two-phase 3D-culture systems to evaluate its importance in follicle maturation.

5 References

- 1 United Nations, D. o. E. a. S. A., Population Division *World Population Prospects 2019: Highlights (ST/ESA/SER.A/423)*. Vol. United Nations, Department of Economic and Social Affairs, Population Division (United Nations, 2019).
- 2 Wilson, E. O. *The future of life*. (Vintage, 2002).
- 3 Steptoe, P. C. & Edwards, R. G. Birth after the reimplantation of a human embryo. *Lancet* **2**, 366, doi:10.1016/s0140-6736(78)92957-4 (1978).
- 4 Nardo, L. G. & Sallam, H. N. Progesterone supplementation to prevent recurrent miscarriage and to reduce implantation failure in assisted reproduction cycles. *Reproductive biomedicine online* **13**, 47-57 (2006).
- 5 Csapo, A. I., Pulkkinen, M. O. & Kaihola, H. L. The relationship between the timing of luteectomy and the incidence of complete abortions. *American journal of obstetrics and gynecology* **118**, 985-989, doi:10.1016/0002-9378(74)90671-1 (1974).
- 6 Morran, L. T., Schmidt, O. G., Gelarden, I. A., Parrish, R. C., 2nd & Lively, C. M. Running with the Red Queen: host-parasite coevolution selects for biparental sex. *Science* **333**, 216-218, doi:10.1126/science.1206360 (2011).
- 7 Romao, G. S. *et al*. Oocyte diameter as a predictor of fertilization and embryo quality in assisted reproduction cycles. *Fertil Steril* **93**, 621-625, doi:10.1016/j.fertnstert.2008.12.124 (2010).
- 8 Cavilla, J. L., Kennedy, C. R., Byskov, A. G. & Hartshorne, G. M. Human immature oocytes grow during culture for IVM. *Human reproduction (Oxford, England)* **23**, 37-45, doi:10.1093/humrep/dem178 (2008).
- 9 Griffin, J., Emery, B. R., Huang, I., Peterson, C. M. & Carrell, D. T. Comparative analysis of follicle morphology and oocyte diameter in four mammalian species (mouse, hamster, pig, and human). *J Exp Clin Assist Reprod* **3**, 2, doi:10.1186/1743-1050-3-2 (2006).
- 10 Kristensen, S. G., Rasmussen, A., Byskov, A. G. & Andersen, C. Y. Isolation of pre-antral follicles from human ovarian medulla tissue. *Human reproduction (Oxford, England)* **26**, 157-166, doi:10.1093/humrep/deq318 (2011).
- 11 Motta, P. M., Makabe, S. & Nottola, S. A. The ultrastructure of human reproduction. I. The natural history of the female germ cell: origin, migration and differentiation inside the developing ovary. *Human reproduction update* **3**, 281-295, doi:10.1093/humupd/3.3.281 (1997).
- 12 Baker, T. G. A Quantitative and Cytological Study of Germ Cells in Human Ovaries. *Proc R Soc Lond B Biol Sci* **158**, 417-433, doi:10.1098/rspb.1963.0055 (1963).
- 13 Kristensen, S. G., Pors, S. E. & Andersen, C. Y. Diving into the oocyte pool. *Curr Opin Obstet Gynecol* **29**, 112-118, doi:10.1097/GCO.0000000000000359 (2017).
- 14 Craig, J. *et al*. Gonadotropin and intra-ovarian signals regulating follicle development and atresia: the delicate balance between life and death. *Front Biosci* **12**, 3628-3639 (2007).
- 15 Cataldo, N. A., Dumesic, D. A., Goldsmith, P. C. & Jaffe, R. B. Immunolocalization of Fas and Fas ligand in the ovaries of women with polycystic ovary syndrome: relationship to apoptosis. *Human reproduction (Oxford, England)* **15**, 1889-1897, doi:10.1093/humrep/15.9.1889 (2000).
- 16 Persani, L., Rossetti, R. & Cacciatori, C. Genes involved in human premature ovarian failure. *Journal of molecular endocrinology* **45**, 257-279, doi:10.1677/JME-10-0070 (2010).
- 17 Fernald, K. & Kurokawa, M. Evading apoptosis in cancer. *Trends Cell Biol* **23**, 620-633, doi:10.1016/j.tcb.2013.07.006 (2013).
- 18 Wallace, W. H. & Kelsey, T. W. Human ovarian reserve from conception to the menopause. *PLoS One* **5**, e8772, doi:10.1371/journal.pone.0008772 (2010).
- 19 Georges, A. *et al*. FOXL2: a central transcription factor of the ovary. *Journal of molecular endocrinology* **52**, R17-33, doi:10.1530/JME-13-0159 (2014).
- 20 Rodgers, R. J. & Irving-Rodgers, H. F. Formation of the ovarian follicular antrum and follicular fluid. *Biol Reprod* **82**, 1021-1029, doi:10.1095/biolreprod.109.082941 (2010).
- 21 Bristol-Gould, S. K. *et al*. Postnatal regulation of germ cells by activin: the establishment of the initial follicle pool. *Dev Biol* **298**, 132-148, doi:10.1016/j.ydbio.2006.06.025 (2006).

- 22 Tilly, J. L. Commuting the death sentence: how oocytes strive to survive. *Nat Rev Mol Cell Biol* **2**, 838-848, doi:10.1038/35099086 (2001).
- 23 Findlay, J. *et al.* in *The Ovary* 3-21 (Elsevier, 2019).
- 24 Livera, G. *et al.* p63 null mutation protects mouse oocytes from radio-induced apoptosis. *Reproduction* **135**, 3-12, doi:10.1530/REP-07-0054 (2008).
- 25 Suh, E. K. *et al.* p63 protects the female germ line during meiotic arrest. *Nature* **444**, 624-628, doi:10.1038/nature05337 (2006).
- 26 Regan, S. L. P. *et al.* Granulosa Cell Apoptosis in the Ovarian Follicle-A Changing View. *Front Endocrinol (Lausanne)* **9**, 61, doi:10.3389/fendo.2018.00061 (2018).
- 27 Shen, M. *et al.* Involvement of the up-regulated FoxO1 expression in follicular granulosa cell apoptosis induced by oxidative stress. *The Journal of biological chemistry* **287**, 25727-25740, doi:10.1074/jbc.M112.349902 (2012).
- 28 Yamoto, M., Minami, S., Nakano, R. & Kobayashi, M. Immunohistochemical localization of inhibin/activin subunits in human ovarian follicles during the menstrual cycle. *The Journal of clinical endocrinology and metabolism* **74**, 989-993, doi:10.1210/jcem.74.5.1569176 (1992).
- 29 Weil, S., Vendola, K., Zhou, J. & Bondy, C. A. Androgen and follicle-stimulating hormone interactions in primate ovarian follicle development. *The Journal of clinical endocrinology and metabolism* **84**, 2951-2956, doi:10.1210/jcem.84.8.5929 (1999).
- 30 Almeida, F. *et al.* Presence of anti-Mullerian hormone (AMH) during follicular development in the porcine ovary. *PLoS One* **13**, e0197894, doi:10.1371/journal.pone.0197894 (2018).
- 31 Matzuk, M. M. Revelations of ovarian follicle biology from gene knockout mice. *Mol Cell Endocrinol* **163**, 61-66, doi:10.1016/s0303-7207(99)00241-5 (2000).
- 32 Wright, C. S. *et al.* Effects of follicle-stimulating hormone and serum substitution on the in-vitro growth of human ovarian follicles. *Human reproduction (Oxford, England)* **14**, 1555-1562, doi:10.1093/humrep/14.6.1555 (1999).
- 33 Rabin, D. *et al.* Isolated deficiency of follicle-stimulating hormone. Clinical and laboratory features. *N Engl J Med* **287**, 1313-1317, doi:10.1056/NEJM197212282872602 (1972).
- 34 Aittomaki, K. *et al.* Clinical features of primary ovarian failure caused by a point mutation in the follicle-stimulating hormone receptor gene. *The Journal of clinical endocrinology and metabolism* **81**, 3722-3726, doi:10.1210/jcem.81.10.8855829 (1996).
- 35 Xu, J. *et al.* Survival, growth, and maturation of secondary follicles from prepubertal, young, and older adult rhesus monkeys during encapsulated three-dimensional culture: effects of gonadotropins and insulin. *Reproduction* **140**, 685-697, doi:10.1530/REP-10-0284 (2010).
- 36 Xu, J. *et al.* Secondary follicle growth and oocyte maturation during encapsulated three-dimensional culture in rhesus monkeys: effects of gonadotrophins, oxygen and fetuin. *Human reproduction (Oxford, England)* **26**, 1061-1072, doi:10.1093/humrep/der049 (2011).
- 37 Orisaka, M. *et al.* Growth differentiation factor 9 is antiapoptotic during follicular development from preantral to early antral stage. *Molecular endocrinology (Baltimore, Md.)* **20**, 2456-2468, doi:10.1210/me.2005-0357 (2006).
- 38 Thompson, W. E. *et al.* Regulation of prohibitin expression during follicular development and atresia in the mammalian ovary. *Biol Reprod* **71**, 282-290, doi:10.1095/biolreprod.103.024125 (2004).
- 39 Meng, L. *et al.* Preantral follicular atresia occurs mainly through autophagy, while antral follicles degenerate mostly through apoptosis. *Biol Reprod* **99**, 853-863, doi:10.1093/biolre/i0y116 (2018).
- 40 Howles, C. M. Role of LH and FSH in ovarian function. *Mol Cell Endocrinol* **161**, 25-30, doi:10.1016/s0303-7207(99)00219-1 (2000).
- 41 Knobil, E. in *Proceedings of the 1979 Laurentian Hormone Conference*. 53-88 (Elsevier).
- 42 Oxberry, B. A. & Greenwald, G. S. An autoradiographic study of the binding of 125 I-labeled follicle-stimulating hormone, human chorionic gonadotropin and prolactin to the hamster ovary throughout the estrous cycle. *Biol Reprod* **27**, 505-516, doi:10.1095/biolreprod27.2.505 (1982).
- 43 Regan, S. L. P. *et al.* The effect of ovarian reserve and receptor signalling on granulosa cell apoptosis during human follicle development. *Mol Cell Endocrinol* **470**, 219-227, doi:10.1016/j.mce.2017.11.002 (2018).
- 44 Dorrington, J. H., Moon, Y. S. & Armstrong, D. T. Estradiol-17beta biosynthesis in cultured granulosa cells from hypophysectomized immature rats; stimulation by follicle-stimulating hormone. *Endocrinology* **97**, 1328-1331, doi:10.1210/endo-97-5-1328 (1975).

- 45 Fauser, B. C. & Van Heusden, A. M. Manipulation of human ovarian function: physiological concepts and clinical consequences. *Endocrine reviews* **18**, 71-106, doi:10.1210/edrv.18.1.0290 (1997).
- 46 Hunzicker-Dunn, M. & Maizels, E. T. FSH signaling pathways in immature granulosa cells that regulate target gene expression: branching out from protein kinase A. *Cellular signalling* **18**, 1351-1359, doi:10.1016/j.cellsig.2006.02.011 (2006).
- 47 Quirk, S. M., Cowan, R. G. & Harman, R. M. The susceptibility of granulosa cells to apoptosis is influenced by oestradiol and the cell cycle. *J Endocrinol* **189**, 441-453, doi:10.1677/joe.1.06549 (2006).
- 48 Chun, S. Y. *et al.* Hormonal regulation of apoptosis in early antral follicles: follicle-stimulating hormone as a major survival factor. *Endocrinology* **137**, 1447-1456, doi:10.1210/endo.137.4.8625923 (1996).
- 49 Vaskivuo, T. E. & Tapanainen, J. S. Apoptosis in the human ovary. *Reproductive biomedicine online* **6**, 24-35 (2003).
- 50 Chaudhary, G. R. *et al.* Necroptosis in stressed ovary. *J Biomed Sci* **26**, 11, doi:10.1186/s12929-019-0504-2 (2019).
- 51 Zhou, J., Peng, X. & Mei, S. Autophagy in Ovarian Follicular Development and Atresia. *Int J Biol Sci* **15**, 726-737, doi:10.7150/ijbs.30369 (2019).
- 52 Christenson, L. K. & Stouffer, R. L. Follicle-stimulating hormone and luteinizing hormone/chorionic gonadotropin stimulation of vascular endothelial growth factor production by macaque granulosa cells from pre- and periovulatory follicles. *The Journal of clinical endocrinology and metabolism* **82**, 2135-2142, doi:10.1210/jcem.82.7.4169 (1997).
- 53 Chaffin, C. L., Dissen, G. A. & Stouffer, R. L. Hormonal regulation of steroidogenic enzyme expression in granulosa cells during the peri-ovulatory interval in monkeys. *Mol Hum Reprod* **6**, 11-18, doi:10.1093/molehr/6.1.11 (2000).
- 54 Fatemi, H. M. *et al.* The luteal phase of recombinant follicle-stimulating hormone/gonadotropin-releasing hormone antagonist in vitro fertilization cycles during supplementation with progesterone or progesterone and estradiol. *Fertil Steril* **87**, 504-508, doi:10.1016/j.fertnstert.2006.07.1521 (2007).
- 55 Daya, S. Luteal support: progestogens for pregnancy protection. *Maturitas* **65 Suppl 1**, S29-34, doi:10.1016/j.maturitas.2009.09.012 (2009).
- 56 Small, C. M. *et al.* Menstrual cycle characteristics: associations with fertility and spontaneous abortion. *Epidemiology* **17**, 52-60 (2006).
- 57 Dal, J., Vural, B., Caliskan, E., Ozkan, S. & Yucesoy, I. Power Doppler ultrasound studies of ovarian, uterine, and endometrial blood flow in regularly menstruating women with respect to luteal phase defects. *Fertil Steril* **84**, 224-227, doi:10.1016/j.fertnstert.2004.12.059 (2005).
- 58 Fuller, P. J., Leung, D. & Chu, S. Genetics and genomics of ovarian sex cord-stromal tumors. *Clin Genet* **91**, 285-291, doi:10.1111/cge.12917 (2017).
- 59 Jamieson, S. & Fuller, P. J. Molecular pathogenesis of granulosa cell tumors of the ovary. *Endocrine reviews* **33**, 109-144, doi:10.1210/er.2011-0014 (2012).
- 60 Young, R. & Scully, R. in *Gynecological Tumors* 113-164 (Springer, 1992).
- 61 Young, R. H. Ovarian sex cord-stromal tumours and their mimics. *Pathology* **50**, 5-15, doi:10.1016/j.pathol.2017.09.007 (2018).
- 62 Young, R. H., Dickersin, G. R. & Scully, R. E. Juvenile granulosa cell tumor of the ovary. A clinicopathological analysis of 125 cases. *Am J Surg Pathol* **8**, 575-596 (1984).
- 63 Zaloudek, C. & Norris, H. J. Granulosa tumors of the ovary in children: a clinical and pathologic study of 32 cases. *Am J Surg Pathol* **6**, 503-512 (1982).
- 64 Shah, S. P. *et al.* Mutation of FOXL2 in granulosa-cell tumors of the ovary. *N Engl J Med* **360**, 2719-2729, doi:10.1056/NEJMoa0902542 (2009).
- 65 Jamieson, S. *et al.* The FOXL2 C134W mutation is characteristic of adult granulosa cell tumors of the ovary. *Mod Pathol* **23**, 1477-1485, doi:10.1038/modpathol.2010.145 (2010).
- 66 Chu, S. *et al.* FSH-regulated gene expression profiles in ovarian tumours and normal ovaries. *Mol Hum Reprod* **8**, 426-433, doi:10.1093/molehr/8.5.426 (2002).
- 67 Leung, D. T. H. *et al.* Combined PPARGamma Activation and XIAP Inhibition as a Potential Therapeutic Strategy for Ovarian Granulosa Cell Tumors. *Molecular cancer therapeutics* **18**, 364-375, doi:10.1158/1535-7163.MCT-18-0078 (2019).
- 68 Fulda, S. Smac Mimetics to Therapeutically Target IAP Proteins in Cancer. *International review of cell and molecular biology* **330**, 157-169, doi:10.1016/bs.ircmb.2016.09.004 (2017).

- 69 Benayoun, B. A. *et al.* Adult ovarian granulosa cell tumor transcriptomics: prevalence of FOXL2 target genes misregulation gives insights into the pathogenic mechanism of the p.Cys134Trp somatic mutation. *Oncogene* **32**, 2739-2746, doi:10.1038/onc.2012.298 (2013).
- 70 Clarke, P. G. & Clarke, S. Nineteenth century research on naturally occurring cell death and related phenomena. *Anat Embryol (Berl)* **193**, 81-99 (1996).
- 71 Kerr, J. F., Wyllie, A. H. & Currie, A. R. Apoptosis: a basic biological phenomenon with wide-ranging implications in tissue kinetics. *Br J Cancer* **26**, 239-257, doi:10.1038/bjc.1972.33 (1972).
- 72 Schweichel, J. U. & Merker, H. J. The morphology of various types of cell death in prenatal tissues. *Teratology* **7**, 253-266, doi:10.1002/tera.1420070306 (1973).
- 73 Tang, D., Kang, R., Berghe, T. V., Vandenabeele, P. & Kroemer, G. The molecular machinery of regulated cell death. *Cell Res* **29**, 347-364, doi:10.1038/s41422-019-0164-5 (2019).
- 74 Degtarev, A. *et al.* Chemical inhibitor of nonapoptotic cell death with therapeutic potential for ischemic brain injury. *Nat Chem Biol* **1**, 112-119, doi:10.1038/nchembio711 (2005).
- 75 Galluzzi, L. *et al.* Molecular mechanisms of cell death: recommendations of the Nomenclature Committee on Cell Death 2018. *Cell Death Differ* **25**, 486-541, doi:10.1038/s41418-017-0012-4 (2018).
- 76 Hussein, M. R. Apoptosis in the ovary: molecular mechanisms. *Human reproduction update* **11**, 162-177, doi:10.1093/humupd/dmi001 (2005).
- 77 Elmore, S. Apoptosis: a review of programmed cell death. *Toxicol Pathol* **35**, 495-516, doi:10.1080/01926230701320337 (2007).
- 78 Tilly, J. L., Kowalski, K. I., Johnson, A. L. & Hsueh, A. J. Involvement of apoptosis in ovarian follicular atresia and postovulatory regression. *Endocrinology* **129**, 2799-2801, doi:10.1210/endo-129-5-2799 (1991).
- 79 Delbridge, A. R., Grabow, S., Strasser, A. & Vaux, D. L. Thirty years of BCL-2: translating cell death discoveries into novel cancer therapies. *Nature reviews. Cancer* **16**, 99-109, doi:10.1038/nrc.2015.17 (2016).
- 80 Llambi, F. *et al.* BOK Is a Non-canonical BCL-2 Family Effector of Apoptosis Regulated by ER-Associated Degradation. *Cell* **165**, 421-433, doi:10.1016/j.cell.2016.02.026 (2016).
- 81 Vitale, I., Manic, G., De Maria, R., Kroemer, G. & Galluzzi, L. DNA Damage in Stem Cells. *Molecular cell* **66**, 306-319, doi:10.1016/j.molcel.2017.04.006 (2017).
- 82 Czabotar, P. E., Lessene, G., Strasser, A. & Adams, J. M. Control of apoptosis by the BCL-2 protein family: implications for physiology and therapy. *Nat Rev Mol Cell Biol* **15**, 49-63, doi:10.1038/nrm3722 (2014).
- 83 Pihan, P., Carreras-Sureda, A. & Hetz, C. BCL-2 family: integrating stress responses at the ER to control cell demise. *Cell Death Differ* **24**, 1478-1487, doi:10.1038/cdd.2017.82 (2017).
- 84 Brumatti, G., Salmanidis, M. & Ekert, P. G. Crossing paths: interactions between the cell death machinery and growth factor survival signals. *Cell Mol Life Sci* **67**, 1619-1630, doi:10.1007/s00018-010-0288-8 (2010).
- 85 Nunez, G. *et al.* Deregulated Bcl-2 gene expression selectively prolongs survival of growth factor-deprived hemopoietic cell lines. *J Immunol* **144**, 3602-3610 (1990).
- 86 Li, K. *et al.* Cytochrome c deficiency causes embryonic lethality and attenuates stress-induced apoptosis. *Cell* **101**, 389-399, doi:10.1016/s0092-8674(00)80849-1 (2000).
- 87 Du, C., Fang, M., Li, Y., Li, L. & Wang, X. Smac, a mitochondrial protein that promotes cytochrome c-dependent caspase activation by eliminating IAP inhibition. *Cell* **102**, 33-42, doi:10.1016/s0092-8674(00)00008-8 (2000).
- 88 Li, P. *et al.* Cytochrome c and dATP-dependent formation of Apaf-1/caspase-9 complex initiates an apoptotic protease cascade. *Cell* **91**, 479-489, doi:10.1016/s0092-8674(00)80434-1 (1997).
- 89 Zhou, M. *et al.* Atomic structure of the apoptosome: mechanism of cytochrome c- and dATP-mediated activation of Apaf-1. *Genes Dev* **29**, 2349-2361, doi:10.1101/gad.272278.115 (2015).
- 90 Julien, O. & Wells, J. A. Caspases and their substrates. *Cell Death Differ* **24**, 1380-1389, doi:10.1038/cdd.2017.44 (2017).
- 91 Chaitanya, G. V., Steven, A. J. & Babu, P. P. PARP-1 cleavage fragments: signatures of cell-death proteases in neurodegeneration. *Cell Commun Signal* **8**, 31, doi:10.1186/1478-811X-8-31 (2010).
- 92 Salvesen, G. S. & Duckett, C. S. IAP proteins: blocking the road to death's door. *Nat Rev Mol Cell Biol* **3**, 401-410, doi:10.1038/nrm830 (2002).

- 93 Eckelman, B. P., Salvesen, G. S. & Scott, F. L. Human inhibitor of apoptosis proteins: why XIAP is the black sheep of the family. *EMBO Rep* **7**, 988-994, doi:10.1038/sj.embor.7400795 (2006).
- 94 Silke, J. & Meier, P. Inhibitor of apoptosis (IAP) proteins-modulators of cell death and inflammation. *Cold Spring Harb Perspect Biol* **5**, doi:10.1101/cshperspect.a008730 (2013).
- 95 Aggarwal, B. B., Gupta, S. C. & Kim, J. H. Historical perspectives on tumor necrosis factor and its superfamily: 25 years later, a golden journey. *Blood* **119**, 651-665, doi:10.1182/blood-2011-04-325225 (2012).
- 96 Green, D. R. & Llambi, F. Cell Death Signaling. *Cold Spring Harb Perspect Biol* **7**, doi:10.1101/cshperspect.a006080 (2015).
- 97 Micheau, O. & Tschopp, J. Induction of TNF receptor I-mediated apoptosis via two sequential signaling complexes. *Cell* **114**, 181-190, doi:10.1016/s0092-8674(03)00521-x (2003).
- 98 Brenner, D., Blaser, H. & Mak, T. W. Regulation of tumour necrosis factor signalling: live or let die. *Nat Rev Immunol* **15**, 362-374, doi:10.1038/nri3834 (2015).
- 99 Hsu, H., Huang, J., Shu, H. B., Baichwal, V. & Goeddel, D. V. TNF-dependent recruitment of the protein kinase RIP to the TNF receptor-1 signaling complex. *Immunity* **4**, 387-396 (1996).
- 100 Liu, Z. G., Hsu, H., Goeddel, D. V. & Karin, M. Dissection of TNF receptor 1 effector functions: JNK activation is not linked to apoptosis while NF-kappaB activation prevents cell death. *Cell* **87**, 565-576, doi:10.1016/s0092-8674(00)81375-6 (1996).
- 101 DiDonato, J. A., Hayakawa, M., Rothwarf, D. M., Zandi, E. & Karin, M. A cytokine-responsive IkkappaB kinase that activates the transcription factor NF-kappaB. *Nature* **388**, 548-554, doi:10.1038/41493 (1997).
- 102 Fulda, S. & Vucic, D. Targeting IAP proteins for therapeutic intervention in cancer. *Nat Rev Drug Discov* **11**, 109-124, doi:10.1038/nrd3627 (2012).
- 103 Hanahan, D. & Weinberg, R. A. Hallmarks of cancer: the next generation. *Cell* **144**, 646-674, doi:10.1016/j.cell.2011.02.013 (2011).
- 104 Hasegawa, T. *et al.* Expression of the inhibitor of apoptosis (IAP) family members in human neutrophils: up-regulation of cIAP2 by granulocyte colony-stimulating factor and overexpression of cIAP2 in chronic neutrophilic leukemia. *Blood* **101**, 1164-1171, doi:10.1182/blood-2002-05-1505 (2003).
- 105 Grant, J. *et al.* Over-expression of X-linked inhibitor of apoptosis protein modulates multiple aspects of neuronal Ca²⁺ signaling. *Neurochem Res* **38**, 847-856, doi:10.1007/s11064-013-0989-0 (2013).
- 106 Tchoghandjian, A. *et al.* Inhibitor of apoptosis protein expression in glioblastomas and their in vitro and in vivo targeting by SMAC mimetic GDC-0152. *Cell Death Dis* **7**, e2325, doi:10.1038/cddis.2016.214 (2016).
- 107 Bagrezaei, F., Hassanshahi, G., Mahmoodi, M., Khanamani Falahati-Pour, S. & Mirzaei, M. R. Expression of Inhibitor of Apoptosis Gene Family Members in Bladder Cancer Tissues and the 5637 Tumor Cell Line. *Asian Pac J Cancer Prev* **19**, 529-532, doi:10.22034/APJCP.2018.19.2.529 (2018).
- 108 Birnbaum, M. J., Clem, R. J. & Miller, L. K. An apoptosis-inhibiting gene from a nuclear polyhedrosis virus encoding a polypeptide with Cys/His sequence motifs. *J Virol* **68**, 2521-2528 (1994).
- 109 Wu, G. *et al.* Structural basis of IAP recognition by Smac/DIABLO. *Nature* **408**, 1008-1012, doi:10.1038/35050012 (2000).
- 110 Budhidarmo, R. & Day, C. L. The ubiquitin-associated domain of cellular inhibitor of apoptosis proteins facilitates ubiquitylation. *The Journal of biological chemistry* **289**, 25721-25736, doi:10.1074/jbc.M113.545475 (2014).
- 111 Mace, P. D. *et al.* Structures of the cIAP2 RING domain reveal conformational changes associated with ubiquitin-conjugating enzyme (E2) recruitment. *The Journal of biological chemistry* **283**, 31633-31640, doi:10.1074/jbc.M804753200 (2008).
- 112 Lopez, J. *et al.* CARD-mediated autoinhibition of cIAP1's E3 ligase activity suppresses cell proliferation and migration. *Molecular cell* **42**, 569-583, doi:10.1016/j.molcel.2011.04.008 (2011).
- 113 Liu, J. *et al.* X-linked inhibitor of apoptosis protein (XIAP) mediates cancer cell motility via Rho GDP dissociation inhibitor (RhoGDI)-dependent regulation of the cytoskeleton. *The Journal of biological chemistry* **286**, 15630-15640, doi:10.1074/jbc.M110.176982 (2011).
- 114 Dogan, T. *et al.* X-linked and cellular IAPs modulate the stability of C-RAF kinase and cell motility. *Nat Cell Biol* **10**, 1447-1455, doi:10.1038/ncb1804 (2008).
- 115 Oberoi, T. K. *et al.* IAPs regulate the plasticity of cell migration by directly targeting Rac1 for degradation. *EMBO J* **31**, 14-28, doi:10.1038/emboj.2011.423 (2012).

- 116 Mehrotra, S. *et al.* IAP regulation of metastasis. *Cancer Cell* **17**, 53-64, doi:10.1016/j.ccr.2009.11.021 (2010).
- 117 Van Themsche, C., Leblanc, V., Parent, S. & Asselin, E. X-linked inhibitor of apoptosis protein (XIAP) regulates PTEN ubiquitination, content, and compartmentalization. *The Journal of biological chemistry* **284**, 20462-20466, doi:10.1074/jbc.C109.009522 (2009).
- 118 LaCasse, E. C. *et al.* Preclinical characterization of AEG35156/GEM 640, a second-generation antisense oligonucleotide targeting X-linked inhibitor of apoptosis. *Clin Cancer Res* **12**, 5231-5241, doi:10.1158/1078-0432.CCR-06-0608 (2006).
- 119 Deveraux, Q. L., Takahashi, R., Salvesen, G. S. & Reed, J. C. X-linked IAP is a direct inhibitor of cell-death proteases. *Nature* **388**, 300-304, doi:10.1038/40901 (1997).
- 120 Eckelman, B. P. & Salvesen, G. S. The human anti-apoptotic proteins cIAP1 and cIAP2 bind but do not inhibit caspases. *The Journal of biological chemistry* **281**, 3254-3260, doi:10.1074/jbc.M510863200 (2006).
- 121 Huang, H. *et al.* The inhibitor of apoptosis, cIAP2, functions as a ubiquitin-protein ligase and promotes in vitro monoubiquitination of caspases 3 and 7. *The Journal of biological chemistry* **275**, 26661-26664, doi:10.1074/jbc.C000199200 (2000).
- 122 Feoktistova, M. *et al.* cIAPs block Ripoptosome formation, a RIP1/caspase-8 containing intracellular cell death complex differentially regulated by cFLIP isoforms. *Molecular cell* **43**, 449-463, doi:10.1016/j.molcel.2011.06.011 (2011).
- 123 Varfolomeev, E. *et al.* Cellular inhibitors of apoptosis are global regulators of NF-kappaB and MAPK activation by members of the TNF family of receptors. *Sci Signal* **5**, ra22, doi:10.1126/scisignal.2001878 (2012).
- 124 Zarnegar, B. J. *et al.* Noncanonical NF-kappaB activation requires coordinated assembly of a regulatory complex of the adaptors cIAP1, cIAP2, TRAF2 and TRAF3 and the kinase NIK. *Nat Immunol* **9**, 1371-1378, doi:10.1038/ni.1676 (2008).
- 125 Varfolomeev, E. *et al.* IAP antagonists induce autoubiquitination of c-IAPs, NF-kappaB activation, and TNFalpha-dependent apoptosis. *Cell* **131**, 669-681, doi:10.1016/j.cell.2007.10.030 (2007).
- 126 Scialdone, A., Menchini, U., Pietroni, C. & Brancato, R. Unilateral proliferative diabetic retinopathy and uveitis in the fellow eye: report of a case. *Ann Ophthalmol* **23**, 259-261 (1991).
- 127 Xu, L. *et al.* c-IAP1 cooperates with Myc by acting as a ubiquitin ligase for Mad1. *Molecular cell* **28**, 914-922, doi:10.1016/j.molcel.2007.10.027 (2007).
- 128 Tamm, I. *et al.* Expression and prognostic significance of IAP-family genes in human cancers and myeloid leukemias. *Clin Cancer Res* **6**, 1796-1803 (2000).
- 129 Foster, F. M. *et al.* Targeting inhibitor of apoptosis proteins in combination with ErbB antagonists in breast cancer. *Breast Cancer Res* **11**, R41, doi:10.1186/bcr2328 (2009).
- 130 Zender, L. *et al.* Identification and validation of oncogenes in liver cancer using an integrative oncogenomic approach. *Cell* **125**, 1253-1267, doi:10.1016/j.cell.2006.05.030 (2006).
- 131 Liu, Z. *et al.* Structural basis for binding of Smac/DIABLO to the XIAP BIR3 domain. *Nature* **408**, 1004-1008, doi:10.1038/35050006 (2000).
- 132 Owens, T. W., Gilmore, A. P., Streuli, C. H. & Foster, F. M. Inhibitor of Apoptosis Proteins: Promising Targets for Cancer Therapy. *J Carcinog Mutagen Suppl* **14**, doi:10.4172/2157-2518.S14-004 (2013).
- 133 Holler, N. *et al.* Fas triggers an alternative, caspase-8-independent cell death pathway using the kinase RIP as effector molecule. *Nat Immunol* **1**, 489-495, doi:10.1038/82732 (2000).
- 134 He, S., Liang, Y., Shao, F. & Wang, X. Toll-like receptors activate programmed necrosis in macrophages through a receptor-interacting kinase-3-mediated pathway. *Proc Natl Acad Sci U S A* **108**, 20054-20059, doi:10.1073/pnas.1116302108 (2011).
- 135 Upton, J. W., Kaiser, W. J. & Mocarski, E. S. DAI/ZBP1/DLM-1 complexes with RIP3 to mediate virus-induced programmed necrosis that is targeted by murine cytomegalovirus vIRA. *Cell Host Microbe* **11**, 290-297, doi:10.1016/j.chom.2012.01.016 (2012).
- 136 Schock, S. N. *et al.* Induction of necroptotic cell death by viral activation of the RIG-I or STING pathway. *Cell Death Differ* **24**, 615-625, doi:10.1038/cdd.2016.153 (2017).
- 137 Wang, X., He, Z., Liu, H., Yousefi, S. & Simon, H. U. Neutrophil Necroptosis Is Triggered by Ligation of Adhesion Molecules following GM-CSF Priming. *J Immunol* **197**, 4090-4100, doi:10.4049/jimmunol.1600051 (2016).

- 138 Vercammen, D. *et al.* Inhibition of caspases increases the sensitivity of L929 cells to necrosis mediated by tumor necrosis factor. *J Exp Med* **187**, 1477-1485, doi:10.1084/jem.187.9.1477 (1998).
- 139 Silke, J., Rickard, J. A. & Gerlic, M. The diverse role of RIP kinases in necroptosis and inflammation. *Nat Immunol* **16**, 689-697, doi:10.1038/ni.3206 (2015).
- 140 Cottet, S. *et al.* cFLIP protein prevents tumor necrosis factor-alpha-mediated induction of caspase-8-dependent apoptosis in insulin-secreting betaTc-Tet cells. *Diabetes* **51**, 1805-1814, doi:10.2337/diabetes.51.6.1805 (2002).
- 141 Teng, X. *et al.* NLRP3 Inflammasome Is Involved in Q-VD-OPH Induced Necroptosis Following Cerebral Ischemia-Reperfusion Injury. *Neurochem Res* **43**, 1200-1209, doi:10.1007/s11064-018-2537-4 (2018).
- 142 Degtarev, A. *et al.* Identification of RIP1 kinase as a specific cellular target of necrostatins. *Nat Chem Biol* **4**, 313-321, doi:10.1038/nchembio.83 (2008).
- 143 Xie, T. *et al.* Structural insights into RIP3-mediated necroptotic signaling. *Cell Rep* **5**, 70-78, doi:10.1016/j.celrep.2013.08.044 (2013).
- 144 Sun, X., Yin, J., Starovasnik, M. A., Fairbrother, W. J. & Dixit, V. M. Identification of a novel homotypic interaction motif required for the phosphorylation of receptor-interacting protein (RIP) by RIP3. *The Journal of biological chemistry* **277**, 9505-9511, doi:10.1074/jbc.M109488200 (2002).
- 145 Zhang, D. W. *et al.* RIP3, an energy metabolism regulator that switches TNF-induced cell death from apoptosis to necrosis. *Science* **325**, 332-336, doi:10.1126/science.1172308 (2009).
- 146 Cho, Y. S. *et al.* Phosphorylation-driven assembly of the RIP1-RIP3 complex regulates programmed necrosis and virus-induced inflammation. *Cell* **137**, 1112-1123, doi:10.1016/j.cell.2009.05.037 (2009).
- 147 Sun, L. *et al.* Mixed lineage kinase domain-like protein mediates necrosis signaling downstream of RIP3 kinase. *Cell* **148**, 213-227, doi:10.1016/j.cell.2011.11.031 (2012).
- 148 Zhao, J. *et al.* Mixed lineage kinase domain-like is a key receptor interacting protein 3 downstream component of TNF-induced necrosis. *Proc Natl Acad Sci U S A* **109**, 5322-5327, doi:10.1073/pnas.1200012109 (2012).
- 149 Huang, Z. *et al.* RIP1/RIP3 binding to HSV-1 ICP6 initiates necroptosis to restrict virus propagation in mice. *Cell Host Microbe* **17**, 229-242, doi:10.1016/j.chom.2015.01.002 (2015).
- 150 Petrie, E. J. *et al.* Conformational switching of the pseudokinase domain promotes human MLKL tetramerization and cell death by necroptosis. *Nature communications* **9**, 2422, doi:10.1038/s41467-018-04714-7 (2018).
- 151 Zhao, X. M. *et al.* Hsp90 modulates the stability of MLKL and is required for TNF-induced necroptosis. *Cell Death Dis* **7**, e2089, doi:10.1038/cddis.2015.390 (2016).
- 152 Dondelinger, Y. *et al.* MLKL compromises plasma membrane integrity by binding to phosphatidylinositol phosphates. *Cell Rep* **7**, 971-981, doi:10.1016/j.celrep.2014.04.026 (2014).
- 153 Dovey, C. M. *et al.* MLKL Requires the Inositol Phosphate Code to Execute Necroptosis. *Molecular cell* **70**, 936-948 e937, doi:10.1016/j.molcel.2018.05.010 (2018).
- 154 Ros, U. *et al.* Necroptosis Execution Is Mediated by Plasma Membrane Nanopores Independent of Calcium. *Cell Rep* **19**, 175-187, doi:10.1016/j.celrep.2017.03.024 (2017).
- 155 Xia, B. *et al.* MLKL forms cation channels. *Cell Res* **26**, 517-528, doi:10.1038/cr.2016.26 (2016).
- 156 Blohberger, J. *et al.* Readthrough acetylcholinesterase (AChE-R) and regulated necrosis: pharmacological targets for the regulation of ovarian functions? *Cell Death Dis* **6**, e1685, doi:10.1038/cddis.2015.51 (2015).
- 157 Tsui, K. H., Wang, P. H., Lin, L. T. & Li, C. J. DHEA protects mitochondria against dual modes of apoptosis and necroptosis in human granulosa HO23 cells. *Reproduction* **154**, 101-110, doi:10.1530/REP-17-0016 (2017).
- 158 Colombini, M. Ceramide channels and mitochondrial outer membrane permeability. *J Bioenerg Biomembr* **49**, 57-64, doi:10.1007/s10863-016-9646-z (2017).
- 159 Merrill, A. H. in *Biochemistry of Lipids, Lipoproteins and Membranes (Fifth Edition)* (eds Dennis E. Vance & Jean E. Vance) 363-397 (Elsevier, 2008).
- 160 Obeid, L. M., Linardic, C. M., Karolak, L. A. & Hannun, Y. A. Programmed cell death induced by ceramide. *Science* **259**, 1769-1771, doi:10.1126/science.8456305 (1993).
- 161 Venable, M. E., Lee, J. Y., Smyth, M. J., Bielawska, A. & Obeid, L. M. Role of ceramide in cellular senescence. *The Journal of biological chemistry* **270**, 30701-30708, doi:10.1074/jbc.270.51.30701 (1995).
- 162 Smith, E. R., Merrill, A. H., Obeid, L. M. & Hannun, Y. A. Effects of sphingosine and other sphingolipids on protein kinase C. *Methods Enzymol* **312**, 361-373, doi:10.1016/s0076-6879(00)12921-0 (2000).

- 163 Hla, T. Physiological and pathological actions of sphingosine 1-phosphate. *Semin Cell Dev Biol* **15**, 513-520, doi:10.1016/j.semcdb.2004.05.002 (2004).
- 164 Hannun, Y. A. & Obeid, L. M. The Ceramide-centric universe of lipid-mediated cell regulation: stress encounters of the lipid kind. *The Journal of biological chemistry* **277**, 25847-25850, doi:10.1074/jbc.R200008200 (2002).
- 165 Linn, S. C. *et al.* Regulation of de novo sphingolipid biosynthesis and the toxic consequences of its disruption. *Biochem Soc Trans* **29**, 831-835, doi:10.1042/0300-5127:0290831 (2001).
- 166 Pewzner-Jung, Y., Ben-Dor, S. & Futerman, A. H. When do Lasses (longevity assurance genes) become CerS (ceramide synthases)? Insights into the regulation of ceramide synthesis. *The Journal of biological chemistry* **281**, 25001-25005, doi:10.1074/jbc.R600010200 (2006).
- 167 Causeret, C., Geeraert, L., Van der Hoeven, G., Mannaerts, G. P. & Van Veldhoven, P. P. Further characterization of rat dihydroceramide desaturase: tissue distribution, subcellular localization, and substrate specificity. *Lipids* **35**, 1117-1125 (2000).
- 168 Wijesinghe, D. S. *et al.* Substrate specificity of human ceramide kinase. *J Lipid Res* **46**, 2706-2716, doi:10.1194/jlr.M500313-JLR200 (2005).
- 169 Raas-Rothschild, A., Pankova-Kholmyansky, I., Kacher, Y. & Futerman, A. H. Glycosphingolipidoses: beyond the enzymatic defect. *Glycoconj J* **21**, 295-304, doi:10.1023/B:GLYC.0000046272.38480.ef (2004).
- 170 Tafesse, F. G., Ternes, P. & Holthuis, J. C. The multigenic sphingomyelin synthase family. *The Journal of biological chemistry* **281**, 29421-29425, doi:10.1074/jbc.R600021200 (2006).
- 171 Marchesini, N. & Hannun, Y. A. Acid and neutral sphingomyelinases: roles and mechanisms of regulation. *Biochem Cell Biol* **82**, 27-44, doi:10.1139/o03-091 (2004).
- 172 Gorelik, A., Liu, F., Illes, K. & Nagar, B. Crystal structure of the human alkaline sphingomyelinase provides insights into substrate recognition. *The Journal of biological chemistry* **292**, 7087-7094, doi:10.1074/jbc.M116.769273 (2017).
- 173 Khan, W. A. *et al.* Use of D-erythro-sphingosine as a pharmacological inhibitor of protein kinase C in human platelets. *Biochem J* **278** (Pt 2), 387-392, doi:10.1042/bj2780387 (1991).
- 174 Hait, N. C., Oskeritzian, C. A., Paugh, S. W., Milstien, S. & Spiegel, S. Sphingosine kinases, sphingosine 1-phosphate, apoptosis and diseases. *Biochim Biophys Acta* **1758**, 2016-2026, doi:10.1016/j.bbamem.2006.08.007 (2006).
- 175 Bandhuvula, P. & Saba, J. D. Sphingosine-1-phosphate lyase in immunity and cancer: silencing the siren. *Trends Mol Med* **13**, 210-217, doi:10.1016/j.molmed.2007.03.005 (2007).
- 176 Kitatani, K., Idkowiak-Baldys, J. & Hannun, Y. A. The sphingolipid salvage pathway in ceramide metabolism and signaling. *Cellular signalling* **20**, 1010-1018, doi:10.1016/j.cellsig.2007.12.006 (2008).
- 177 Tettamanti, G., Bassi, R., Viani, P. & Riboni, L. Salvage pathways in glycosphingolipid metabolism. *Biochimie* **85**, 423-437, doi:10.1016/s0300-9084(03)00047-6 (2003).
- 178 Gillard, B. K., Clement, R. G. & Marcus, D. M. Variations among cell lines in the synthesis of sphingolipids in de novo and recycling pathways. *Glycobiology* **8**, 885-890, doi:10.1093/glycob/8.9.885 (1998).
- 179 Hannun, Y. A. & Obeid, L. M. Principles of bioactive lipid signalling: lessons from sphingolipids. *Nat Rev Mol Cell Biol* **9**, 139-150, doi:10.1038/nrm2329 (2008).
- 180 Bielawski, J., Szulc, Z. M., Hannun, Y. A. & Bielawska, A. Simultaneous quantitative analysis of bioactive sphingolipids by high-performance liquid chromatography-tandem mass spectrometry. *Methods* **39**, 82-91, doi:10.1016/j.ymeth.2006.05.004 (2006).
- 181 Mishra, S. K., Stephenson, D. J., Chalfant, C. E. & Brown, R. E. Upregulation of human glycolipid transfer protein (GLTP) induces necroptosis in colon carcinoma cells. *Biochim Biophys Acta Mol Cell Biol Lipids* **1864**, 158-167, doi:10.1016/j.bbalip.2018.11.002 (2019).
- 182 Ogretmen, B. Sphingolipid metabolism in cancer signalling and therapy. *Nature reviews. Cancer* **18**, 33-50, doi:10.1038/nrc.2017.96 (2018).
- 183 Heinrich, M. *et al.* Cathepsin D links TNF-induced acid sphingomyelinase to Bid-mediated caspase-9 and -3 activation. *Cell Death Differ* **11**, 550-563, doi:10.1038/sj.cdd.4401382 (2004).
- 184 Wang, G. *et al.* Direct binding to ceramide activates protein kinase Czeta before the formation of a proapoptotic complex with PAR-4 in differentiating stem cells. *The Journal of biological chemistry* **280**, 26415-26424, doi:10.1074/jbc.M501492200 (2005).

- 185 Garcia-Barros, M. *et al.* Tumor response to radiotherapy regulated by endothelial cell apoptosis. *Science* **300**, 1155-1159, doi:10.1126/science.1082504 (2003).
- 186 Morita, Y. *et al.* Oocyte apoptosis is suppressed by disruption of the acid sphingomyelinase gene or by sphingosine-1-phosphate therapy. *Nat Med* **6**, 1109-1114, doi:10.1038/80442 (2000).
- 187 Chipuk, J. E. *et al.* Sphingolipid metabolism cooperates with BAK and BAX to promote the mitochondrial pathway of apoptosis. *Cell* **148**, 988-1000, doi:10.1016/j.cell.2012.01.038 (2012).
- 188 Siskind, L. J., Kolesnick, R. N. & Colombini, M. Ceramide channels increase the permeability of the mitochondrial outer membrane to small proteins. *The Journal of biological chemistry* **277**, 26796-26803, doi:10.1074/jbc.M200754200 (2002).
- 189 Zhang, X. *et al.* Ceramide Nanoliposomes as a MLKL-Dependent, Necroptosis-Inducing, Chemotherapeutic Reagent in Ovarian Cancer. *Molecular cancer therapeutics* **17**, 50-59, doi:10.1158/1535-7163.MCT-17-0173 (2018).
- 190 Nganga, R., Oleinik, N. & Ogretmen, B. Mechanisms of Ceramide-Dependent Cancer Cell Death. *Adv Cancer Res* **140**, 1-25, doi:10.1016/bs.acr.2018.04.007 (2018).
- 191 Bailey, L. J., Alahari, S., Tagliaferro, A., Post, M. & Caniggia, I. Augmented trophoblast cell death in preeclampsia can proceed via ceramide-mediated necroptosis. *Cell Death Dis* **8**, e2590, doi:10.1038/cddis.2016.483 (2017).
- 192 Sawai, H., Ogiso, H. & Okazaki, T. Differential changes in sphingolipids between TNF-induced necroptosis and apoptosis in U937 cells and necroptosis-resistant sublines. *Leukemia research* **39**, 964-970, doi:10.1016/j.leukres.2015.06.002 (2015).
- 193 Parisi, L. R., Li, N. & Atilla-Gokcumen, G. E. Very Long Chain Fatty Acids Are Functionally Involved in Necroptosis. *Cell Chem Biol* **24**, 1445-1454 e1448, doi:10.1016/j.chembiol.2017.08.026 (2017).
- 194 Nganga, R. *et al.* Receptor-interacting Ser/Thr kinase 1 (RIPK1) and myosin IIA-dependent ceramidosomes form membrane pores that mediate blebbing and necroptosis. *The Journal of biological chemistry* **294**, 502-519, doi:10.1074/jbc.RA118.005865 (2019).
- 195 Henkes, L. E. *et al.* Acid sphingomyelinase involvement in tumor necrosis factor alpha-regulated vascular and steroid disruption during luteolysis in vivo. *Proc Natl Acad Sci U S A* **105**, 7670-7675, doi:10.1073/pnas.0712260105 (2008).
- 196 Kim, J. H., Han, J. S. & Yoon, Y. D. Biochemical and morphological identification of ceramide-induced cell cycle arrest and apoptosis in cultured granulosa cells. *Tissue & cell* **31**, 531-539, doi:10.1054/tice.1999.0061 (1999).
- 197 Xie, Y. L. *et al.* Palmitic acid in chicken granulosa cell death-lipotoxic mechanisms mediate reproductive inefficacy of broiler breeder hens. *Theriogenology* **78**, 1917-1928, doi:10.1016/j.theriogenology.2012.07.004 (2012).
- 198 Witty, J. P., Bridgham, J. T. & Johnson, A. L. Induction of apoptotic cell death in hen granulosa cells by ceramide. *Endocrinology* **137**, 5269-5277, doi:10.1210/endo.137.12.8940345 (1996).
- 199 Hernandez-Coronado, C. G. *et al.* Sphingosine-1-phosphate and ceramide are associated with health and atresia of bovine ovarian antral follicles. *Animal* **9**, 308-312, doi:10.1017/S1751731114002341 (2015).
- 200 Pru, J. K., Hendry, I. R., Davis, J. S. & Rueda, B. R. Soluble Fas ligand activates the sphingomyelin pathway and induces apoptosis in luteal steroidogenic cells independently of stress-activated p38(MAPK). *Endocrinology* **143**, 4350-4357, doi:10.1210/en.2002-220229 (2002).
- 201 Kaipia, A., Chun, S. Y., Eisenhauer, K. & Hsueh, A. J. Tumor necrosis factor-alpha and its second messenger, ceramide, stimulate apoptosis in cultured ovarian follicles. *Endocrinology* **137**, 4864-4870, doi:10.1210/endo.137.11.8895358 (1996).
- 202 Santana, P. *et al.* Ceramide mediates tumor necrosis factor effects on P450-aromatase activity in cultured granulosa cells. *Endocrinology* **136**, 2345-2348, doi:10.1210/endo.136.5.7720683 (1995).
- 203 Chowdhury, I. *et al.* Prohibitin (PHB) acts as a potent survival factor against ceramide induced apoptosis in rat granulosa cells. *Life sciences* **89**, 295-303, doi:10.1016/j.lfs.2011.06.022 (2011).
- 204 Li, Q. L. *et al.* Inhibition of steroidogenesis and induction of apoptosis in rat luteal cells by cell-permeable ceramide in vitro. *Sheng Li Xue Bao* **53**, 142-146 (2001).
- 205 Mu, Y. M. *et al.* Saturated FFAs, palmitic acid and stearic acid, induce apoptosis in human granulosa cells. *Endocrinology* **142**, 3590-3597, doi:10.1210/endo.142.8.8293 (2001).

- 206 Perks, C. M. *et al.* Prolactin acts as a potent survival factor against C2-ceramide-induced apoptosis in
human granulosa cells. *Human reproduction (Oxford, England)* **18**, 2672-2677,
doi:10.1093/humrep/deg496 (2003).
- 207 Leonelli, S. & Ankeny, R. A. What makes a model organism? *Endeavour* **37**, 209-212 (2013).
- 208 Davies, J. A. Developmental biologists' choice of subjects approximates to a power law, with no evidence
for the existence of a special group of 'model organisms'. *BMC Dev Biol* **7**, 40, doi:10.1186/1471-213X-7-
40 (2007).
- 209 Bolker, J. A. Model systems in developmental biology. *Bioessays* **17**, 451-455, doi:10.1002/bies.950170513
(1995).
- 210 Davis, M. M. A prescription for human immunology. *Immunity* **29**, 835-838,
doi:10.1016/j.immuni.2008.12.003 (2008).
- 211 Schnabel, J. Neuroscience: Standard model. *Nature* **454**, 682-685, doi:10.1038/454682a (2008).
- 212 Geerts, H. Of mice and men: bridging the translational disconnect in CNS drug discovery. *CNS Drugs* **23**,
915-926, doi:10.2165/11310890-000000000-00000 (2009).
- 213 von Herrath, M. G. & Nepom, G. T. Lost in translation: barriers to implementing clinical
immunotherapeutics for autoimmunity. *J Exp Med* **202**, 1159-1162, doi:10.1084/jem.20051224 (2005).
- 214 Bolker, J. Model organisms: There's more to life than rats and flies. *Nature* **491**, 31-33,
doi:10.1038/491031a (2012).
- 215 Plant, T. M. A comparison of the neuroendocrine mechanisms underlying the initiation of the preovulatory
LH surge in the human, Old World monkey and rodent. *Front Neuroendocrinol* **33**, 160-168,
doi:10.1016/j.yfrne.2012.02.002 (2012).
- 216 Adkins, R. M., Walton, A. H. & Honeycutt, R. L. Higher-level systematics of rodents and divergence time
estimates based on two congruent nuclear genes. *Mol Phylogenet Evol* **26**, 409-420 (2003).
- 217 Springer, M. S. *et al.* Macroevolutionary dynamics and historical biogeography of primate diversification
inferred from a species supermatrix. *PLoS One* **7**, e49521, doi:10.1371/journal.pone.0049521 (2012).
- 218 Springer, M. S., Murphy, W. J., Eizirik, E. & O'Brien, S. J. Placental mammal diversification and the
Cretaceous-Tertiary boundary. *Proc Natl Acad Sci U S A* **100**, 1056-1061, doi:10.1073/pnas.0334222100
(2003).
- 219 Byers, S. L., Wiles, M. V., Dunn, S. L. & Taft, R. A. Mouse estrous cycle identification tool and images.
PLoS One **7**, e35538, doi:10.1371/journal.pone.0035538 (2012).
- 220 Plumel, M. I. *et al.* Litter size manipulation in laboratory mice: an example of how proteomic analysis can
uncover new mechanisms underlying the cost of reproduction. *Front Zool* **11**, 41, doi:10.1186/1742-9994-
11-41 (2014).
- 221 Ecochard, R. & Gougeon, A. Side of ovulation and cycle characteristics in normally fertile women. *Human
reproduction (Oxford, England)* **15**, 752-755, doi:10.1093/humrep/15.4.752 (2000).
- 222 Butler, H. Evolutionary trends in primate sex cycles. *Contrib Primatol* **3**, 2-35 (1974).
- 223 Murray, S. A. *et al.* Mouse gestation length is genetically determined. *PLoS One* **5**, e12418,
doi:10.1371/journal.pone.0012418 (2010).
- 224 Brooks, H. L., Pollow, D. P. & Hoyer, P. B. The VCD Mouse Model of Menopause and Perimenopause for
the Study of Sex Differences in Cardiovascular Disease and the Metabolic Syndrome. *Physiology
(Bethesda)* **31**, 250-257, doi:10.1152/physiol.00057.2014 (2016).
- 225 Greendale, G. A., Lee, N. P. & Arriola, E. R. The menopause. *Lancet* **353**, 571-580, doi:10.1016/S0140-
6736(98)05352-5 (1999).
- 226 Billiar, R. B., Zachos, N. C., Burch, M. G., Albrecht, E. D. & Pepe, G. J. Up-regulation of alpha-inhibin
expression in the fetal ovary of estrogen-suppressed baboons is associated with impaired fetal ovarian
folliculogenesis. *Biol Reprod* **68**, 1989-1996, doi:10.1095/biolreprod.102.011908 (2003).
- 227 Chen, Y., Jefferson, W. N., Newbold, R. R., Padilla-Banks, E. & Pepling, M. E. Estradiol, progesterone, and
genistein inhibit oocyte nest breakdown and primordial follicle assembly in the neonatal mouse ovary in
vitro and in vivo. *Endocrinology* **148**, 3580-3590, doi:10.1210/en.2007-0088 (2007).
- 228 Chaffin, C. L. & Vandervoort, C. A. Follicle growth, ovulation, and luteal formation in primates and rodents:
a comparative perspective. *Exp Biol Med (Maywood)* **238**, 539-548, doi:10.1177/1535370213489437
(2013).

- 229 Andersen, A. G., Als-Nielsen, B., Hornnes, P. J. & Franch Andersen, L. Time interval from human chorionic gonadotrophin (HCG) injection to follicular rupture. *Human reproduction (Oxford, England)* **10**, 3202-3205, doi:10.1093/oxfordjournals.humrep.a135888 (1995).
- 230 Stouffer, R. in *Knobil and Neill's physiology of reproduction* 475-526 (Elsevier Inc., 2006).
- 231 Stocco, C., Telleria, C. & Gibori, G. The molecular control of corpus luteum formation, function, and regression. *Endocrine reviews* **28**, 117-149, doi:10.1210/er.2006-0022 (2007).
- 232 Mihm, M., Gangooly, S. & Muttukrishna, S. The normal menstrual cycle in women. *Anim Reprod Sci* **124**, 229-236, doi:10.1016/j.anireprosci.2010.08.030 (2011).
- 233 Woodruff, T. K., D'Agostino, J., Schwartz, N. B. & Mayo, K. E. Dynamic changes in inhibin messenger RNAs in rat ovarian follicles during the reproductive cycle. *Science* **239**, 1296-1299, doi:10.1126/science.3125611 (1988).
- 234 Davis, J. S. & Rueda, B. R. The corpus luteum: an ovarian structure with maternal instincts and suicidal tendencies. *Front Biosci* **7**, d1949-1978, doi:10.2741/davis1 (2002).
- 235 Banerjee, P. & Fazleabas, A. T. Endometrial responses to embryonic signals in the primate. *The International journal of developmental biology* **54**, 295-302, doi:10.1387/ijdb.082829pb (2010).
- 236 Hearn, J. P. The embryo-maternal dialogue during early pregnancy in primates. *J Reprod Fertil* **76**, 809-819, doi:10.1530/jrf.0.0760809 (1986).
- 237 Allen, W. R. & Stewart, F. Equine placentation. *Reprod Fertil Dev* **13**, 623-634 (2001).
- 238 Phillips, K. A. *et al.* Why primate models matter. *Am J Primatol* **76**, 801-827, doi:10.1002/ajp.22281 (2014).
- 239 Xu, J. *et al.* Primate follicular development and oocyte maturation in vitro. *Adv Exp Med Biol* **761**, 43-67, doi:10.1007/978-1-4614-8214-7_5 (2013).
- 240 Xu, M. *et al.* Encapsulated three-dimensional culture supports development of nonhuman primate secondary follicles. *Biol Reprod* **81**, 587-594, doi:10.1095/biolreprod.108.074732 (2009).
- 241 Telfer, E. E. Future developments: In vitro growth (IVG) of human ovarian follicles. *Acta Obstet Gynecol Scand* **98**, 653-658, doi:10.1111/aogs.13592 (2019).
- 242 Magnusson, A., Kallen, K., Thurin-Kjellberg, A. & Bergh, C. The number of oocytes retrieved during IVF: a balance between efficacy and safety. *Human reproduction (Oxford, England)* **33**, 58-64, doi:10.1093/humrep/dex334 (2018).
- 243 Al-Inany, H. G., Aboulghar, M., Mansour, R. & Proctor, M. Recombinant versus urinary human chorionic gonadotrophin for ovulation induction in assisted conception. *Cochrane Database Syst Rev*, CD003719, doi:10.1002/14651858.CD003719.pub2 (2005).
- 244 Hershko Klement, A. & Shulman, A. hCG Triggering in ART: An Evolutionary Concept. *International journal of molecular sciences* **18**, doi:10.3390/ijms18051075 (2017).
- 245 Casarini, L. *et al.* LH and hCG action on the same receptor results in quantitatively and qualitatively different intracellular signalling. *PLoS One* **7**, e46682, doi:10.1371/journal.pone.0046682 (2012).
- 246 Choi, J. & Smitz, J. Luteinizing hormone and human chorionic gonadotropin: origins of difference. *Mol Cell Endocrinol* **383**, 203-213, doi:10.1016/j.mce.2013.12.009 (2014).
- 247 Wen, X. *et al.* Human granulosa-lutein cell in vitro production of progesterone, inhibin A, inhibin B, and activin A are dependent on follicular size and not the presence of the oocyte. *Fertil Steril* **89**, 1406-1413, doi:10.1016/j.fertnstert.2007.03.086 (2008).
- 248 Kossowska-Tomaszczuk, K. *et al.* The multipotency of luteinizing granulosa cells collected from mature ovarian follicles. *Stem cells (Dayton, Ohio)* **27**, 210-219, doi:10.1634/stemcells.2008-0233 (2009).
- 249 Ferrero, H. *et al.* Efficiency and purity provided by the existing methods for the isolation of luteinized granulosa cells: a comparative study. *Human reproduction (Oxford, England)* **27**, 1781-1789, doi:10.1093/humrep/des096 (2012).
- 250 Imai, M. *et al.* Spontaneous transformation of human granulosa cell tumours into an aggressive phenotype: a metastasis model cell line. *BMC Cancer* **8**, 319, doi:10.1186/1471-2407-8-319 (2008).
- 251 Havelock, J. C., Rainey, W. E. & Carr, B. R. Ovarian granulosa cell lines. *Mol Cell Endocrinol* **228**, 67-78, doi:10.1016/j.mce.2004.04.018 (2004).
- 252 van den Berg-Bakker, C. A. *et al.* Establishment and characterization of 7 ovarian carcinoma cell lines and one granulosa tumor cell line: growth features and cytogenetics. *International journal of cancer* **53**, 613-620, doi:10.1002/ijc.2910530415 (1993).

- 253 Zhang, H. *et al.* Characterization of an immortalized human granulosa cell line (COV434). *Mol Hum Reprod* **6**, 146-153, doi:10.1093/molehr/6.2.146 (2000).
- 254 Nishi, Y. *et al.* Establishment and characterization of a steroidogenic human granulosa-like tumor cell line, KGN, that expresses functional follicle-stimulating hormone receptor. *Endocrinology* **142**, 437-445, doi:10.1210/endo.142.1.7862 (2001).
- 255 Ishiwata, I., Ishiwata, C., Soma, M., Kobayashi, N. & Ishikawa, H. Establishment and characterization of an estrogen-producing human ovarian granulosa tumor cell line. *J Natl Cancer Inst* **72**, 789-800 (1984).
- 256 Blohberger, J. *et al.* L-DOPA in the human ovarian follicular fluid acts as an antioxidant factor on granulosa cells. *Journal of ovarian research* **9**, 62, doi:10.1186/s13048-016-0269-0 (2016).
- 257 Urra, J., Blohberger, J., Tiszavari, M., Mayerhofer, A. & Lara, H. E. In vivo blockade of acetylcholinesterase increases intraovarian acetylcholine and enhances follicular development and fertility in the rat. *Sci Rep* **6**, 30129, doi:10.1038/srep30129 (2016).
- 258 Wuttke, W., Pitzel, L., Seidlova-Wuttke, D. & Hinney, B. LH pulses and the corpus luteum: the luteal phase deficiency LPD). *Vitam Horm* **63**, 131-158 (2001).
- 259 Windham, G. C. *et al.* Ovarian hormones in premenopausal women: variation by demographic, reproductive and menstrual cycle characteristics. *Epidemiology* **13**, 675-684, doi:10.1097/00001648-200211000-00012 (2002).
- 260 Kim, H., Kim, H. & Ku, S. Y. Fertility preservation in pediatric and young adult female cancer patients. *Ann Pediatr Endocrinol Metab* **23**, 70-74, doi:10.6065/apem.2018.23.2.70 (2018).
- 261 Forman, E. J., Anders, C. K. & Behera, M. A. A nationwide survey of oncologists regarding treatment-related infertility and fertility preservation in female cancer patients. *Fertil Steril* **94**, 1652-1656, doi:10.1016/j.fertnstert.2009.10.008 (2010).
- 262 Yee, S., Fuller-Thomson, E., Lau, A. & Greenblatt, E. M. Fertility preservation practices among Ontario oncologists. *J Cancer Educ* **27**, 362-368, doi:10.1007/s13187-011-0301-4 (2012).
- 263 Huang, Z. & Wells, D. The human oocyte and cumulus cells relationship: new insights from the cumulus cell transcriptome. *Mol Hum Reprod* **16**, 715-725, doi:10.1093/molehr/gaq031 (2010).
- 264 Chronowska, E. High-throughput analysis of ovarian granulosa cell transcriptome. *Biomed Res Int* **2014**, 213570, doi:10.1155/2014/213570 (2014).
- 265 Perlman, S. *et al.* Transcriptome analysis of FSH and FSH variant stimulation in granulosa cells from IVM patients reveals novel regulated genes. *Mol Hum Reprod* **12**, 135-144, doi:10.1093/molehr/gah247 (2006).
- 266 Kahsar-Miller, M. D., Conway-Myers, B. A., Boots, L. R. & Azziz, R. Steroidogenic acute regulatory protein (StAR) in the ovaries of healthy women and those with polycystic ovary syndrome. *American journal of obstetrics and gynecology* **185**, 1381-1387, doi:10.1067/mob.2001.118656 (2001).
- 267 Stocco, D. M. StAR protein and the regulation of steroid hormone biosynthesis. *Annual review of physiology* **63**, 193-213, doi:10.1146/annurev.physiol.63.1.193 (2001).
- 268 Kiriakidou, M., McAllister, J. M., Sugawara, T. & Strauss, J. F., 3rd. Expression of steroidogenic acute regulatory protein (StAR) in the human ovary. *The Journal of clinical endocrinology and metabolism* **81**, 4122-4128, doi:10.1210/jcem.81.11.8923870 (1996).
- 269 Zhang, Y. *et al.* Transcriptome Landscape of Human Folliculogenesis Reveals Oocyte and Granulosa Cell Interactions. *Molecular cell* **72**, 1021-1034 e1024, doi:10.1016/j.molcel.2018.10.029 (2018).
- 270 Shen, X. *et al.* Proteomic analysis of human follicular fluid associated with successful in vitro fertilization. *Reprod Biol Endocrinol* **15**, 58, doi:10.1186/s12958-017-0277-y (2017).
- 271 Mesen, T. B. & Young, S. L. Progesterone and the luteal phase: a requisite to reproduction. *Obstet Gynecol Clin North Am* **42**, 135-151, doi:10.1016/j.ogc.2014.10.003 (2015).
- 272 van der Linden, M., Buckingham, K., Farquhar, C., Kremer, J. A. & Metwally, M. Luteal phase support for assisted reproduction cycles. *Cochrane Database Syst Rev*, CD009154, doi:10.1002/14651858.CD009154.pub2 (2011).
- 273 Miyake, A., Aono, T., Kinugasa, T., Tanizawa, O. & Kurachi, K. Suppression of serum levels of luteinizing hormone by short- and long-loop negative feedback in ovariectomized women. *J Endocrinol* **80**, 353-356, doi:10.1677/joe.0.0800353 (1979).
- 274 Smitz, J. *et al.* Pituitary gonadotrophin secretory capacity during the luteal phase in superovulation using GnRH-agonists and HMG in a desensitization or flare-up protocol. *Human reproduction (Oxford, England)* **7**, 1225-1229, doi:10.1093/oxfordjournals.humrep.a137831 (1992).

- 275 Beckers, N. G. *et al.* Nonsupplemented luteal phase characteristics after the administration of recombinant human chorionic gonadotropin, recombinant luteinizing hormone, or gonadotropin-releasing hormone (GnRH) agonist to induce final oocyte maturation in in vitro fertilization patients after ovarian stimulation with recombinant follicle-stimulating hormone and GnRH antagonist cotreatment. *The Journal of clinical endocrinology and metabolism* **88**, 4186-4192, doi:10.1210/jc.2002-021953 (2003).
- 276 Fatemi, H. M. The luteal phase after 3 decades of IVF: what do we know? *Reproductive biomedicine online* **19 Suppl 4**, 4331 (2009).
- 277 Chaffin, C. L., Hess, D. L. & Stouffer, R. L. Dynamics of periovulatory steroidogenesis in the rhesus monkey follicle after ovarian stimulation. *Human reproduction (Oxford, England)* **14**, 642-649, doi:10.1093/humrep/14.3.642 (1999).
- 278 Suzuki, T. *et al.* Cyclic changes of vasculature and vascular phenotypes in normal human ovaries. *Human reproduction (Oxford, England)* **13**, 953-959, doi:10.1093/humrep/13.4.953 (1998).
- 279 Kim, M. *et al.* Melatonin released from granulosa cells (GCs) may have positive role in oocyte maturation in late folliculogenesis. *Fertility and Sterility* **94**, S142 (2010).
- 280 Parinaud, J., Beaur, A., Bourreau, E., Vieitez, G. & Pontonnier, G. Effect of a luteinizing hormone-releasing hormone agonist (Buserelin) on steroidogenesis of cultured human preovulatory granulosa cells. *Fertil Steril* **50**, 597-602, doi:10.1016/s0015-0282(16)60190-5 (1988).
- 281 Meinel, S. *et al.* Pro-nerve growth factor in the ovary and human granulosa cells. *Hormone molecular biology and clinical investigation* **24**, 91-99, doi:10.1515/hmbci-2015-0028 (2015).
- 282 Bagnjuk, K. *et al.* Necroptosis in primate luteolysis: a role for ceramide. *Cell Death Discov* **5**, 67, doi:10.1038/s41420-019-0149-7 (2019).
- 283 Hild-Petito, S. A., Shiigi, S. M. & Stouffer, R. L. Isolation and characterization of cell subpopulations from the monkey corpus luteum of the menstrual cycle. *Biol Reprod* **40**, 1075-1085, doi:10.1095/biolreprod40.5.1075 (1989).
- 284 O'Shea, J. D., Rodgers, R. J. & D'Occhio, M. J. Cellular composition of the cyclic corpus luteum of the cow. *J Reprod Fertil* **85**, 483-487, doi:10.1530/jrf.0.0850483 (1989).
- 285 Kamat, B. R., Brown, L. F., Manseau, E. J., Senger, D. R. & Dvorak, H. F. Expression of vascular permeability factor/vascular endothelial growth factor by human granulosa and theca lutein cells. Role in corpus luteum development. *Am J Pathol* **146**, 157-165 (1995).
- 286 Pharriss, B. B. & Wyngarden, L. J. The effect of prostaglandin F₂alpha on the progesterone content of ovaries from pseudopregnant rats. *Proc Soc Exp Biol Med* **130**, 92-94, doi:10.3181/00379727-130-33495 (1969).
- 287 Silvia, W. J., Lewis, G. S., McCracken, J. A., Thatcher, W. W. & Wilson, L., Jr. Hormonal regulation of uterine secretion of prostaglandin F₂ alpha during luteolysis in ruminants. *Biol Reprod* **45**, 655-663, doi:10.1095/biolreprod45.5.655 (1991).
- 288 Peterson, A. J., Fairclough, R. J., Payne, E. & Smith, J. F. Hormonal changes around bovine luteolysis. *Prostaglandins* **10**, 675-684 (1975).
- 289 Zarco, L., Stabenfeldt, G. H., Quirke, J. F., Kindahl, H. & Bradford, G. E. Release of prostaglandin F₂alpha and the timing of events associated with luteolysis in ewes with oestrous cycles of different lengths. *J Reprod Fertil* **83**, 517-526, doi:10.1530/jrf.0.0830517 (1988).
- 290 Morales, C. *et al.* Different patterns of structural luteolysis in the human corpus luteum of menstruation. *Human reproduction (Oxford, England)* **15**, 2119-2128, doi:10.1093/humrep/15.10.2119 (2000).
- 291 Shikone, T. *et al.* Apoptosis of human corpora lutea during cyclic luteal regression and early pregnancy. *The Journal of clinical endocrinology and metabolism* **81**, 2376-2380, doi:10.1210/jcem.81.6.8964880 (1996).
- 292 Hojo, T. *et al.* Programmed necrosis - a new mechanism of steroidogenic luteal cell death and elimination during luteolysis in cows. *Sci Rep* **6**, 38211, doi:10.1038/srep38211 (2016).
- 293 Hojo, T. *et al.* Receptor interacting protein kinases-dependent necroptosis as a new, potent mechanism for elimination of the endothelial cells during luteolysis in cow. *Theriogenology* **128**, 193-200, doi:10.1016/j.theriogenology.2019.01.035 (2019).
- 294 Wang, Z. *et al.* Prostaglandin F₂alpha-induced functional regression of the corpus luteum and apoptosis in rodents. *J Pharmacol Sci* **92**, 19-27, doi:10.1254/jphs.92.19 (2003).
- 295 Gaytan, F. *et al.* Macrophages, cell proliferation, and cell death in the human menstrual corpus luteum. *Biol Reprod* **59**, 417-425, doi:10.1095/biolreprod59.2.417 (1998).

- 296 Sugino, N. & Okuda, K. Species-related differences in the mechanism of apoptosis during structural luteolysis. *J Reprod Dev* **53**, 977-986, doi:10.1262/jrd.19047 (2007).
- 297 Doyle, L. L., Barclay, D. L., Duncan, G. W. & Kirton, K. T. Human luteal function following hysterectomy as assessed by plasma progesterone. *American journal of obstetrics and gynecology* **110**, 92-97, doi:10.1016/0002-9378(71)90221-3 (1971).
- 298 Neill, J. D., Johansson, E. D. & Knobil, E. Failure of hysterectomy to influence the normal pattern of cyclic progesterone secretion in the rhesus monkey. *Endocrinology* **84**, 464-465, doi:10.1210/endo-84-2-464 (1969).
- 299 Dozier, B. L., Watanabe, K. & Duffy, D. M. Two pathways for prostaglandin F₂ alpha synthesis by the primate periovulatory follicle. *Reproduction* **136**, 53-63, doi:10.1530/REP-07-0514 (2008).
- 300 Bogan, R. L., Murphy, M. J., Stouffer, R. L. & Hennebold, J. D. Prostaglandin synthesis, metabolism, and signaling potential in the rhesus macaque corpus luteum throughout the luteal phase of the menstrual cycle. *Endocrinology* **149**, 5861-5871, doi:10.1210/en.2008-0500 (2008).
- 301 Summers, P. M., Wennink, C. J. & Hodges, J. K. Cloprostenol-induced luteolysis in the marmoset monkey (*Callithrix jacchus*). *J Reprod Fertil* **73**, 133-138, doi:10.1530/jrf.0.0730133 (1985).
- 302 Antonova, M., Wienecke, T., Olesen, J. & Ashina, M. Prostaglandins in migraine: update. *Curr Opin Neurol* **26**, 269-275, doi:10.1097/WCO.0b013e328360864b (2013).
- 303 Nakahata, K. *et al.* Vasodilation mediated by inward rectifier K⁺ channels in cerebral microvessels of hypertensive and normotensive rats. *Anesth Analg* **102**, 571-576, doi:10.1213/01.ane.0000194303.00844.5e (2006).
- 304 Yu, Y. *et al.* Prostaglandin F₂alpha elevates blood pressure and promotes atherosclerosis. *Proc Natl Acad Sci U S A* **106**, 7985-7990, doi:10.1073/pnas.0811834106 (2009).
- 305 Takayama, K. *et al.* Thromboxane A₂ and prostaglandin F₂alpha mediate inflammatory tachycardia. *Nat Med* **11**, 562-566, doi:10.1038/nm1231 (2005).
- 306 Jovanovic, N., Pavlovic, M., Mircevski, V., Du, Q. & Jovanovic, A. An unexpected negative inotropic effect of prostaglandin F₂alpha in the rat heart. *Prostaglandins Other Lipid Mediat* **80**, 110-119, doi:10.1016/j.prostaglandins.2006.05.014 (2006).
- 307 Saleem, S., Ahmad, A. S., Maruyama, T., Narumiya, S. & Dore, S. PGF₂(alpha) FP receptor contributes to brain damage following transient focal brain ischemia. *Neurotox Res* **15**, 62-70, doi:10.1007/s12640-009-9007-3 (2009).
- 308 Ricciotti, E. & FitzGerald, G. A. Prostaglandins and inflammation. *Arterioscler Thromb Vasc Biol* **31**, 986-1000, doi:10.1161/ATVBAHA.110.207449 (2011).
- 309 Sotrel, G., Helvacioğlu, A., Dowers, S., Scommegna, A. & Auletta, F. J. Mechanism of luteolysis: effect of estradiol and prostaglandin F₂ alpha on corpus luteum luteinizing hormone/human chorionic gonadotropin receptors and cyclic nucleotides in the rhesus monkey. *American journal of obstetrics and gynecology* **139**, 134-140, doi:10.1016/0002-9378(81)90434-8 (1981).
- 310 Auletta, F. J., Agins, H. & Scommegna, A. Prostaglandin F mediation of the inhibitory effect of estrogen on the corpus luteum of the rhesus monkey. *Endocrinology* **103**, 1183-1189, doi:10.1210/endo-103-4-1183 (1978).
- 311 Kim, S. O., Markosyan, N., Pepe, G. J. & Duffy, D. M. Estrogen promotes luteolysis by redistributing prostaglandin F₂alpha receptors within primate luteal cells. *Reproduction* **149**, 453-464, doi:10.1530/REP-14-0412 (2015).
- 312 Mukku, V. & Moudgal, N. R. Relative sensitivity of the corpus luteum of different days of pregnancy to LH-deprivation in the rat and hamster. *Mol Cell Endocrinol* **6**, 71-80, doi:10.1016/0303-7207(76)90045-9 (1976).
- 313 Hutchison, J. S. & Zeleznik, A. J. The corpus luteum of the primate menstrual cycle is capable of recovering from a transient withdrawal of pituitary gonadotropin support. *Endocrinology* **117**, 1043-1049, doi:10.1210/endo-117-3-1043 (1985).
- 314 Hanson, F. W., Powell, J. E. & Stevens, V. C. Effects of HCG and human pituitary LH on steroid secretion and functional life of the human corpus luteum. *The Journal of clinical endocrinology and metabolism* **32**, 211-215, doi:10.1210/jcem-32-2-211 (1971).
- 315 Cole, L. A. Biological functions of hCG and hCG-related molecules. *Reprod Biol Endocrinol* **8**, 102, doi:10.1186/1477-7827-8-102 (2010).

- 316 Sachet, M., Liang, Y. Y. & Oehler, R. The immune response to secondary necrotic cells. *Apoptosis* **22**, 1189-1204, doi:10.1007/s10495-017-1413-z (2017).
- 317 Snyder, A. G. *et al.* Intratumoral activation of the necroptotic pathway components RIPK1 and RIPK3 potentiates antitumor immunity. *Sci Immunol* **4**, doi:10.1126/sciimmunol.aaw2004 (2019).
- 318 Espey, L. L. Ovulation as an inflammatory reaction--a hypothesis. *Biol Reprod* **22**, 73-106, doi:10.1095/biolreprod22.1.73 (1980).
- 319 Bishop, C. V., Xu, F., Molskness, T. A., Stouffer, R. L. & Hennebold, J. D. Dynamics of Immune Cell Types Within the Macaque Corpus Luteum During the Menstrual Cycle: Role of Progesterone. *Biol Reprod* **93**, 112, doi:10.1095/biolreprod.115.132753 (2015).
- 320 Penny, L. A. *et al.* Immune cells and cytokine production in the bovine corpus luteum throughout the oestrous cycle and after induced luteolysis. *J Reprod Fertil* **115**, 87-96, doi:10.1530/jrf.0.1150087 (1999).
- 321 Walusimbi, S. S. & Pate, J. L. Physiology and Endocrinology Symposium: role of immune cells in the corpus luteum. *J Anim Sci* **91**, 1650-1659, doi:10.2527/jas.2012-6179 (2013).
- 322 Takamatsu, K., Mikami, M., Kiguchi, K., Nozawa, S. & Iwamori, M. Structural characteristics of the ceramides of neutral glycosphingolipids in the human female genital tract--their menstrual cycle-associated change in the cervical epithelium and uterine endometrium, and their dissociation in the mucosa of the fallopian tube with the menstrual cycle. *Biochim Biophys Acta* **1165**, 177-182 (1992).
- 323 Rylova, S. N., Somova, O. G. & Dyatlovitskaya, E. V. Comparative investigation of sphingoid bases and fatty acids in ceramides and sphingomyelins from human ovarian malignant tumors and normal ovary. *Biochemistry (Mosc)* **63**, 1057-1060 (1998).
- 324 Andreasian, G. O., Malykh Ia, N. & Diatlovitskaia, E. V. [Ceramides and gangliosides in benign and malignant human ovarian tumors]. *Vopr Med Khim* **42**, 248-253 (1996).
- 325 Romiti, E. *et al.* Characterization of sphingomyelinase activity released by thrombin-stimulated platelets. *Mol Cell Biochem* **205**, 75-81, doi:10.1023/a:1007041329052 (2000).
- 326 Becker, K. P., Kitatani, K., Idkowiak-Baldys, J., Bielawski, J. & Hannun, Y. A. Selective inhibition of juxtannuclear translocation of protein kinase C beta11 by a negative feedback mechanism involving ceramide formed from the salvage pathway. *The Journal of biological chemistry* **280**, 2606-2612, doi:10.1074/jbc.M409066200 (2005).
- 327 Weitzel, J. M., Vernunft, A., Kruger, B., Plinski, C. & Viergutz, T. Inactivation of the LOX-1 pathway promotes the Golgi apparatus during cell differentiation of mural granulosa cells. *J Cell Physiol* **229**, 1946-1951, doi:10.1002/jcp.24644 (2014).
- 328 Pru, J. K., Lynch, M. P., Davis, J. S. & Rueda, B. R. Signaling mechanisms in tumor necrosis factor alpha-induced death of microvascular endothelial cells of the corpus luteum. *Reprod Biol Endocrinol* **1**, 17 (2003).
- 329 Kisliouk, T. *et al.* Expression pattern of prokineticin 1 and its receptors in bovine ovaries during the estrous cycle: involvement in corpus luteum regression and follicular atresia. *Biol Reprod* **76**, 749-758, doi:10.1095/biolreprod.106.054734 (2007).
- 330 Cardoso-Moreira, M. *et al.* Gene expression across mammalian organ development. *Nature* **571**, 505-509, doi:10.1038/s41586-019-1338-5 (2019).
- 331 Lee, S. J. *et al.* American Society of Clinical Oncology recommendations on fertility preservation in cancer patients. *Journal of clinical oncology : official journal of the American Society of Clinical Oncology* **24**, 2917-2931, doi:10.1200/JCO.2006.06.5888 (2006).
- 332 Oktay, K. *et al.* Fertility Preservation in Patients With Cancer: ASCO Clinical Practice Guideline Update. *Journal of clinical oncology : official journal of the American Society of Clinical Oncology* **36**, 1994-2001, doi:10.1200/JCO.2018.78.1914 (2018).
- 333 Pacheco, F. & Oktay, K. Current Success and Efficiency of Autologous Ovarian Transplantation: A Meta-Analysis. *Reprod Sci* **24**, 1111-1120, doi:10.1177/1933719117702251 (2017).
- 334 Meirow, D. *et al.* Transplantations of frozen-thawed ovarian tissue demonstrate high reproductive performance and the need to revise restrictive criteria. *Fertil Steril* **106**, 467-474, doi:10.1016/j.fertnstert.2016.04.031 (2016).
- 335 Muller, A. *et al.* Replantation of cryopreserved ovarian tissue: the first live birth in Germany. *Dtsch Arztebl Int* **109**, 8-13, doi:10.3238/arztebl.2012.0008 (2012).
- 336 Madhusoodhan, P. P., Carroll, W. L. & Bhatla, T. Progress and Prospects in Pediatric Leukemia. *Curr Probl Pediatr Adolesc Health Care* **46**, 229-241, doi:10.1016/j.cpped.2016.04.003 (2016).

- 337 Baskar, R., Lee, K. A., Yeo, R. & Yeoh, K. W. Cancer and radiation therapy: current advances and future directions. *Int J Med Sci* **9**, 193-199, doi:10.7150/ijms.3635 (2012).
- 338 Du, Y., Bagnjuk, K., Lawson, M. S., Xu, J. & Mayerhofer, A. Acetylcholine and necroptosis are players in follicular development in primates. *Sci Rep* **8**, 6166, doi:10.1038/s41598-018-24661-z (2018).
- 339 Bagnjuk, K. *et al.* Inhibitor of apoptosis proteins are potential targets for treatment of granulosa cell tumors - implications from studies in KGN. *Journal of ovarian research* **12**, 76, doi:10.1186/s13048-019-0549-6 (2019).
- 340 Cha, K. Y. *et al.* Pregnancy after in vitro fertilization of human follicular oocytes collected from nonstimulated cycles, their culture in vitro and their transfer in a donor oocyte program. *Fertil Steril* **55**, 109-113, doi:10.1016/s0015-0282(16)54068-0 (1991).
- 341 Trounson, A., Wood, C. & Kausche, A. In vitro maturation and the fertilization and developmental competence of oocytes recovered from untreated polycystic ovarian patients. *Fertil Steril* **62**, 353-362, doi:10.1016/s0015-0282(16)56891-5 (1994).
- 342 Steptoe, P. C. & Edwards, R. G. Laparoscopic recovery of preovulatory human oocytes after priming of ovaries with gonadotrophins. *Lancet* **1**, 683-689, doi:10.1016/s0140-6736(70)90923-2 (1970).
- 343 Hatirnaz, S. *et al.* Oocyte in vitro maturation: A systematic review. *Turk J Obstet Gynecol* **15**, 112-125, doi:10.4274/tjod.23911 (2018).
- 344 Sauerbrun-Cutler, M. T., Vega, M., Keltz, M. & McGovern, P. G. In vitro maturation and its role in clinical assisted reproductive technology. *Obstet Gynecol Surv* **70**, 45-57, doi:10.1097/OGX.000000000000150 (2015).
- 345 Shalom-Paz, E. *et al.* Fertility preservation for breast-cancer patients using IVM followed by oocyte or embryo vitrification. *Reproductive biomedicine online* **21**, 566-571, doi:10.1016/j.rbmo.2010.05.003 (2010).
- 346 Jeruss, J. S. & Woodruff, T. K. Preservation of fertility in patients with cancer. *N Engl J Med* **360**, 902-911, doi:10.1056/NEJMra0801454 (2009).
- 347 Donnez, J. *et al.* Livebirth after orthotopic transplantation of cryopreserved ovarian tissue. *Lancet* **364**, 1405-1410, doi:10.1016/S0140-6736(04)17222-X (2004).
- 348 Xiao, S. *et al.* In vitro follicle growth supports human oocyte meiotic maturation. *Sci Rep* **5**, 17323, doi:10.1038/srep17323 (2015).
- 349 Eppig, J. J. & Schroeder, A. C. Capacity of mouse oocytes from preantral follicles to undergo embryogenesis and development to live young after growth, maturation, and fertilization in vitro. *Biol Reprod* **41**, 268-276, doi:10.1095/biolreprod41.2.268 (1989).
- 350 Morohaku, K. *et al.* Complete in vitro generation of fertile oocytes from mouse primordial germ cells. *Proc Natl Acad Sci U S A* **113**, 9021-9026, doi:10.1073/pnas.1603817113 (2016).
- 351 Woodruff, T. K. & Shea, L. D. A new hypothesis regarding ovarian follicle development: ovarian rigidity as a regulator of selection and health. *Journal of assisted reproduction and genetics* **28**, 3-6, doi:10.1007/s10815-010-9478-4 (2011).
- 352 Xiao, S. *et al.* Size-specific follicle selection improves mouse oocyte reproductive outcomes. *Reproduction* **150**, 183-192, doi:10.1530/REP-15-0175 (2015).
- 353 Nubbemeyer, R., Heistermann, M., Oerke, A. K. & Hodges, J. K. Reproductive efficiency in the common marmoset (*Callithrix jacchus*): a longitudinal study from ovulation to birth monitored by ultrasonography. *J Med Primatol* **26**, 139-146 (1997).
- 354 Oerke, A. K., Einspanier, A. & Hodges, J. Noninvasive monitoring of follicle development, ovulation, and corpus luteum formation in the marmoset monkey (*Callithrix jacchus*) by ultrasonography. *American Journal of Primatology* **39**, 99-113 (1996).
- 355 Bishop, C. V. *et al.* Evaluation of antral follicle growth in the macaque ovary during the menstrual cycle and controlled ovarian stimulation by high-resolution ultrasonography. *Am J Primatol* **71**, 384-392, doi:10.1002/ajp.20664 (2009).
- 356 Takahashi, N. *et al.* Necrostatin-1 analogues: critical issues on the specificity, activity and in vivo use in experimental disease models. *Cell Death Dis* **3**, e437, doi:10.1038/cddis.2012.176 (2012).
- 357 Puccetti, P. & Grohmann, U. IDO and regulatory T cells: a role for reverse signalling and non-canonical NF-kappaB activation. *Nat Rev Immunol* **7**, 817-823, doi:10.1038/nri2163 (2007).

- 358 Kollmann, Z., Schneider, S., Fux, M., Bersinger, N. A. & von Wolff, M. Gonadotrophin stimulation in IVF alters the immune cell profile in follicular fluid and the cytokine concentrations in follicular fluid and serum. *Human reproduction (Oxford, England)* **32**, 820-831, doi:10.1093/humrep/dex005 (2017).
- 359 Wu, R., Van der Hoek, K. H., Ryan, N. K., Norman, R. J. & Robker, R. L. Macrophage contributions to ovarian function. *Human reproduction update* **10**, 119-133, doi:10.1093/humupd/dmh011 (2004).
- 360 Loukides, J. A. *et al.* Human follicular fluids contain tissue macrophages. *The Journal of clinical endocrinology and metabolism* **71**, 1363-1367, doi:10.1210/jcem-71-5-1363 (1990).
- 361 Vidal, J. D. & Dixon, D. in *Boorman's Pathology of the Rat* 523-536 (Elsevier, 2018).
- 362 Vince, J. E. *et al.* IAP antagonists target cIAP1 to induce TNFalpha-dependent apoptosis. *Cell* **131**, 682-693, doi:10.1016/j.cell.2007.10.037 (2007).
- 363 Wu, H., Tschopp, J. & Lin, S. C. Smac mimetics and TNFalpha: a dangerous liaison? *Cell* **131**, 655-658, doi:10.1016/j.cell.2007.10.042 (2007).
- 364 Troeger, A. *et al.* Survivin and its prognostic significance in pediatric acute B-cell precursor lymphoblastic leukemia. *Haematologica* **92**, 1043-1050, doi:10.3324/haematol.10675 (2007).
- 365 Hundsdorfer, P., Dietrich, I., Schmelz, K., Eckert, C. & Henze, G. XIAP expression is post-transcriptionally upregulated in childhood ALL and is associated with glucocorticoid response in T-cell ALL. *Pediatr Blood Cancer* **55**, 260-266, doi:10.1002/pbc.22541 (2010).
- 366 Miura, K. *et al.* Inhibitor of apoptosis protein family as diagnostic markers and therapeutic targets of colorectal cancer. *Surg Today* **41**, 175-182, doi:10.1007/s00595-010-4390-1 (2011).
- 367 Che, X. *et al.* Nuclear cIAP1 overexpression is a tumor stage- and grade-independent predictor of poor prognosis in human bladder cancer patients. *Urol Oncol* **30**, 450-456, doi:10.1016/j.urolonc.2010.12.016 (2012).
- 368 Yang, X. H. *et al.* XIAP is a predictor of cisplatin-based chemotherapy response and prognosis for patients with advanced head and neck cancer. *PLoS One* **7**, e31601, doi:10.1371/journal.pone.0031601 (2012).
- 369 Ponten, F., Jirstrom, K. & Uhlen, M. The Human Protein Atlas--a tool for pathology. *J Pathol* **216**, 387-393, doi:10.1002/path.2440 (2008).
- 370 Li, J. *et al.* Expression of inhibitor of apoptosis proteins (IAPs) in rat granulosa cells during ovarian follicular development and atresia. *Endocrinology* **139**, 1321-1328, doi:10.1210/endo.139.3.5850 (1998).
- 371 Li, W. *et al.* BV6, an IAP antagonist, activates apoptosis and enhances radiosensitization of non-small cell lung carcinoma in vitro. *J Thorac Oncol* **6**, 1801-1809, doi:10.1097/JTO.0b013e318226b4a6 (2011).
- 372 Rettinger, E. *et al.* SMAC Mimetic BV6 Enables Sensitization of Resistant Tumor Cells but also Affects Cytokine-Induced Killer (CIK) Cells: A Potential Challenge for Combination Therapy. *Front Pediatr* **2**, 75, doi:10.3389/fped.2014.00075 (2014).
- 373 Fischer, K. *et al.* The Smac Mimetic BV6 Improves NK Cell-Mediated Killing of Rhabdomyosarcoma Cells by Simultaneously Targeting Tumor and Effector Cells. *Front Immunol* **8**, 202, doi:10.3389/fimmu.2017.00202 (2017).
- 374 Hehlhans, S. *et al.* The SMAC mimetic BV6 sensitizes colorectal cancer cells to ionizing radiation by interfering with DNA repair processes and enhancing apoptosis. *Radiat Oncol* **10**, 198, doi:10.1186/s13014-015-0507-4 (2015).
- 375 El-Mesery, M., Shaker, M. E. & Elgaml, A. The SMAC mimetic BV6 induces cell death and sensitizes different cell lines to TNF-alpha and TRAIL-induced apoptosis. *Exp Biol Med (Maywood)* **241**, 2015-2022, doi:10.1177/1535370216661779 (2016).
- 376 Bildik, G. *et al.* Endogenous c-Jun N-terminal kinase (JNK) activity marks the boundary between normal and malignant granulosa cells. *Cell Death Dis* **9**, 421, doi:10.1038/s41419-018-0459-3 (2018).
- 377 Lee, F. A. *et al.* Randomized Phase II Study of the X-linked Inhibitor of Apoptosis (XIAP) Antisense AEG35156 in Combination With Sorafenib in Patients With Advanced Hepatocellular Carcinoma (HCC). *Am J Clin Oncol* **39**, 609-613, doi:10.1097/COC.000000000000099 (2016).
- 378 Schimmer, A. D. *et al.* Phase I/II trial of AEG35156 X-linked inhibitor of apoptosis protein antisense oligonucleotide combined with idarubicin and cytarabine in patients with relapsed or primary refractory acute myeloid leukemia. *Journal of clinical oncology : official journal of the American Society of Clinical Oncology* **27**, 4741-4746, doi:10.1200/JCO.2009.21.8172 (2009).
- 379 Mahadevan, D. *et al.* Phase I trial of AEG35156 an antisense oligonucleotide to XIAP plus gemcitabine in patients with metastatic pancreatic ductal adenocarcinoma. *Am J Clin Oncol* **36**, 239-243, doi:10.1097/COC.0b013e3182467a13 (2013).

- 380 Schimmer, A. D. *et al.* Addition of AEG35156 XIAP antisense oligonucleotide in reinduction chemotherapy does not improve remission rates in patients with primary refractory acute myeloid leukemia in a randomized phase II study. *Clin Lymphoma Myeloma Leuk* **11**, 433-438, doi:10.1016/j.clml.2011.03.033 (2011).
- 381 Fauser, B. C. *et al.* Minimal ovarian stimulation for IVF: appraisal of potential benefits and drawbacks. *Human reproduction (Oxford, England)* **14**, 2681-2686, doi:10.1093/humrep/14.11.2681 (1999).
- 382 Whelan, J. G., 3rd & Vlahos, N. F. The ovarian hyperstimulation syndrome. *Fertil Steril* **73**, 883-896, doi:10.1016/s0015-0282(00)00491-x (2000).
- 383 Fauser, B. C. & Devroey, P. Reproductive biology and IVF: ovarian stimulation and luteal phase consequences. *Trends Endocrinol Metab* **14**, 236-242 (2003).
- 384 Blumenfeld, Z. The Ovarian Hyperstimulation Syndrome. *Vitam Horm* **107**, 423-451, doi:10.1016/bs.vh.2018.01.018 (2018).
- 385 Fauser, B. C. *et al.* Endocrine profiles after triggering of final oocyte maturation with GnRH agonist after cotreatment with the GnRH antagonist ganirelix during ovarian hyperstimulation for in vitro fertilization. *The Journal of clinical endocrinology and metabolism* **87**, 709-715, doi:10.1210/jcem.87.2.8197 (2002).
- 386 European Recombinant, L. H. S. G. Human recombinant luteinizing hormone is as effective as, but safer than, urinary human chorionic gonadotropin in inducing final follicular maturation and ovulation in in vitro fertilization procedures: results of a multicenter double-blind study. *The Journal of clinical endocrinology and metabolism* **86**, 2607-2618, doi:10.1210/jcem.86.6.7599 (2001).
- 387 Devoto, L., Kohen, P., Munoz, A. & Strauss, J. F., 3rd. Human corpus luteum physiology and the luteal-phase dysfunction associated with ovarian stimulation. *Reproductive biomedicine online* **18 Suppl 2**, 19-24, doi:10.1016/s1472-6483(10)60444-0 (2009).
- 388 von Wolff, M. The role of Natural Cycle IVF in assisted reproduction. *Best Pract Res Clin Endocrinol Metab* **33**, 35-45, doi:10.1016/j.beem.2018.10.005 (2019).
- 389 Steward, K. & Raja, A. in *StatPearls* (2019).
- 390 Sugino, N., Matsuoka, A., Taniguchi, K. & Tamura, H. Angiogenesis in the human corpus luteum. *Reprod Med Biol* **7**, 91-103, doi:10.1111/j.1447-0578.2008.00205.x (2008).
- 391 Arru, M. *et al.* Arterial devices for regional hepatic chemotherapy: transaxillary versus laparotomic access. *J Vasc Access* **1**, 93-99 (2000).
- 392 Fulda, S. Promises and Challenges of Smac Mimetics as Cancer Therapeutics. *Clin Cancer Res* **21**, 5030-5036, doi:10.1158/1078-0432.CCR-15-0365 (2015).
- 393 Marci, R. *et al.* Radiations and female fertility. *Reprod Biol Endocrinol* **16**, 112, doi:10.1186/s12958-018-0432-0 (2018).
- 394 Blumenfeld, Z. Chemotherapy and fertility. *Best Pract Res Clin Obstet Gynaecol* **26**, 379-390, doi:10.1016/j.bpobgyn.2011.11.008 (2012).

6 Acknowledgements

This present dissertation would not be possible without the encouragement, motivation, endurance and personal support of many people in my environment. Although the following acknowledgements could never meet the grade the people who supported me are deserving, I want to verbalize my thanks in this section.

Thank you, Prof. Dr. Artur Mayerhofer, for giving me the opportunity to work on this interesting project within your group and for the freedom to manifest my own thoughts and interests in new projects and experiments. I want to thank you for your infinite optimism, which amplified my motivation, even in hard times. Your implicit support, especially in the time when I started my own little family, gave me the security I needed to continue my work purposefully and concentrated. Without your input and help during the preparation of the published papers and the dissertation, I would not have succeeded. I truly can say that you are the best principal I've ever had.

Thank you, PD. Dr. Lars Kunz, for being such an outstanding doctorate supervisor. You always gave me the right hints at the right time to conduct the experiments that are needed for clear results. Only because of your help with the interpretations, your critical view and your effort in proof reading the work, we were able to publish far reaching results that might impact clinical use cases in future. Furthermore, I am grateful for the time you spend reading this dissertation over and over again and for the useful remarks, which helped me to finalize a version I am happy with.

Prof. Dr. Gisela Grupe deserves a special thank you for her readiness to join the commission for the present dissertation as the second examiner. Thank you for the effort you spent reading the dissertation and writing a report. In this context I want to thank Prof. Dr. Jörg Nickelsen, PD Dr. Annette Müller-Taubenberger, Prof. Dr. Angelika Böttger and Prof. Dr. Wolfgang Enard for being part of the examining board. Further I want to thank PD Dr. Annette Müller-Taubenberger for the helpful discussions and remarks in regards to my work and presentations in the department.

The present dissertation is a result of fruitful cooperation's that significantly affected the success and outcome of this research. Therefore, I want to thank Prof. Dr. Dieter Berg,

Dr. Ulrike Berg and the laboratory team of the Kinderwunschzentrum A.R.T. in Bogenhausen for their trust and for providing the foundation for this present work, the IVF-derived luteinized granulosa cells. I am also grateful for the precious cooperation with Jing Xu, Ph.D. from the Oregon National Primate Research Center of the OHSU, who helped us with the follicle study and the primate tissue material. In this regard, I want to thank Prof. Dr. Rüdiger Behr for the *C. jacchus* tissue samples and the interesting tour through the Deutsches Primatenzentrum in Göttingen. Special thanks go to Prof. Dr. Doris Mayr for sharing the tissue micro arrays and the deep knowledge about gynecological tumor diseases. The group around Dr. Thomas Fröhlich and especially Jan-Bernd Stöckl were vital to this work, since they performed the mass spectrometry analysis and helped with their expertise in data evaluation. Therefore, I want to thank all of you.

Prof. Dr. Artur Mayerhofer's lab is truly a place where you want to be during your doctoral studies. Next to the cooperative nature of the group, the people in here are making even the hardest day very pleasant. You guys helped me to improve my mood when experiments or other things went wrong and you made the conferences very special by combining the exchange of scientific knowledge with the pleasure of being together. Therefore, I want to acknowledge Daniel Aigner, Dr. Jan Blohberger, Dr. Theresa Buck, Kim Dietrich, Katja Eubler, Theo Hack, Carola Herrmann, Melanie Kaseder, Verena Kast, Karin Metzrath, Annika Missel, Nina Schmid, Astrid Tiefenbacher, Dr. Harald Welter and Dr. Lena Walenta. A special thank you goes to my Master student Verena Kast, who conducted most of the hands-on work on the SMAC mimetics paper. Annika Missel deserves to earn a honorable mention for proof reading the present work and all the helpful discussions within the lab. Further the technicians Kim Dietrich, Astrid Tiefenbacher and Carola Herrmann deserve a special acknowledgment for keeping the lab alive and for the readiness to help out whenever they were needed.

Next to the AM group, I want to thank the helping hands at the BMC, which are Rico Schieweck, Dr. Max Harner, Siavash Khosravi, Dr. Saskia Hutten and Ralf Bigiel, who were there with a helpful advice in terms of mitochondria, antibody selection, transfection methods or the all destroying Mac update that crashed the remaining programs.

The work environment was crucial for the success of this present dissertation, but another group of people made it possible for me to pursue this goal. I want to thank these people

in my mother tongue to make sure everybody who this part is dedicated to will understand it.

Hiermit möchte ich meinen Eltern, Ekaterina und Walerij Bagnjuk dafür danken, dass sie mir ein sorgloses Leben mit offenen Wegen geschenkt haben. Ich danke euch, dass ihr mich bei jeder meiner Entscheidungen unterstützt habt und dass ihr alles in eurer Macht stehende getan habt, damit ich jeden Stolperstein erfolgreich meistern konnte. Von euch habe ich die größte aller Tugenden erfahren – die Selbstlosigkeit. Auch meinem Bruder, Ewgenij Bagnjuk, gebührt besonderer Dank. Du hast mir stets das Gefühl der Sicherheit gegeben und dafür gesorgt, dass ich auf der richtigen Bahn bleibe und die wesentlichen Ziele im Leben verfolge. Du warst und bist mir stets das größte Vorbild. Ihr drei habt mich die bedingungslose Liebe gelehrt, die ich jetzt meiner eigenen kleinen Familie geben kann. Ich danke dir Joana-Sophie Bagnjuk für dein Sein, du bist jemand, der die Welt besser macht. Um dich und deinen Wert in meinem Leben zu umschreiben fehlen mir die Worte. Du unterstützt mich, gibst mir Mut und Halt, lehrst mich eines Besseren und sorgst dafür, dass ich jeden Abend gerne nach Hause komme. Ohne dein Vertrauen und deine Liebe wäre all das hier nicht möglich gewesen. Du bist wahrlich die Ehefrau, die ich mir an meiner Seite wünsche. Du bist meine beste Freundin. Neben meiner Ehefrau möchte ich in dieser Danksagung meinen Sohn Nikita Jonathan Bagnjuk erwähnen. Seit deiner Geburt bist du der Mittelpunkt meines Lebens und das Fundament meiner Motivation geworden. Ich möchte dir das gleiche unbeschwerte Leben schenken, welches meine Eltern mir geschenkt haben. Aus diesem Grund bist du es, der mich von innen antreibt stetig besser zu werden. Du bist es, der jeden Tag unvergesslich macht und zusammen mit deiner Mutter macht ihr mein Leben zu dem, was es ist – ein wundervolles Abenteuer. Ich liebe euch.

7 List of publications

- First author: Title: Necroptosis in primate luteolysis: a role for ceramide
Bagnjuk K. et al. (2019), Cell Death Discovery
DOI: 10.1038/s41420-019-0149-7
- Title: Acetylcholine and necroptosis are key players in follicular development in primates
Du Y., Bagnjuk K. et al. (2018), Scientific Reports
DOI: 10.1038/s41598-018-24661-z
- Title: SMAC mimetics are novel therapeutics for granulosa cell tumors – implications from studies in KGN
Bagnjuk K., Kast V. et al. (2019), Journal of Ovarian Research
DOI: 10.1186/s13048-019-0549-6
- Title: Human IVF-derived granulosa cells – a model for the Corpus luteum (Review)
Bagnjuk K. and Mayerhofer A. (2019), Frontiers in Endocrinology
DOI: 10.3389/fendo.2019.00452
- Co-author: Title: A Role for H₂O₂ and TRPM2 in the Induction of Cell Death: Studies in KGN Cells
Hack CT. et al (2019), Antioxidants
DOI: 10.3390/antiox8110518